



Ghent University

Faculty of Engineering

Department of Flow, Heat and Combustion

Academic Year 2011-2012

**Application of Zone- and Field codes to model heat and smoke propagation in support of
Fire Hazard Analyses of Nuclear Power Plants.**

Feng Xu

Supervisor: Bart MERCI

Promoter: Bart MERCI

Master thesis submitted in the Erasmus Mundus Study Programme

International Master of Science in Fire Safety Engineering

DISCLAIMER

This thesis is submitted in partial fulfilment of the requirements for the degree of *The International Master of Science in Fire Safety Engineering (IMFSE)*. This thesis has never been submitted for any degree or examination to any other University/programme. The author(s) declare(s) that this thesis is original work except where stated. This declaration constitutes an assertion that full and accurate references and citations have been included for all material, directly included and indirectly contributing to the thesis.

This document may contain confidential information which falls under the restrictions set by the OECD PRISME project. Therefore, nothing may be made public in any way without the prior permission of the PRISME management board. The PRISME Management Board (MB) deliberated that the Project data be kept confidential for a period of three years following the completion of the Project. This would not preclude that publication of the main test results be made in e.g. conferences or technical literature during the course of the Project, as requested by several partners. These publications would however require the MB approval, which can be requested by e-mail via the NEA secretariat. In the frame of the PRISME agreement, Bel V and Tractebel Engineering are responsible for the project deliverables in Belgium. It is therefore strictly forbidden to publish, cite or make public in any way this document or any part thereof without the express written permission of Bel V and the MB. Under no circumstance this document may be communicated to or put at the disposal of third parties; photocopying or duplicating it in any other way is strictly prohibited. Disregarding the confidential nature of this document may cause irremediable damage.

The restrictions set above expire on the 1st of July 2014 as the PRISME project was ended in June 2011. Nevertheless, the PRISME MB can one-sidedly decide to alter this term.

The author(s) gives (give) permission to make this master thesis available for consultation and to copy parts of this master thesis for personal use. In the case of any other use, the limitations of the copyright have to be respected, in particular with regard to the obligation to state expressly the source when quoting results from this master thesis. The thesis supervisor must be informed when data or results are used.

Feng Xu
2012/04/30

ABSTRACT

CFD model ISIS and two-zone model SYLVIA are used to simulate four experiments conducted by PRISME, which aims to study the leakage during fire in Nuclear Power Plant. The models are validated and evaluated regarding to their ability to simulate leakage scenarios. A discussion is made about different sources of uncertainty of the simulation.

Explanation for several abnormal outputs of ISIS is proposed and solutions are given. Recommendations are given for the usage of ISIS in simulating leakage scenarios.

A database is built for further research. With the database current and further validation work can be integrated together to give a statistic evaluation of the models.

Advice regarding to further research is made for BelV.

CONTENTS

ABSTRACT.....	II
CONTENTS.....	III
ABBREVIATIONS	V
FIGURES.....	VIII
TABLES	XII
1. INTRODUCTION	1
1.1 Objective.....	1
1.2 Methodology.....	1
1.2.1 NPP Fire Scenarios	2
1.2.2 Fire Modeling Codes.....	4
1.2.3 Documentation of the Calculation Method.....	4
1.2.4 Assess the Experimental Data.....	5
1.2.5 Fire Modeling Parameters.....	5
1.2.6 Verification	8
1.2.7 Quantitative Validation.....	8
1.2.8 Report Results.....	8
2. TEST SERIES DESCRIPTION AND MODEL INPUT DATA.....	9
2.1 Test Series Description	9
2.2 Model Input.....	11
2.2.1 ISIS	11
2.2.2 Sylvia	20
3. UNCERTAINTY	25
3.1 Introduction.....	25
3.2 Measurement Uncertainty.....	25
3.3 Model Input Uncertainty.....	26
3.4 Combined Uncertainty	27
3.5 Application of Combined Uncertainty.....	28
4. RESULTS	30
4.1 Results Presenting Methodology	30
4.2 ISIS	30
4.2.1 Relative Difference	30
4.2.2 Attribute-time Curve.....	39
4.3 Sylvia	54
4.3.1 Relative Difference	54
4.3.2 Attribute-time Curve.....	60
5. DISCUSSION	70
5.1 Further Uncertainty for Real Application.....	70
5.2 Time Aspects in Validation Process	71

5.3 Quantitative Criteria.....	72
6. CONCLUSIONS.....	74
7. ACKNOWLEDGEMENTS.....	76
8. REFERENCES	77
9. APPENDICES	I
9.1 ISIS script.....	I
9.2 Sylvia script	XX

ABBREVIATIONS

A	area [m ²]
ADM	Admission Branch
ASTM	American Society of Testing and Materials
B	low
CFD	Computational Fluid Dynamics
c_p	specific heat
D	characteristic dimension [m]
DIVA	Dispositif Incendie, Ventilation et A érocontamination
EBU	Eddy Break-up Model
EXT	Exhaust Branch
FVS	Soot Volume Fraction
H	height [m]
HAUT	High
HRR	Heat Release Rate
IH	Interface Height
IRSN	Institut de Radioprotection et de S éret éNucl éaire (France)
ISIS	Incendie SIMul é pour la S éret é
ISO	International Organization for Standardization
k	turbulent kinetic energy [m ² /s ²]
L	length [m]
L2	room 2
L3	room 3
LOL	Lower Oxygen Limit
m	mass [kg]
\dot{m}	mass flow rate [kg/s]
MLR	Mass Loss Rate
N	North
NE	North-East
NFPA	National Fire Protection Association (USA)
NPP	Nuclear Power Plant
NW (nw)	North-West
OECD	Organisation for Economic Co-operation and Development
P	Pressure [Pa]
PRISME	French acronym for “Fire Propagation in Elementary Multi-room Scenarios”
Q	heat flux [kW/m ²]
Q^*	fire froude number
\dot{Q}	heat release rate [kW]
R	Resistance
R2	room 2
R3	room 3
RHF	Radiative Heat Flux
S	South
s_{con}	soot concentration
Sc	Turbulent Schmidt
SE (se)	South-East

SFPE	Society of Fire Protection Engineers
SGDH	Turbulent Production Due to Buoyance
SPSS	Statistical Package for the Social Sciences
SW (sw)	South-West
T	Temperature (°C or K)
THF	Total Heat Flux
TINF	Cold Layer Temperature
TPH	Hydrogenated tetra-propylene
TSUP	Upper Layer Temperature
U_{ε}	combined uncertainty
U_E	measurement uncertainty
U_M	model input uncertainty
ULT	Upper Layer Temperature
\dot{V}	flow rate [m ³ /s]
V	volume [m ³]
V&V	Verification and Validation
W	West
wsggm	Gray-medium Assumption with the Cell Size
Y	mass fraction
y_s	soot yield fraction
ε	dissipation rate [m ² /s ³]
ϵ	emmissitivity
φ	equivalence ratio
ρ	density [kg/m ³]
$\tilde{\sigma}_E$	relative standard deviation of the experimental data
$\tilde{\sigma}_M$	relative standard deviation of the model
α	thermal diffusivity [m ² /s]
γ	view factor
ΔH_c	heat of combustion [kJ/kg]
ΔH_{O_2}	heat of combustion of oxygen [kJ/kg]
ΔP	pressure difference [Pa]
Δt	time step [s]

Subscripts

b	beginning
c	ceiling
E	experimental measurement
e	end
f	flame
fuel	fuel
G	soot
leak	leak
m	model (simulation)
net	net

o	stable state
p	peak
pool	pool
r	radiation
rad	radiation
s	static
soot	soot
t	total

Units

SI units are used throughout the text. It is always indicated when deflecting.

FIGURES

Figure 1 Overview of the approach for V&V study of selected fire models for nuclear power plant applications (Adopted from Figure 2-1 of [34])	2
Figure 2 Pictorial representation of the fire scenarios and corresponding fire modeling parameters (Source: [17])	7
Figure 3 Design of DIVA facility	9
Figure 4 Description of the scenario involving two circular leakages.....	10
Figure 5 Description of the Leak2 scenario.....	10
Figure 6 Description of Leak3 scenario.....	10
Figure 7 Description of Leak4 scenario.....	11
Figure 8 Dimension of fire pool in reality	12
Figure 9 Fire pool in structured mesh.....	12
Figure 10 Dimension of leakage pipe in reality.....	12
Figure 11 Leak pipe in structured mesh.....	12
Figure 12 Schematic of the grid.....	13
Figure 13 Schematic of the extraction of cells for boundary condition.....	13
Figure 14 Schematic of the Leak1 grid (a)along +Z axis (b)along +Y axis (c)along +X axis (d)perspective.....	14
Figure 15 Refinement level influence (Source: [43])	14
Figure 16 Schematic of the Leak 1 grid by gambit (a)along +Z axis (b)along +Y axis (c)along +X axis (d)perspective.....	15
Figure 17 Six parts of mesh (a) the rest of the two rooms (b) transition in both rooms (c) leakage pipes.....	15
Figure 18 Hierarchy of the abstraction of the DIVA facility to the Sylvia input. (a)DIVA facility (b)ventilation network of DIVA (c) abstraction of ventilation network(d) Sylvia input	21
Figure 19 Scatter plots depicting validation results in and out of the range of combined uncertainty (original source: Figure 2-10 of NUREG 1824[34])	28
Figure 20 Summary of prediction of radiative heat flux.....	31
Figure 21 Summary of prediction of radiative heat flux (adjusted value).....	32
Figure 22 Wall temperature in the fire room	33
Figure 23 Wall temperature in the target room and floor temperature	33

Figure 24 Soot concentration	34
Figure 25 Oxygen concentration.....	35
Figure 26 CO ₂ concentration	35
Figure 27 Flow rate through leakage pipes.....	36
Figure 28 Gas temperature in the SW axis of fire room.....	37
Figure 29 Gas temperature in the NE axis of fire room.....	37
Figure 30 Gas temperature in the central axis of fire room	38
Figure 31 Gas temperature in the NE axis of target room	38
Figure 32 Gas temperature in the NW axis of target room.....	39
Figure 33 Gas temperature in the CC axis of target room	39
Figure 34 Coordinate system in room 2 (fire room) and room 3 (target room) (Source: [7])	40
Figure 35 Radiative heat flux.....	41
Figure 36 Adjusted radiative heat flux.....	41
Figure 37 Radiative heat flux on the ceiling.....	42
Figure 38 Radiative heat flux on the ceiling.....	42
Figure 39 Wall temperature in fire room	43
Figure 40 Floor wall temperature	44
Figure 41 Wall temperature in target room.....	44
Figure 42 Soot concentration in the exhaust branches.....	45
Figure 43 Oxygen concentration in the fire room.....	46
Figure 44 Oxygen concentration in the target room	46
Figure 45 CO ₂ concentration in the fire room	46
Figure 46 CO ₂ concentration in the target room.....	47
Figure 47 Relative pressure	47
Figure 48 Flow rate in fire room.....	48
Figure 49 Flow rate in target room	48
Figure 50 Gas temperature in the extraction point of fire room	49
Figure 51 Mass flow equilibrium.....	49
Figure 52 Mass flow rate through leakage pipes	50

Figure 53 Resistance of upper leakage by ISIS	50
Figure 54 Energy flow through leakage.....	51
Figure 55 Temperatures of gases in room 2 - CENTRAL axis	52
Figure 56 Temperatures of gases in room 2 - NE axis	52
Figure 57 Temperatures of gases in room 2 - SW axis.....	52
Figure 58 Temperatures of gases in room 3 - CENTRAL axis	53
Figure 59 Temperatures of gases in room 3 - NE axis	53
Figure 60 Temperatures of gases in room 3 - SW axis.....	53
Figure 61 Radiative heat flux prediction by Sylvia	54
Figure 62 HRR of Leak4.....	55
Figure 63 Radiative heat flux prediction by Sylvia	55
Figure 64 Soot concentration prediction by Sylvia.....	56
Figure 65 Gas property in room2 and room3 predicted by Sylvia for Leak1 scenario	57
Figure 66 Oxygen concentration prediction by Sylvia	57
Figure 67 Carbon dioxide concentration prediction by Sylvia	58
Figure 68 Relative pressure prediction by Sylvia.....	58
Figure 69 Hot gas layer temperature.....	59
Figure 70 Interface height (a)Leak1 (b)Leak2 (c)Leak3 (d)Leak4.....	59
Figure 71 Ventilation flow rate prediction by Sylvia	60
Figure 72 Radiative heat flux.....	60
Figure 73 Wall temperature in fire room	61
Figure 74 Floor temperature in the fire room	61
Figure 75 Wall temperature in target room.....	62
Figure 76 Soot concentration in the exhaust branches.....	62
Figure 77 Oxygen concentration in the fire room.....	63
Figure 78 Oxygen concentration in the target room	63
Figure 79 CO ₂ concentration in the fire room	64
Figure 80 CO ₂ concentration in the target room.....	64
Figure 81 Measured static pressure and flow rate before ignition.....	65
Figure 82 Relative pressure	66

Figure 83 flow rate in fire room.....	66
Figure 84 flow rate in target room	66
Figure 85 Flow rate through leakage pipes.....	67
Figure 86 Mass flow rate through leakage pipes	67
Figure 87 Energy flow rate through leakage pipes predicted by Sylvia.....	68
Figure 88 Two zone temperature in fire room	68
Figure 89 Two zone temperature in target room	69
Figure 90 Interface height.....	69
Figure 91 HRR input for leak 4 scenario.....	70
Figure 92 Gas temperature prediction by two models	71

TABLES

Table 1 Range of normalized parameter	3
Table 2 List of fire scenarios and fire modeling parameters involved (Adopted and adjusted from [17]).....	8
Table 3 Overview of simulations	11
Table 4 Soot fraction of each leak scenario	17
Table 5 External pressure and resistance	18
Table 6 Material properties input.....	23
Table 7 Experimental measurement uncertainty(Source: [15]).....	26
Table 8 Model input uncertainty (Adopted and adjusted from [14]).....	26
Table 9 Combined uncertainty.....	27
Table 10 Position of heat flux sensor.....	40
Table 11 Wall temperature measurement points	43
Table 12 Position of gas concentration measurement points.....	45
Table 13 Position of pressure measurement point	47
Table 14 Position of thermocouple trees	51
Table 15 Relative differences for maximum value.....	71
Table 16 Prediction of activation time.....	72
Table 17 Database structure for statistical analysis of V&V study	73
Table 18 Overview of models' capability	74

1. INTRODUCTION

1.1 Objective

The objective of this thesis is to establish confidence for the application of two fire codes to NPP scenarios. The fire codes involved here are CFD model ISIS and the two-zone model SYLVIA. Validation of the fire codes is conducted in this thesis in order to achieve the objective. Test data used for the validation process is obtained from the PRISME project [1][5].

1.2 Methodology

The use of fire models to support fire protection decision making requires a good understanding of their limitations and predictive capabilities. NFPA 805 [2] states that fire models shall only be applied within the limitations of the given model and shall be verified and validated. ASTM E 1355 [3] provides definitions of the terms model verification and model validation.

Model Verification is the process of determining that the implementation of a calculation method accurately represents the developer's conceptual description of the calculation method and the solution to the calculation method. The fundamental strategy of verification of computational models is the identification and quantification of error in the computational model and its solution.

Model Validation is the process of determining the degree to which a calculation method is an accurate representation of the real world from the perspective of the intended uses of the calculation method. The fundamental strategy of validation is the identification and quantification of error and uncertainty in the conceptual and computational models with respect to intended users.

ASTM E 1355 [3] and ISO 16730 [4] establishes a process for conducting a V&V study of a fire model. BONTE [23] modified this process for NPP fire scenarios to fit it in for PRISME. The methodology for the assessment of fire models proposed in this work is as follows:

- (1) Define a list of typical NPP fire scenarios.
- (2) Select and describe the fire models for which an evaluation can be conducted.
- (3) Assess the documentation of the calculation method:
- (4) Technical documentation that explains the scientific basis of the calculation method.
- (5) Assess the experimental data.
- (6) Define fire modelling parameters.
- (7) Conduct the verification study for each fire modelling tool.
- (8) Conduct the quantitative validation study for each fire modelling tool.
- (9) Report validation results.

Figure 1 graphically represents this approach. The following sections describe the steps of this approach in greater detail.

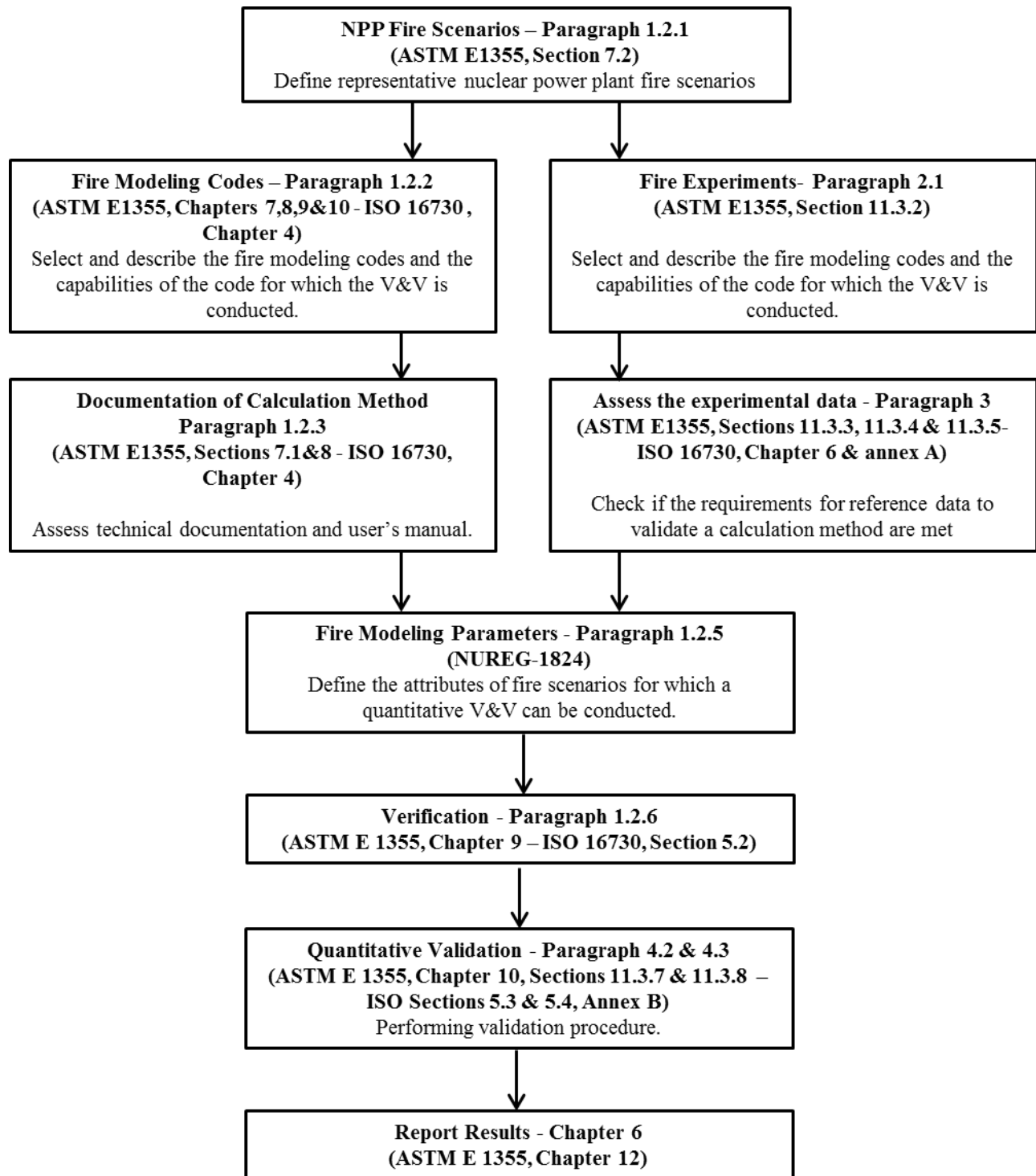


Figure 1 Overview of the approach for V&V study of selected fire models for nuclear power plant applications (Adopted from Figure 2-1 of [34])

1.2.1 NPP Fire Scenarios

Fire scenarios are the basis for the V&V study and thus the choice of them are of significance. For the purpose of the V&V study, a fire scenario definition should include a complete

description of the phenomena of interest in the evaluation to facilitate appropriate application of the model. In the context of this V&V study, the list of scenarios captures all the phenomena of interest that would be predicted by some fire models, but may or may not have experimental data to support a quantitative model evaluation. It is not the intent of this thesis to conduct V&V study on ISIS and Sylvia for every aspect. The focus of this thesis is on the fire models' capability in predicting attributes for fire scenarios involving leakage. The fire scenarios chosen are thus four fire tests from PRISME.

The PRISME project consists of a series of fire and smoke propagation tests in a dedicated facility at the French Institut de radioprotection et de sûreté nucléaire (IRSN) centre at Cadarache. The facility is used to investigate room-to-room heat and smoke propagation, the effect of network ventilation and the resulting thermal stresses to sensitive safety equipment of such room configurations [5].

Several propagation modes are being studied in PRISME. In this thesis, four tests from PRISME that are dedicated to leakage are studied.

The applicability of the validation results can be determined using normalized parameters traditionally used in fire modeling applications [17]. Normalized parameters allow users to compare results from scenarios of different scales by normalizing physical characteristics of the scenario.

Table 1 Range of normalized parameter

Quantity	Normalized Parameter	Range for ISIS (Leak1~Leak2)	Range for Sylvia (Leak1~Leak4)
Fire Froude Number	$Q^* = \frac{\dot{Q}}{\rho_{\infty} c_p T_{\infty} D^2 \sqrt{gD}}$	1.17~1.23	1.17~2.78
Flame Length Ratio	$\frac{H_f + L_f}{H_c}$	0.74~0.75	0.74~1
Equivalence Ratio	$\varphi = \frac{\dot{Q}}{\Delta H_{O_2} \dot{m}_{O_2}}$ $\dot{m}_{O_2} = 0.23 \rho_{\infty} \dot{V}$	0.56~0.6	0.56~1.33
Compartment Aspect Ratio	L/H or W/H	1.25~1.5	1.25~1.5
Radial Distance Ratio	$\frac{r}{D}$	3.4~4	3.4~4
Leakage Ratio	$\frac{3600 * \dot{V}}{V}$	5~6.25	5~6.25

In [17] there is one more normalized parameter: ceiling jet distance ratio, which is used to express the horizontal distance from target to plume. As there is no ceiling jet involved in the PRISME Leak Tests, this parameter is not included in Table 1.

One parameter specific for fire scenarios involving leakage is proposed in this thesis. This parameter is called leakage ratio. It is the ratio between the hourly leakage and the volume of the target room. Higher leakage ratio value means that there is lots of gas leakage compared to the volume of the room.

1.2.2 Fire Modeling Codes

Two zone model Sylvia and CFD model ISIS are studied in this thesis.

The ISIS code (Incendie SIMulé pour la Sûreté, in French) is a CFD software developed by IRSN that can cope with a wide range of applications, including laminar or turbulent flows, possibly reactive, governed by incompressible or low-Mach number Navier-Stokes equations.

An extensive description of the physical modelling of the ISIS code is described in [6].

The first public release of the software was April 4, 2008. Since then, several verification and validation studies have been performed by the developer ([37] , [38]). An overview of the validation of the ISIS CFD code for fire simulations is given in [12]. Because the model is relatively new, external verification and validation work is scarce.

The Sylvia software system, developed by IRSN, simulates the consequences of a fire in an industrial facility featuring a ventilation network. It calculates the development of the fire, the transportation of hot gases and soot, the resuspension and the transportation of aerosols, whether radioactive or not, the clogging of filters and the damage of isolating equipment such as firebreak doors and fire dampers.

Modelling of the fire is a zone-based approach: the volume of each room is divided into two zones of variable height in which the thermodynamic properties (pressure, temperature and concentration of the gaseous and particulate species) are uniform, the upper zone containing the hot gases and soot. The ventilation network is modeled using a set of elements, conduits, filters, valves, fans, etc. Mass and heat exchange correlations (between zones, flame and walls) supplement the mass and energy balance equations for the zones. The rates of suspension and deposition of the aerosols on the walls of the rooms and in the ventilation network are also estimated. Constant attention is paid to system validation, particularly on the basis of the numerous full-scale tests performed by the IRSN.

An extensive description of the physical modelling of the Sylvia code is described in [39].

1.2.3 Documentation of the Calculation Method

The documentation shall include technical documentation that explains the scientific basis of the calculation method and a user's manual in the case of a computer program. The documentation for Sylvia and ISIS is either available now or being prepared by the developers [6][44][39][12][40].

1.2.4 Assess the Experimental Data

Reference data to validate a calculation method can be obtained from experiments, surveys on well documented fire events, or other validated calculation methods, as appropriate for the parameters and other quantities to be validated. Care should be taken to ensure that the test, the published full-scale data or the documented experience closely matches the scenario for which evaluation is sought. The ASTM E1355, sections 11.3.3 to 11.3.5 give good guidance on this matter.

The data provided in the framework of the OECD PRISME project is without question elaborate and detailed to use for validation purposes. However, the uncertainty of the experimental data should still be assessed, which is done in chapter 3.

1.2.5 Fire Modeling Parameters

A complete validation of ISIS/Sylvia for a given NPP fire scenario is not possible because (i) the availability of experimental data is limited, and/or (ii) the selected fire models have limited modeling capabilities. In this thesis, as many as fire modeling attributes are chosen within the limit of both the availability of experimental data and capability of fire models. Therefore, this section of ‘fire modeling parameters’ is intended to benefit as much as possible from the available data to establish the modeling capabilities and limitations of the selected fire models in typical NPP fire scenarios [34].

An important consideration in evaluating the capabilities of fire models in NPPs is the range of fire scenarios for which the models may be used. From a fire modeling perspective, most NPPs have similar configurations and fire hazards. That is, fire scenarios are characterized by similar attributes. One V&V study for other PRISME scenarios has been done by BONTE [23]. In his work 15 attributes were chosen. Similar attributes are chosen in this thesis. However some of them are not chosen here because of lack of experimental data. However, the flow rate of the leakage is added, because it is one of the most important parameters for NPP fire scenarios involving leakage.

The selection of fire modeling attributes is outlined below (Adopted from [23] and adapted for the leakage scenarios)

(1) Hot gas layer temperature: The hot gas layer temperature is particularly important in NPP fire scenarios because it can provide an indication of target damage away from the ignition source. Models predict the increase in environmental temperature attributable to the energy released by a fire in a volume. However, different models define this volume in different ways. In the Sylvia two-zone model, the room is divided into upper and lower control volumes. Thus, the hot gas layer temperature output from this two-zone model is at a uniform temperature in the upper control volume. This layer is also referred to as the hot gas layer because it accumulates hot gases that are transported to the upper part of the room by the fire plume. In the ISIS field model, the room is divided into numerous control volumes. Consequently, ISIS can provide

outputs for the average temperature of the control volumes in the upper layer of the computational domain, as determined by a reduction of temperature profile data. Nevertheless, it was decided to not validate this deduced parameter for the ISIS code.

(2) Hot gas layer height: The height of the hot gas layer is also important in NPP fire scenarios because it indicates whether a given target is immersed in and affected by hot gas layer temperatures. The concept of hot gas layer height is most relevant in the two-zone model Sylvia, in which this attribute defines the interface between the upper and lower control volumes. The ISIS field model does not provide the hot gas layer height as a direct output, but this parameter can be calculated from the temperature profile within the height of the room[35]. Nevertheless, it was decided to not validate this deduced parameter for the ISIS code.

(3) Plume temperature: The fire plume is the buoyant flow rising above the ignition source, which carries the hot gases that ultimately accumulate in the upper part of a room to form the hot gas layer. The plume is characterized by a distinct temperature profile, which is expected to be higher than the ceiling jet and hot gas layer. This attribute is particularly important in NPP fires because of the numerous postulated scenarios that involve targets directly above a potential fire source. The plume temperature can be obtained from the ISIS model by inspecting the temperature profile in the pre-defined grid. The Sylvia model does not provide plume temperatures as an output.

(4) Radiated heat flux to walls: Radiation is an important mode of heat transfer in fire events. Sylvia and ISIS have sophisticated heat transfer models that account for radiation exchanges between room surfaces and the upper and lower gas layers. Therefore, the incident thermal radiation to which a given target is exposed is a result of the heat balance at the surface of the target (which includes all of the exchanges), as well as the thermal radiation received from the flames.

(5) Wall temperature: This attribute was included as a separate attribute in the NUREG-1824 V&V study to evaluate model capabilities to determine the temperature of walls, floors, and ceilings. Sylvia and ISIS provide the temperatures of these surfaces as outputs, since such outputs are part of the calculations required to determine the heat losses through boundaries. However, the walls in leak scenarios are insulated by THERMIPAN which makes the boundary condition as multilayer. ISIS is not able to specify boundary condition to multilayer situation.

(6) Smoke concentration: The smoke concentration can be an important attribute in NPP fire scenarios that involve rooms where operators may need to perform actions during a fire. This attribute specifically refers to soot concentration, which affects how far a person can see through the smoke (visibility). Sylvia and ISIS calculate smoke concentration as a function of time. These models determine smoke concentration as the fire plume carries combustion products into the hot gas layer.

(7) Oxygen concentration: Oxygen concentration is an important attribute potentially influencing the outcome of fires in NPPs because of the compartmentalized nature of NPPs. Oxygen concentration has a direct influence on the burning behaviour of a fire, especially if the concentration is relatively low. The Sylvia two-zone model calculates the oxygen concentration in the upper and lower layers, and the ISIS model calculates the oxygen concentration in each control volume defined in the computational domain.

(8) Total relative room pressure: Room pressure is a rarely used attribute in NPP fire modeling. It may be important when it contributes to smoke migration to adjacent compartments or when characterizing the aeraulic behaviour of the fire room and the effects on the ventilation network during a fire. Sylvia and ISIS calculate room pressure as they solve energy and mass balance equations in the control volume.

(9) Volume flow rate at the admission and extraction branches of the ventilation network: this attribute is at present a rarely used attribute in NPP fire modeling. Together with the total relative pressure, this attribute describes the aeraulic behaviour of the fire room and the effects on the ventilation network during the fire. As for oxygen concentration, this attribute can also be important because it influences the outcome of under-ventilated fires. In the near future, the possible integration of the ISIS model in the SYLVIA system will make it possible to simulate 3-D fire developments in a compartment together with the description of a complete and realistic ventilation network.

(10) Leakage volume flow rate: This attribute determines the energy flow from the fire room to the adjacent rooms. The other attributes in the target room are determined by the leakage flow rate to great extent. Sylvia and ISIS calculate the leakage volume flow rate and provide it as direct output.

Those fire modeling parameters are chosen with good reasons. Figure 2 is a pictorial representation of application of the fire modeling parameters in fire scenario.

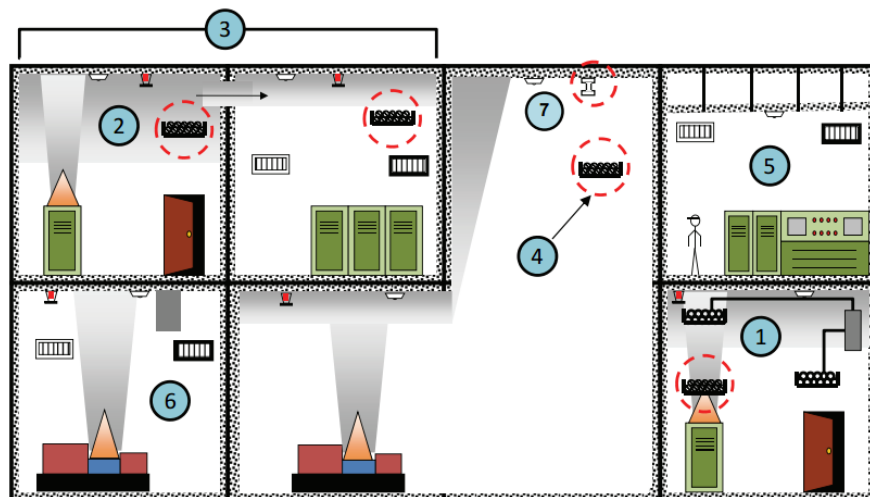


Figure 2 Pictorial representation of the fire scenarios and corresponding fire modeling parameters (Source: [17])

The numbers in the figure above stands for different fire scenarios. They are described in the table below:

Table 2 List of fire scenarios and fire modeling parameters involved (Adopted and adjusted from [17])

Number	Scenario Description	Fire Modeling Parameters involved
1	Scenarios consisting of determining time to damage of cables above the ignition source located inside the flames or the fire plume.	Plume temperature.
2	Scenarios consisting of determining time to damage of cables located inside or outside the HGL. This scenario also includes a secondary fuel source (i.e., propagation to cable trays).	Hot gas layer temperature.
3	Scenarios consisting of determining time to damage of cables located in an adjacent room to the room of fire origin.	Leakage flow rate. Gas temperature.
4	Scenarios consisting of determining time to damage of cables located inside or outside the HGL in rooms with complex geometries.	Hot gas layer temperature, Hot gas layer height.
5	Scenarios consisting of determining time to loss of habitability of the main control room.	Gas temperature, Smoke concentration, Oxygen concentration.
6	Scenarios consisting of determining time to smoke or heat detector activation.	Gas temperature, Smoke concentration.
7	Scenarios consisting of determining temperature of structural elements.	Wall temperature, Gas temperature

1.2.6 Verification

Model Verification is the process of determining that the implementation of a calculation method accurately represents the developer’s conceptual description of the calculation method and the solution to the calculation method.

The verification of ISIS has already been performed by the developer in [40]. There is currently no verification work done for Sylvia. However, the verification is not within the scope of this thesis.

1.2.7 Quantitative Validation

The validation study is conducted by comparing the experimental data with the model predictions. The quantitative validation is conducted by both relative difference and attribute-time curve. The validation procedure is presented in Chapter 4.

1.2.8 Report Results

In Chapter 6, an overview of the validation results is provided. The results are valid within the normalized parameter range.

2. TEST SERIES DESCRIPTION AND MODEL INPUT DATA

2.1 Test Series Description

The PRISME Leak Fire experiments were carried out in the DIVA facility. DIVA (the name DIVA is a French acronym for "experimental facility for the study of fires, ventilation and airborne contamination") was built by IRSN in order to study fires in several rooms configuration [22]. DIVA is situated in JUPITER compartment. Two rooms are involved (see Figure 3): Room 2 (also called fire room) which holds the pool fire located in its center and Room 3 (also called target room), the adjacent room, in which the impact of smoke and hot gases propagation will be analyzed. These two rooms have identical sizes (length*width*height=6*5*4m). They are connected to the ventilation network to manage accurately the renewal rates of air in fire and adjacent rooms.

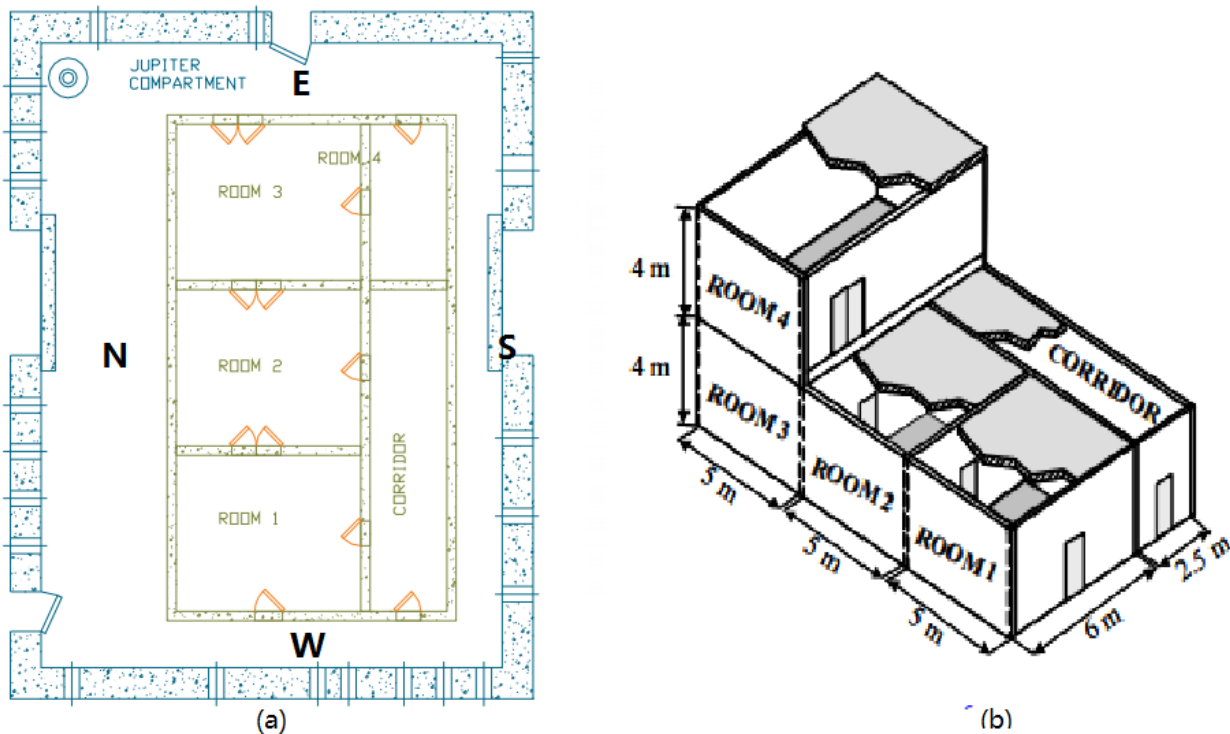


Figure 3 Design of DIVA facility

The four side walls and the ceiling of the fire room are insulated with Rock-wool panels fixed on metallic frames screwed on the concrete. The ceiling of the target room is also insulated with rockwool. The thickness of insulation for ceiling and side walls is 5cm and 3cm respectively.

Leak1 case [7] : The aim is to simulate the leakage between two rooms. The connection between these two rooms consists of two circular pipes of 210mm inner diameter ($A=314\text{cm}^2$) located in the upper part and lower part on the wall between rooms 2 and 3. The pipe is 1.5m long and it is welded on the rectangular steel plate used as crossing plate between the 2 rooms. This scenario is depicted in Figure 4.

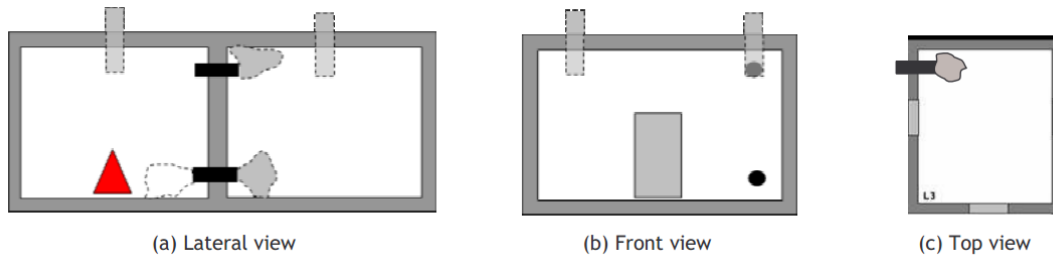


Figure 4 Description of the scenario involving two circular leakages

The first circular duct is located in the upper part of the fire room (center of the pipe 55cm from the top). The second one is located in the lower part of it near the floor (center of the pipe 56cm from the bottom).

Leak2 case [8]: One vertical slot is set between the two rooms. It consists in a vertical slot ($1730\text{mm} \times 16\text{mm} = 279\text{cm}^2$) located at the center of the wall separating the 2 rooms. The depth of the slot is about 60mm. The bottom of the slot is located at 17cm from the ground level.

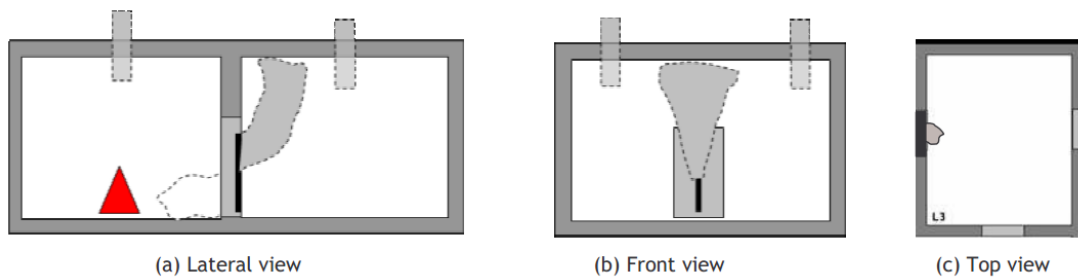


Figure 5 Description of the Leak2 scenario

Leak3 case [9]: Fire room and target room are connected by fire door. The fire door was closed during the test. However the fire door itself is leaky. It has only one leaf with height of 2.054m and width of 0.948m.

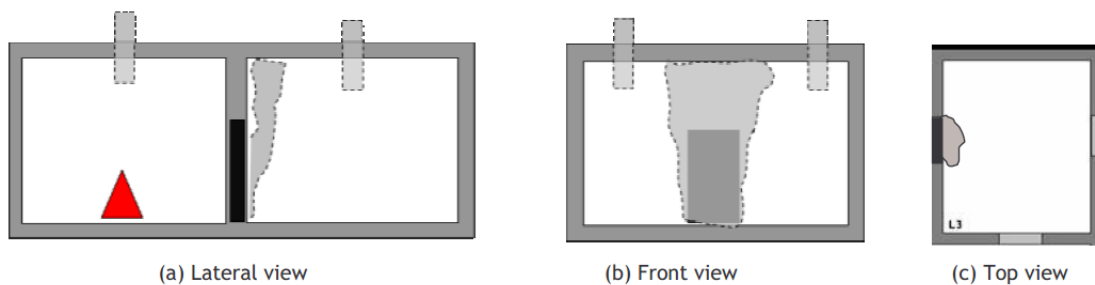


Figure 6 Description of Leak3 scenario

Leak4 case [10]: The connection between the fire room and the target room of Leak4 is the same as Leak3. However, in Leak4 there is one additional internal duct going through the fire room

which ventilates the target room. The internal duct is a rectangular steel duct of $0.4 \times 0.4 \text{ m}^2$ in area. The height of the duct is 3.5m.

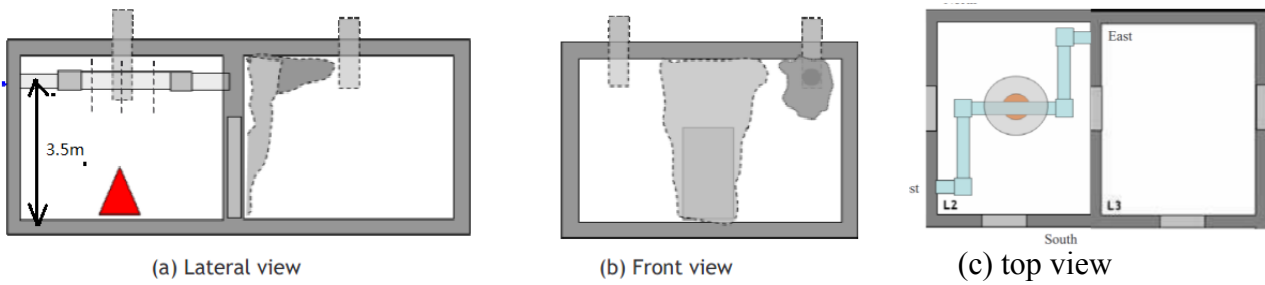


Figure 7 Description of Leak4 scenario

2.2 Model Input

The table below shows the cases that are run by ISIS and Sylvia. Detailed description for the model input is given here only for the Leak1 scenario. For Leak2~Leak4 scenarios, only the difference with Leak1 scenario are mentioned.

Table 3 Overview of simulations

	ISIS	Sylvia
Leak1	ISIS can model leak1. Several simulations are run for this case including sensitivity analysis	Sylvia can model leak1 scenario. Several simulations are run for this case including sensitivity analysis
Leak2	ISIS can model leak2. No sensitivity is made for leak2	Sylvia can model leak2. No sensitivity is made for leak2
Leak3	ISIS is not able to simulate leak3 for the reason that it is unable to model the real firebreak door	Sylvia can model leak3. No sensitivity is made for leak3
Leak4	ISIS is not able to simulate leak4 for the reason that it cannot model the heat transfer to the internal duct	Sylvia can model leak4. No sensitivity is made for leak4

2.2.1 ISIS

2.2.1.1 Version and Platform

Version 3.0.1 [24] of ISIS is used. Openmpi1.4.4 [25] is installed as external library for parallel execution. Metis 4.0.3 [26] is installed as external mesh splitter.

The information for the server on which the simulations are running is as follows:

Server type: Dell PowerEdge 1950

Processor (CPU) : 2x Intel Xeon X5355 Quad-core 2.67GHz

Memory: 32GB (8x 4GB) DDR2 FB 667MHz

Operating system: Scientifix Linux 4.5 64-bit

2.2.1.2 Grid

Both unstructured mesh by gambit and structured mesh are used for simulating Leak1 scenario. However, as ISIS encounters problems when running an unstructured mesh, the gambit mesh is only built for the Leak1 scenario.

The coordinate axes used in both structured and unstructured meshes are the same. The origin locates in the southwest corner of room2 in the floor. The direction of x axis is from west to east. The direction of y axis is from south to north. The direction of z axis is from bottom to up. The direction used in this thesis is depicted in Figure 3.

2.2.1.2.1 Structured Mesh

It is only possible to build a structured mesh for space composed of cuboids, thus the fire pool and leakage pipes are simplified as cuboids although in reality they are cylinders.

The fire pool has a round surface with an inner diameter of 0.874m. In the structured mesh, the fire pool surface is simplified to a square with side length of 0.775m. The side length is chosen as the value so that the surface area is the same as the round face in reality ($S=0.6m^2$).

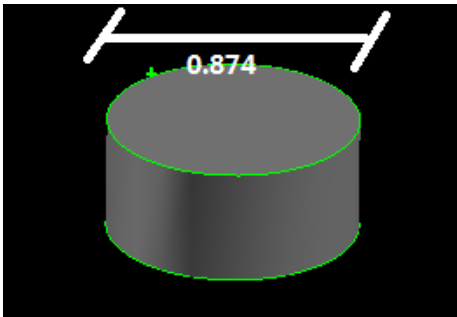


Figure 8 Dimension of fire pool in reality

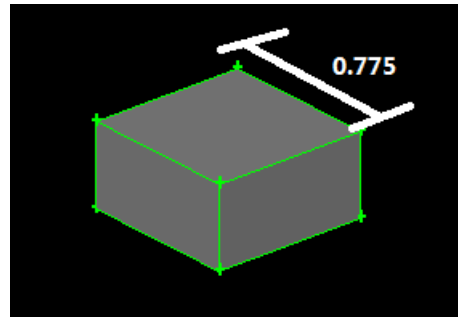


Figure 9 Fire pool in structured mesh

A cuboid with dimension of 0.186*0.186*1.5 m is used to model the leakage pipe, which is in reality a cylinder with inner diameter of 0.21m and length of 1.5m.

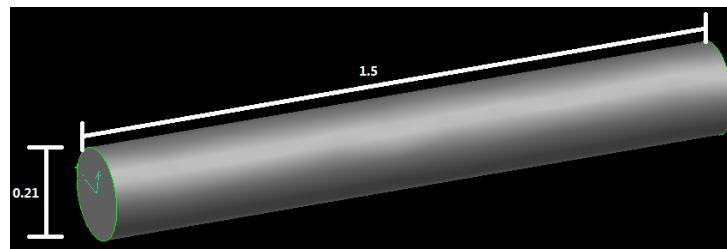


Figure 10 Dimension of leakage pipe in reality

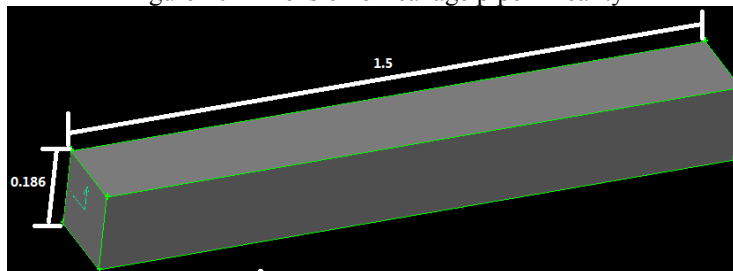


Figure 11 Leak pipe in structured mesh

The ventilation pipes are cuboids thus they are represented as they are.

In ISIS it is only possible to specify boundary condition to faces that are on the boundary of the computational domain. This could cause problems for inner walls of multi-room scenarios. For this reason the cells in the wall between two rooms should be extracted so that the boundary condition can be specified to this wall. As can be seen from Figure 12, all of the cells in the connecting wall are extracted from the computation domain except for the cells in the leakage pipes.

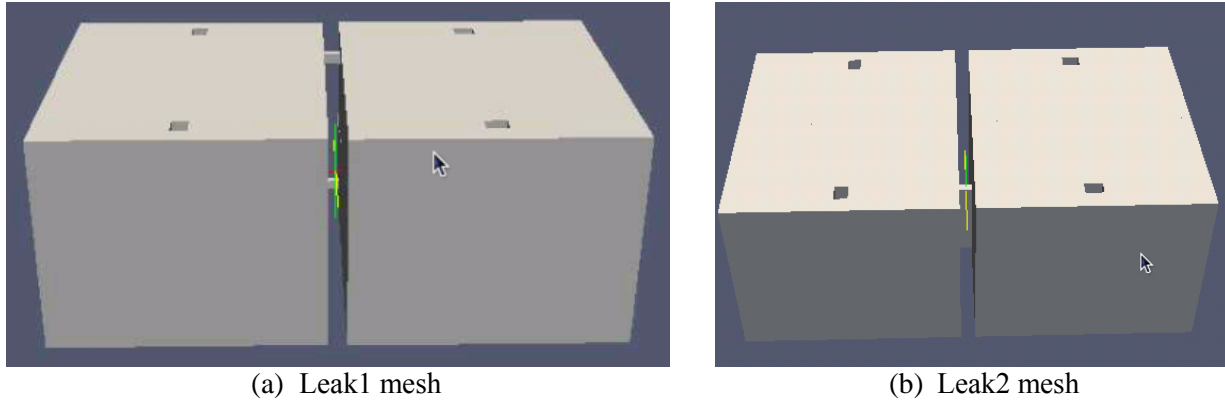


Figure 12 Schematic of the grid

The leakage pipes are 1.5m long, which means that most part of the leakage pipes are immersed inside the rooms. To specify a boundary condition to the pipe walls, one layer of cells around the leakage pipe is also extracted from the computation domain. The picture below shows the extraction in a black color. It is the schema for the cut plane of the x-z plane through the leakpipes. The black color indicates the cells that are being extracted so that boundary conditions can be specified.



Figure 13 Schematic of the extraction of cells for boundary condition

For Leak1, there are 69, 45 and 31 cells along x, y and z axis respectively. The size of the cells is chosen in such a way so that they are as close to 15cm as possible and at the same time any edges of objects in the domain are on the sides of cells. For Leak2, there are 72, 45 and 29 cells along x, y and z axis respectively.

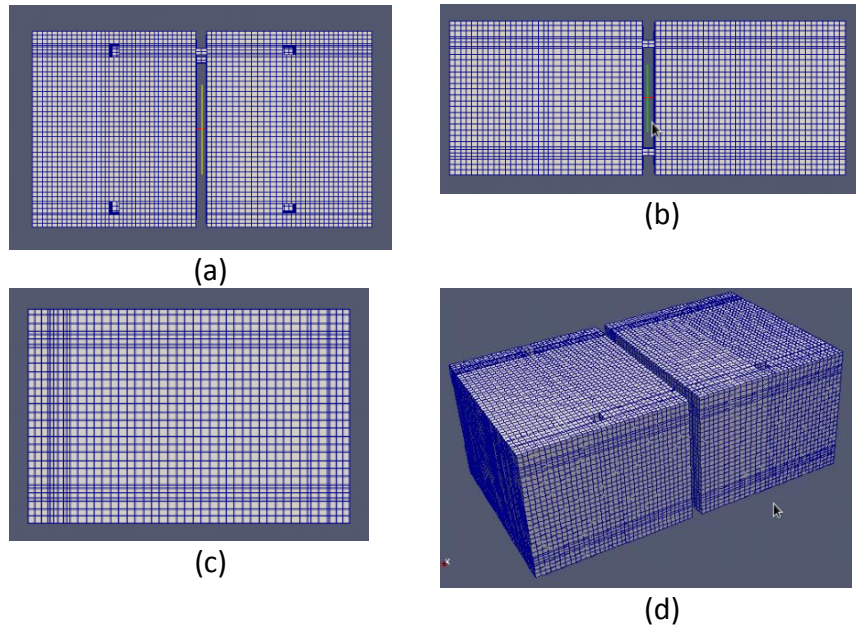


Figure 14 Schematic of the Leak1 grid (a)along +Z axis (b)along +Y axis (c)along +X axis (d)perspective

For further study on the base case, local refinement is executed on the mesh. ISIS is able to define an area where the number of cells can be multiplied by a certain degree, which is determined by the input 'level'. With a higher value of level, a higher level of refinement is obtained. The figure below shows the influence of different value of level.

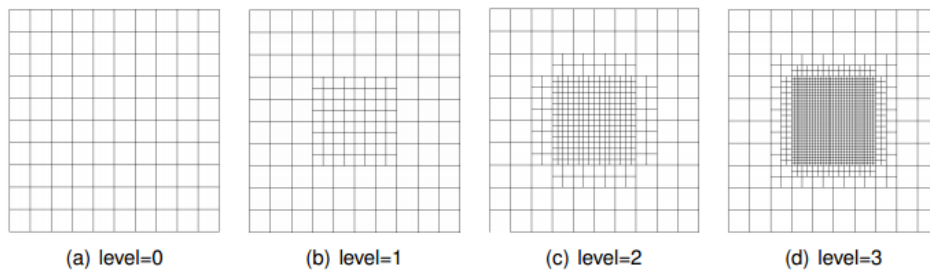


Figure 15 Refinement level influence (Source: [42])

2.2.1.2.2 Unstructured Mesh

From version 3.0.0 on, ISIS is able to support unstructured mesh with limitations. Within this thesis work it is found that ISIS 3.0.0 does not support unstructured mesh containing curved components. A newer version of 3.0.1 was released to solve this problem. Even with the latest eversion, ISIS only supports hexahedron elements. What is more, the simulation results show that key parameters become negative during the process. The values for k , ϵ and fuel mass fraction become negative during the simulation. With all of these problems, unstructured mesh cannot be used to model PRISME projects currently. However, unstructured mesh is still introduced here. It can be useful when further improvement of ISIS is made.

The whole volume is first created in Gambit. The whole volume is then splitted into six parts for meshing. The six parts are upper leakage, lower leakage, transition in the fire room, transition in the target room, the rest of the fire room and the rest of the target room (see Figure 17). The grid size is controlled by ‘interval size’ in the gambit. For the leakage pipes, the interval size is 4cm and for transition the value is 8cm. For the rest of the room the interval size is 15cm. The transition part is there to maintain a smooth transition between fine grid in the leakage pipes and coarse grid in the rooms.

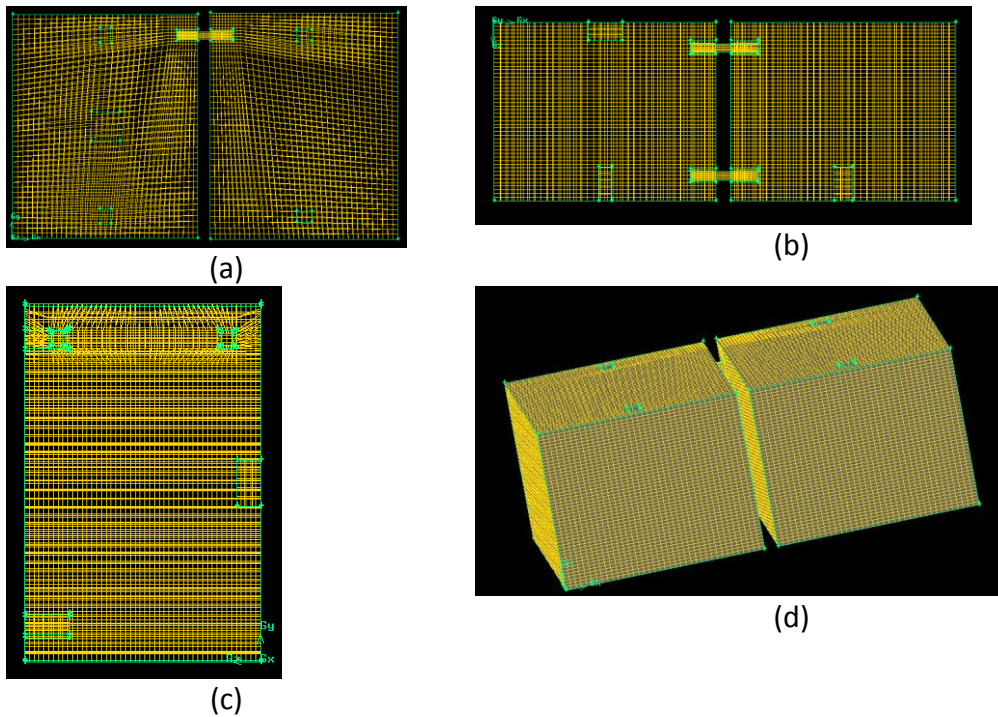


Figure 16 Schematic of the Leak 1 grid by gambit (a)along +Z axis (b)along +Y axis (c)along +X axis (d)perspective

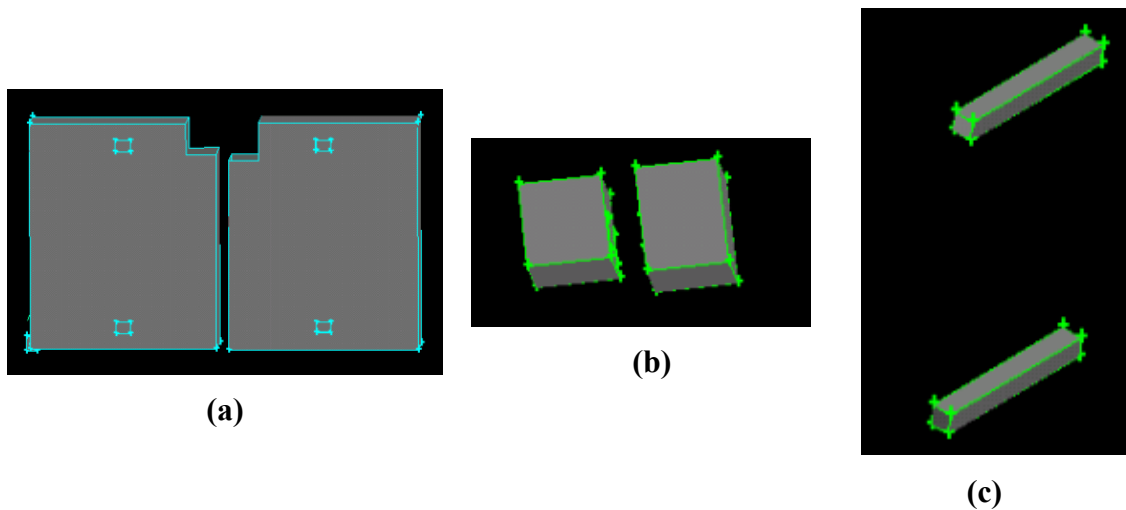


Figure 17 Six parts of mesh (a) the rest of the two rooms (b) transition in both rooms (c) leakage pipes

2.2.1.3 ISIS Input

The values for some key ISIS settings are:

execution_mode	Parallel
geometry	Cartesian_3D
split_on_processors	METIS/coordinate_splitting
near-wall treatment	
♦ type	Log-law
♦ delta	Cell_size
♦ cell_size_fraction	0.25
turbulent production	SGDH

The automatic mesh partitioner METIS which is coupled with ISIS is used in the thesis for a more uniform distribution of cells to different processors. Sensitivity analysis shows that two different mesh split methods do not have significant influence on the simulation results.

For the physical model, the inputs are as follows:

Flow	Navier-Stokes in the low Mach number regime
Turbulence	Standard k-ε model with buoyancy effects
♦ Constants for k-ε transport equation	Default value
♦ Maximal_mixing_length	0.6m
Energy	Enthalpy
Species	Mixture fraction and fuel mass fraction (EBU combustion model)
Radiative heat transfer	Finite Volume Method
♦ Angular discretization	Automatic
♦ Number of subdivision each octant	8
Soot model	
♦ Soot fraction	Fixed_soot_fraction 0.0239

The soot fraction is not given in the PRISME reports directly. The value 0.0239 is calculated from the soot concentration and the mass flow rate in the exhaust branch.

$$m_{soot} = \sum \dot{Q} s_{con}$$

Where m_{soot} is the amount of soot that goes out of the rooms, \dot{Q} is the mass flow rate in the exhaust branch and s_{con} is the soot concentration in the exhaust branches.

In total there is 0.26705kg of soot that is exhausted from the rooms. Assume that 35% of the total soot deposits inside the rooms, the total amount of soot produced is:

$$0.26705/0.65=0.41\text{kg}$$

The weight of the fuel is 17.38 for leak1 case. The soot fraction is thus:

$$\text{soot fraction} = \frac{m_{\text{soot}}}{m_{\text{fuel}}} = \frac{0.41}{17.38} = 0.023$$

The above calculation is based on Leak1 data. For the other scenarios, the soot fractions are calculated by the same method. The results are showed in the table below. The fuel used is Tetra Propylene Hydrogenated, which is a hydrocarbon. Tewarson [11] shows that the soot yield fraction for hydrocarbon is 0.059. The calculated value deviates from the recommended value. However, the final results show that the calculated soot yield fraction shows better agreement with experimental data.

Table 4 Soot fraction of each leak scenario

	Leak1	Leak2	Leak3	Leak4
Soot fraction	0.023	0.021	0.024	0.025

The properties of air are:

Laminar viscosity	Sutherland, $\mu_0 = 1.68 \times 10^{-5}$ Pa.s, $T_0 = 273$ K, $S = 110.5$ K
Specific heat capacity	
Reference temperature	
Turbulent Prandtl	
Density	
Turbulent Schmidt	
Soot absorption coefficient	
Gas absorption	
Gas emmissivity	

The standard gravity field is applied.

The properties of fuel are:

Heat of combustion	$\Delta H_c = 4.55 \times 10^7$ J/kg
Boiling point	

The fuel is treated as dodecane with incomplete combustion: $C_{12}H_{26} + (18.5 - s) O_2 + N_2 \rightarrow 13 H_2O + (12 - s) CO_2 + N_2 + sC$

The value of s is determined by:

$$s = y_s \frac{W_{\text{fuel}}}{W_c} = 0.023 * \frac{170}{12} = 0.33$$

The HRR is calculated for each PRISME tests using oxygen depletion method [18]. It is possible to give HRR as input in ISIS. However in that case, information about gas concentration would be lost. One way to make sure that the HRR is the same in both simulation and test is by using

the calculated heat of combustion. The mass loss rate from the test is used as an input for ISIS. At the same time, the heat of combustion of the fuel is calculated as:

$$\Delta H_c = \frac{\sum HRR\Delta t}{\sum m\Delta t} = 4.55 * 10^7 \text{ J/kg}$$

With the calculated ΔH_c , the HRR of the simulation is the same as that in the test, even though the input for ISIS is through the MLR.

The initial conditions are:

Velocity	0.0 0.0 0.0 m/s
Gas and wall temperature	$T_0 = 300 \text{ K}$
Thermodynamic pressure	$P_0 = 101325 \text{ Pa}$
Turbulence kinetic energy	$k_0 = 1.E-6 \text{ m}^2/\text{s}^2$
Dissipation rate of turbulent	$\varepsilon_0 = 1.E-9 \text{ m}^2/\text{s}^3$
Mixture fraction	0.0
Fuel mass fraction	0.0

The boundaries of the computation domain can be divided into four groups by the type of boundary condition that is applied to them.

Ventilation Openings

The admission openings and exhaust openings of the ventilation branches are specified to the boundary type of ‘pipe_junction’, which represents a confined compartment connected to a ventilation system. A steady Bernoulli equation was solved for each branch of the system. Pressures at the extremity of each branch and the corresponding air flow resistances were deduced from the experimental data at steady state before ignition. The external pressure and resistance for each of the ventilation openings is as follows:

Table 5 External pressure and resistance

	External relative pressure(Pa)	Resistance (m^{-1})
Admission(fire room)	495	2107
Exhaust(fire room)	-902	2501
Admission(target room)	504	50852
Exhaust(target room)	-900	64437

In all PRISME leak scenarios, a steady state is reached before ignition. The steady state here means that before ignition the pressure and flow rate of the whole ventilation system remains constant. The measured relative pressure in the ventilation branches in this steady state is used to determined ‘external relative pressure’.

The resistance is calculated by:

$$R = \frac{\Delta P}{Q^2 \rho}$$

Where Q is the volume flow rate, ΔP the pressure difference between the opening external pressure and room pressure, and ρ the density of air.

The properties of the air coming from the ventilation openings are:

Mixture fraction	0
Fuel_mass_fraction	0
Radiative intensity	Incoming radiation
Turbulence intensity	0.01
Mixing length scale	0.03m ¹
temperature	298.15K

Walls

Convective heat transfer between the rooms and the boundary in this group is calculated by wall-law. The laminar prandtl is 0.7 and turbulent prandtl 0.7.

As for radiative heat transfer, the walls are treated as gray surface in this group. The emissivity of the surfaces is 0.95 for THERMIPAN and 0.7 for concrete.

The heat transfer inside the walls is calculated by conduction. The thermal properties of the wall materials (thermapian or concrete) are such as stated in [20]. A mesh is specified to the surfaces for conduction calculation.

The boundary condition with the external is assumed to be adiabatic.

Ceiling, floor, insulation walls in the fire room and concrete walls in the target room are specified with this kind of boundary condition.

Adiabatic Walls

The ventilation branches, the fire pool surfaces other than the fuel surface and the leakage pipes are modeled as adiabatic walls.

Fire Pool

At the pool surface, 'fixed_mass_flow_rate' condition is imposed. The mass flow rate data comes from the test measurements. *Fuel mass fraction* and *mixture fraction* are set as:

$$\begin{cases} 1 & \dot{m}(t) > 0 \\ 0 & \dot{m}(t) \leq 0 \end{cases}$$

The properties for the fuel inflow are:

¹ With the knowledge of u_{inlet} , i , and l , the k_{inlet} and ϵ_{inlet} is fixed (see [13])

density	4.49kg/m^3 $1.E-5\text{ m}^2/\text{s}^2$ $\varepsilon_{\text{pool}}= 1.E-9\text{ m}^2/\text{s}$ 461K
Turbulence kinetic energy	
Dissipation rate of turbulent kinetic energy	
temperature	

As for the radiation heat transfer, the fire pool surface is modeled as gray surface with emissivity of 1 and surface temperature of 461K.

2.2.2 Sylvia

2.2.2.1 Version and Platform

Sylvia 1.5.0 is used for this thesis.

The information of the computer on which simulations ran is:

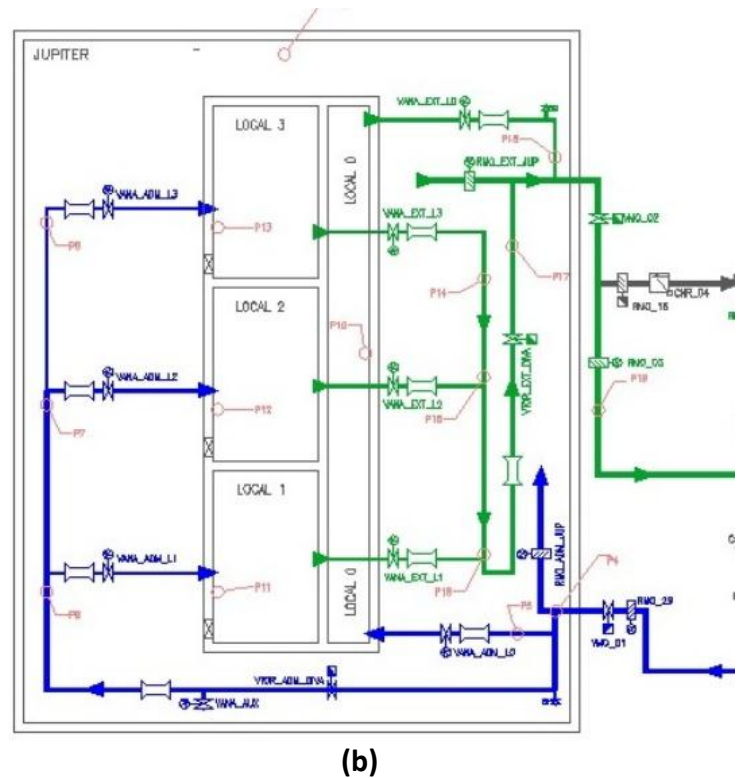
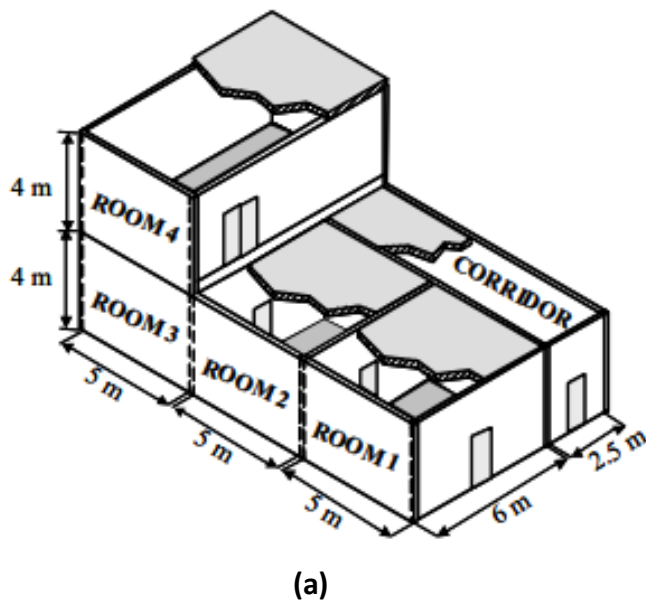
Operation system: Microsoft Windows XP, Service Pack 3

Processor: Intel(R) Core™2 Quad CPU Q9550 @2.83GHz 2.83GHz

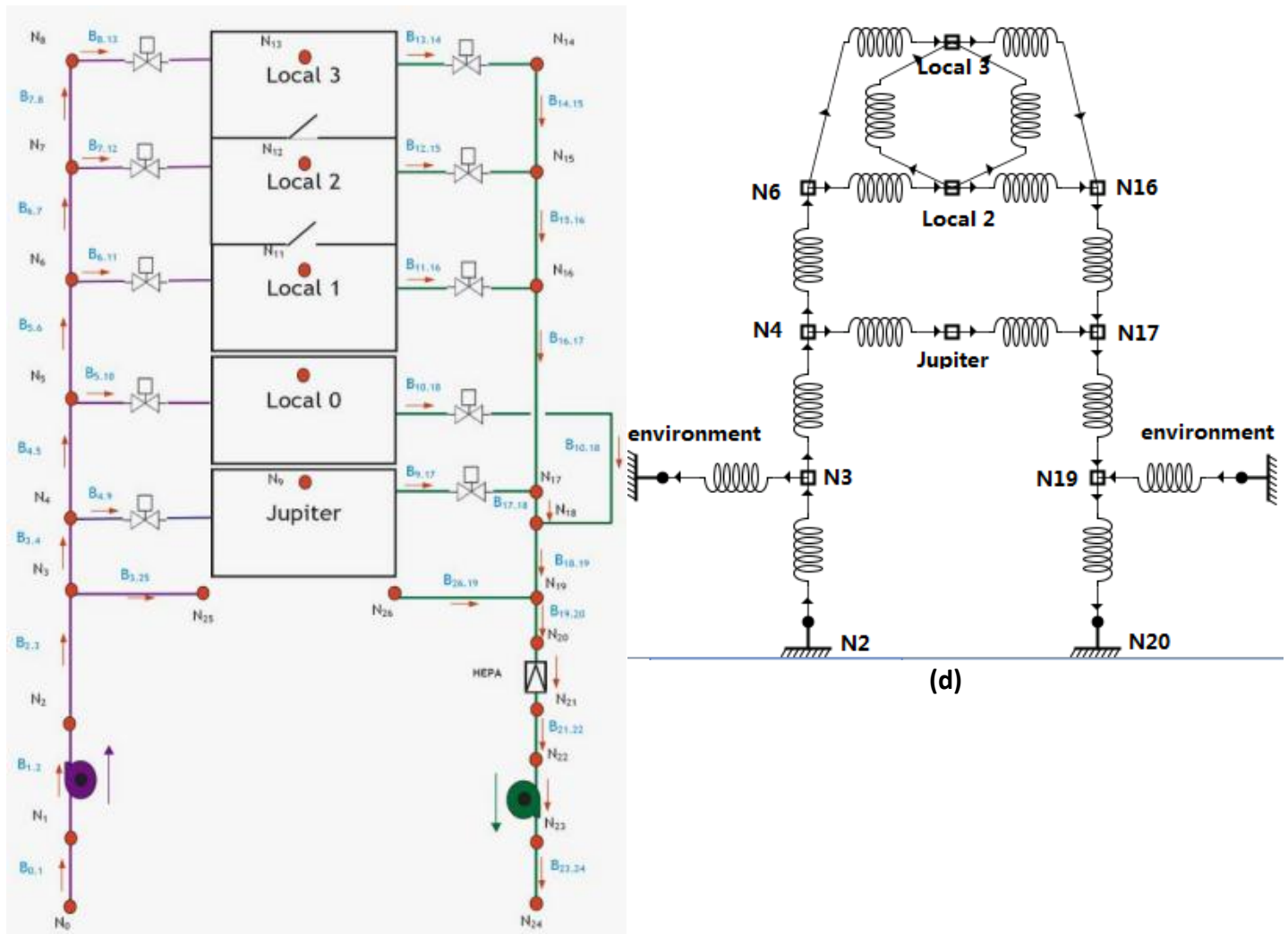
Memory: 3.21GB of RAM

2.2.2.2 General Information

Sylvia is a two zone model which predicts ventilation quite well. As a two zone model, it is possible to include all the DIVA rooms in the simulation. The figure below shows the hierarchy of abstraction of the DIVA facility to the set up in the SYLVIA.



² For k and ε , the recommended values of the PRISME Source validation case as described in [12] were used.



(c)

(d)

Figure 18 Hierarchy of the abstraction of the DIVA facility to the Sylvia input. (a)DIVA facility (b)ventilation network of DIVA (c) abstraction of ventilation network(d) Sylvia input

2.2.2.3 Element List

In SYLVIA all components of a scenario are represented by ‘element’.

□ stands for a ‘zone’, which can be either one zone or two zone space. In the thesis, the fire room and the target room are two zone spaces. All the other rooms are represented as one zone spaces.

The conjunction of ventilation pipes is also represented by this kind of element.

Initial pressure values need to be imposed on the ‘zone’ elements. The steady state pressure value before ignition is used.



stands for branches with quadratic resistance. All of the ventilation pipes and leakage pipes are represented by this kind of element.

The mass flow rate through the branch is calculated by SYLVIA with:

$$Q = \sqrt{\frac{\Delta P \cdot \rho}{R}}$$

Where Q is the mass flow rate, ΔP the pressure difference between the opening external pressure and room pressure, and R the resistance of the branch.

The resistance of the branches is calculated automatically by SYLVIA with the initial pressure difference and initial flow rate that are imposed to the branch element.



stands for node with imposed pressure, temperature and species. It is assumed that the pressure just after the admission fan and before the exhaust fan is constant along the test. These two positions are thus represented by this element. The whole network contains two connections to the atmosphere, which is also represented by this element.

‘wall’ element, ‘BC_TARGET’ element and ‘pool’ element are not showed in the graphical representation of the model (Figure 10 (d)). In SYLVIA ‘wall’ element still needs to be created and attached to ‘zone’ element. ‘BC_TARGET’ element is used when detailed information such as flux value is required for certain location.

In the ‘pool’ element, the mass loss rate of fuel is specified. The data from the test is used as input.

2.2.2.4 Exchange List

Heat transfer between two elements needs to be specified in the exchange list of SYLVIA.

For radiation heat transfer, the radiative property of the soot-gases mixture is calculated by [39]:

$$\epsilon_{G+Soot} = \epsilon_G + \epsilon_{Soot} - \epsilon_G \epsilon_{Soot}$$

For each of the species, the models used to calculate emissivity are:

soot	Sarovim [27]
CO₂	Viskanta [28]
O₂	Viskanta [28]

The only two gray gases SYLVIA accounts for are H₂O and CO₂.

For convective heat transfer, the convection coefficient is calculated by the natural convection correlation [29].

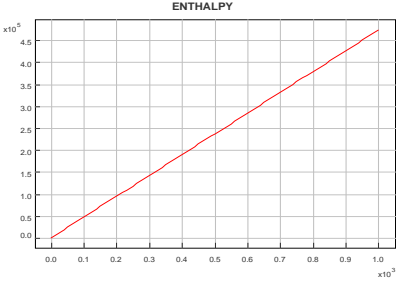
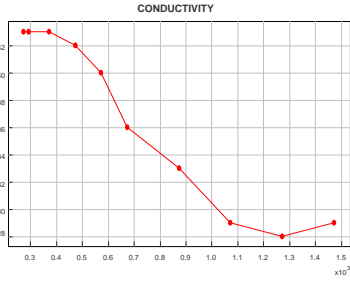
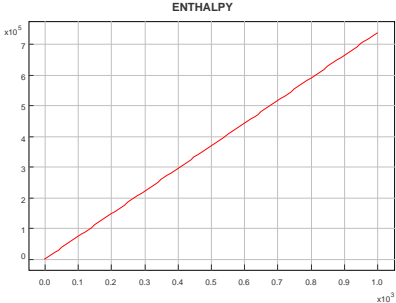
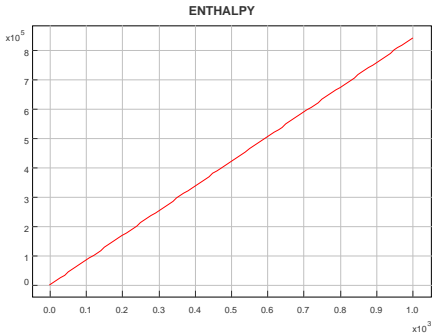
As the properties of the walls need to be specified in the elements list, nothing more has to be specified for conduction heat transfer in this part.

2.2.2.5 Material/Species List

The properties of the material and species are specified in this group.

Concrete, rockwool and blackbody are the three materials used in this scenario. Their properties are as follows [20] :

Table 6 Material properties input

	Enthalpy(J/Kg)	Conductivity(W/mK)	emissivity
	Type: polynom	Type: tabulation	
Black body			1
Concrete	Type: polynom 	Constant: 1.5 W/mK	0.7
rockwool	Type: polynom 	Constant: 0.102 W/mK	0.95

In the species list, the properties of the gases and soot are specified. The properties of H₂O, CO₂, CO and N₂ are not case dependent, thus detail about them are not described here.

For TPH, the fuel, some of its key inputs are:

Oxidant yield	3.4202 kg/kg
Heat of combustion	4.55E07 J/kg
Yield	
♦ CO ₂	3.02 kg/kg
♦ CO	0.006 kg/kg
♦ H ₂ O	1.37647 kg/kg
♦ Soot	0.023 kg/kg

The density of the soot is 1800kg/m³.

2.1.1.1 Other Inputs

Reference values for network buildup:

Time	Pressure	101325 Pa
	density	1.177 kg/m ³
	Begin time	-300s
	End time	1500s

The initial pressure and flow rate imposed are indeed not in balance because of measurement errors. SYLVIA needs several calculation cycles to build up a steady state. For that reason begin time is 300 seconds ahead of ignition so that steady state can be achieved in SYLVIA before ignition.

3. UNCERTAINTY

3.1 Introduction

Uncertainties must be investigated within the validation process. Uncertainties come from different sources.

The measurement uncertainty is the uncertainty associated with the measurement devices in the different experiments. Each device or method has its accuracy level. For the PRIMSE project, the measurement uncertainty is provided in the deliverables.

The model uses the HRR/MLR data as an input for simulation. The HRR/MLR data are also an experimental measurement, which inevitable includes certain amount of uncertainty. The uncertainty of the input value will result in the uncertainty of the output data. The degree of uncertainty of the output data caused by the input uncertainty can be calculated by analytic analysis. Chapter 4 of NUREG 1934 [17] provides detailed information about calculation of the model uncertainty.

Typically, it is possible to provide rational estimates of the experimental measurement uncertainty and the experimental model input uncertainty. Both are related to measurements. Another type of uncertainty, the model intrinsic uncertainty, is far more difficult to quantify.

The measurement uncertainty and model input uncertainty can be treated together as combined uncertainty. The combined uncertainty is then used as the criteria to judge the performance of fire codes. The method to calculate the combined uncertainty is described in Chapter1 of Volume 2 of NUREG 1824 [14]. The same method would be followed in this thesis.

3.2 Measurement Uncertainty

The deliverables for the Leak Tests of PRISME do not contain explicated and direct assessment of the measurement uncertainty. However, the measurement uncertainty assessment is given in the Door Test of PRISME. Given that the facilities used in these two tests are similar to each other and that it is the same group of persons that conducted the tests, the measurement uncertainty from Door Test is used to evaluate the data from Leak Test.

Table 7 Experimental measurement uncertainty (Source: [15])

Measurement	Range	Standard absolute or relative uncertainty $\pm u_s$	Coverage factor	Expanded absolute or relative uncertainty $\pm u_e$
Pressures P_Li_MIC (i = 1,2,3)	[-200 ; +200] Pa	2Pa	2	4Pa
Pressures P_Li_MIN (i = 1,2,3)	[-2500 ; +2500] Pa	4Pa	2	8Pa
Pressures P_Li_MOY (i = 1,2,3)	[-7000 ; +10000] Pa	11Pa	2	22Pa
O ₂ concentrations	[0 ; 25] %v	0.3 %	3	1 %
CO concentrations	[0 ; 5000] ppm or [0 ; 2500] ppm	1.6 %	3	5 %
CO ₂ concentrations	[0 ; 10] %v or [0 ; 20] %v	2 %	-	2 %
THC concentrations	[0 ; 1000] ppm	1 %	5	5 %
Temperatures (K type) in hot sooty zone and near the flame	[0-1300] °C	-	-	8%
Temperatures (K type) in cold slightly sooty zone near the flame	[0-1300] °C	-	-	15 %
Temperatures (K type) out of the flame radiations	[0-1300] °C	1 %	3	3 %
Total heat fluxes on the walls	[0-10000] W/m ²	3 %	3	10 %
Radiant fluxes	[0-2000] W/m ² [0-5000] W/m ² [0-10000] W/m ²	15 %	2	30 %
Soot concentrations	-	-	-	30 %
Mass	[0-300] kg	0.015 kg	1	0.015 kg
Flow rates in DIVA ventilation network	Q > 180m ³ .h ⁻¹	u _s (Q)/Q < 5 %	2	u _e (Q)/Q < 10 %
	110m ³ .h ⁻¹ < Q < 180m ³ .h ⁻¹	5 % < u _s (Q)/Q < 10 %		10% < u _e (Q)/Q < 20 %
	60m ³ .h ⁻¹ < Q < 110m ³ .h ⁻¹	10 % < u _s (Q)/Q < 25 %		20% < u _e (Q)/Q < 50 %

3.3 Model Input Uncertainty

Model input uncertainty is associated with parameters derived from experimental measurements that are used as model input. The most influential input is the HRR for most of the outputs.

The uncertainty for the HRR measurement is not given in the deliverables of PRISME LEAK tests. However, the measurement uncertainty for HRR is given as 20% in [30] for PRISME source tests. Suggestions for reducing the HRR measurement uncertainty are also given, thus a 15% value is estimated for the Leak tests. With a 15% uncertainty in the HRR, expanded uncertainty for each of the parameters can be calculated by the way stated in NUREG-1824 [14].

Table 8 Model input uncertainty (Adopted and adjusted from [14])

Quantity	Input Parameter	Power Dependence	Expanded Uncertainty
HGL Temperature	\dot{Q}	2/3	10
HGL Depth	\dot{Q}, A, H	$\frac{L}{D} = 3.7 \dot{Q}^{2/5} - 1.02$; $\dot{Q}^* = \frac{\dot{Q}}{\rho_\infty c_p T_\infty \sqrt{g D D^2}}$	-1
Plume Temperature	\dot{Q}	2/5 1.3 < z/D* < 3.3	6
		2/3 3.3 < z/D*	10

Quantity	Input Parameter	Power Dependence	Expanded Uncertainty
Gas Concentrations	\dot{Q}	1/2	8
Smoke Concentration	\dot{Q}, y_s	$\frac{\delta M_s}{M_s} = [2/3 \frac{T_\infty}{T_g} - 1/6] \frac{\delta \dot{Q}}{\dot{Q}} + \frac{\delta y_s}{y_s}$	18
Pressure	$\dot{Q}, A_{leak}, \dot{V}_{vent}$	2,2,2	No forced ventilation: 30 With ventilation: 75
Heat Flux	\dot{Q}, χ_{rac}	Fire: $\frac{\delta \dot{q}''}{\dot{q}''} = \frac{\delta \dot{Q}}{\dot{Q}} + \frac{\delta x_{rad}}{x_{rad}} - 2 \frac{\delta r}{r}$	22
		Upper layer: $\frac{\delta \dot{q}''}{\dot{q}''} = 4 \frac{\delta T_g}{T_g} = 8/3 \frac{\delta \dot{Q}}{\dot{Q}} (1 - \frac{T_\infty}{T_g})$	15
Surface Temperature	\dot{Q}	2/3	10

3.4 Combined Uncertainty

With the information on measurement uncertainty and model input uncertainty, the combined uncertainty can be calculated by formula:

$$U_\varepsilon \approx (U_M + U_E)^{1/2}$$

The result is showed in the table below:

Table 9 Combined uncertainty

Quality	Measurement uncertainty(U_E)	Model input uncertainty(U_M)	Combined uncertainty
Radiative Heat flux	30%	22%	37%
Wall temperature	3%	10%	11%
Floor temperature of fire room	15%	10%	18%
Soot concentration	30%	18%	35%
CO2 concentration	2%	8%	8%
O2 concentration	1%	8%	8%
pressure	1%	75%	75%
Flow rate	10%	10%	14%
Gas temperature in the fire room	8%	10%	13%
Gas temperature in the target room	3%	10%	11%
HGL temperature/depth ³	-	-	13%

³ The combined uncertainty for HGL is taken as the same as NUREG report [16] as there is no information given in the PRISME reports regarding to its uncertainty.

3.5 Application of Combined Uncertainty

3.5.1 Single point comparison

The measured and predicted values are compared in terms of combined uncertainty. The graph below shows this strategy. If the models and experiments were in perfect agreement, the data points would fall along the 45 degree line indicated in the graph. The data in the left picture are such that the models are in agreement with the experiments within the bounds of the combined uncertainties. In contrast, the right picture shows data in which the models and experiments are not in agreement within the bound of the combined uncertainties.

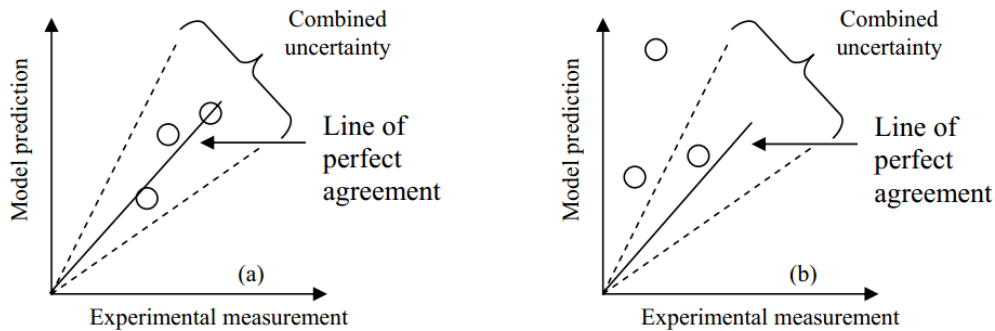


Figure 19 Scatter plots depicting validation results in and out of the range of combined uncertainty (original source: Figure 2-10 of NUREG 1824[34])

This approach is in fact comparing the “relative difference” between the measured and predicted values with the combined uncertainty. The relative difference is defined as the following equation:

$$\varepsilon = \frac{\Delta M - \Delta E}{\Delta E} = \frac{(M_p - M_o) - (E_p - E_o)}{(E_p - E_o)}$$

Where ΔM is the difference between peak value of the model prediction and the ambient value, and ΔE is the difference between the experimental observation and the ambient value.

Combined uncertainty, U_ε , can be calculated by [14]:

$$U_\varepsilon \approx (U_M + U_E)^{1/2}$$

It has been demonstrated [14] that, if $|\varepsilon| < U_\varepsilon$, the variation between simulation and test results can be explained by the uncertainties. In other word, the simulation tool is reliable within the uncertainty level. In this thesis, this criterion is used to determine the capability of fire models in predicting the fire attributes.

3.5.2 Time-dependent Variants Comparison

The aforementioned criterion only deals with local point data, that is, max/min value through the fire scenario. However, single point information alone cannot provide full information in safety perspective. The time of the max/min point and the shape of the curve are just as important in some scenarios [31].

For time-dependent variants, the “relative difference” can be defined as :

$$\varepsilon = \frac{\|\vec{E} - \vec{m}\|}{\|\vec{E}\|}$$

Where \vec{E} is the experimental data vector, and \vec{m} is the model data vector. Several different definition of norm can be utilized here. Euclidean, Hellinger, Secant and Hybrid inner product and norm have been used by BONTE [23] and L. Audouin [31] to analysis time-dependent variance. They each provide one aspect of the information for the vectors. For example, the Hellinger norm can provide a sensitive measure of comparison of the shape of two vectors and Secand norm large-scale differences between vectors.

There are no rigor criteria for assessing the agreement between a model vector and an experiment vector. Beside, there is lack of information regarding to how the discrepancy between time-dependent variables would affect the target. However, the information from time-dependent variables can be at least utilized as a criterion for comparing the closeness of the curve shape from simulation with that of experiments for different fire models. Consequently, one is not able to say how good the model result is regarding to the shape of curve in a quantified manner. However one is at least able to say that model A is better than model B in predicting the shape of certain parameter. More effort should be made to make a better use of the vector information. This needs more research and could be one possible future R&D work for Bel V.

4. RESULTS

4.1 Results Presenting Methodology

Results of this thesis are presented in two ways.

Firstly they are presented in the form of relative differences between fire model predictions and experimental data for attributes such as gas temperature that are important to NPP fire modeling applications. While the relative differences show agreement in some cases, they show both under-prediction and over-prediction in other cases. These relative differences are determined jointly by the capabilities of the fire models, the availability of reliable experimental data, and the experimental uncertainty of these data. Based on those relative differences, judgments are made on the two fire models' capability to predict attributes important to NPP fire modeling applications.

The results are also analyzed by presenting attribute-time curves of both fire models predictions and experimental data. Although the relative differences alone could lead to conclusion regarding to fire models' capability to predict certain attributes, the time curve could provide readers with more detailed information for each attributes. Explanations are given for the deviation of the models' predictions from experimental data. Besides, relative difference does not include any information for time, which also plays an important role in NPP fire scenarios [23]. The time curves could provide an intuitive overview of the time factors.

4.2 ISIS

There are four leak scenarios within the PRISME project. ISIS is not capable to simulate a real fire-broken door as a leakage route, thus is unable to model leak3 and leak4 scenarios.

Relative differences from all available simulation results will be presented together. The idea is to make judgment of the model's capability based on a range of different scenarios instead only one specific case. The criterion for judgment of the capability of ISIS in predicting fire attributes is by comparing relative difference against combined uncertainty [14].

$$|\varepsilon| < U_\varepsilon$$

Where $|\varepsilon|$ is the relative difference and U_ε the combined uncertainty.

Detailed attribute-time curve and explanation for deviations are provided here for leak1 scenario. Some of the weakness and incapability of ISIS are revealed during the simulation process.

4.2.1 Relative Difference

The numerical comparison between an experimental observation and a corresponding model prediction is referred to as "relative difference". Relative differences have been calculated for each of the attributes listed in Section 5.1 using point estimate peak values from fire experiments

and model predictions. The following equation[34], which is described in chapter 2, has been selected for relative difference calculations

$$\varepsilon = \frac{\Delta M - \Delta E}{\Delta E} = \frac{(M_p - M_o) - (E_p - E_o)}{(E_p - E_o)}$$

where ΔM is the difference between the peak value (M_p) of the model prediction and the ambient value (M_o), and ΔE is the difference between the experimental observation (E_p) and the ambient value (E_o). In the context of this study, for the parameters Oxygen Concentration and HGL Height, the “peak” value is actually the minimum value.

Radiative Heat Flux

Radiative heat flux measurements are available from PRISME Leak scenarios. The figures below summarize the relative differences for the radiative heat flux predictions.

The radiative heat flux predictions by the ISIS are indeed the net radiative heat flux between the environment and the walls, which are at high temperature during the test. While in the experiment, the radiative heat flux is measured by radiometer with a water cooling device. As a result, the radiative heat flux from model prediction and experimental data are indeed two different attributes in principle. ISIS under-predicts all radiative heat flux for this reason.

However, it is possible to make an adjustment to the ISIS predictions. Readers are referred to section 4.2.2 for detailed description on this adjustment. The relative differences for the adjusted radiative heat flux are also presented in the figures below. The relative differences all fall within combined uncertainty. With proper adjustment, ISIS can predict the radiative heat flux satisfactory.

In real applications the heat flux to a target is the most significant value. In that sense, ISIS can provide prediction directly.

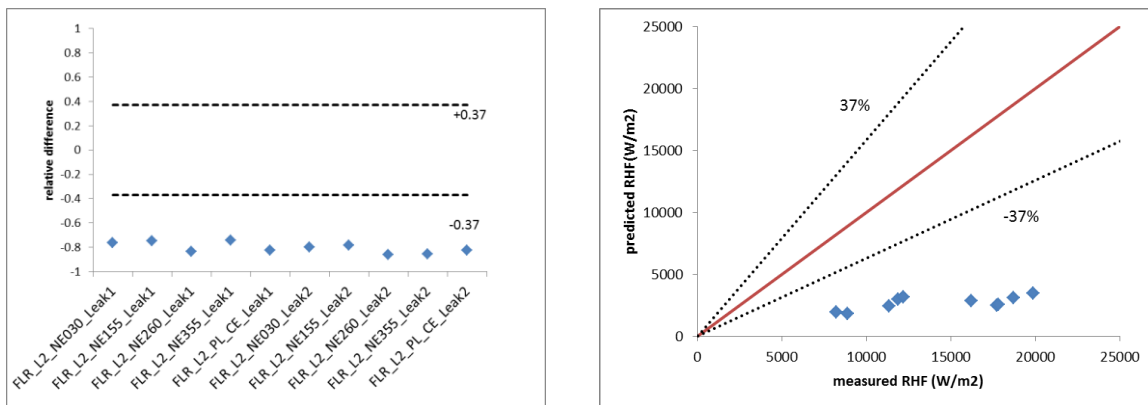


Figure 20 Summary of prediction of radiative heat flux

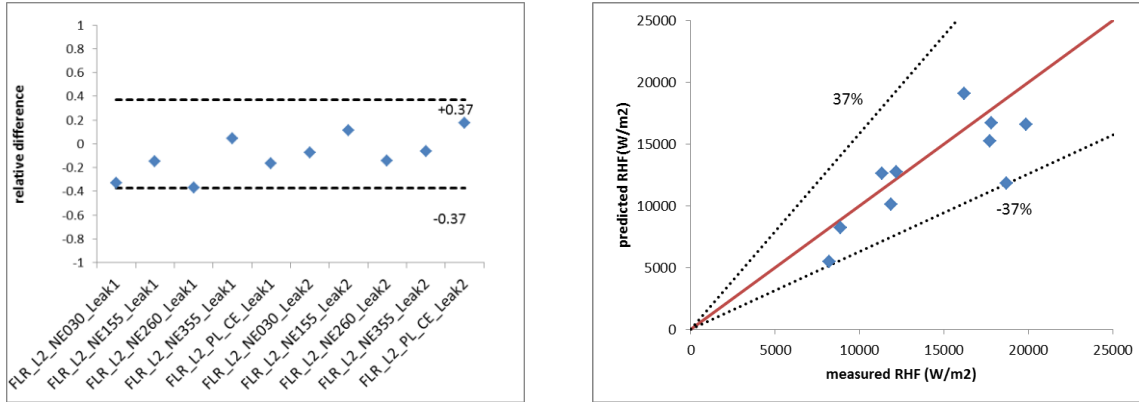


Figure 21 Summary of prediction of radiative heat flux (adjusted value)

Wall Temperature

Wall surface temperature measurements are available from PRISME Leak scenarios for several points in the north wall and also one point on the floor.

The walls and ceiling of experimental rooms were insulated with THERMIPAN to create higher temperature inside the fire room [36]. Also with insulation, there could be more intensive heat attack on the target room. There are two layers of two different materials for the boundary condition. The duration for the fires is around 1200s for PRISME Leak tests. The thermal penetration depth in the THERMIPAN during the test is [42]:

$$2\sqrt{\alpha t} = 2\sqrt{8.67 * 10^{-7} * 1200} = 0.065m$$

Where α is the thermal diffusivity of the THERMIPAN (m^2/s), t the time.

The thickness of the THERMIPAN is 0.03m for the wall and 0.05m for the ceiling. They are both less than the thermal penetration depth, which means that the insulation layer is thermal thin during the later period of the fire. It is thus necessary to specify a multilayer boundary condition, which is beyond the capability of ISIS.

Besides, the thermocouples on the surface of insulation were damaged because of the high fire intensity. The available wall temperature measurements in the fire room are between the concrete wall and the insulation. Thus the wall temperature results are analyzed in two groups. The first group is for the temperature between two layers in the fire room (with THERMIPAN insulation). The other group is for temperature in the other positions (without THERMIPAN insulation).

ISIS overpredicts the temperature in the first group to great extent. The relative difference can be as high as 30%. However, the temperature measurement points are different in test and simulation. The large difference here does not prove that ISIS is bad at predicting wall temperature. Instead, the weakness of ISIS in modeling multi-layer boundary condition is revealed. However, if the duration of fire is relative short and in that case the the first layer can be treated as thermal thick. It is valid to just model one layer material in that case.

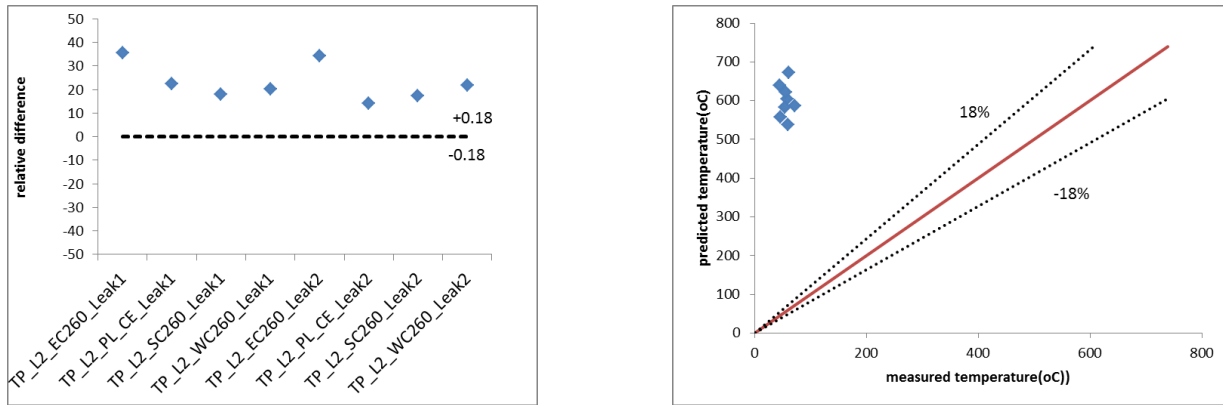


Figure 22 Wall temperature in the fire room

The figure below shows the relative differences of the wall and floor temperature in the target room, where there is no insulation. In this situation, ISIS prediction of wall temperature is quite satisfactory. As the temperature rise in the target room is relatively small, the relative difference becomes quite large, even with a small amount of deviation. Besides, the figure shows a trend of overprediction of wall temperature. However, the boundary condition specified to the ISIS models would in fact reduce the heat loss through walls, and thus enhance both the wall temperature and gas temperature.

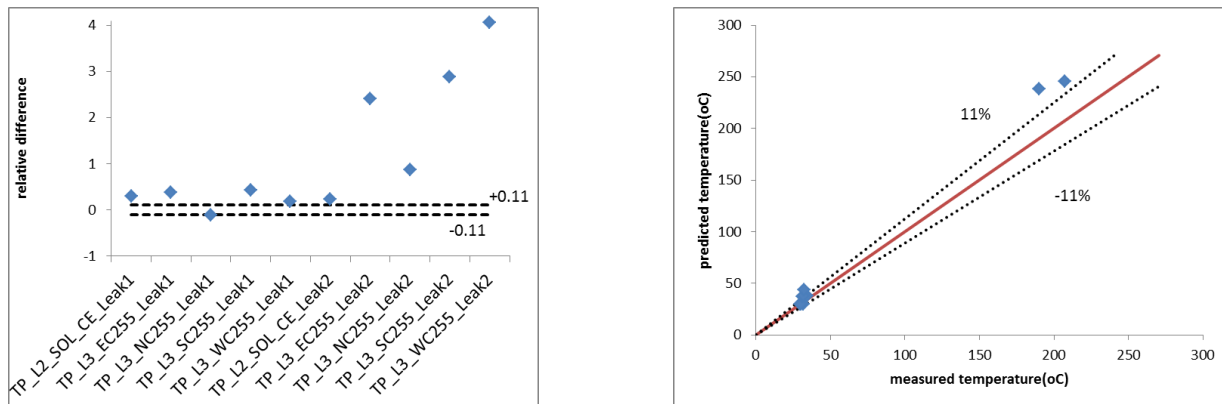


Figure 23 Wall temperature in the target room and floor temperature

The wall temperature prediction from ISIS can be utilized in real application even though some of the relative differences are beyond combined uncertainty.

The wall temperature prediction, however, is not reliable while the boundary is multilayered. Suggestion is given to the ISIS develop group to improve the ISIS's ability to model multilayer condition.

Soot Concentration

Soot concentration of the exhausted gas from both rooms is available from PRISME leak scenarios. The most important input parameter for the soot concentration is 'soot yield fraction'. The soot yield fraction input for ISIS is calculated based on the test data. SFPE also provides

soot yield fraction data for hydrocarbon, which is 0.059 [11]. Sensitivity analysis shows that the soot yield fraction influence the soot concentration result greatly. For real application of ISIS there is no test data for soot yield fraction. Thus although ISIS provides good prediction of soot concentration in this thesis, it does not guarantee as good prediction in real application where there is no test data to determine the soot yield fraction.

One possible way to solve the problem with soot yield fraction is using Moss Model [32][33] for soot production. The Moss model is a two equations model which takes into account the processes of nucleation, surface growth and coagulation. The soot yield fraction can be calculated by this model. The Moss Model for soot production has not been utilized in this thesis because of lack of time. This can be one future R&D work for Bel V.

However, the soot concentration prediction in the target room is much higher than experimental data. ISIS is able to predict the soot concentration in the fire room correctly but not in the target room.

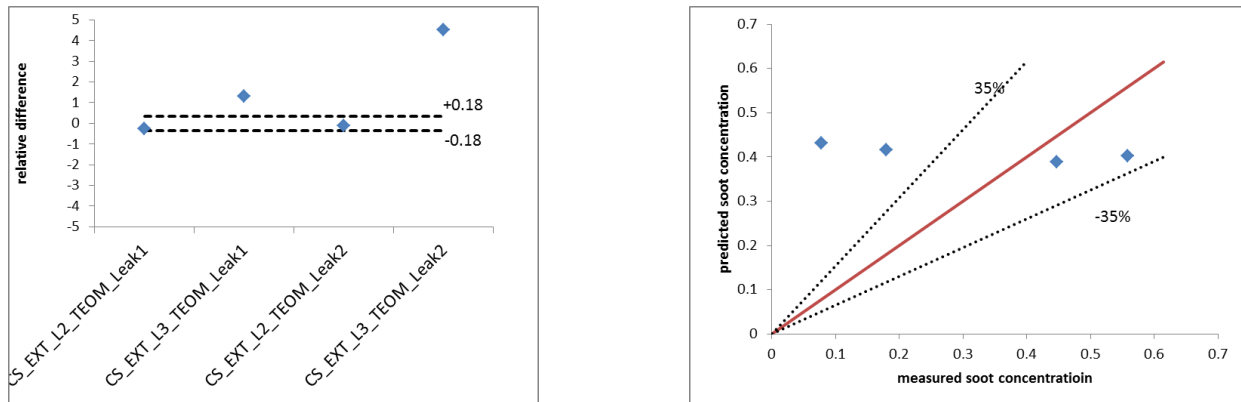


Figure 24 Soot concentration

Oxygen Concentration and Carbon Dioxide Concentration

ISIS uses a mixture fraction combustion model [6], meaning that the concentrations of all of the major gas species are related to a single scalar variable for which a single transport equation is solved. Assuming that the basic stoichiometry of the combustion process is known, predicting oxygen and carbon dioxide concentrations is similar, mathematically, to predicting temperatures. Gas sampling data is available from PRISME leak scenarios.

The figures below show the relative differences for oxygen and carbon dioxide concentration. These two gas species show similar behavior. In general, the gas concentration predictions in the fire room by ISIS are satisfactory. However, for both gases the concentration in the target room is overpredicted. The accurate prediction in the fire room shows that ISIS is reliable in calculating the combustion products. The overpredictions in the target room, however, show that the simulation of leakage is not perfect.

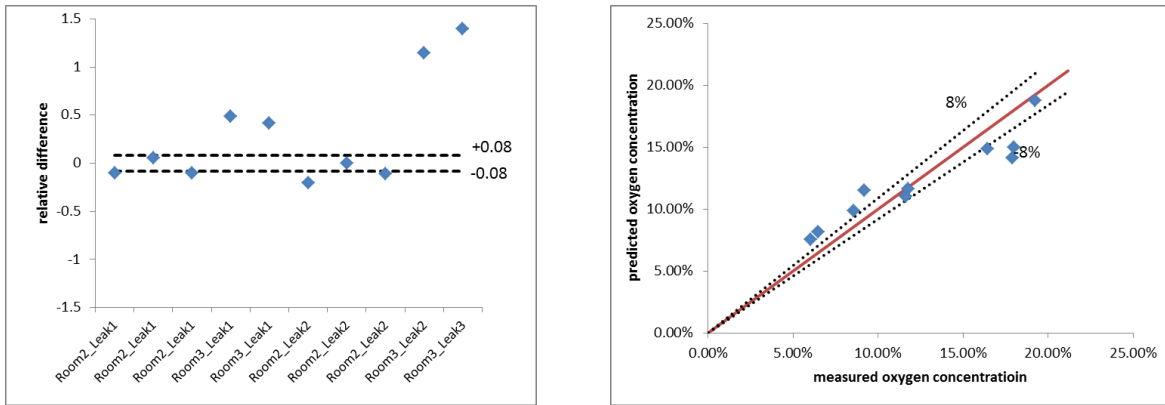


Figure 25 Oxygen concentration

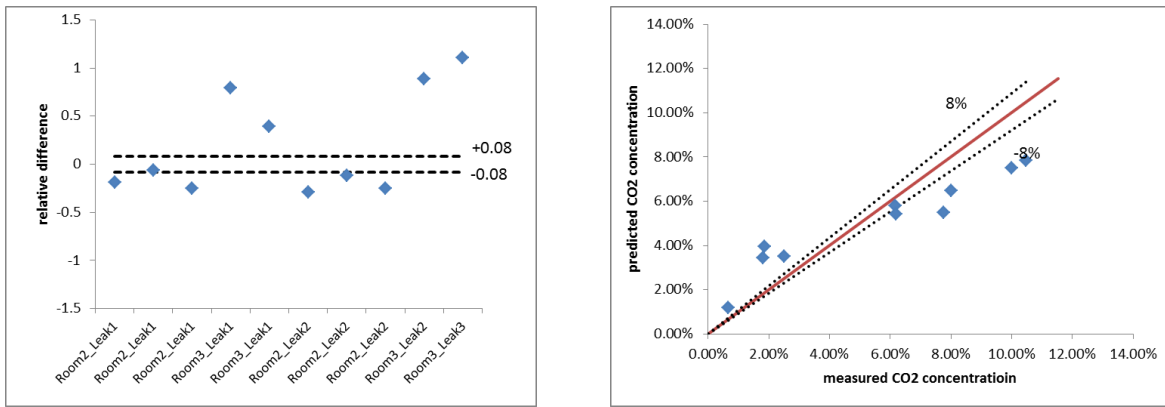


Figure 26 CO₂ concentration

Pressure

Total relative pressure measurements are available in both rooms for PRISME leak scenarios. However, the predictions of the relative pressure are absurdly wrong and are thus not presented here. Detailed pressure-time curve is given for Leak1 in the next section.

Leakage Flow Rate

The flow rate from the fire room to the target room by leakage is an key attribute for PRISME Leak Scenarios. However, the leakage flow rate measurement is only available for Leak1 scenario, where two circular pipes were used as leak route. Although it is the total flow from the fire room to the target room that determines the thermal response in the target room, here the local maximum flow rate is compared for the consistence of the methodology.

The figure below shows the relative differences of the leak flow rate. ISIS predicts the leak flow rate quite well. The relative differences fall within the combined uncertainty.

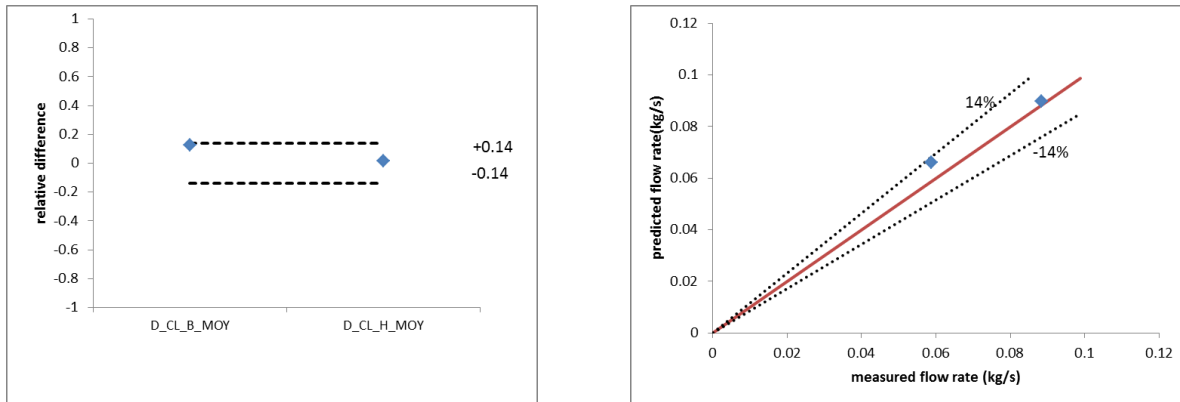


Figure 27 Flow rate through leakage pipes

Gas Temperature

The gas temperature measurements are available from PRISME Leak scenarios. Several thermocouple trees were put in different positions of both rooms. Vertical temperature distribution can be obtained from the measurements. The thermocouple couple tree located in the center of the fire room is indeed providing the information for fire plume temperature. As there are plenty of gas temperature data from PRISME and the gas temperature predictions of leak1 and leak2 scenarios are almost the same, here only the relative differences for leak1 scenario is presented.

The gas temperature in the SW and NE axis shows similar trend. This is not surprising since the position of these two axis is symmetric. ISIS overpredicts the gas temperature in the lower part of the room. For the higher part of the room, the gas temperature is predicted quite accurate by ISIS. One common problem with the gas temperature measurement is the influence of radiation from fire plumes. The temperature of the bare thermocouple bead is in fact not the real gas temperature. A common approach is to correct for radiation. This however is burdensome because the radiative exchange correction may depend on the character of the thermocouple. The experimental data from the PRISME data is not adjusted for radiation. In the upper part of the room the thermocouples are immersed in thick smoke and thus they are less influenced by the flame radiation. Also, as the gas temperature in the higher altitude is high by itself, which means the thermocouple there would also emit radiation compensating with the radiation from the fire source. That is why the prediction for the upper part gas temperature is more accurate. However in the lower part of the room the thermocouples are more susceptible to the fire radiation.

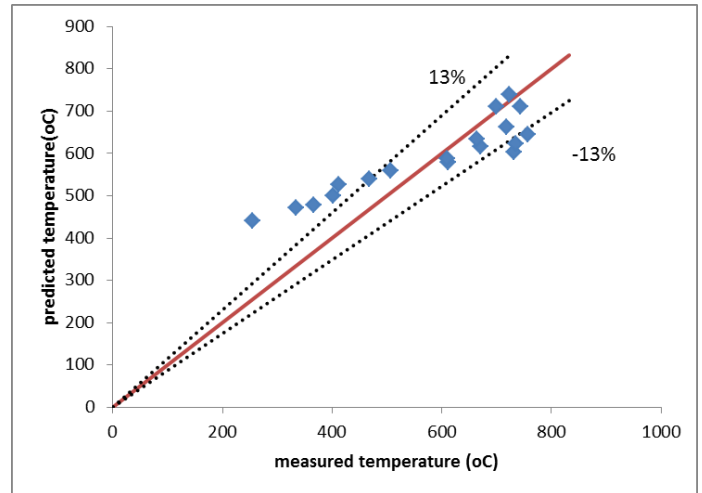
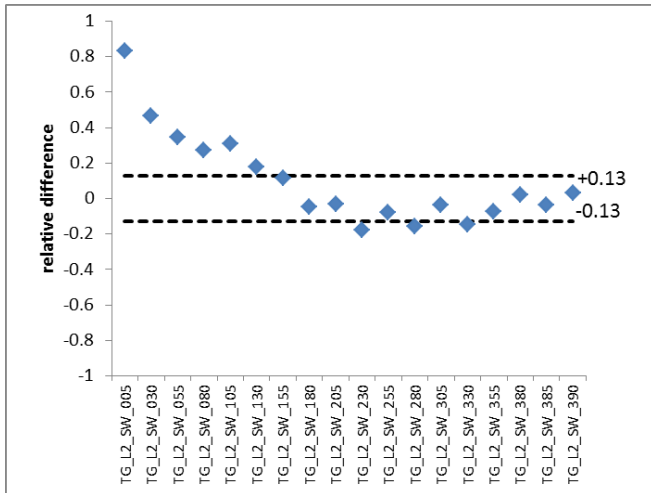


Figure 28 Gas temperature in the SW axis of fire room

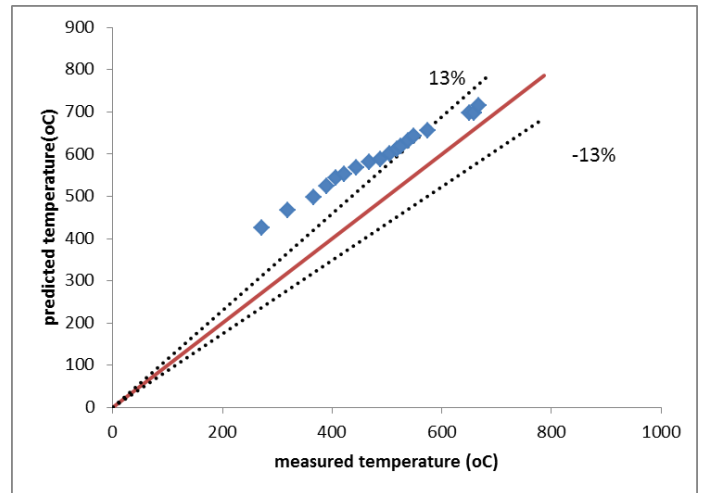
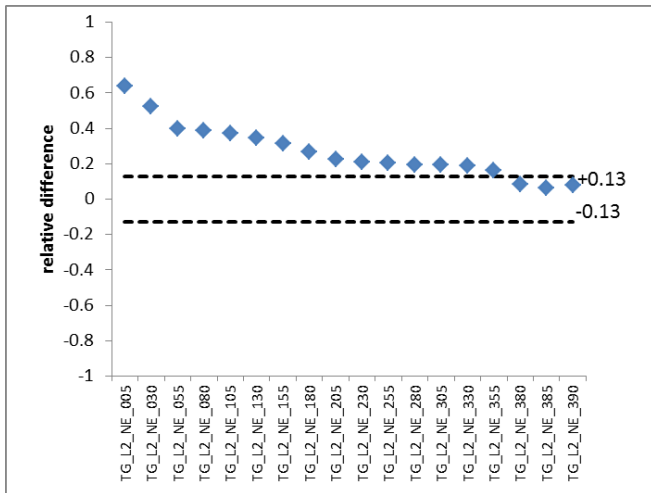


Figure 29 Gas temperature in the NE axis of fire room

The figure below shows the gas temperature in the fire plume. ISIS overpredicts the fire plume temperature in each point. This again can be explained by the radiation exchange between the thermocouple and the environment. In the experiments, the thermocouples in the fire plume are at very high temperature. The wall temperature of the room, on the other hand, is much lower. The thermocouple bead would lose heat by radiation to the wall surface and thus give lower value for the plume temperature. In this sense, the plume temperature prediction from the ISIS might be even more accurate than the experimental data.

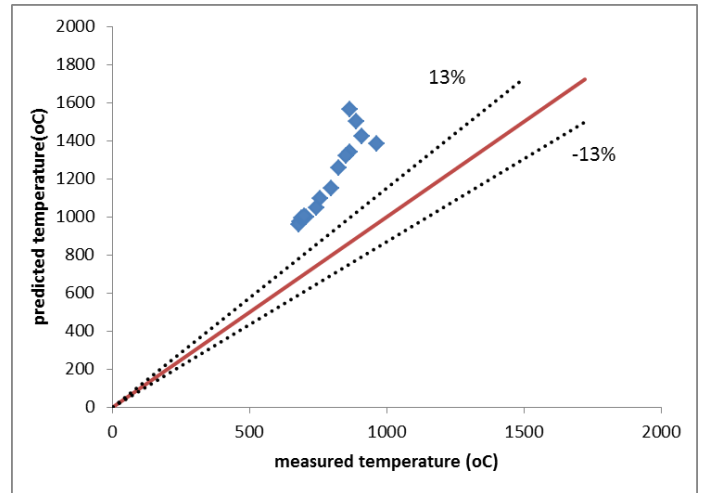
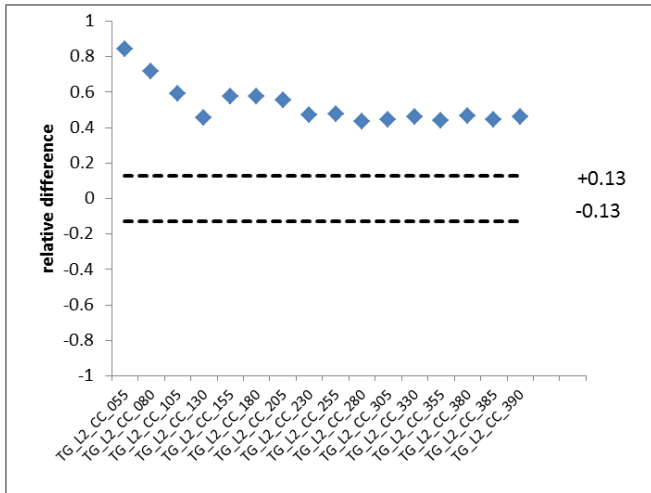


Figure 30 Gas temperature in the central axis of fire room

The figures below present the relative differences for the gas temperature in the target room. ISIS generally predicts the gas temperature in the target room well. However as the temperature rise in the target room is relatively small. As a result the relative difference is large even with small amount of deviation. As explained before, the current boundary condition of ISIS would reduce the heat loss through the wall and thus enhance the gas temperature inside the fire room. Consequently gas with higher temperature spread to the target room through leakage. The gas temperature in the target room is consequently higher.

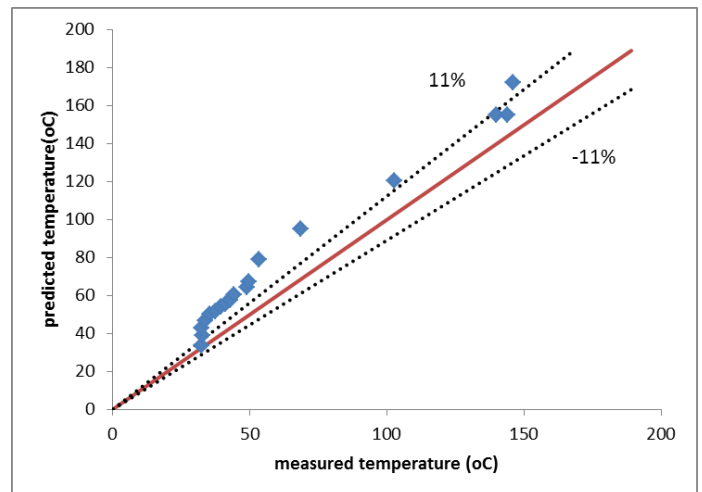
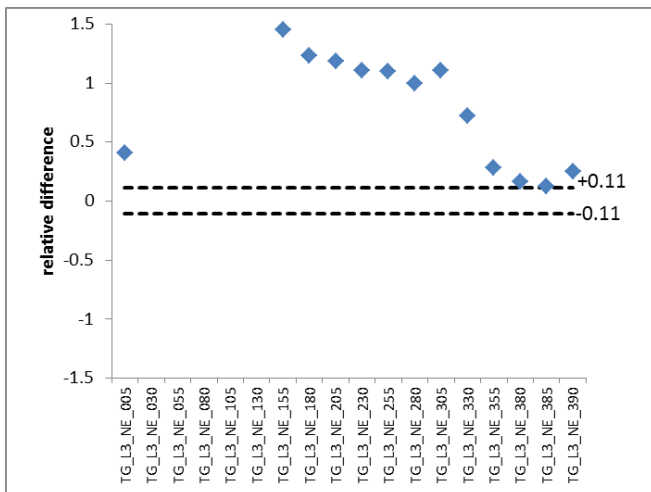


Figure 31 Gas temperature in the NE axis of target room

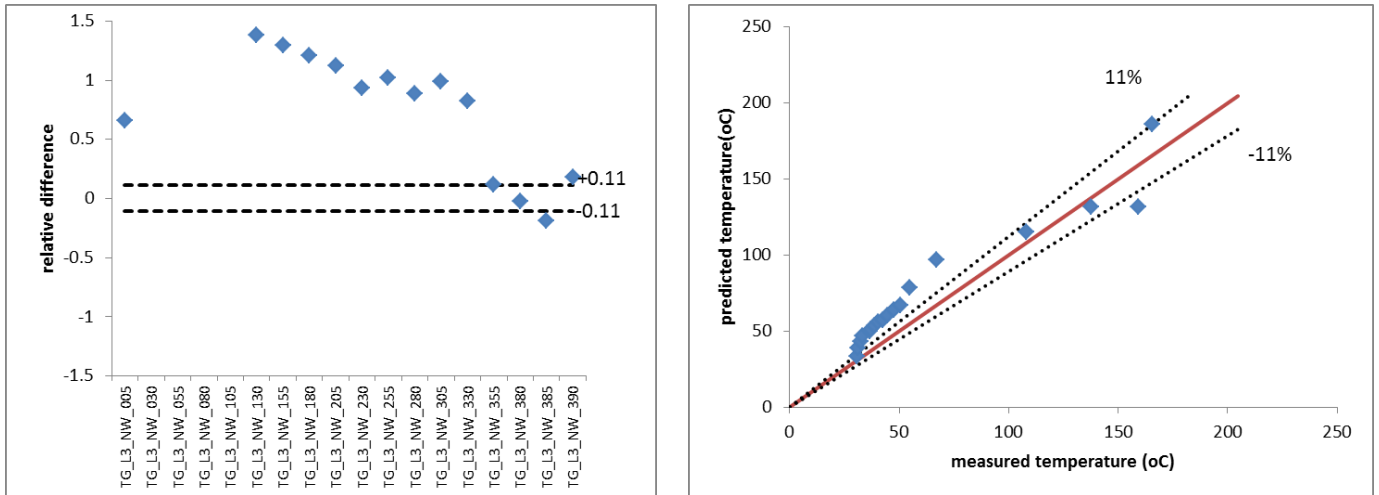


Figure 32 Gas temperature in the NW axis of target room

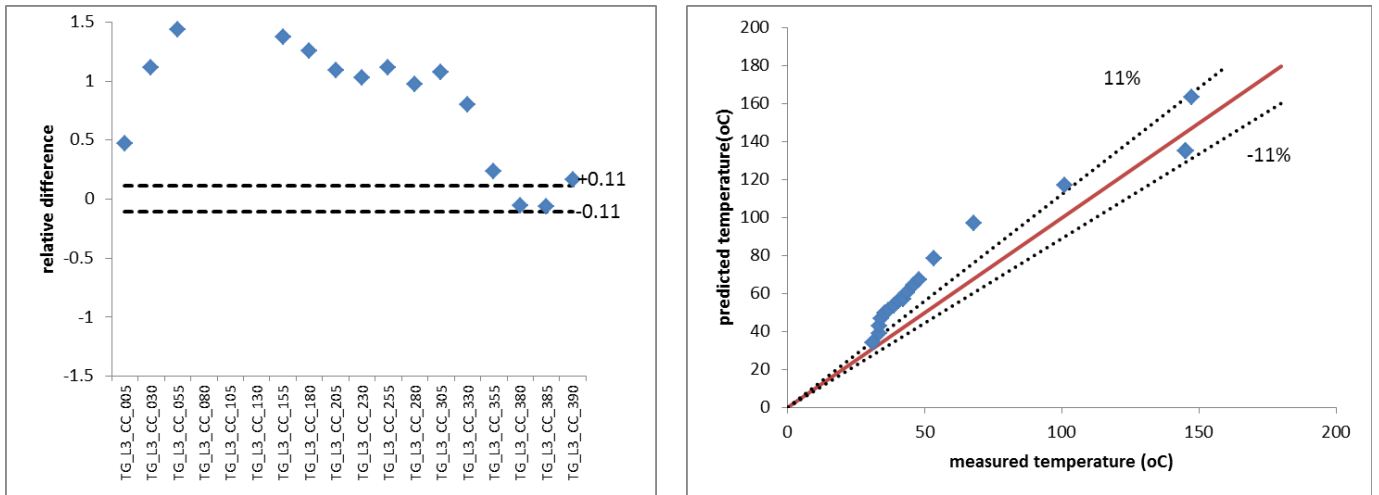


Figure 33 Gas temperature in the CC axis of target room

4.2.2 Attribute-time Curve

The simulation results are also presented by time curves. More detailed information about the quality of predictions can be obtained from this kind of curves. Explanations are also given for deviation of the prediction for certain attributes. The position information for each measurement is also described here to give the reader a clear picture about where all experimental data is measured inside the rooms.

In this thesis a coordinate system is used to indicate the position of measurement points. Two coordinate systems are used whose origins locate in the center of the fire room and the target room respectively. They are named as SC_L2 and SC_L3. The figure below shows these two coordinate systems.

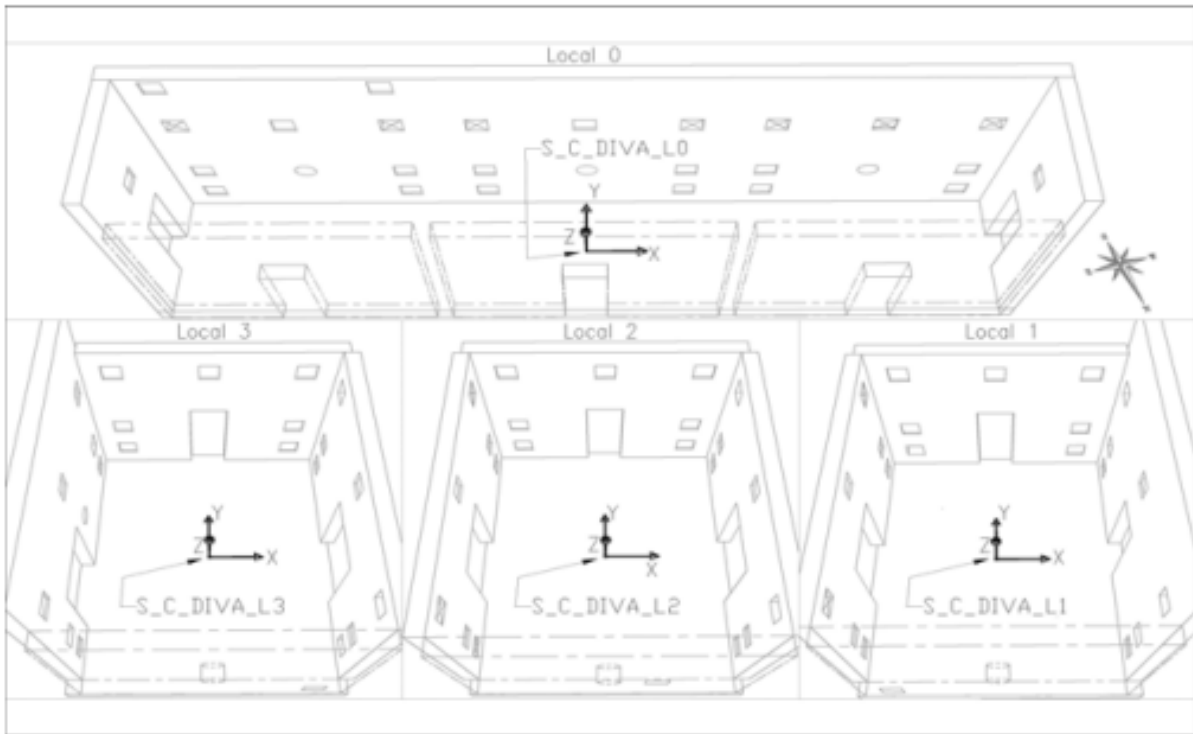


Figure 34 Coordinate system in room 2 (fire room) and room 3 (target room) (Source: [7])

Heat Flux:

Both total heat flux and radiative heat flux are measured during the PRISME leak tests. However, the total heat flux sensors broke down because of the severity of the fire. As a result, only radiative heat flux experimental data is available. In total radiative heat flux at five different positions are measured. Radiative heat fluxes on the north wall of the fire room at four different heights and on the ceiling were measured. Their location information is summarized in the table below.

Table 10 Position of heat flux sensor

Name	CS	X	Y	Z	Description
FLR_L2_NE030	SC_L2	-165	-286	28	Radiative heat flux on North wall in room 2 - NE axis - z = 30 cm
FLR_L2_NE155	SC_L2	-163	-286	155	Radiative heat flux on North wall in room 2 - NE axis - z = 155 cm
FLR_L2_NE260	SC_L2	-162	-286	261	Radiative heat flux on North wall in room 2 - NE axis - z = 260 cm
FLR_L2_NE355	SC_L2	-162	-286	355	Radiative heat flux on North wall in room 2 - NE axis - z = 355 cm
FLR_L2_PL_CE	SC_L2	-182	-4	394	Radiative heat flux on ceiling in room 2

The following figure shows the radiave heat flux from both test and simulation.

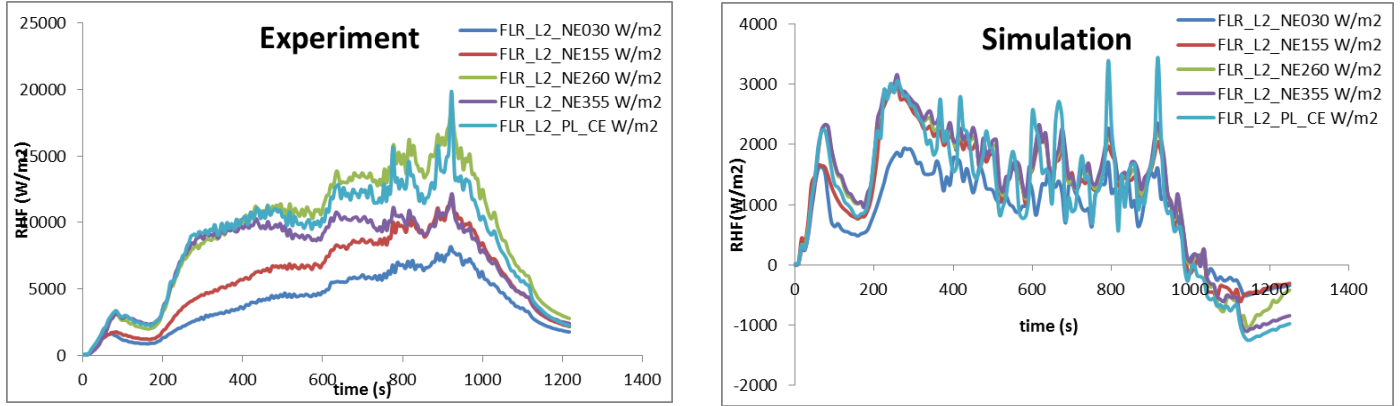


Figure 35 Radiative heat flux

The results show a great discrepancy for radiative heat flux between experiment and simulation. The much lower value predicted by ISIS can be explained by the fact that the surface temperature of the radiometer sensor is much lower than the wall temperature. The surface temperature of the radiometer sensor is kept around 298K by the cooling water. The wall surface temperature during the test is quite high compared to 298K. The radiative heat fluxes compared above are the net radiative heat fluxes between target and the whole environment.

The wall surface temperature at those measurement points is also available from ISIS. The radiative heat flux is adjusted taking into account the wall surface temperature by:

$$Q_{r,adj} = Q_{r,m} + \gamma(\epsilon\sigma T_{wall}^4 - \epsilon\sigma 298^4)$$

Where $Q_{r,adj}$ is the adjusted radiative heat flux, $Q_{r,m}$ the radiative heat flux calculated by the model, ϵ the emissivity of the wall, which is 0.95 in this case, T_{wall} the wall surface temperature at the same position and γ the factor taking into account the view factor and gas absorptivity.

γ value is difficult to determine by hand. A value of 0.4 is chosen so that the result would show the best match with the experimental data. The following figure shows the comparison between the experiment and the adjusted simulation results. The result is a much better agreement. Not only the maximum local value but also the shape of the radiative heat flux curve is better predicted.

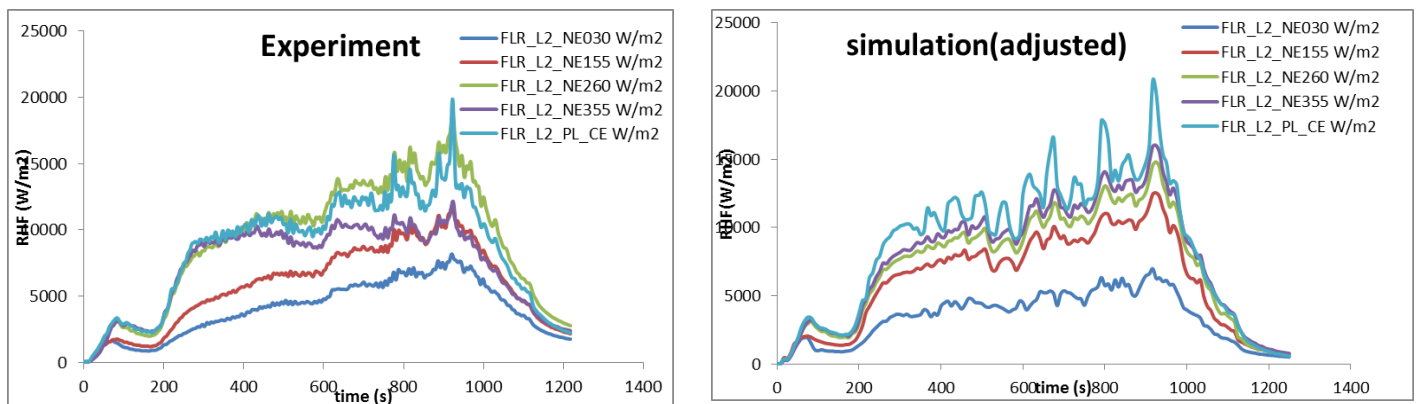


Figure 36 Adjusted radiative heat flux

To demonstrate that the adjustment made above is valid, one special case is ran. The cell on which the measurement point is is specified with the boundary condition so that the wall surface temperature for this point would stay low during the fire⁴. The figure below shows the radiative heat flux on the ceiling. With the same condition as measurement, the ISIS can predict the radiative heat flux much better even without adjustment.

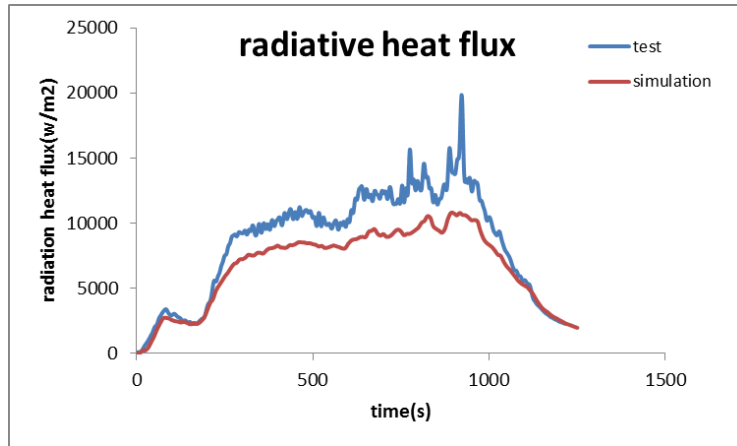


Figure 37 Radiative heat flux on the ceiling

The figure below also shows that the radiative heat flux is higher on the part of the ceiling with the new boundary condition.

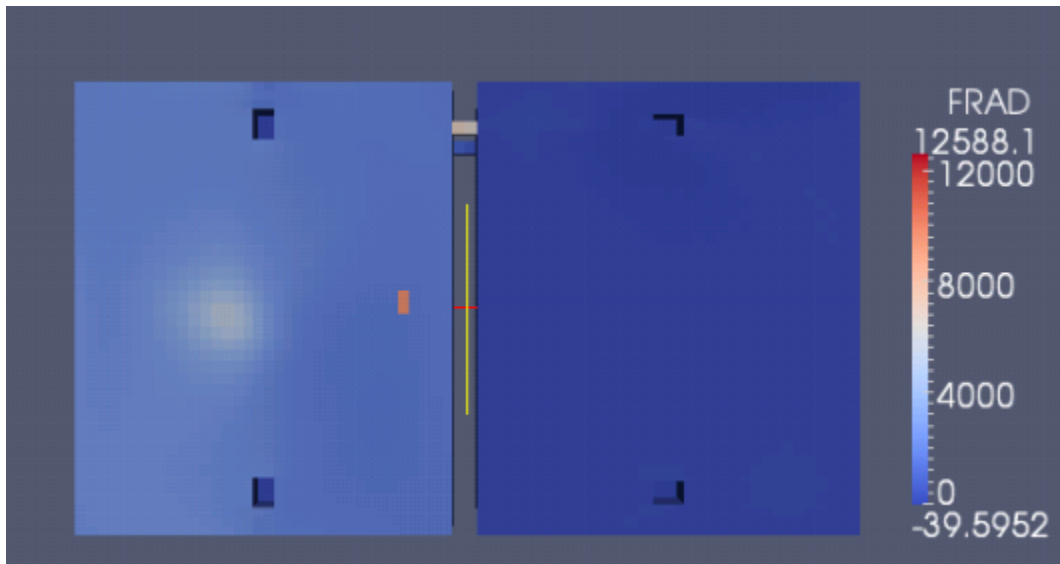


Figure 38 Radiative heat flux on the ceiling

⁴ The wall properties are set so that the thermal inertial (kpc) is quite large, which means that surface temperature rise would be quite slow [42]. It is best to specify fixed temperature boundary condition. However in that case it is not possible to get radiative heat flux data from ISIS.

It can be concluded that the radiative heat flux predicted by ISIS is indeed reliable. However, I would suggest the developer of ISIS to make it possible to model radiometer, which means that ISIS should be able to model the radiative heat flux to a target with fixed temperature.

Wall Temperature

Wall temperature at ten different positions is measured during the PRISME test. Their location information is showed in the table below.

Table 11 Wall temperature measurement points

Name	CS	X	Y	Z	Description
TP_L2_EC260	SC_L2	-250	9	260	East wall temperature in room 2
TP_L2_NC260	SC_L2	-16	-300	262	North wall temperature in room 2
TP_L2_PL_CE	SC_L2	-235	0	400	Ceiling temperature in room 2
TP_L2_SC260	SC_L2	9	300	260	South wall temperature in room 2
TP_L2_SOL_CE	SC_L2	-123	0	0	Floor temperature in room 2
TP_L2_WC260	SC_L2	250	-16	260	West wall temperature in room 2
TP_L3_EC255	SC_L3	-250	-14	252	East wall temperature in room 3
TP_L3_NC255	SC_L3	13	-300	251	North wall temperature in room 3
TP_L3_SC255	SC_L3	18	300	255	South wall temperature in room 3
TP_L3_WC255	SC_L3	250	16	249	West wall temperature in room 3

The wall temperature measured during test is in fact the temperature of the concrete wall. However the wall temperature given by ISIS is the wall temperature of the first layer, which is THERMIPAN for walls in room 2.

The following figure shows the wall temperature in the fire room. As they present wall temperature at different points, the large difference does not. However, this does reveal the weakness of ISIS in modeling multilayer boundary conditions.

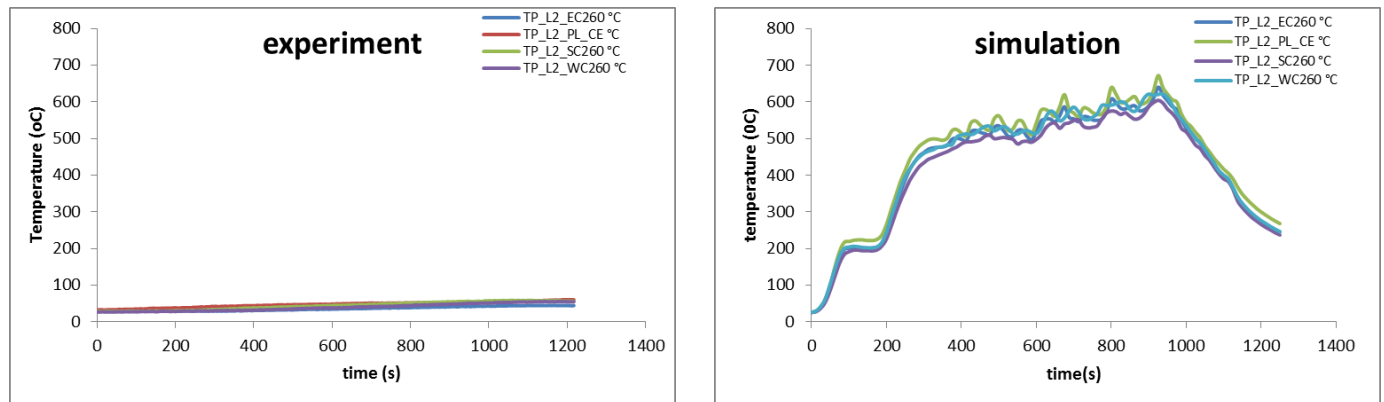


Figure 39 Wall temperature in fire room

In room 2, there is no insulation on the floor, thus it is possible to compare wall temperature on the floor.

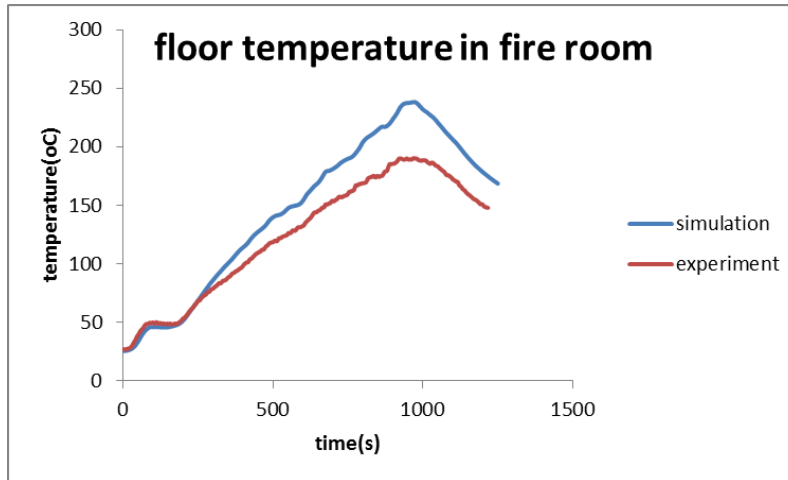


Figure 40 Floor wall temperature

The floor temperature is predicted quite well in the beginning of the fire. However as fire continues to grow, ISIS starts to overpredict the floor temperature. This can be explained by the fact that the THERMIPAN becomes thermal thin as fire develops which makes the boundary condition inappropriate for the insulation walls. The insulated wall temperature is thus overpredicted and thus cast more radiation to the floor, making the floor temperature higher than reality.

The prediction of floor temperature starts to deviate from experiment value from about 240s. At time of 240s, the characteristic thickness is [42]:

$$2\sqrt{\alpha t} = 2\sqrt{8.67 * 10^{-7} * 240} = 0.0288m$$

The thickness of the wall insulation layer is 0.03m. After 240 seconds, ISIS is not able to model the wall temperature well and that also affect the floor temperature prediction.

The figure below shows the wall temperature in the target room. ISIS predicts the wall temperature in the target room quite well.

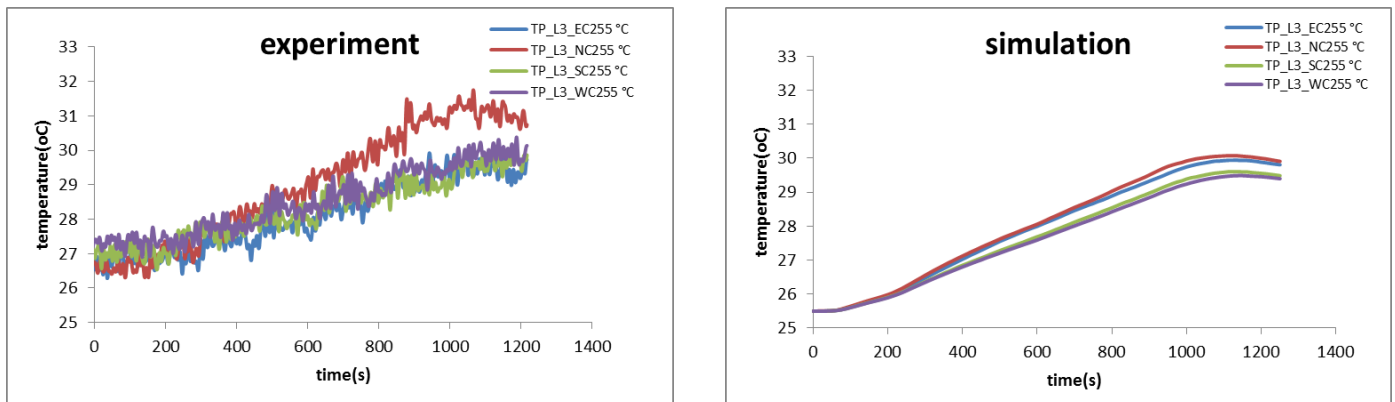


Figure 41 Wall temperature in target room

Soot Concentration

Soot concentration in the exhaust branches of both rooms are measured by PRISME Leak scenarios. The output from ISIS is for the point which is on the exhaust branch boundary face. Soot concentration data is available at the two exhaust branch in room2 and room3.

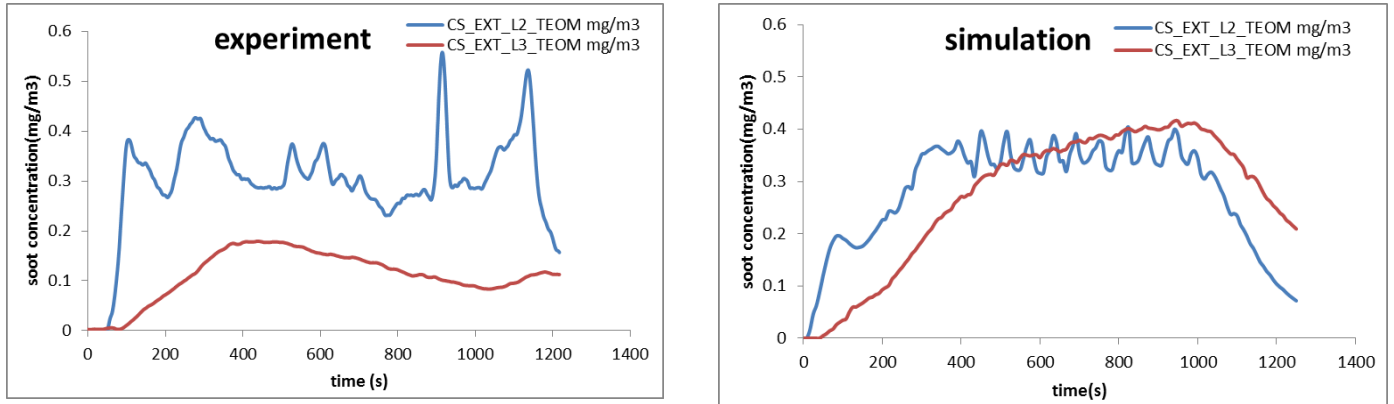


Figure 42 Soot concentration in the exhaust branches

ISIS predicts the soot concentration in the exhaust branch of fire room well. However, the soot concentration in the target room is not predicted well.

The soot yield value used for simulation is calculated from experiment data and is much lower than the recommended value from Tweason [11]. The soot concentration results show that using the soot yield value calculated from data is a better choice than Tweason data. Here better means that the simulation result shows better agreement with experimental data.

One possible way to solve the problem with the soot yield fraction input is to apply Moss soot production model [32][33]. This model does not require input for soot yield fraction. Instead, soot yield fraction is an output of this soot production model. However, more research is needed for the application of Moss Model.

Gas Concentration

O₂, CO₂, and CO concentration is measured. Gas concentration at seven positions is measured and compared. Their location information is showed in the table below:

Table 12 Position of gas concentration measurement points

Name	CS	X	Y	Z	Description
L2_BAS	SC_L2	-125	140	73	Concentration at bottom of room 2. SE axis
L2_FP	SC_L2	-120	-40	35	Concentration near the pool
L2_HAUT	SC_L2	-123	139	333	Concentration at top of room 2. SE axis
EXT_L3	SC_JUP	250	540	107	Concentration in the exhaust duct of room 3
EXT_L2	SC_JUP	780	540	107	Concentration in the exhaust duct of room 2
L3_BAS	SC_L3	127	-152	80	Concentration at bottom of room 3. NW axis
L3_HAUT	SC_L3	124	-157	327	Concentration at top of room 3. NW axis

Oxygen Concentration

The figure below shows the oxygen concentration in the fire room. The oxygen concentration at different places in fire room is predicted quite well by ISIS.

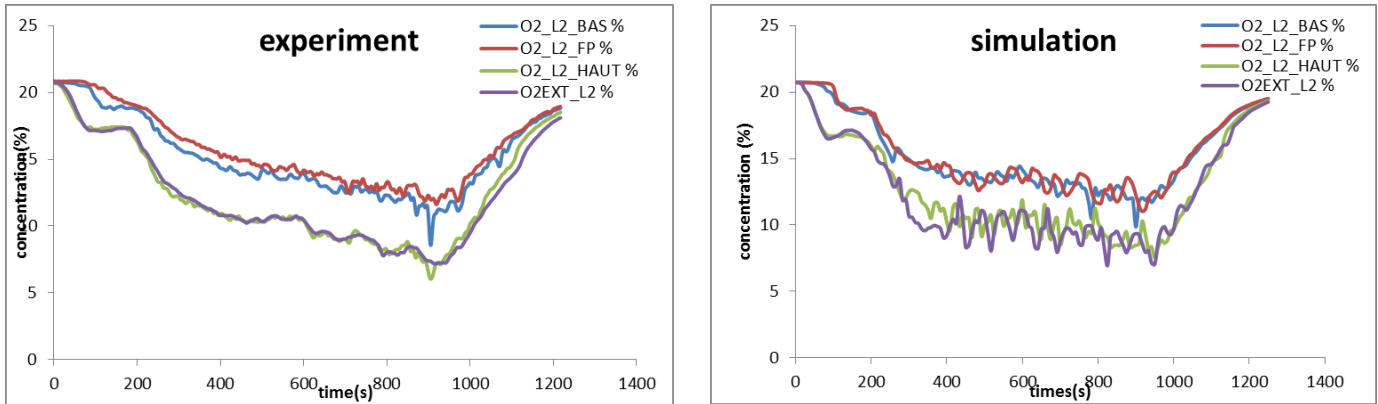


Figure 43 Oxygen concentration in the fire room

The figure below shows the oxygen concentration in the target room. Except for the point at the top of room 3, ISIS predicts the oxygen concentration quite well.

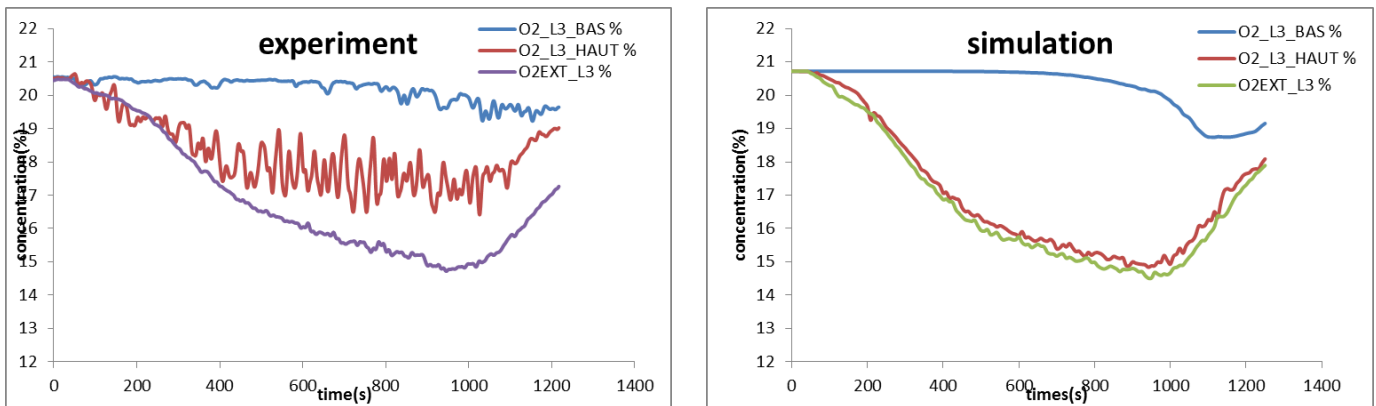


Figure 44 Oxygen concentration in the target room

CO₂ Concentration

The figure below shows the CO₂ concentration in the fire room. The CO₂ concentration at different places in fire room is predicted quite well by ISIS.

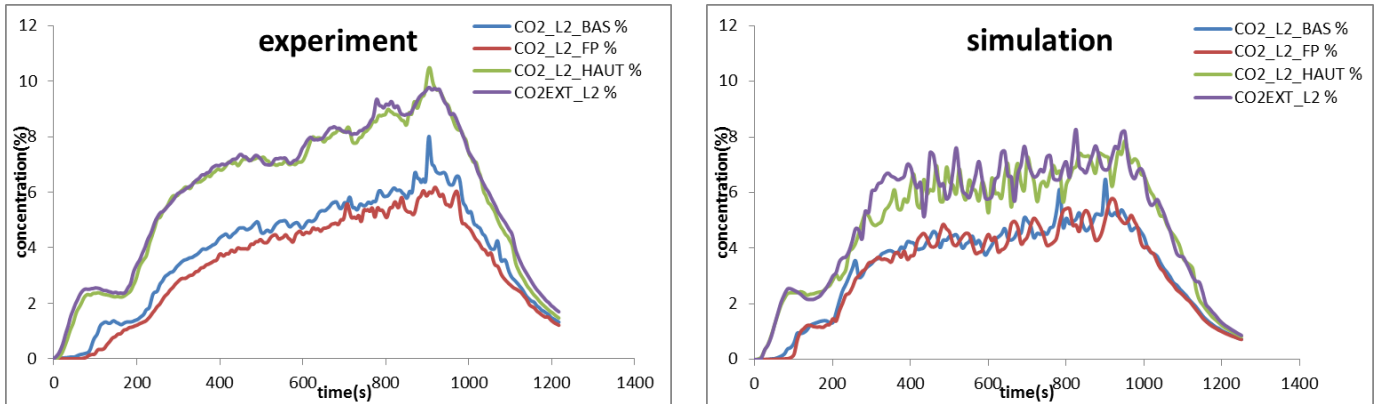


Figure 45 CO₂ concentration in the fire room

The figure below shows the CO₂ concentration in the target room. Except for the point at the top of room 3, ISIS predicts the CO₂ concentration quite well. In fact, for oxygen concentration at the same position it is not well predicted. As in the target room the gas concentration is determined by the transportation of gas from fire room to the target room, the difference of gas concentration at this point may be due to the fact that in the experiment there is mixture of fresh air and gas from fire room at point HAUT.

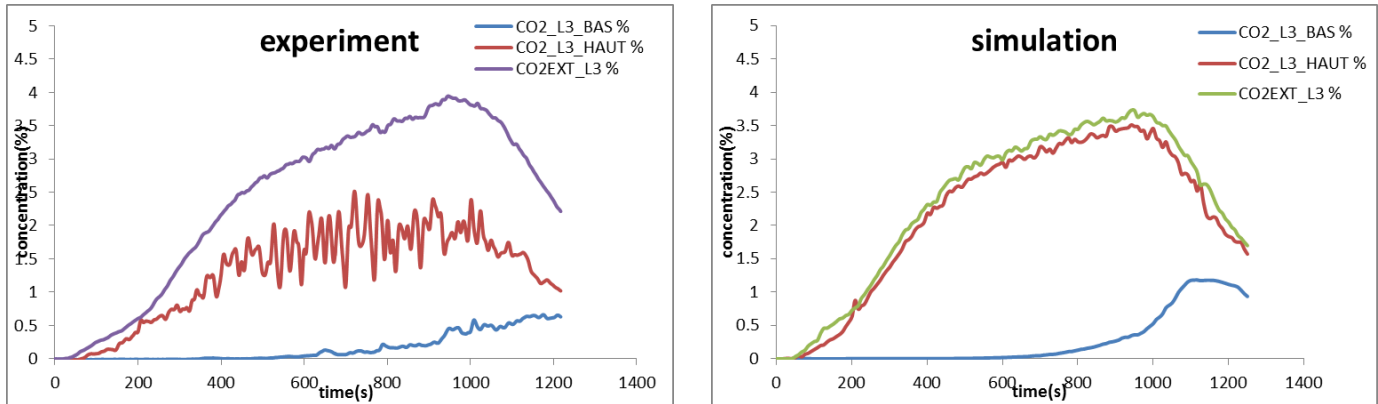


Figure 46 CO₂ concentration in the target room

Pressure

The relative pressure in the fire room and the target room is measured. Their position information is showed in the table below.

Table 13 Position of pressure measurement point

Name	CS	X	Y	Z	Description
L2_BAS	SC_L2	-125	140	73	Concentration at bottom of room 2. SE axis
L3_HAUT	SC_L3	124	-157	327	Concentration at top of room 3. NW axis

The following picture shows the relative pressure. The predicted relative pressure deviates from the experimental value to great extent. The flow rate of ventilation braches, which is determined by the pressure in the room, is predicted correctly. The good prediction of flow rate demonstrates that the pressure used by ISIS to calculate the flow rate is correct. No explanation can be found for the weird pressure prediction.

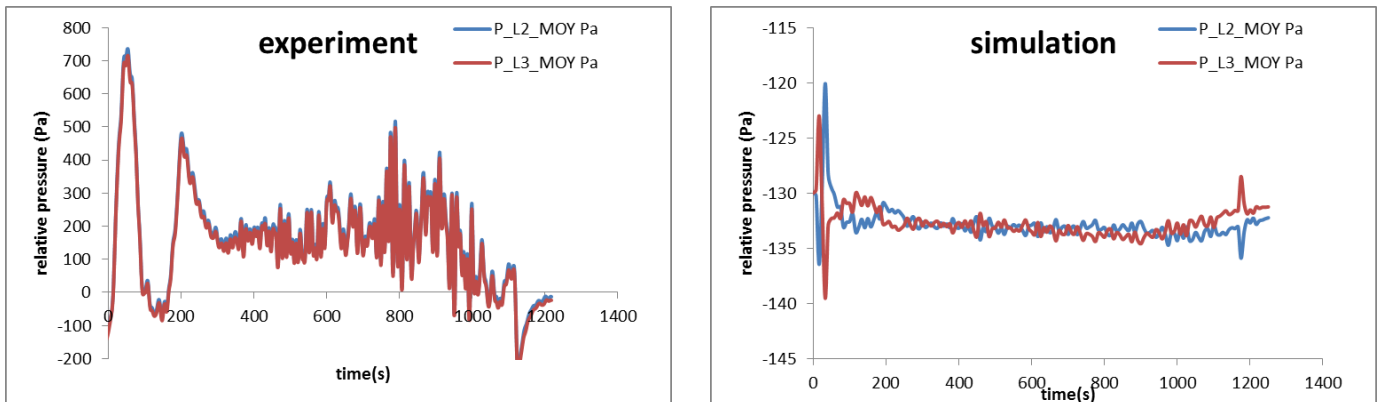


Figure 47 Relative pressure

Flow Rate

The figure below shows the flow rate at the admission and extraction branches of the ventilation network. Both volume and mass flow rate are compared. Mass flow rate in both rooms are well predicted by ISIS. However, the volume flow rate in the admission branch of room 2 is not well predicted. This can be explained by the fact that ISIS overpredicts the gas temperature in the extraction point, which can be seen in the Figure below. The density is thus underpredicted at the same point, which leads to error in the prediction of the volume flow rate.

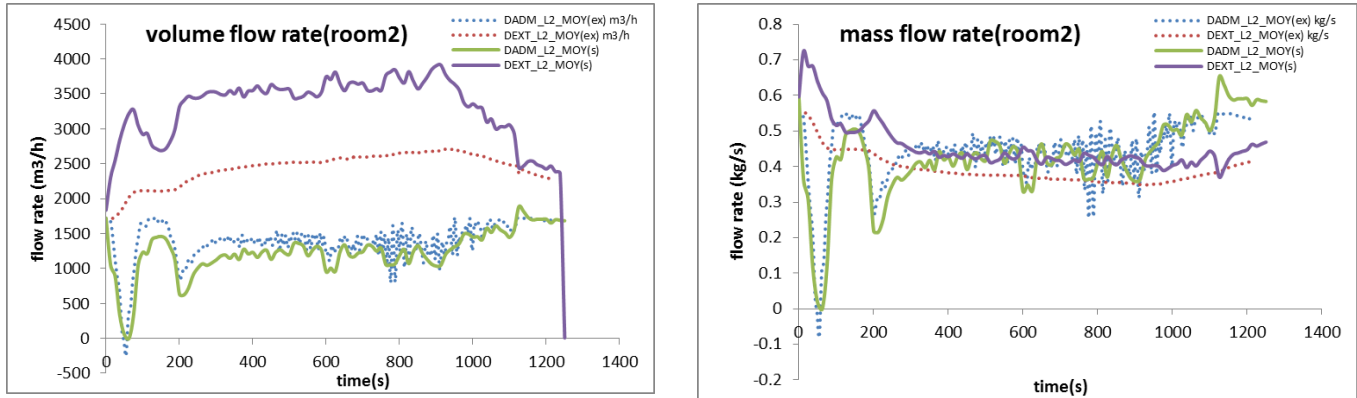


Figure 48 Flow rate in fire room

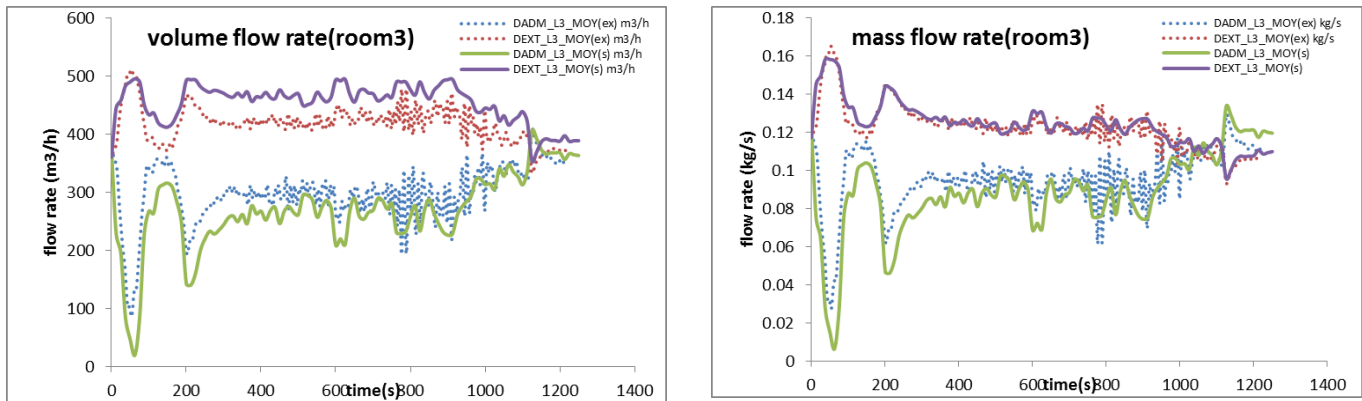


Figure 49 Flow rate in target room

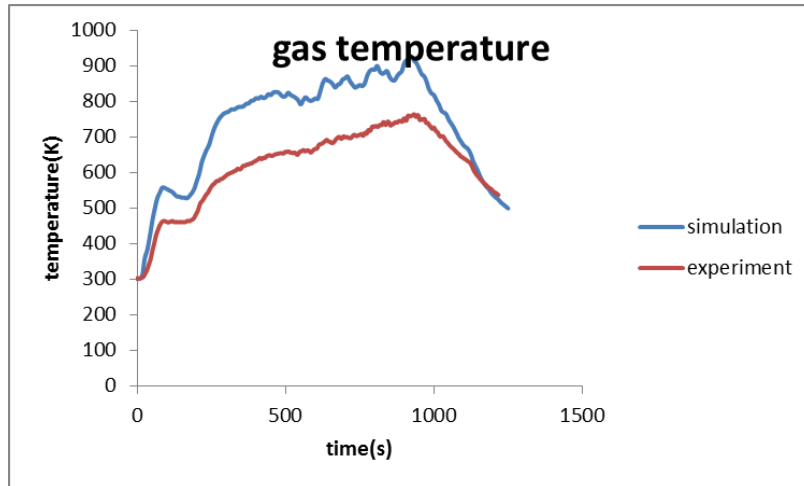


Figure 50 Gas temperature in the extraction point of fire room

The following figure shows the mass flow equilibrium of the whole system⁵. The blue line shows the instant net mass flow rate to the whole system. The green line shows the net mass flow into the system.

$$m_{net} = m_e - m_b$$

Where m_e is the total mass of the air in the two rooms in the end of the test and m_b is the total mass in the beginning. m_{net} is the net mass brought by ventilation branches into the rooms throughout the test.

At the end of the test the density of the air inside both rooms is lower than the beginning because of higher temperature, which means that at the end of test the total mass inside the system is less than the beginning ($m_e < m_b$). ISIS prediction follows the mass equilibrium law, thus the net mass into the whole system is minus in the end. The positive value (29kg) indicated by experiment shows the measurement error of experiment.

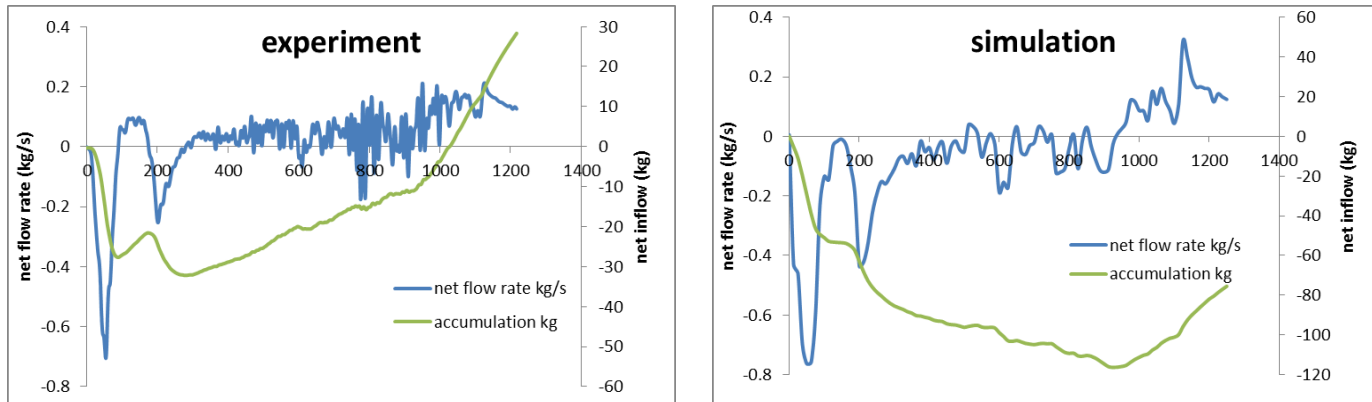


Figure 51 Mass flow equilibrium

⁵ It is assumed here that the leakage to the environment is negligible since the facility is quite air-tight.

Flow Rate of the Leakage

The following figure shows the mass flow rate through the leakage pipes. ISIS is able to predict the transportation of gases from the fire room to the target room. The relative pressure in the two ends of the leakage pipes are also given by ISIS. The resistance of the two pipes is also calculated.

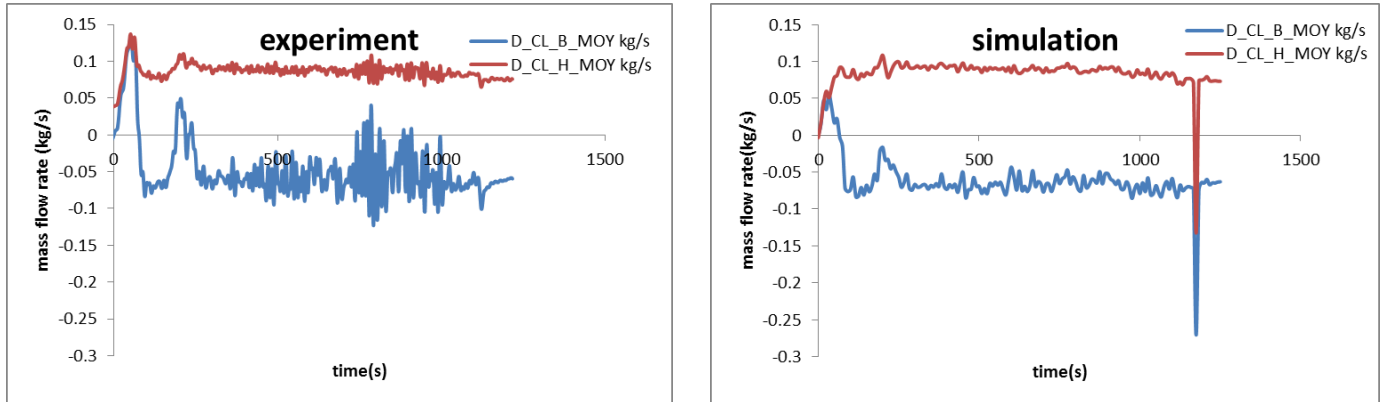


Figure 52 Mass flow rate through leakage pipes

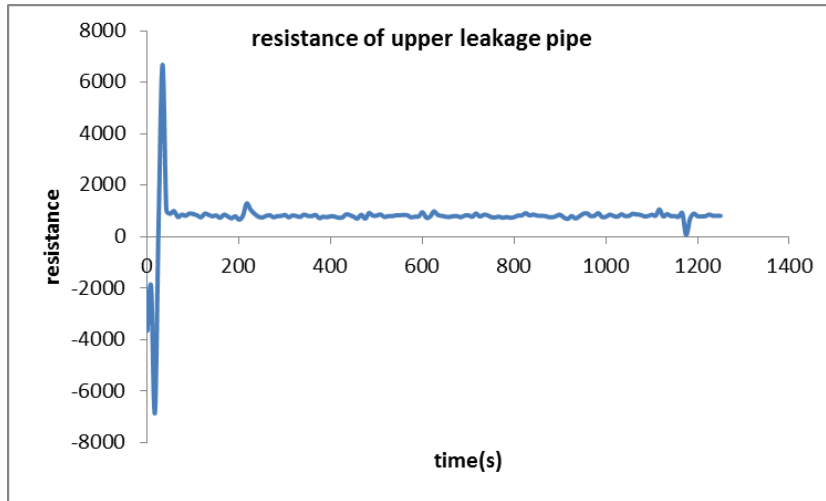


Figure 53 Resistance of upper leakage by ISIS

The static relative pressure before and after the leakage pipes is exported as output. The density of the gas in the middle of the leakage pipe is also exported. The flow rate of the leakage pipe data is also exported. The resistance of leakage pipe can thus be calculated by:

$$R(t) = \frac{\Delta P(t)}{Q(t)^2 \rho(t)}$$

The resistance calculated from ISIS is 815 for the stable state. The resistance of the upper leakage calculated by the experiment is 1080 [19]. There is 20% difference in predicting the resistance. However, the flow rate of the leakage is predicted well.

The temperature in the target room is determined both by leakage flow rate and the temperature of the leakage gases. The flow rate and temperature determine the energy flow from the fire room to the target room. The figure below shows the energy flow through leakage. The energy flow rate is calculated by:

$$\dot{Q} = \dot{m}c_p(T - 300)$$

ISIS overpredicts the energy flow through leakage. This can be explained by the fact that the gas temperature is overpredicted by ISIS because of the boundary conditions. However, the prediction is still satisfactory with local point difference of 7%.

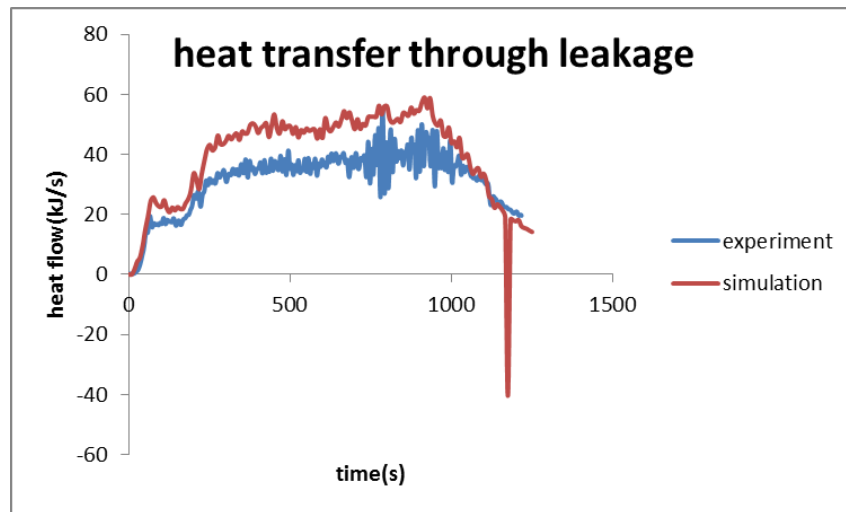


Figure 54 Energy flow through leakage

Gas Temperature

Five thermocouple trees were used to record the temperature profile during the test. The table below shows their position information

Table 14 Position of thermocouple trees

Name	CS	X	Y	Z	Description
TG_L2_CC	SC_L2	0	0	-	Temperatures of gases in room 2 - CENTRAL axis
TG_L2_NE	SC_L2	-125	-150	-	Temperatures of gases in room 2 - NE axis
TG_L2_SW	SC_L2	125	150	-	Temperatures of gases in room 2 - SW axis
TG_L3_CC	SC_L3	0	0	-	Temperatures of gases in room 3 - CENTRAL axis
TG_L3_NE	SC_L3	-125	-150	-	Temperatures of gases in room 3 - NE axis
TG_L3_SW	SC_L3	125	150	-	Temperatures of gases in room 3 - SW axis

The following figures show the comparison of gas temperature.

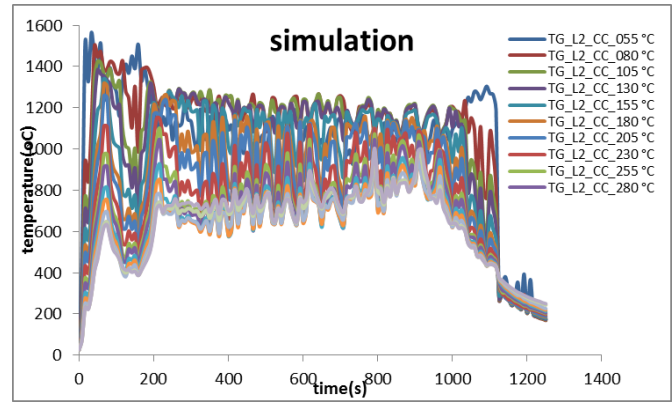
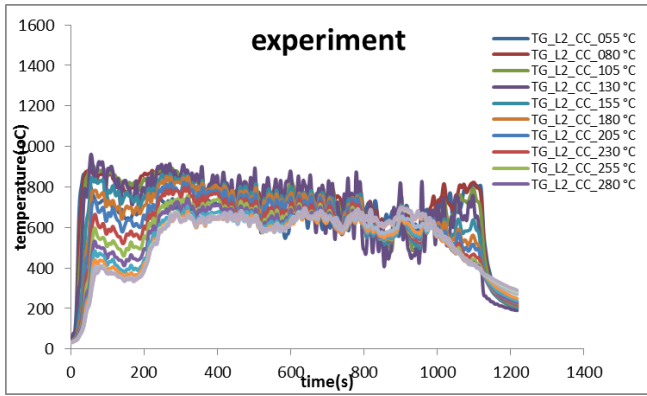


Figure 55 Temperatures of gases in room 2 - CENTRAL axis

ISIS overpredicts the flame temperature to great extent. However, for the gas temperature out of the flame region, ISIS predicts gas temperature well.

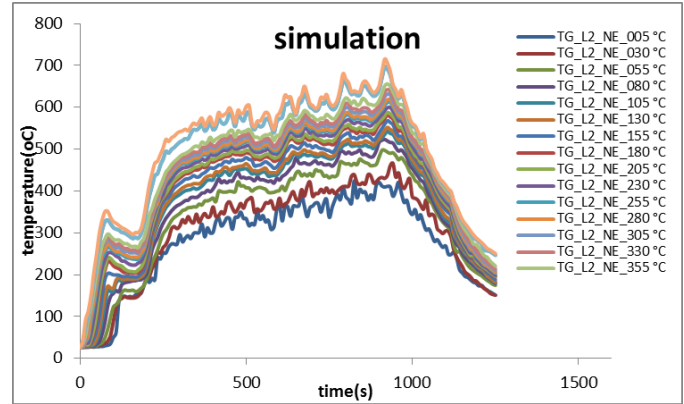
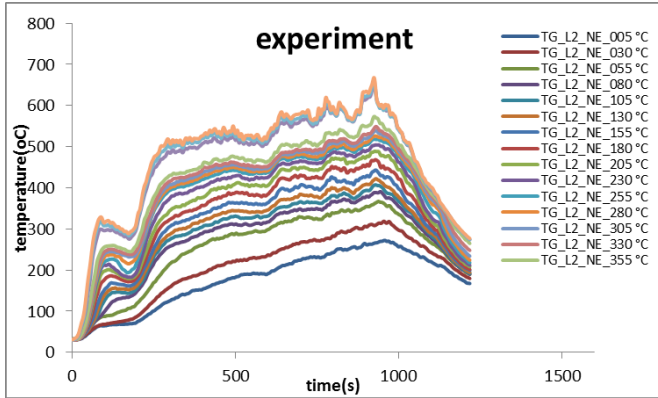


Figure 56 Temperatures of gases in room 2 - NE axis

The upper layer temperature is predicted better than the lower layer temperature by ISIS. Readers are referred to section 4.2.1 for detailed discussion for gas temperature prediction by ISIS.

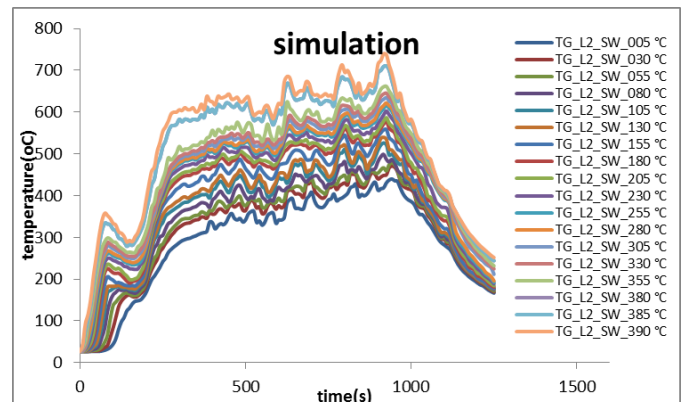
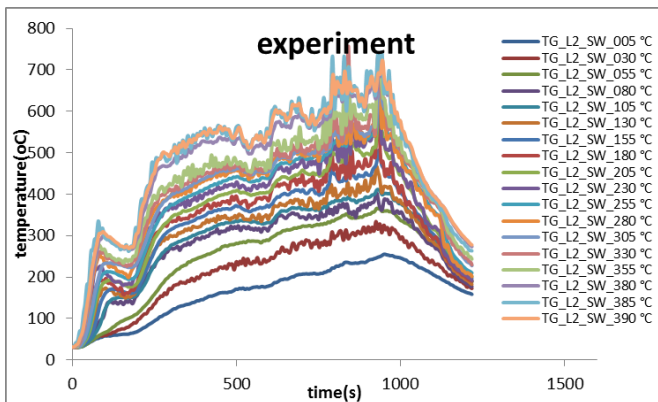


Figure 57 Temperatures of gases in room 2 - SW axis

The upper layer temperature is predicted better than the lower layer temperature by ISIS. Readers are referred to section 4.2.1 for detailed discussion for gas temperature prediction by ISIS.

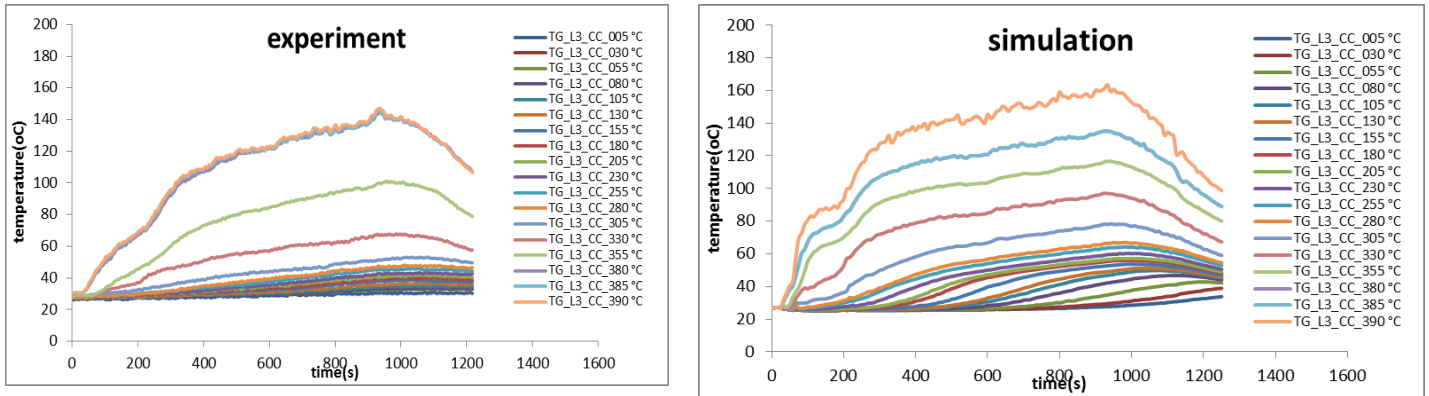


Figure 58 Temperatures of gases in room 3 - CENTRAL axis

The highest temperature in the target room is predicted well by ISIS.

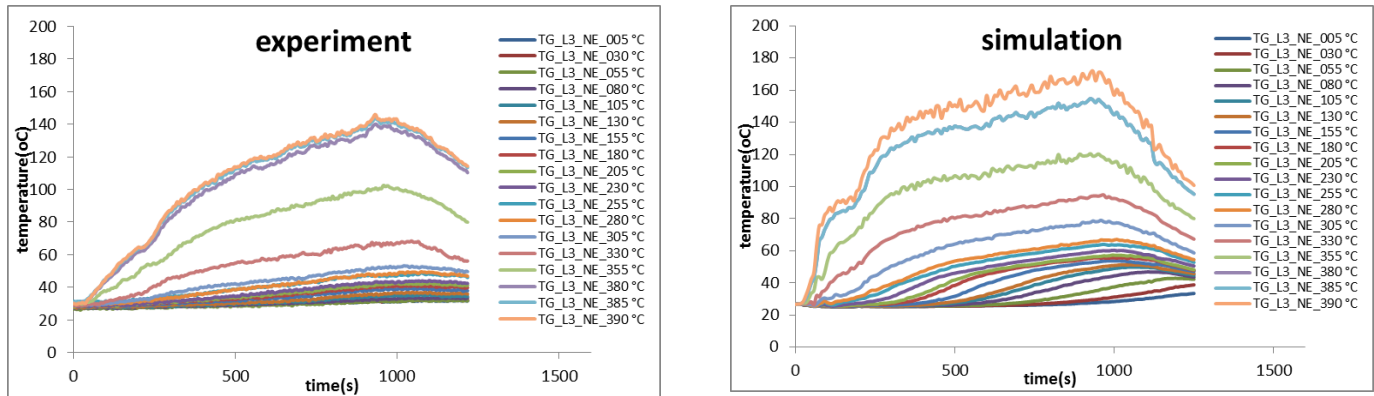


Figure 59 Temperatures of gases in room 3 - NE axis

ISIS overpredicts the gas temperature in the NE axis of room 3.

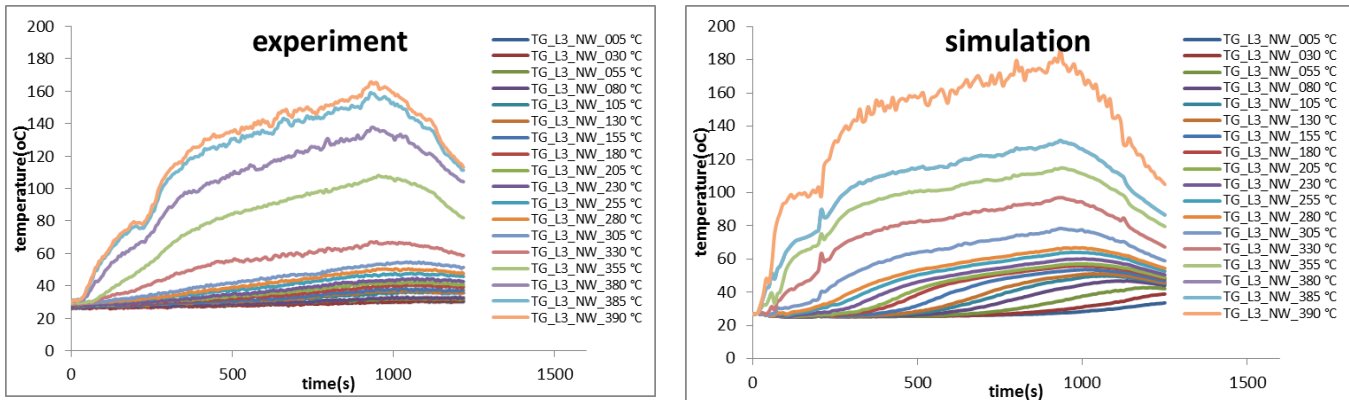


Figure 60 Temperatures of gases in room 3 - SW axis

ISIS overpredicts the gas temperature in the room 3.

4.3 Sylvia

In the first part, all results from four leak scenarios will be compared by single point value. In the second part detailed simulation results for Leak1 scenario will be presented.

The information for the position of measurement points is the same as that in ISIS (section 4.2.2), thus it is not presented again in this part.

4.3.1 Relative Difference

Heat Flux:

Sylvia overpredicts radiative heat flux for all four leak scenarios. There seems to be problem with Sylvia to predict adiation heat flux: there exists radiation even with a radiation fraction of zero. The overpredicted radiation also leads to inaccuracy of the prediction of other parameters.

The figure below also shows that the prediction from Sylvia is biased by a factor of around two. This is partly because of the instric average nature of zone model.

Also, as Sylvia overpridicts the radiative heat flux, by lowering the radiation fraction one should be able to get better results. Here better results means greater matchness with the experimental data. However, as mentioned above, radiation fraction does not affect the radiative heat flux in Sylvia. This is not normal and may reveal possible problem with Sylvia.

As the Sylvia overpredicts the radiative heat flux, it is deemed more conservative for real application.

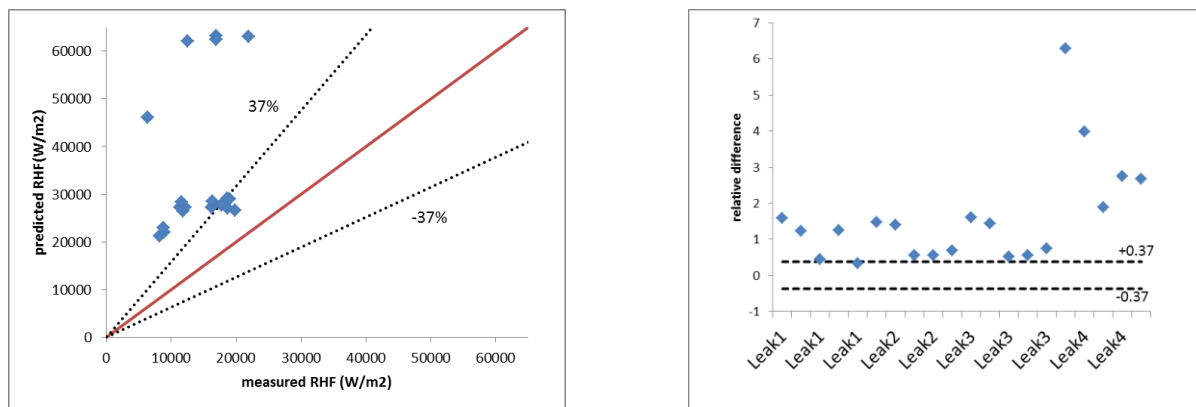


Figure 61 Radiative heat flux prediction by Sylvia

Wall Temperature

For Leak1 ~ Leak 3 scenarios, Sylvia overpredicts the wall temperature in some points while underpredicts the wall temperature in other points. This can be explained by the average nature of zone model. The temperature given by Sylvia is more averaged, which makes the temperature

prediction higher in some parts while lower in other parts. The temperature is predicted unbiased, as the relative differences scatter around zero.

However, in Leak 4 scenario, there was a sudden rise in the HRR in the later period of fire as showed in the figure below. Sylvia seems to overrate the effect of this short period of high HRR on the wall temperature and gas temperature. As the relative differences are calculated based on the local maximum values, wall temperature in Leak4 is overpredicted. The same explanation can be given to the overpredicted heat flux in Leak4 scenario.

To conclude, Sylvia is reliable in predicting the wall temperature.

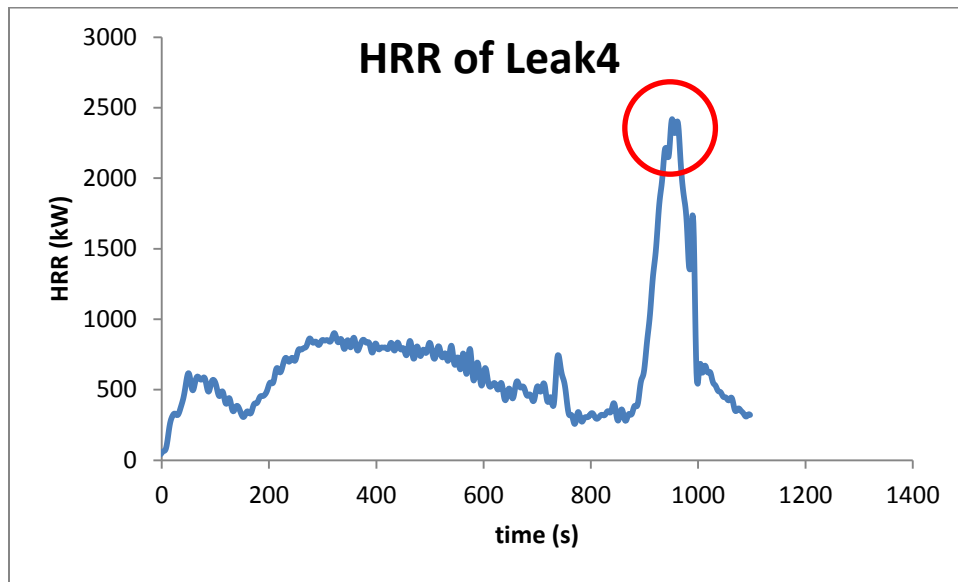


Figure 62 HRR of Leak4

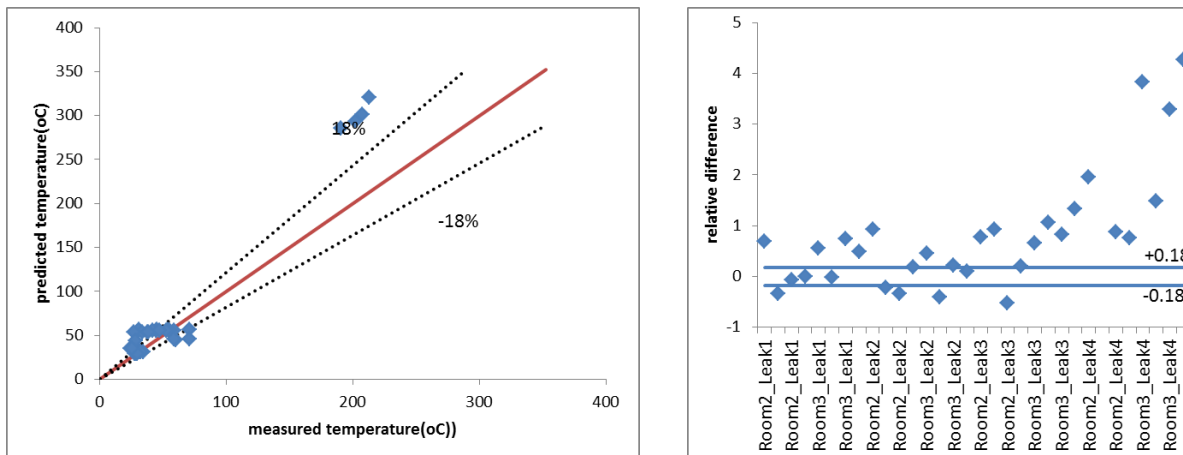


Figure 63 Radiative heat flux prediction by Sylvia

Soot Concentration

Sylvia overpredicts the soot concentration. The soot yield fraction is calculated taking into account the deposition of soot. In the simulation Sylvia does not calculate the deposition, resulting in higher soot concentration in the air. On the other hand, the soot concentration is very sensitive to the input parameter ‘soot yield’. The wrong soot yield may also lead to the higher prediction.

Also, it can be observed that the soot concentration in the target room (room 2) is overpredicted by greater factor.

Sylvia is able to model the deposition of soot in nodes. There are two options for the deposition model: the fixed deposition model and the calculated deposition model [39]. With implementation of the deposition model, the soot concentration in both rooms would be lower and give better results. Here better results mean better matchness with experimental data. In this thesis the deposition model is not implemented. More research effort is needed for the input parameters of deposition model. Effect of deposition model on the soot concentration can be another future R&D work for Bel V.

To conclude, with proper input for soot yield fraction and implementation of deposition model, Sylvia can give good predictions for soot concentration.

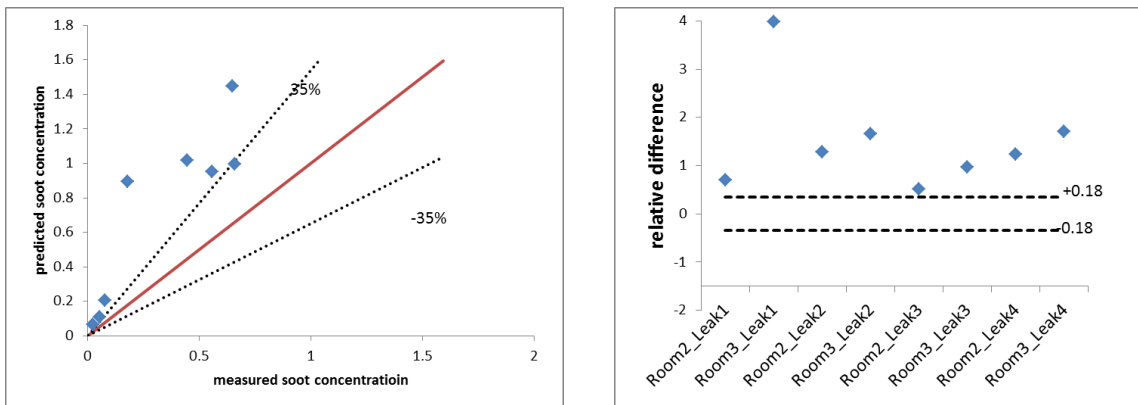


Figure 64 Soot concentration prediction by Sylvia

Oxygen Concentration

Sylvia, as a two-zone model, only provides oxygen concentration in the upper layer and lower layer. The oxygen concentration in the lower layer is predicted the same as environment, and thus is not compared here. The upper layer oxygen concentration from prediction is analyzed here.

Generally speaking Sylvia predicts the oxygen concentration quite well except for the oxygen concentration in the upper layer of the target room in the Leak 1 scenario. As the relative difference is calculated by the deviation from normal state, the positive relative difference for oxygen concentration means that the oxygen concentration is underpredicted.

The large relative difference for the oxygen concentration prediction in the target room reveals the fact that Sylvia might not be suitable for modeling leakage scenarios as in Leak1, which involves two circular pipes connecting two adjacent rooms. Indeed, the gas property in the upper layer of the target room is predicted almost the same as the gas property in the upper layer of the fire room (as showed in the figure below). This is obvious incorrect. The gas from the upper layer of room2 would spread to the upper layer of room3 and mix with with the ventilation air to room3.

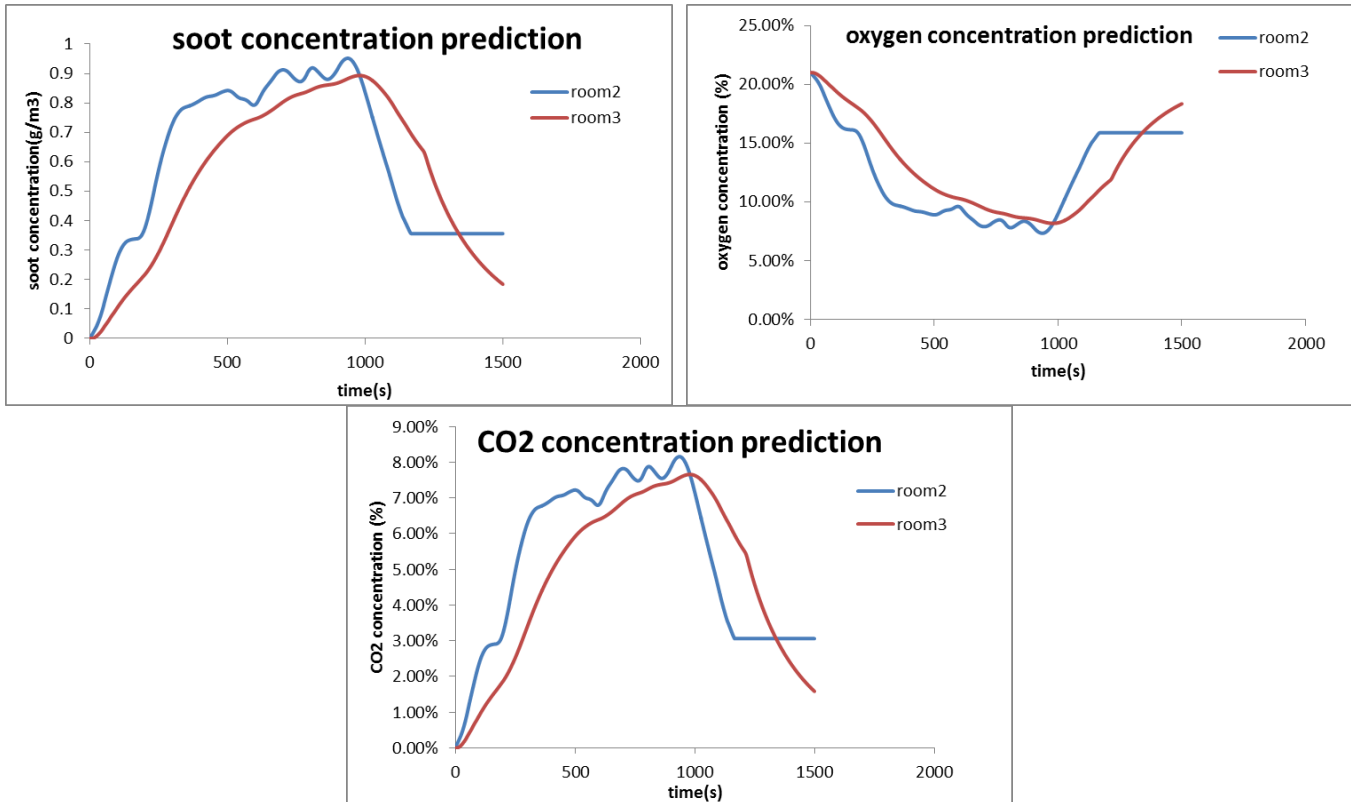


Figure 65 Gas property in room2 and room3 predicted by Sylvia for Leak1 scenario

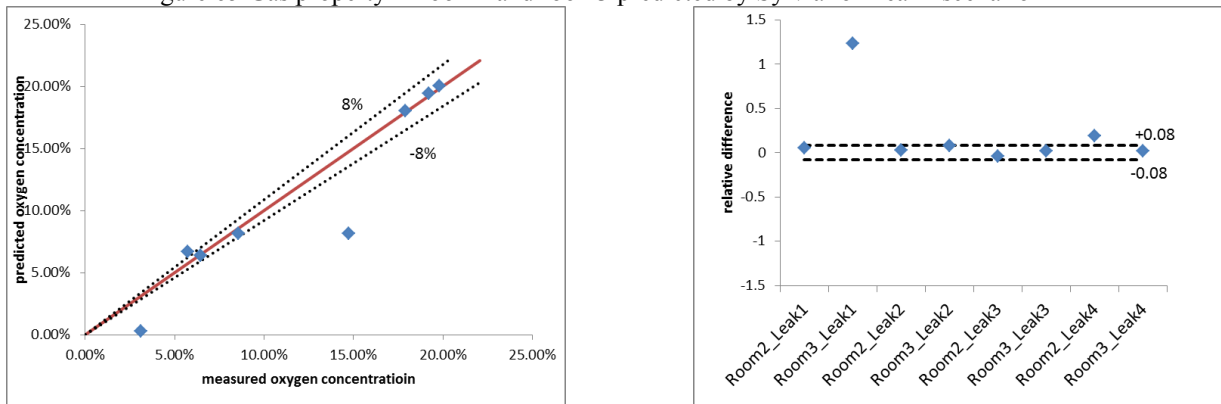


Figure 66 Oxygen concentration prediction by Sylvia

Carbon Dioxide Concentration

The upper layer carbon dioxide concentration from prediction is analyzed here. Generally speaking Sylvia predicts the dioxide concentration quite well, except for the upper layer of the target room in the Leak 1 scenario. This reveals the fact that Sylvia is not suitable for modeling leakage scenarios as in Leak1, which involves two circular pipes connecting two adjacent rooms. The same inaccuracy prediction for gas concentration also happens for oxygen concentration in this point.

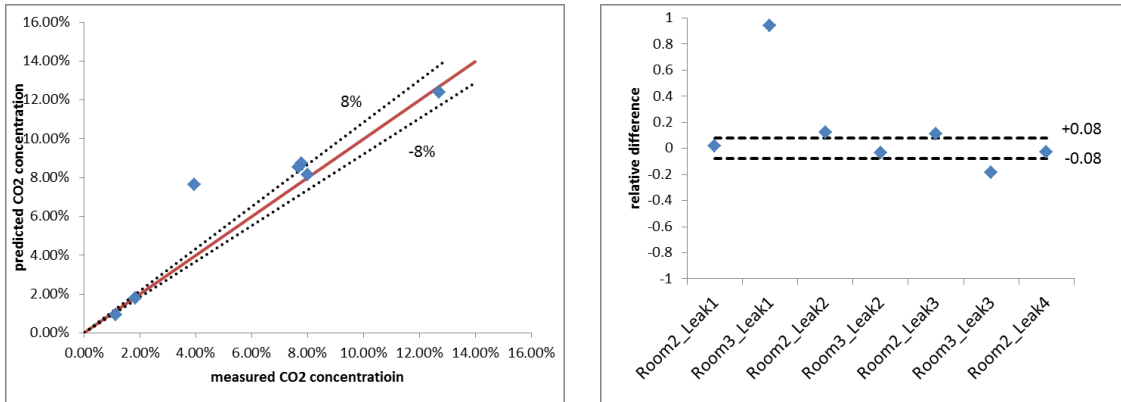


Figure 67 Carbon dioxide concentration prediction by Sylvia

Pressure

The combined uncertainty for the pressure measurement is quite large (± 0.75). All of the pressure predictions fall within the uncertainty boundary. Sylvia works quite well in regarding to prediction of pressure.

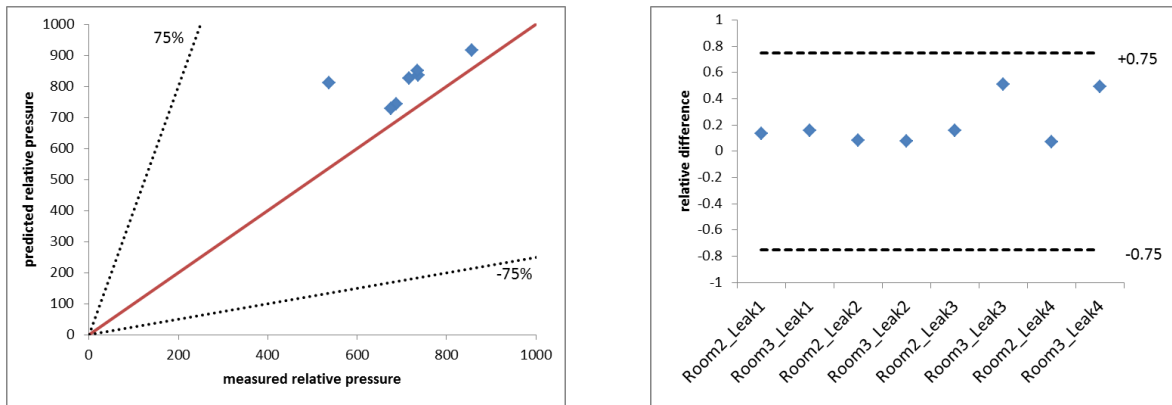


Figure 68 Relative pressure prediction by Sylvia

Gas Temperature

Sylvia overpredicts the hot gas layer temperature. This is due to the fact that Sylvia cannot predict the interface height well for scenarios with leakage.

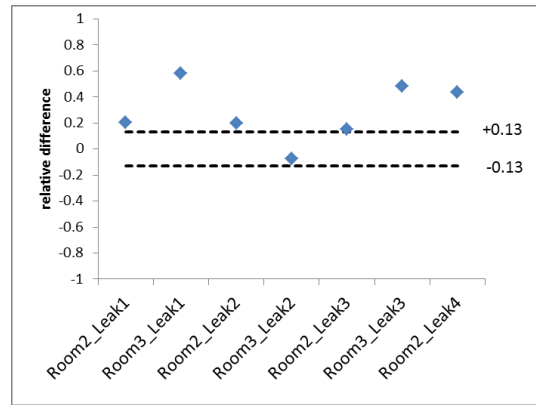
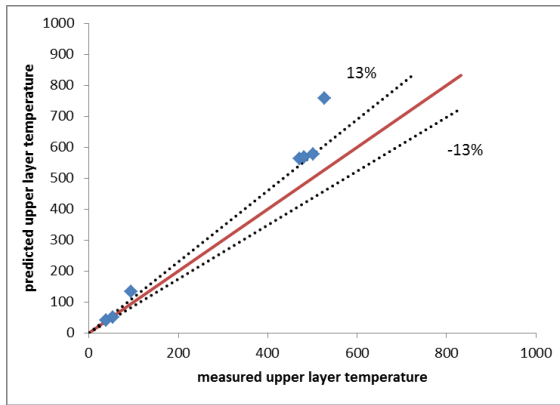
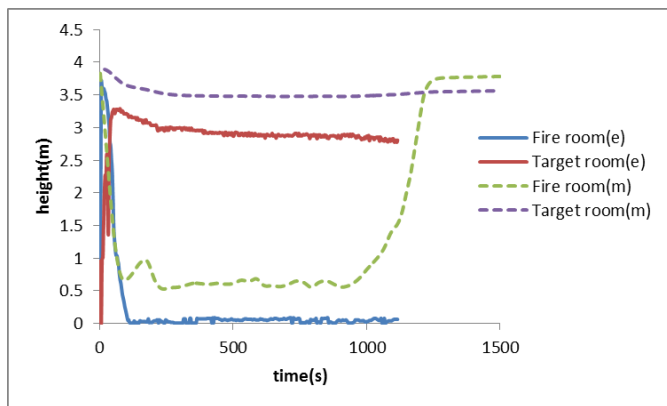


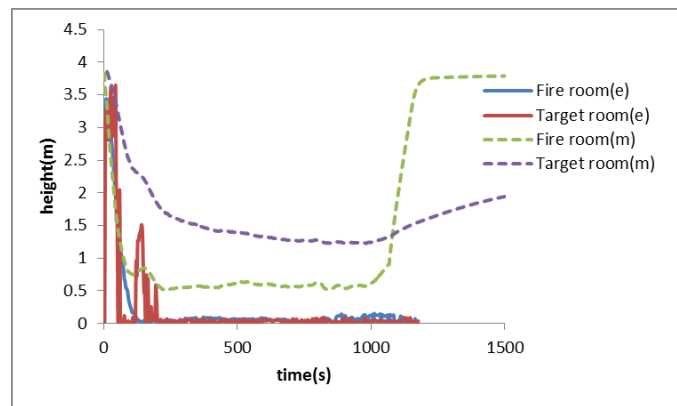
Figure 69 Hot gas layer temperature

Interface Height

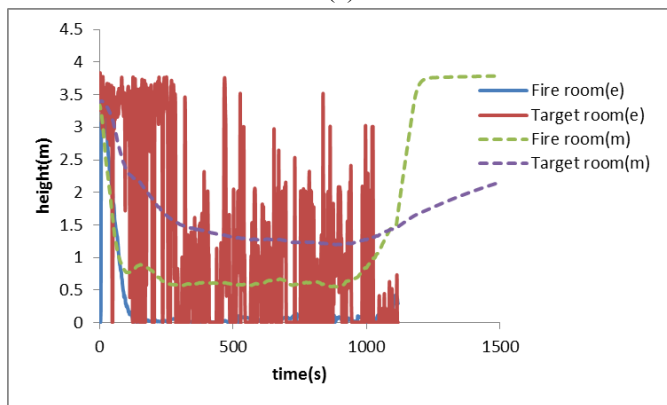
The figures below show the interface height from the four leakage scenarios. Sylvia predicts none of them correctly. It can be concluded that Sylvia cannot predict the two zone interface height correctly for scenarios involving leakage between two adjacent rooms. Indeed the wrong prediction of interface height would also lead to wrong prediction of gas temperature and other parameters.



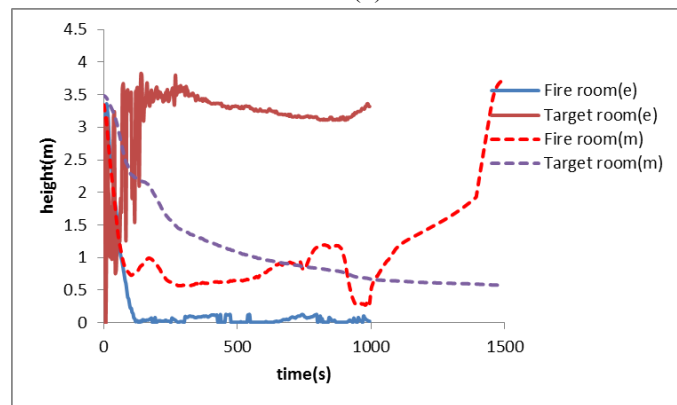
(a)



(b)



(c)



(d)

Figure 70 Interface height (a)Leak1 (b)Leak2 (c)Leak3 (d)Leak4

Ventilation Flow Rate

The ventilation flow rate prediction by Sylvia is satisfactory in the sense that all of the relative difference fall within uncertainty limit.

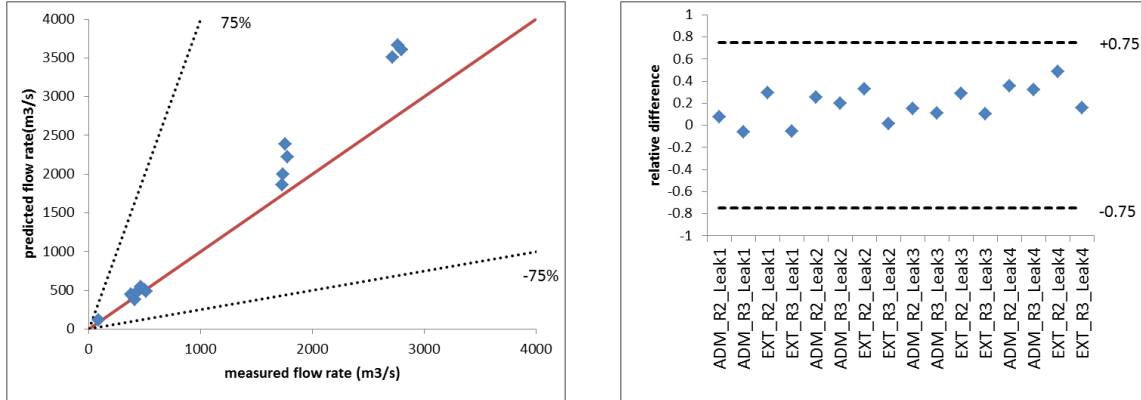


Figure 71 Ventilation flow rate prediction by Sylvia

4.3.2 Attribute-time Curve

Heat Flux:

The following figure shows the radiave heat flux from both test and simulation.

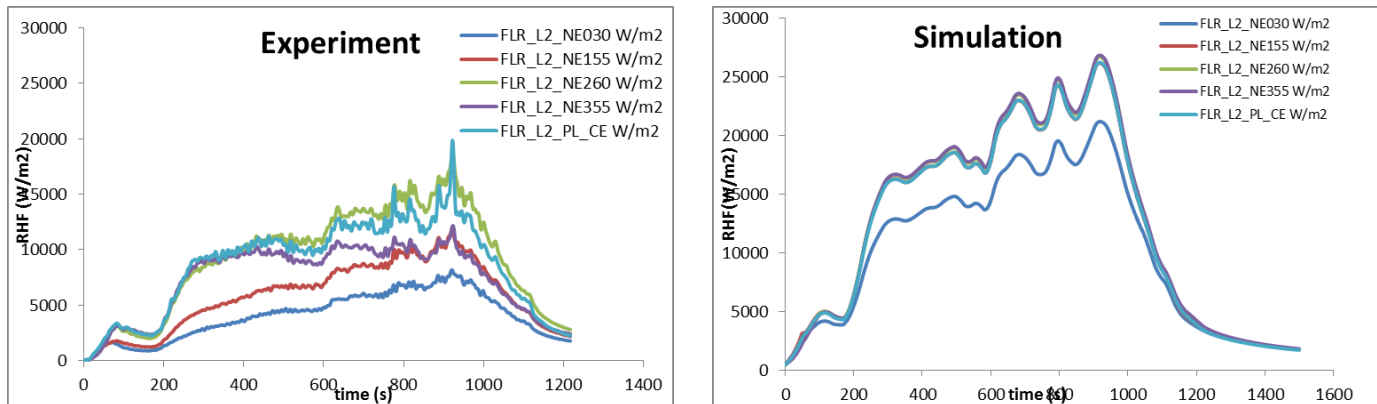


Figure 72 Radiative heat flux

Sylvia predicts the radiative heat flux well in regarding of general shape. However, as a two-zone model, Sylvia tends to give a well-mixed result. Sylvia also tends to overpredict the radiative heat flux. One interesting phenomenon is that the radiation fraction won't influence the radiative heat flux prediction of Sylvia. The flame temperature also has little difference on the radiative heat flux.

In Sylvia, it is possible to define a target with a fixed temperature so that the radiative heat flux calculated by Sylvia is identical to the radiative heat flux measured by radiometer used during the PRISME tests. No adjust as in ISIS is necessary here.

Wall Temperature

The following figure shows the wall temperature in the fire room.

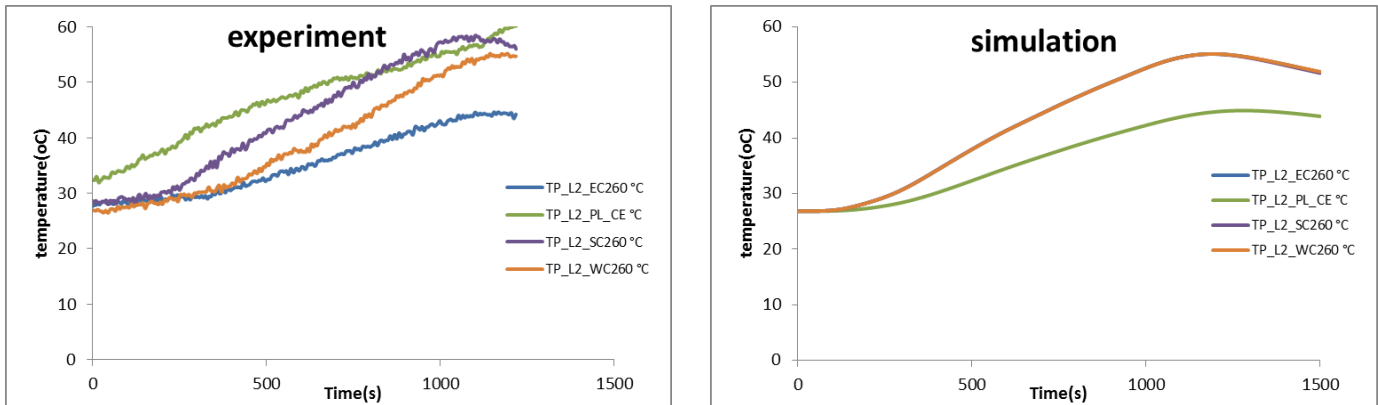


Figure 73 Wall temperature in fire room

The wall temperature is well predicted by Sylvia though an identical value is predicted for all walls. In Sylvia the wall has only one temperature regardless of its height in the wall. The value predicted by Sylvia is thus the average of the whole wall. This can also be the reason why there is discrepancy between simulation and experiment results.

The floor temperature is overpredicted, which can be explained by the fact that the radiative heat flux is overpredicted by Sylvia, leading to higher floor temperature.

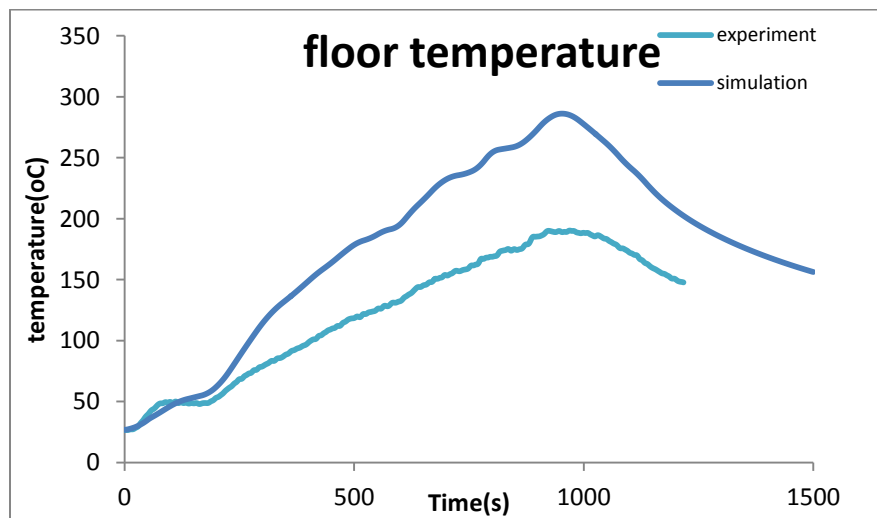


Figure 74 Floor temperature in the fire room

The figure below shows the wall temperature in the target room.

Sylvia gives one temperature for different positions in the target room. However, Sylvia still provides a satisfactory prediction for wall temperature in the target room.

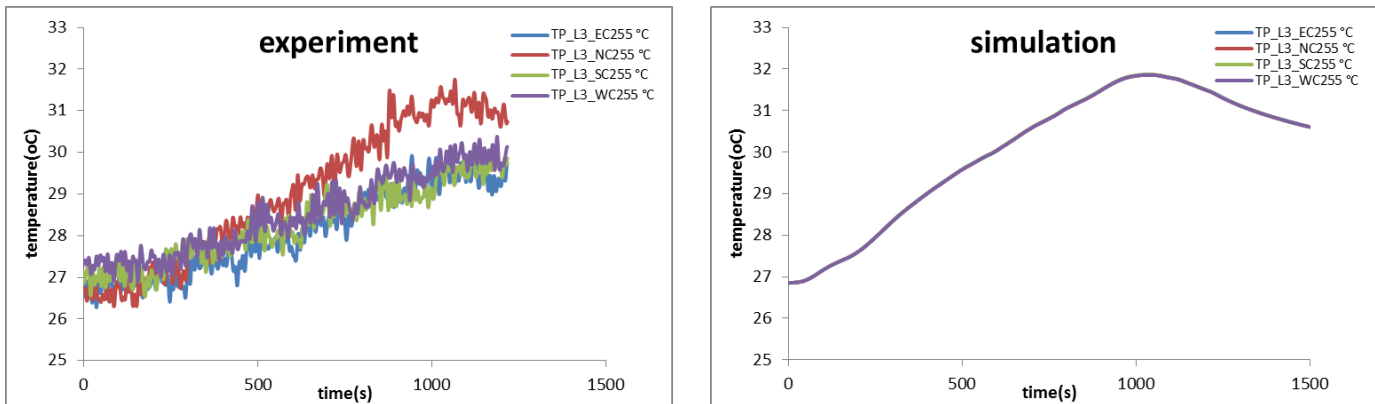


Figure 75 Wall temperature in target room

Soot Concentration

In Sylvia the soot concentration at the exhaust point is the same as in the upper layer. The soot concentration for tests and Sylvia is showed in the picture below.

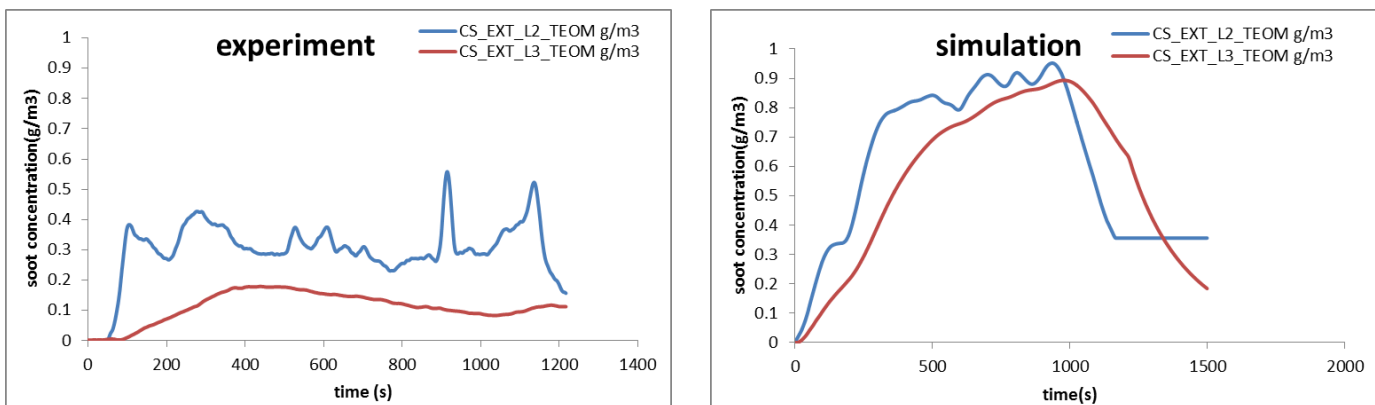


Figure 76 Soot concentration in the exhaust branches

Sylvia overpredicts the soot concentration in both rooms. This can be explained by the fact that in Sylvia the disposition of soot is not modeled and thus lead to higher soot concentration in the air. What is more, in the two-zone model turbulence in point is eliminated and thus in the Sylvia result there is no spikes. The soot concentration in the target room shows a very strange behavior. The same behavior has also been observed by ISIS. The soot concentration in the target room is even higher than that in the fire room by prediction.

The soot yield value used for simulation is calculated from experiment data and is much lower than the recommended value from SFPE. The soot concentration results show that using the soot yield value calculated from data is a better choice than SFPE book.

Oxygen Concentration

The figure below shows the oxygen concentration in the fire room. The lower layer oxygen concentration is predicted as the same as atmosphere. The upper layer oxygen concentration is very similar to that of the oxygen concentration near pool measured in test. If the oxygen concentration prediction is used to calculate the burning rate of fuel, then the prediction of Sylvia is satisfactory.

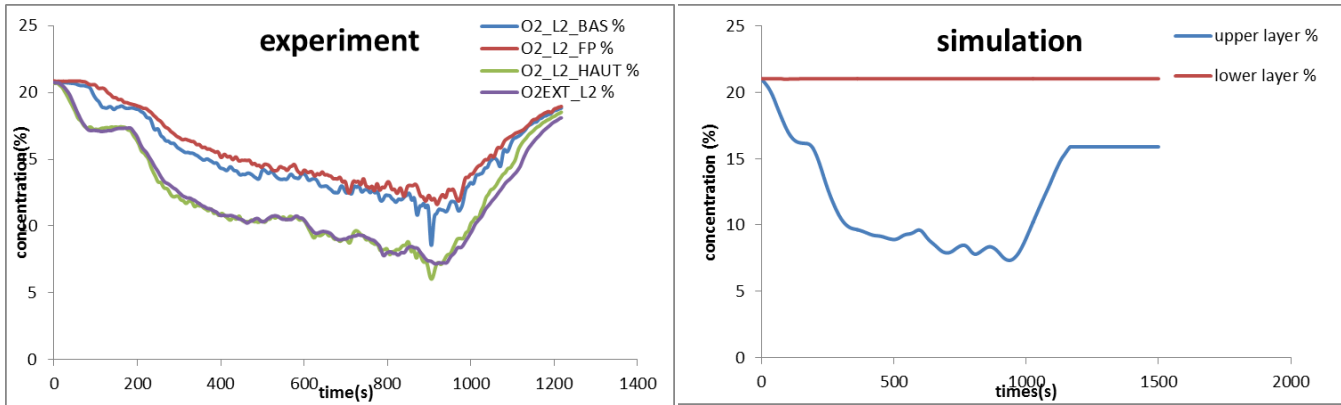


Figure 77 Oxygen concentration in the fire room

The figure below shows the oxygen concentration in the target room. The oxygen concentration in the upper layer is predicted almost equal to that in the upper layer of the fire room.

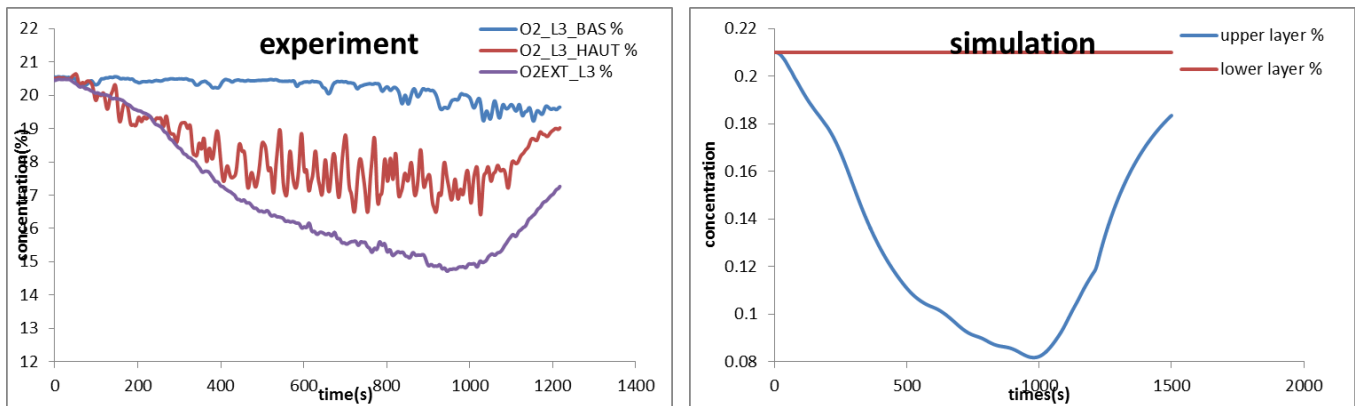


Figure 78 Oxygen concentration in the target room

CO₂ Concentration

The figure below shows the CO₂ concentration in the fire room. The CO₂ concentration predicted by Sylvia resembles the CO₂ concentration near the pool. The same behavior happens with oxygen concentration prediction too. Thus, Sylvia is able to predict the near pool gas concentration well.

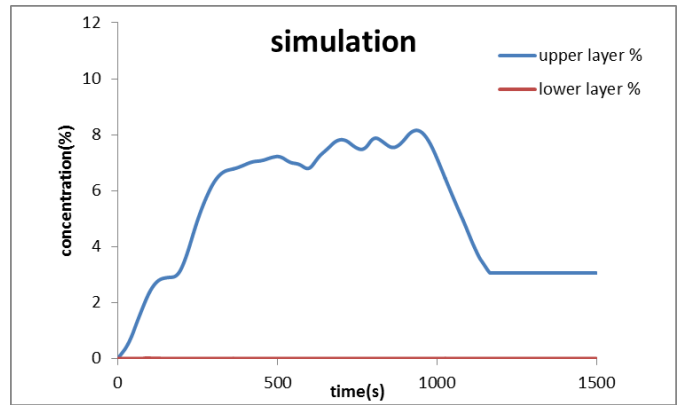
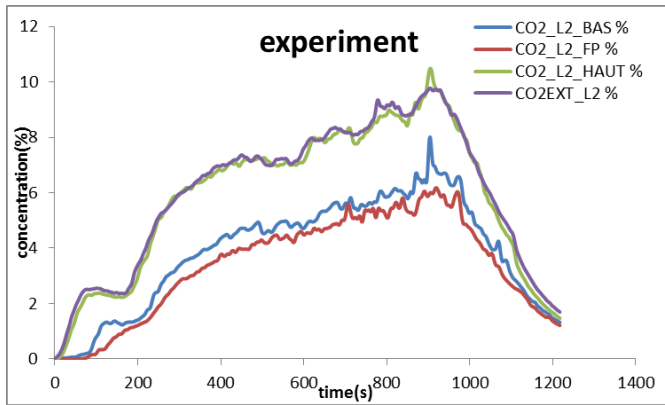


Figure 79 CO₂ concentration in the fire room

The figure below shows the CO₂ concentration in the target room. The CO₂ concentration in the upper layer is predicted almost equal to that in the upper layer of fire room.

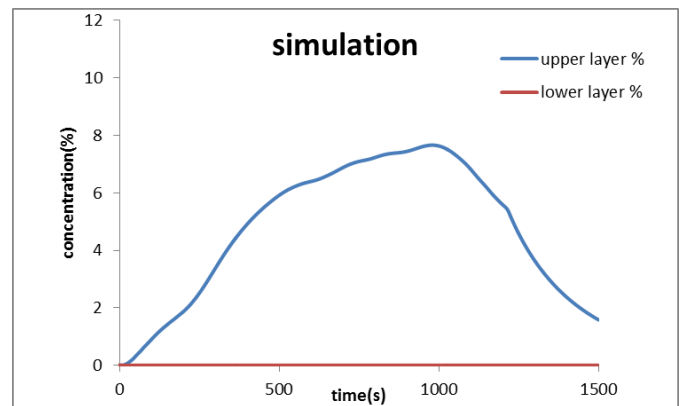
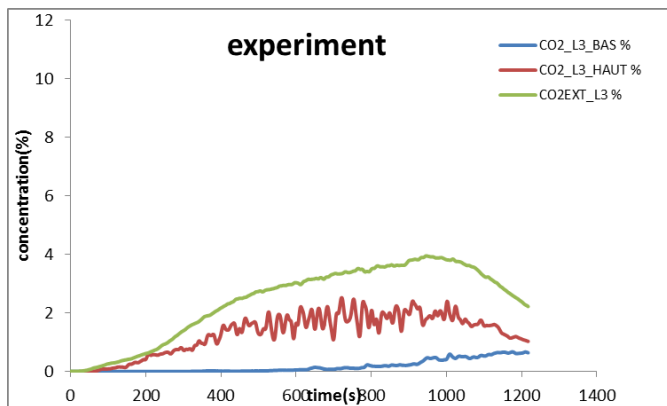


Figure 80 CO₂ concentration in the target room

Pressure

Figure 82 shows the relative pressure. Sylvia predicts the relative pressure quite well. However, the relative pressure stabilizes at a different value before ignition because of the inequilibrium of the ventilation network input.

In fact, the pressure inside both rooms stabilizes around zero before ignition. The pressure from prediction during the fire is consequently constantly higher than experimental data. The author studies the experimental data carefully and find out that there was one huge measurement mistake within the experimental data, which was used as model input.

The figure below shows the stable state of the ventilation system of DIVA used as initial condition in Sylvia. The green numbers mean the flow rate and the red numbers mean the node pressure. Inside the red circle is the inaccurate experimental data. In reality the flow rate 1 and the flow rate 2 should add up to the flow rate 3. However, the experimental data shows that $\dot{V}_1 + \dot{V}_2 = 11866 + 13339 = 25205 \text{ m}^3/\text{h}$ and $\dot{V}_3 = 21836 \text{ m}^3/\text{h}$. There is $(25205 - 21836)/21836 = 15.4\%$ of inbalance of flow rate for these three branches. It is hard to decide

which measurement is wrong for these three branches, thus the initial conditions are set as the experimental data is. The same problems happen with all PRISME leak scenarios.

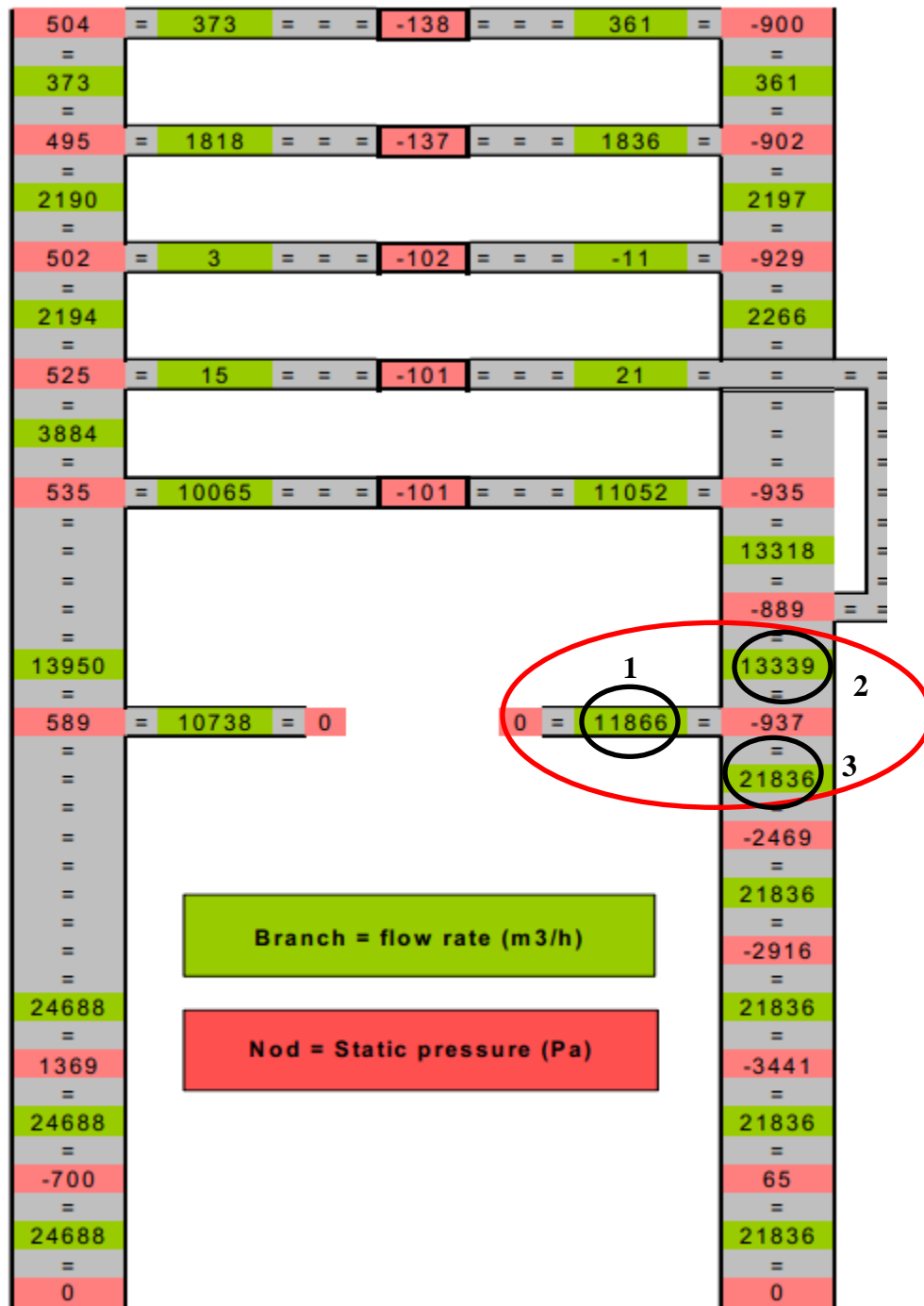


Figure 81 Measured static pressure and flow rate before ignition

Final results show that the inaccuracy of the model input from experimental data makes Sylvia overpredict the room pressure. With accurate experimental data, Sylvia should be able to predict the pressure even better.

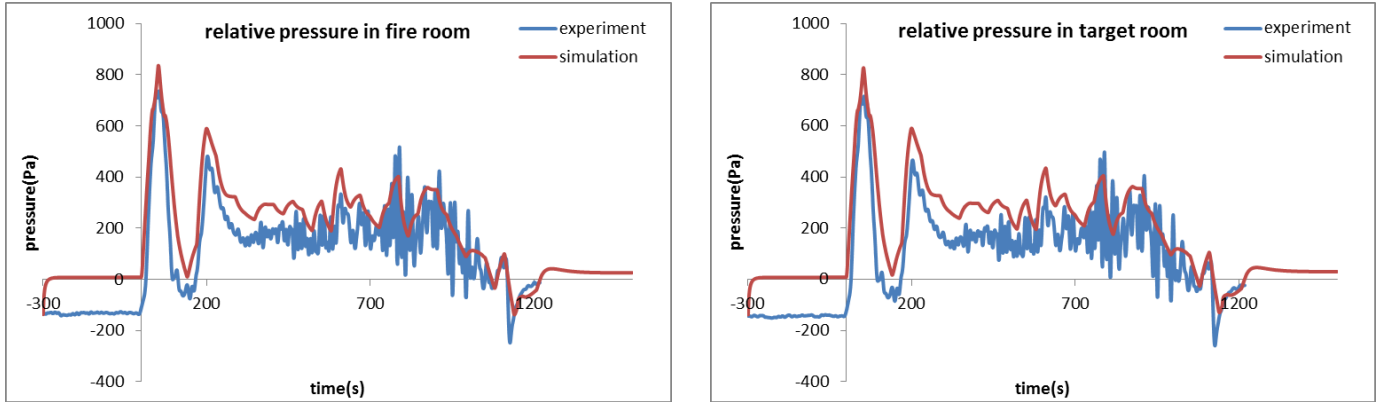


Figure 82 Relative pressure

Flow Rate

The figure below shows the flow rate at the admission and extraction branches of the ventilation network. Both volume and mass flow rate are compared. Flow rate in the target room is better predicted. Only volume flow rate in the exhaust branch of fire room is not predicted well. This can be explained by the fact that the exhaust gas temperature is not well predicted.

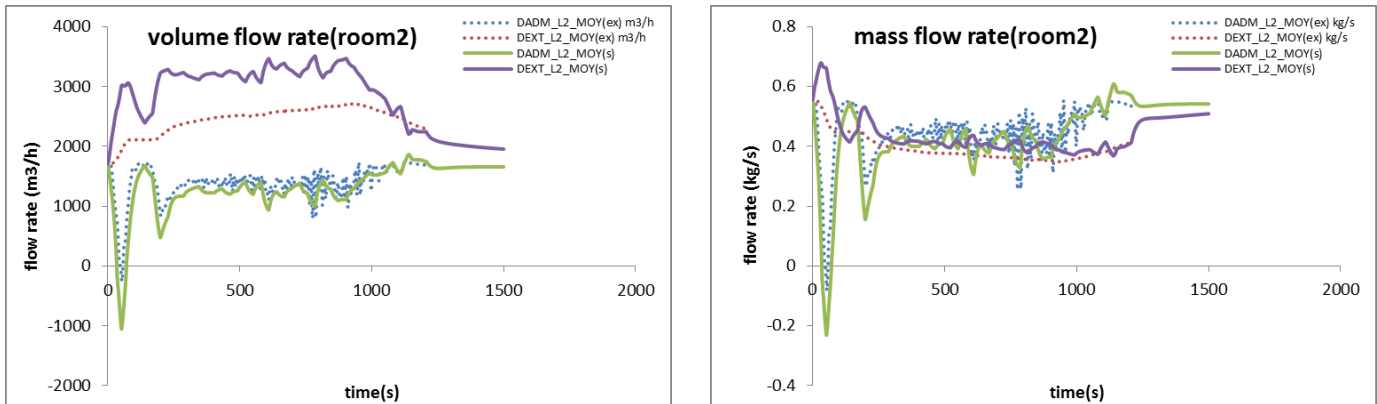


Figure 83 Flow rate in fire room

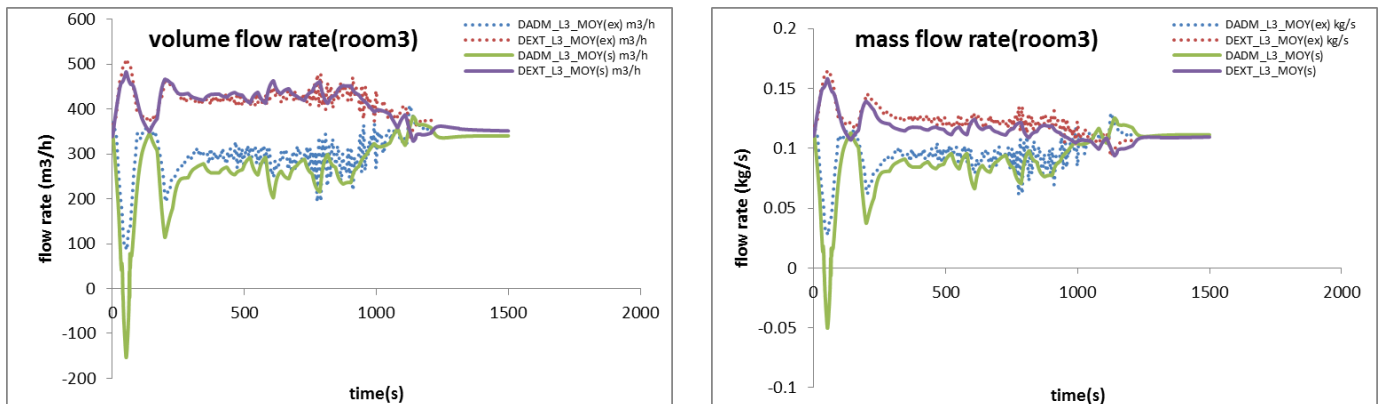


Figure 84 Flow rate in target room

Flow Rate of the Leakage

The mass flow rate and the volume flow rate through the leakage pipes are showed in the pictures below. The leakage flow rate is predicted quite well.

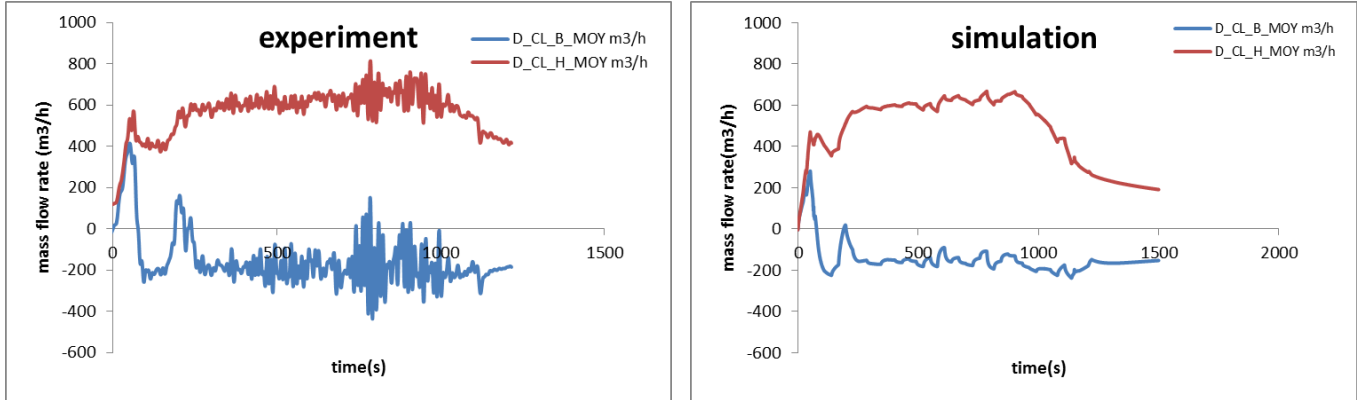


Figure 85 Flow rate through leakage pipes

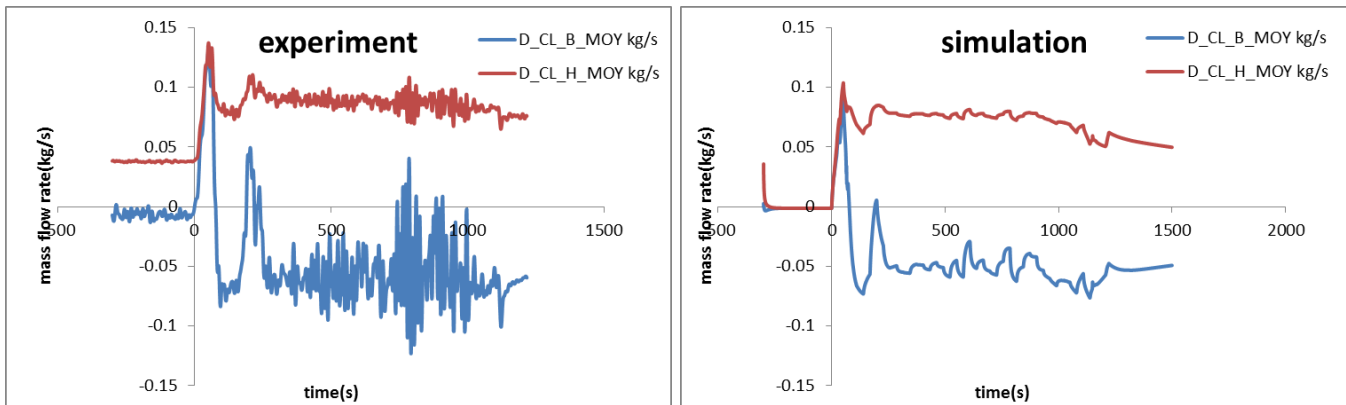


Figure 86 Mass flow rate through leakage pipes

The heat transferred from the fire room to the target room is determined jointly by the gas temperature and flow rate. Energy flow rate can be used to express the amount of energy transferred by leakage. The figure below shows the energy flow through leakage pipes. The energy flow through leakage is predicted quite well by Sylvia.

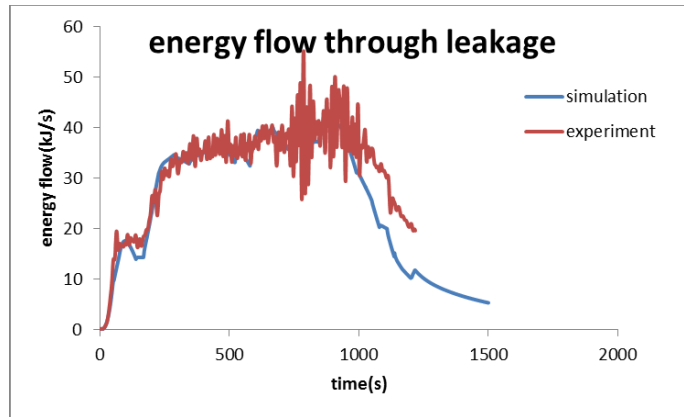


Figure 87 Energy flow rate through leakage pipes predicted by Sylvia

Gas Temperature

The hot gas layer temperature is compared below. The hot gas layer temperature of the experiments is calculated from the vertical temperature distribution [20].

The figures below show the two zone temperature in the rooms. Sylvia overpredicts the higher layer temperature in the fire room. However, Sylvia underpredicts the lower layer temperature in the fire room. This can be explained by the fact that Sylvia does not predict the interface height correctly. In the experiment the interface height is close to zero about 100 seconds after ignition. The lower layer temperature given by the reduction method [20] is indeed the temperature from the lowest thermocouple, which is also in the higher layer. That is why the lower layer temperature from experiment data is higher than that from the simulation. As the lower layer temperature is underpredicted in Sylvia, the upper layer temperature should be higher so that the energy balance can be kept.

The overprediction of the higher layer temperature in the target room can be explained by the fact the upper layer temperature in the fire room is overpredicted. Hotter gas would come into the upper layer of target room and as a result the upper layer temperature in the target room is overpredicted.

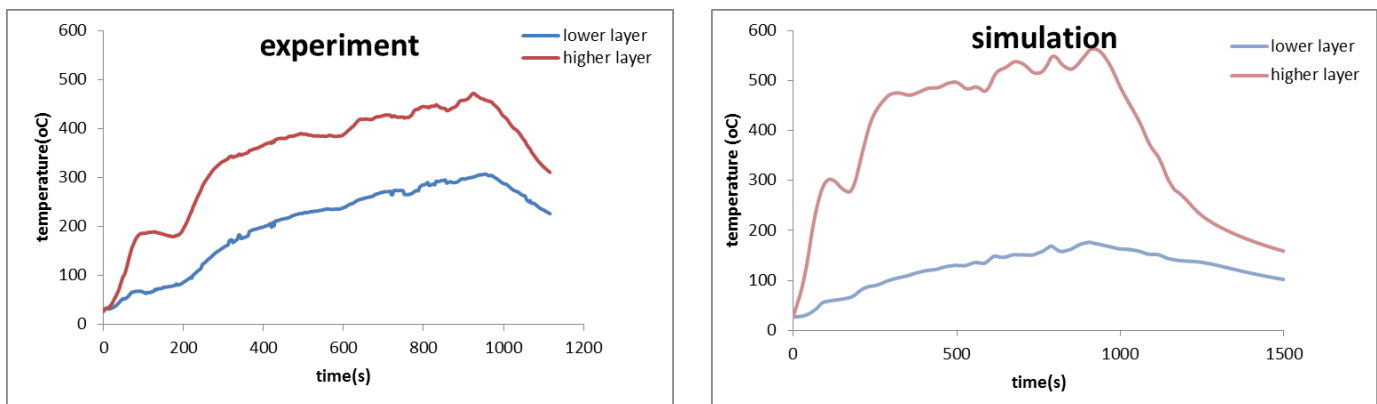


Figure 88 Two zone temperature in fire room

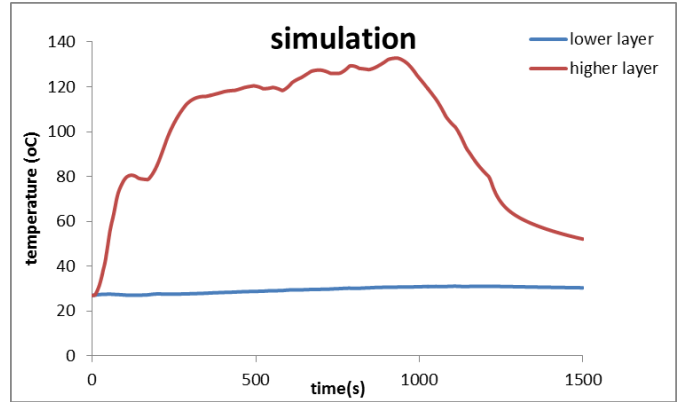
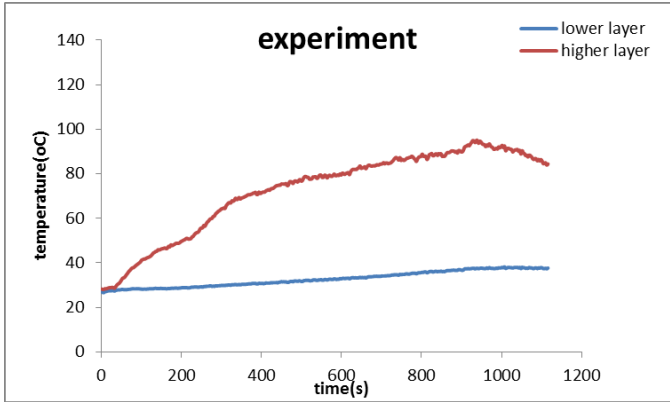


Figure 89 Two zone temperature in target room

The figure below shows the interface height in the rooms. Sylvia cannot predict interface height well. In fact, the interface height stables at the height of leakage pipe in both rooms. In the fire room the interface height is at the same height as the lower leakage pipe, where cold air is brought into from the target room. In the target room the interface height is at the same height the higher leakage pipe, where hot air is brought into from the fire room.

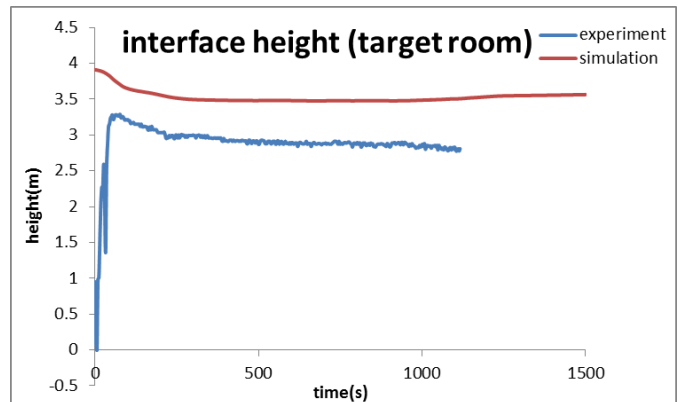
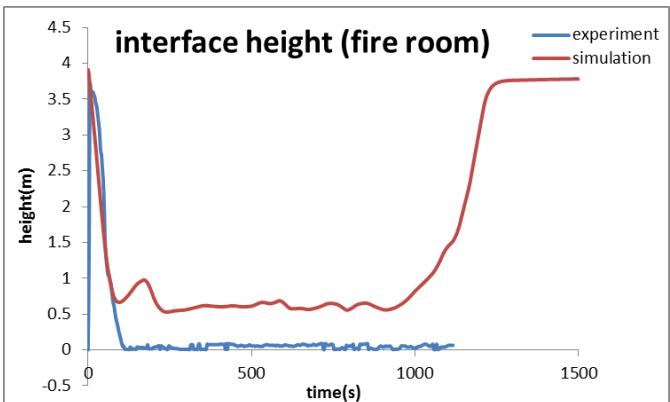


Figure 90 Interface height

5. DISCUSSION

5.1 Further Uncertainty for Real Application

Experimental uncertainty and model input uncertainty have been identified in current V&V studies. The model input uncertainty originates from the uncertainties of the input parameters such as HRR, material properties and dimension of configurations.

In the V&V study, the model input uncertainty is reduced to a minimum because most of the input comes from experimental data.

HRR is the most significant model input for simulation [17]. In most V&V studies, the HRR data is obtained from instrumentation measurements. The uncertainty of the input for HRR is thus the same as the measurement uncertainty of HRR, which varies between 7.1%~13.5% with the oxygen depletion method [41]. However, in real application, there is no experimental data for HRR, thus people need to estimate the HRR of the design fire scenario. In this case, the uncertainty of input HRR is much higher. Sometimes it is easy to estimate HRR as the case in the PRISME leak tests, where the fire source is liquid fuel pool. The mass loss rate of the fuel pool can be calculated by method of Babrauskas [42]. The figure below shows the HRR input for the leak4 scenario by Sylvia. The red curve stands for the HRR in the V&V study, where the measurement value is used. The blue curve stands for the HRR calculated by the method of Bakrauskas. Sylvia is used to produce the estimated HRR with lower oxygen limit. The difference of these two HRR curves reveals the further uncertainty for real application of fire model. What's more, the Bakrauskas calcualtioin method is valid for open air environment. Fire in compartment would further influence the HRR [45].

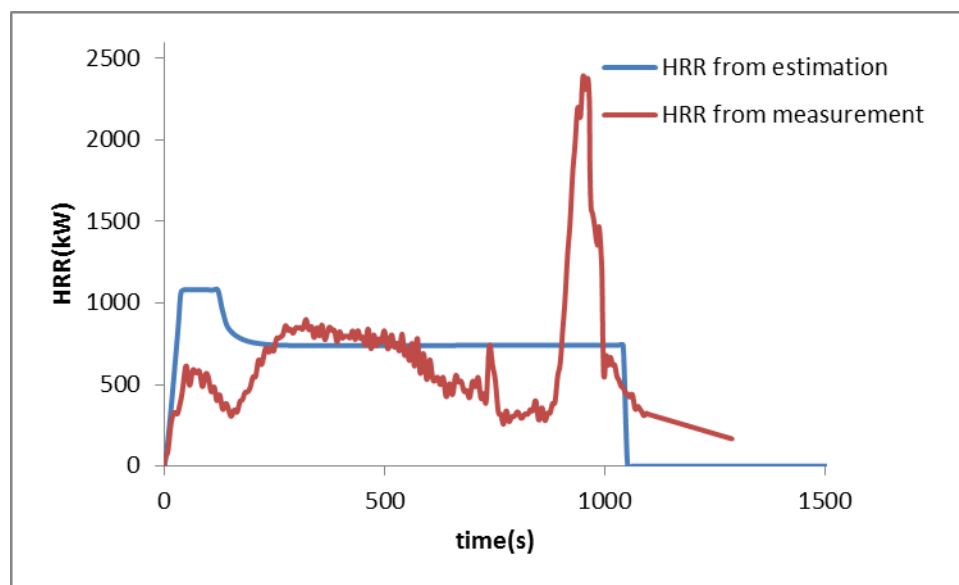


Figure 91 HRR input for leak 4 scenario

Soot yield fraction is another input that could cause large uncertainty. The input of soot yield fraction in this V&V study is calculated from experimental data. While in the real application, the soot yield fraction could be obtained from the SFPE hand book [11]. For the PRISME leak scenarios, the value from experimental data is 0.023; however, the recommended value from the SFPE book is 0.056. This would lead to further uncertainty because the radiation is very sensitive to sooty yield fraction.

A verified and validated fire model does not guarantee good predictions in real applications. As important as the quality of the fire model is the quality of the design fire scenario, where the HRR-curve and other key parameters are determined. It is possible that a model which gives good predictions in V&V study might give wrong predictions in real application. That is why sensitivity analysis is always an important procedure in applying fire models to real application.

5.2 Time Aspects in Validation Process

Metrics are used in this thesis for Quantitative Validation. Single point comparison is used as the criterion for the validation of fire models. For some scenarios, the timing of the fire is also an important attribute. The single criteria of using local single point value comparison can be misleading in some circumstances. Figure 87 shows model prediction for gas temperature with two different fire models.

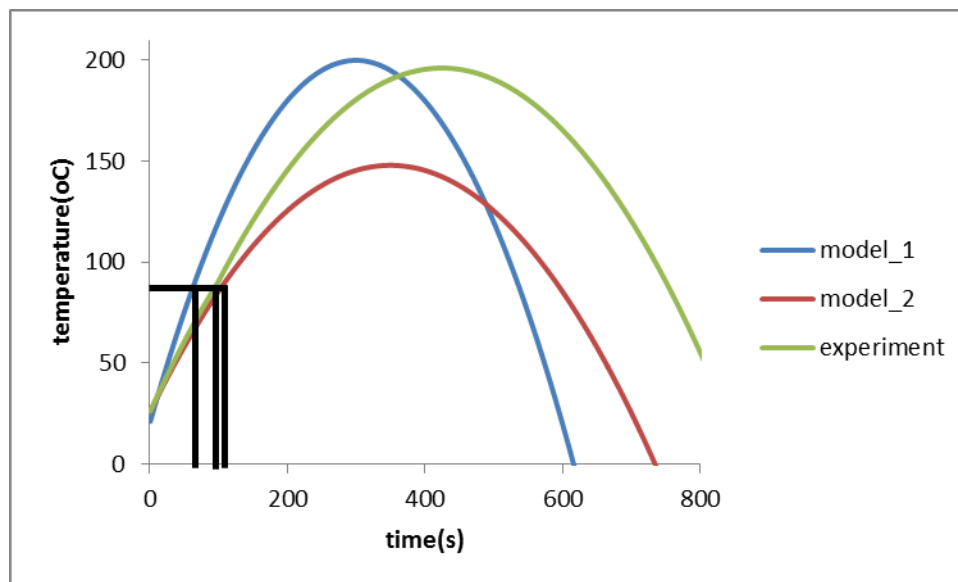


Figure 92 Gas temperature prediction by two models

The relative differences for the maximum gas temperature are:

Table 15 Relative differences for maximum value

	Maximum temperature(°C)	Relative difference
Experimental data	196	N/A
Model 1	200	2%

	Maximum temperature(°C)	Relative difference
Model 2	148	24%

Model 1 is by far better than model 2 if we only compare the maximum value. However, in some situations it can be the other way around. Now consider situation where the gas temperature prediction is used to determine the time for the activation of sprinkler (activation temperature of 85°C). The table below gives the time to for the gas temperature to reach 85°C:

Table 16 Prediction of activation time

	Activation time(s)	Relative difference
Experimental data	91	N/A
Model 1	61	33%
Model 2	100	10%

In this case model 2 provides a better gas temperature prediction for the activation of sprinkler. This simple example illustrates the fact that the maximum value alone cannot be the perfect criterion for fire model V&V study. The time aspects should also be integrated into the V&V study. However, currently there is no established way to incorporate time aspects into V&V study in a quantitative way. BONTE [23] proposed several normalised metrics for time-dependent comparisons. However, there is still no established method to use those normalised metrics in V&V study, which can be one of the future R&D work for Bel V.

Table 16 also indicates that the relative difference methodology can also be applied to time-related values.

5.3 Quantitative Criteria

In most V&V study for fire models, the criterion is to compare the relative difference with the combined uncertainty. If the relative difference is smaller than the combined uncertainty, the capability of the fire model is approved. One problem with this criterion is that it is dichotomic. A fire model can only either pass the criteria or fail it. And there is no way to compare the capabilities of two fire models if their relative differences are both within combined uncertainty range.

In the latest draft version of NUREG-1934 [17], NRC came up with a new quantitative criterion. Two statistical parameters are calculated for each model and each predicted quantity. The first quality, δ , is the bias factor. It indicates the extent to which the model, on average, under or overpredicts the measurements of a given quantity. For example, a bias factor of 1.02 for gas temperature means that the model over-estimates the value by 2% on average. The second statistic is the relative standard deviation of the model, $\tilde{\sigma}_M$, and the experiments, $\tilde{\sigma}_E$. These indicate the uncertainty or degree of “scatter” of the model and the experiments, respectively. Detailed calculation procedure for those statistic parameters can be found in [17]. Those statistic data can provide practical information for the model prediction.

It was the intention of the author of this thesis to apply this new methodology for this V&V study. However, the new method involves a statistic analysis of the model results. The statistic calculation procedure assumes that the quantity $\ln(M/E)$ is normally distributed. This is possible only when there are sufficient points in the sample. The V&V study conducted in this thesis only covers four test scenarios, the number of which is not high enough for statistical analysis. However the V&V study for ISIS and Sylvia is a continuous work at Bel V. Future V&V study for other PRISME tests would be done at Bel V. It is thus important that one standard database structure is established for Bel V so that all the future work results can be integrated together.

The following table shows the structure of this database. For the calculation of the statistical parameters, only the local max/min value of experimental data and simulation prediction of this local max/min value for each test is needed. As for each parameter there might be several measurement points thus one single table cannot contain all of these information. What's more, the value of the normalized parameters of each test should also be recorded. The data would be stored as Excel file and handed in together with the thesis report.

Table 17 Database structure for statistical analysis of V&V study

	ISIS				Sylvia								Experimental uncertainty	
	Leak1		Leak2		Leak1		Leak2		Leak3		Leak4			
	M	E	M	E	M	E	M	E	M	E	M	E		
Radiative heat flux														0.3
Wall temperature														0.11
Soot concentration														0.3
Oxygen concentration														0.01
Carbon dioxide														0.02
Pressure														0.01
Ventilation flow rate														0.1
Leakage flow rate														0.1
Gas temperature														0.08
Interface height														0.13
Two zone temperature														0.13

After several more V&V study by Bel V, there would be enough data available for statistical calculation. Normality test should be conducted for $\ln(M/E)$ of each parameter to determine whether or not data is enough. The normality test can be done by SPSS[43].

6. CONCLUSIONS

The table below gives an overview of the capabilities of fire models in predicting fire modeling attributes. The conclusions are made based on the results which are analyzed in chapter 4.

Table 18 Overview of models' capability

	ISIS	Sylvia
Radiative heat flux	Good prediction ⁶ .	Over-prediction. Possible problem existing with the radiation calculation of Sylvia.
Wall temperature	General good prediction for single layer wall. Unable to predict temperature for multilayer wall.	Unbiased however largely dispersed prediction.
Soot concentration	Good prediction in the fire room. Large relative difference in the target room.	Overprediction in both rooms.
Oxygen concentration	Good prediction.	Good prediction.
Carbon dioxide	Good prediction.	Good prediction.
Pressure	Bad prediction. Possible error with the output of pressure.	Good prediction.
Ventilation flow rate	Good prediction.	Good prediction.
Leakage flow rate	Good prediction.	Good prediction.
Gas temperature	Good prediction of hot gas layer temperature. Overprediction of lower layer temperature. More sensible temperature than experimental data for fire plume.	As two zone temperature.
Interface height	N/A	None of the interface height is predicted correctly.
Two zone temperature	N/A	The hot gas layer temperature is overpredicted because of wrong prediction of interface height.

The validity of the conclusion table is within the range of table 1. For a given set of experiments and NPP fire scenarios, the users can calculate the relevant normalized parameters. These parameters will either be inside, outside, or on the margin of the validation parameter space. NUREG_1934 [17] provides solutions for each situation:

1. If the parameters fall within the ranges that were evaluated in the validation study, then Table 16 can be referenced directly.

⁶ Adjusted simulation radiative heat flux provides good prediction

2. If only some of the parameters fall within the range of the study, additional justification is necessary (see section 2.3.7 of [17] for guidance). This is a common occurrence because realistic fire scenarios involve a variety of fire phenomena, some of which are easier to estimate than others.

3. If the parameters fall outside the range of the study, then a validation determination cannot be made based on the results from the study. The modeler needs to provide independent justification for using the particular model.

7. ACKNOWLEDGEMENTS

I would like to express my gratitude to my promoter, Bart Merici, who always gives me positive energy during my thesis writing process by great encouragement. Bart's expertise and patience, added significantly value to my graduate experience.

I would also like to express my gratitude to my thesis supervisor Bonte Frederick, who came up with my thesis topic and gave me enormous guidance. His truly scientist intuition has made him as a constant oasis of ideas and passions in science, which exceptionally inspire and enrich my growth as a student.

I would also like to thank my family for the support they provided me through my entire life. Although physically we are separated by great distance, mentally we are as close as ever.

In conclusion, I recognize that this research would not have been possible without the help from BelV, who provides me with the precious test data from PRISME projects. I would also like to express my gratitude for the IMFSE program, in which I learn so much during the two years in Europe.

8. REFERENCES

- [1] Laurent Audouin, Hugues Pr érel, William Le Saux, *OVERVIEW OF THE OECD PRISME PROJECT – MAIN EXPERIMENTAL RESULTS*, 21th International Conference on Structural Mechanics in Reactor Technology
- [2] NFPA 805: *Performance-based standard for fire protection for light water reactor electric generating plants*, 2010
- [3] ASTM E1355-05a: *Standard Guide for Evaluating the Predictive Capability of Deterministic Fire Models*. 2009
- [4] ISO 16730, '*Fire Safety Engineering – Assessment, verification and validation of calculation methods*', 2008
- [5] <http://www.oecd-nea.org/jointproj/prisme.html>
- [6] ISIS 3.0.0 - *Physical Modelling in ISIS* DPAM-SEMIC-2011-054/DL Ind.3. 2011
- [7] PRISME LEAK program-*PRS_LK_1 test report*; SERCI-2008-254-PRISME 28
- [8] PRISME LEAK program-*PRS_LK_2 test report*; SERCI-2008-254-PRISME 29
- [9] PRISME LEAK program-*PRS_LK_3 test report*; SERCI-2008-254-PRISME 30
- [10] PRISME LEAK program-*PRS_LK_4 test report*; SERCI-2008-254-PRISME 31
- [11] *SFPE Handbook of Fire Protection Engineering*, Third Edition. National Fire Protection Association
- [12] IRSN, *Validation of the ISIS CFD code for fire simulations*, DPAM/SEMIC-2008-167. 2008
- [13] Yeoh, G.H. and K.K. Yuen, *Computational fluid dynamics in fire engineering: theory, modelling and practice*. Amsterdam: Elsevier. ISBN 978-0-7506-8589-4, 2009.
- [14] *Verification and Validation of Selected Fire Models for Nuclear Power Plant Applications, Volume 2: Experimental Uncertainty*, U.S. Nuclear Regulatory Commission, Office of Nuclear Regulatory Research (RES), Rockville, MD, 2007, and Electric Power Research Institute (EPRI), Palo Alto, CA, NUREG-1824 and EPRI 1011999.
- [15] *PRISME DOOR Programme – Analysis Report*; DPAM/SEREA-2008-157 – PRISME 26
- [16] *Verification and Validation of Selected Fire Models for Nuclear Power Plant Applications, Volume 7: Fire Dynamics Simulator (FDS)*, U.S. Nuclear Regulatory Commission, Office of Nuclear Regulatory Research (RES), Rockville, MD, 2007, and Electric Power Research Institute (EPRI), Palo Alto, CA, NUREG-1824 and EPRI 1011999.
- [17] *Nuclear Power Plant Fire Modeling Application Guide (NPP FIRE MAG)*, Draft Report for Class Discussion U.S. Nuclear Regulatory Commission, Office of Nuclear Regulatory Research (RES), Washington, DC, 2010 and Electric Power Research Institute (EPRI), Palo Alto, CA, NUREG-1934 and EPRI 1023259.
- [18] H. PRETREL and R. THOME, *Theoretical relations for determining the fire Heat Release Rate*, DPAM/SEREA-2006-310 - PRISME - 11

- [19] PRISME LEAK program-*analysis report*; SERCI-2009-410-DR-PRISME 35
- [20] W. LE SAUX, PRISME SUPPORT - *Properties of materials used during the tests performed in the DIVA facility*, DPAM/SEREA-2006-355, PRISME-015
- [21] PRISME-SOURCE *Technical specification of the data* - DPAM/SEREA-2006-099 - PRISME-2006-06
- [22] W. Le Saux, H. Pretrel, J. M. Such, *The DIVA “multiroom” experimental facility and the DIVA-0 program*, 8th International Symposium on Fire Safety Science
- [23] Frederick BONTE, *Validation of Zone and Field Models to Support Fire Hazard Analysis and Fire PSA review of Fire Scenarios encountered in Nuclear Power Plants*
- [24] <https://gforge.irsrn.fr/gf/project/isis/frs/>
- [25] <http://www.open-mpi.org/software/ompi/v1.4/>
- [26] <http://glaros.dtc.umn.edu/gkhome/fetch/sw/metis/OLD/metis-4.0.3.tar.gz>
- [27] A. F. Sarofim and H. C. Hottel. *Radiative transfer in combustion chambers : Influences of alternative fuels*. Sixth Int. Heat Transfer Conf., 6 :119–217, 1978.
- [28] R. Viskanta and M. P. Menguc. *Radiation heat transfert in combustion system*. Prog. Energy Combust. Sci., 13 :97–160, 1987.
- [29] F.P. Incropera and D.P. DeWitt. *Fundamentals of Heat and Mass Transfer*. John Wiley and Sons, 4th edition, 1996.
- [30] *Methods for determining the fire Heat Release rate during PRISME-SOURCE tests*, DPAM/SEREA-2006-0320 - PRISME – 12
- [31] L. Audouin et , *Quantifying differences between computational results and measurements in the case of a large-scale well-confined fire scenario*, Nuclear Engineering and Design 241 (2011) 18–31
- [32] J. B. Moss, C. D. Stewart, and K. J. Syed. *Flowfield modelling of soot formation at elevated pressure*. In Combustion Institute, editor, Symposium International on Combustion, volume 22, pages 413–423, 1988.
- [33] J. B. Moss, C. D. Stewart, and K. J. Young. *Modeling soot formation and burnout in a high temperature laminar diffusion flame burning under oxygen-enriched conditions*. Combustion and Flame, 101:491–500, 1995
- [34] *Verification and Validation of Selected Fire Models for Nuclear Power Plant Applications, Volume 1: Main Report*, U.S. Nuclear Regulatory Commission, Office of Nuclear Regulatory Research (RES), Rockville, MD, 2007, and Electric Power Research Institute (EPRI), Palo Alto, CA, NUREG-1824 and EPRI 1011999.
- [35] Tourniaire B., Audouin L., *Sensitivity analysis of a data reduction method estimating the interface height, the lower and upper temperatures in fire room*, Proceedings of International Seminar on Fire and Explosion Hazards, 2000.
- [36] *Functional Specification for PRISME Leak Experiments*, PRISME-2007-26- January 2007
- [37] S. Suard, L. Audouin, F. Babik, L. Rigollet, and J.-C. Latché *Verification and validation of the ISIS CFD code for fire simulation. In Fire Safety Engineering - Examples on Assessment*,

Verification and Validation of Calculation Methods, Southwest Research Institute, USA, 2006.

- [38] S. Suard, S. Mésis, F. Babik, P. Querre, C. Lapuerta, L. Adouin and L. Rigollet, IRSN/DPAM, *Status of IRSN Fire Codes Development and Validation*, 2007.
- [39] *Physical modelling of the SYLVIA V1.4 code* DPAM-SEMIC-2009-441/Ind. 3
- [40] *ISIS 3.0.0 Verification tests*, DPAM-SEMIC-2011-076/DL Ind.1
- [41] Jesper Axelsson, Petra Andersson, Anders Lönnermark, Patrick Van Hees, Ingrid Wetterlund, *Uncertainties in measuring heat and smoke release rates in the Room/Corner Test and the SBI, NT Techn Report 477, NORDTEST Project No. 1480-00*
- [42] Dougal Drysdale, *An introduction to fire dynamics*, second edition, JOHN WILEY & SONS
- [43] <https://statistics.laerd.com/spss-tutorials/testing-for-normality-using-spss-statistics.php>
- [44] *ISIS 3.0.0 Tutorial*, DPAM-SEMIC-2011-331 Ind.3, IRSN
- [45] HUGUES PRETREL et, *Experimental Study of Burning Rate Behaviour in Confined and Ventilated Fire Compartments*

9. APPENDICES

9.1 ISIS script

```
MODULE ISIS
$$$__short_name="Leak1"
$$$__created_by="fbo"
$$$__creation_date="Thu Sep 16 10:52:53 BST 2010"
$$$__file_name="Leak1.pe1"
SDS_LX=5.0
SDS_Xpool=2.5
SDS_Lxpool=0.63
SDS_Xvent=2.5
SDS_Lxvent=0.4
SDS_minx_pool=(SDS_Xpool-$DS_Lxpool/2.e+00)
SDS_maxx_pool=(SDS_Xpool+$DS_Lxpool/2.e+00)
SDS_minx_adm_s=(SDS_Xvent-$DS_Lxvent/2.e+00)
SDS_maxx_adm_s=(SDS_Xvent+$DS_Lxvent/2.e+00)
SDV_MESH_X=(regular_vector($DS_X1, 14, $DS_X2)
<<
regular_vector($DS_X2, 2, $DS_X3) <<
regular_vector($DS_X3, 2, $DS_X4) <<
regular_vector($DS_X4, 2, $DS_X5) <<
regular_vector($DS_X5, 11, $DS_X6) <<
regular_vector($DS_X6, 4, $DS_X7) <<
regular_vector($DS_X7, 2, $DS_X8) <<
regular_vector($DS_X8, 4, $DS_X9) <<
regular_vector($DS_X9, 9, $DS_X10) <<
regular_vector($DS_X10, 3, $DS_X11) <<
regular_vector($DS_X11, 16, $DS_X12))
SDS_CenterRod1=0.09
SDS_Diamrod=0.02216
SDS_CenterRod2=0.18
SDS_LPlateX=0.266
SDS_tPlate=0.013
SDS_SchiftR2X=5.3
SDS_LY=6.0
SDS_Lypool=0.63
SDS_Lyvent=0.4
SDS_Ypool=3.0
SDS_miny_ext_s=0.4
SDS_maxy_ext_s=(4.e-01+$DS_Lyvent)
SDS_maxy_pool=(SDS_Ypool+$DS_Lypool/2.e+00)
SDS_miny_pool=(SDS_Ypool-$DS_Lypool/2.e+00)
SDS_miny_adm_s=(SDS_LY-$DS_Lyvent-4.e-01)
SDS_maxy_adm_s=(SDS_LY-4.e-01)
SDV_MESH_Y=(regular_vector($DS_Y1, 3, $DS_Y2) <<
regular_vector($DS_Y2, 1, $DS_Y3) <<
regular_vector($DS_Y3, 2, $DS_Y4) <<
regular_vector($DS_Y4, 1, $DS_Y5) <<
regular_vector($DS_Y5, 12, $DS_Y6) <<
regular_vector($DS_Y6, 5, $DS_Y7) <<
regular_vector($DS_Y7, 12, $DS_Y8) <<
regular_vector($DS_Y8, 1, $DS_Y9) <<
regular_vector($DS_Y9, 1, $DS_Y10) <<
regular_vector($DS_Y10, 2, $DS_Y11) <<
regular_vector($DS_Y11, 1, $DS_Y12) <<
regular_vector($DS_Y12, 1, $DS_Y13) <<
regular_vector($DS_Y13, 3, $DS_Y14))
SDS_miny_ext_r=0.45
SDS_maxy_ext_r=0.75
SDS_miny_tray=(SDS_Ypool-$DS_Lytray/2.e+00)
SDS_miny_door=(SDS_Ypool-$DS_Lydoor/2.e+00)
SDS_maxy_door=(SDS_Ypool+$DS_Lydoor/2.e+00)
SDS_maxy_tray=(SDS_Ypool+$DS_Lytray/2.e+00)
SDS_miny_adm_r=(SDS_LY-7.5e-01)
SDS_maxy_adm_r=(SDS_LY-4.5e-01)
SDS_Lytray=1.0
SDS_Lydoor=0.72
SDS_LZ=4.0
SDS_Pan_height=0.4
SDS_minz_vent_s=(SDS_LZ-$DS_Hvent)
SDS_Hvent=0.9
SDS_maxz_vent_s=(SDS_LZ)
SDS_minz_vent_r=(SDS_minz_vent_s)
SDS_maxz_vent_r=(SDS_minz_vent_s+$DS_Hvent_r)
SDS_Hvent_r=0.6
SDV_MESH_Z=(regular_vector($DS_Z1, 3, $DS_Z2) <<
regular_vector($DS_Z2, 1, $DS_Z3) <<
regular_vector($DS_Z3, 2, $DS_Z4) <<
regular_vector($DS_Z4, 1, $DS_Z5) <<
regular_vector($DS_Z5, 17, $DS_Z6) <<
regular_vector($DS_Z6, 1, $DS_Z7) <<
regular_vector($DS_Z7, 2, $DS_Z8) <<
regular_vector($DS_Z8, 1, $DS_Z9) <<
regular_vector($DS_Z9, 2, $DS_Z10) <<
regular_vector($DS_Z10, 1, $DS_Z11))
SDS_PosTray2=0.5
SDS_LPlateZ=0.048
SDS_Lzdoor=2.15
SDS_PosTray1=(SDS_LZ-5.e-01)
SDS_minx_ext_s=(SDS_Xvent-$DS_Lxvent/2.e+00)
SDS_maxx_ext_s=(SDS_Xvent+$DS_Lxvent/2.e+00)
SDS_Small=1.0E-6
SDS_tinit=-10.0
SDS_tend=1250.0
SDS_dt=0.1
SDS_k0=1.0E-6
SDS_epsilon0=1.0E-9
SDS_P0=(SDS_Pref+$DS_Plocal)
SDS_Pref=101325.0
SDS_Plocal=-97.7
SDS_Tref=298.15
SDS_Cp=1020.0
SDS_rho0=(SDS_P0/$DS_Tref/$DS_R)
SDS_R=287.0
SDS_Q=(interpol("Leak1_MLR.txt", $DS_T))
$$$_k_pool="1.e-5"
SDS_k_pool=1.0E-5
$$$_epsilon_pool="1.e-9"
SDS_epsilon_pool=1.0E-9
SDS_TFuel=461.0
SDS_H_pool=(SDS_FuelInj*(SDS_Cp*(SDS_TFuel-
SDS_Tref)+$DS_HcFuelEff))
SDS_FuelInj=(( $DS_Q>0.e+00 ? 1.e+00 : 0.e+00 ) )
SDS_HcFuelEff=(SDS_HcFuel*(1.e+00-$DS_RadFrac))
SDS_HcFuel=4.55E7
SDS_RadFrac=0.0
SDS_DP_ADM=495.0
SDS_R_ADM=2107.0
SDS_DP_EXT=-902.0
SDS_R_EXT=2501.0
```

```

$IS_SAVE=150
$IS_SAVE2=100
$IS_NX=4
$IS_NY=2
$IS_NZ=2
$DV_wall=(stretched_vector(0.e+00, 1.e-04, 5.e-02, 3.e-
01))
$DS_rhoFuel=(($DS_P0*$DS_WCH2H26/8.31e+00/$DS_
TFuel)
$DS_WCH2H26=0.17
$DS_rhoSoot=1800.0
$DS_R_ADM2=50852.0
$DS_R_EXT2=64437.0
$DS_DP_ADM2=504.0
$DS_DP_EXT2=-900.0
$DS_s_soot=0.338
$DS_X1=0.03
$DS_X2=2.1125
$DS_X3=2.35
$DS_X4=2.65
$DS_X5=2.8875
$DS_X6=4.4
$DS_X7=4.97
$DS_X8=5.3
$DS_X9=5.9
$DS_X10=7.6
$DS_X11=8.0
$DS_X12=10.3
$DS_Y1=0.03
$DS_Y2=0.4
$DS_Y3=0.45
$DS_Y4=0.75
$DS_Y5=0.8
$DS_Y6=2.6125
$DS_Y7=3.3875
$DS_Y8=5.2
$DS_Y9=5.25
$DS_Y10=5.317
$DS_Y11=5.503
$DS_Y12=5.55
$DS_Y13=5.6
$DS_Y14=5.97
$DS_Z1=0.0
$DS_Z2=0.4
$DS_Z3=0.467
$DS_Z4=0.653
$DS_Z5=0.71
$DS_Z6=3.25
$DS_Z7=3.307
$DS_Z8=3.493
$DS_Z9=3.55
$DS_Z10=3.85
$DS_Z11=3.95
MODULE meshing
MODULE macro_colors
concrete_walls=<"right" "bottom" "behind" "top" "wall1"
"wall2" "wall3" "wall4" "wall5" "wall6" "wall7">
ceiling=<"front">
adiabatic_walls=<"ad1" "ad2" "ex1" "ex2" "firepool"
"leak1" "leak2" "leak3" "leak4" "leak5" "leak6" "leak7"
"leak8" "leak9" "leak10" "leak11" "leak12" "leak13"
"leak14" "leak15" "leak16">

```

```

admission=<"admission1">
extraction=<"exhaust1">
pool_fire_front=<"pool">
admission2=<"admission20">
extraction2=<"exhaust20">
insulation_walls=<"sw" "nw" "ew1" "ew2" "ew3" "ew4"
"ew5" "ew6" "ew7" "left">
leaku=<"leakup">
leakd=<"leakdown">
END MODULE macro_colors
MODULE GE_Meshing
MODULE GE_Colorist
MODULE faces
admission1=(in_box($DV_X, vector($DS_X3, $DS_Y13-
$DS_Small, $DS_Z6), vector($DS_X4,
$DS_Y13+$DS_Small, $DS_Z10)))
exhaust1=(in_box($DV_X, vector($DS_X3, $DS_Y2-
$DS_Small, $DS_Z6), vector($DS_X4,
$DS_Y2+$DS_Small, $DS_Z10)))
admission20=(in_box($DV_X, vector($DS_X11-
$DS_Small, $DS_Y9, $DS_Z6),
vector($DS_X11+$DS_Small, $DS_Y12, $DS_Z10)))
exhaust20=(in_box($DV_X, vector($DS_X11-$DS_Small,
$DS_Y3, $DS_Z6), vector($DS_X11+$DS_Small,
$DS_Y4, $DS_Z10)))
leakup=(in_box($DV_X, vector($DS_X6-$DS_Small,
$DS_Y10, $DS_Z7), vector($DS_X6+$DS_Small,
$DS_Y11, $DS_Z8)))
leakdown=(in_box($DV_X, vector($DS_X6-$DS_Small,
$DS_Y10, $DS_Z3), vector($DS_X6+$DS_Small,
$DS_Y11, $DS_Z4)))
pool=(in_box($DV_X, vector($DS_X2, $DS_Y6, $DS_Z2-
$DS_Small), vector($DS_X5, $DS_Y7,
$DS_Z2+$DS_Small)))
sw=(in_box($DV_X, vector($DS_X1, $DS_Y1-
$DS_Small, $DS_Z1), vector($DS_X7,
$DS_Y1+$DS_Small, $DS_Z11)))
nw=(in_box($DV_X, vector($DS_X1, $DS_Y14-
$DS_Small, $DS_Z1), vector($DS_X7,
$DS_Y14+$DS_Small, $DS_Z11)))
ew1=(in_box($DV_X, vector($DS_X7-$DS_Small,
$DS_Y1, $DS_Z9), vector($DS_X7+$DS_Small,
$DS_Y14, $DS_Z11)))
ew4=(in_box($DV_X, vector($DS_X7-$DS_Small,
$DS_Y1, $DS_Z5), vector($DS_X7+$DS_Small,
$DS_Y14, $DS_Z6)))
ew7=(in_box($DV_X, vector($DS_X7-$DS_Small,
$DS_Y1, $DS_Z1), vector($DS_X7+$DS_Small,
$DS_Y14, $DS_Z2)))
ew2=(in_box($DV_X, vector($DS_X7-$DS_Small,
$DS_Y12, $DS_Z6), vector($DS_X7+$DS_Small,
$DS_Y14, $DS_Z9)))
ew3=(in_box($DV_X, vector($DS_X7-$DS_Small,
$DS_Y1, $DS_Z6), vector($DS_X7+$DS_Small, $DS_Y9,
$DS_Z9)))
ew5=(in_box($DV_X, vector($DS_X7-$DS_Small,
$DS_Y12, $DS_Z2), vector($DS_X7+$DS_Small,
$DS_Y14, $DS_Z5)))
ew6=(in_box($DV_X, vector($DS_X7-$DS_Small,
$DS_Y1, $DS_Z2), vector($DS_X7+$DS_Small, $DS_Y9,
$DS_Z5)))
END MODULE faces

```

```

END MODULE GE_Colorist
MODULE GE_Meshing
type="box_meshing"
concrete_name="GE_BoxWithBoxes"
mesh_polyhedron=<"GE_Rectangle" "GE_Cuboid">
vertices_coordinate_0=($DV_MESH_X)
vertices_coordinate_1=($DV_MESH_Y)
vertices_coordinate_2=($DV_MESH_Z)
END MODULE GE_Meshing
MODULE holes
wall1=(in_box($DV_X, vector($DS_X7, $DS_Y1,
$DS_Z8), vector($DS_X8, $DS_Y14, $DS_Z11)))
wall2=(in_box($DV_X, vector($DS_X7, $DS_Y1,
$DS_Z7), vector($DS_X8, $DS_Y10, $DS_Z8)))
wall3=(in_box($DV_X, vector($DS_X7, $DS_Y11,
$DS_Z7), vector($DS_X8, $DS_Y14, $DS_Z8)))
wall4=(in_box($DV_X, vector($DS_X7, $DS_Y1,
$DS_Z4), vector($DS_X8, $DS_Y14, $DS_Z7)))
wall5=(in_box($DV_X, vector($DS_X7, $DS_Y1,
$DS_Z3), vector($DS_X8, $DS_Y10, $DS_Z4)))
wall6=(in_box($DV_X, vector($DS_X7, $DS_Y11,
$DS_Z3), vector($DS_X8, $DS_Y14, $DS_Z4)))
wall7=(in_box($DV_X, vector($DS_X7, $DS_Y1,
$DS_Z1), vector($DS_X8, $DS_Y14, $DS_Z3)))
leak1=(in_box($DV_X, vector($DS_X6, $DS_Y9,
$DS_Z8), vector($DS_X7, $DS_Y12, $DS_Z9)))
leak2=(in_box($DV_X, vector($DS_X6, $DS_Y9,
$DS_Z7), vector($DS_X7, $DS_Y10, $DS_Z8)))
leak3=(in_box($DV_X, vector($DS_X6, $DS_Y11,
$DS_Z7), vector($DS_X7, $DS_Y12, $DS_Z8)))
leak4=(in_box($DV_X, vector($DS_X6, $DS_Y9,
$DS_Z6), vector($DS_X7, $DS_Y12, $DS_Z7)))
leak5=(in_box($DV_X, vector($DS_X8, $DS_Y9,
$DS_Z8), vector($DS_X9, $DS_Y12, $DS_Z9)))
leak6=(in_box($DV_X, vector($DS_X8, $DS_Y9,
$DS_Z7), vector($DS_X9, $DS_Y10, $DS_Z8)))
leak7=(in_box($DV_X, vector($DS_X8, $DS_Y11,
$DS_Z7), vector($DS_X9, $DS_Y12, $DS_Z8)))
leak8=(in_box($DV_X, vector($DS_X8, $DS_Y9,
$DS_Z6), vector($DS_X9, $DS_Y12, $DS_Z7)))
leak9=(in_box($DV_X, vector($DS_X6, $DS_Y9,
$DS_Z4), vector($DS_X7, $DS_Y12, $DS_Z5)))
leak10=(in_box($DV_X, vector($DS_X6, $DS_Y9,
$DS_Z3), vector($DS_X7, $DS_Y10, $DS_Z4)))
leak11=(in_box($DV_X, vector($DS_X6, $DS_Y11,
$DS_Z3), vector($DS_X7, $DS_Y12, $DS_Z4)))
leak12=(in_box($DV_X, vector($DS_X6, $DS_Y9,
$DS_Z2), vector($DS_X7, $DS_Y12, $DS_Z3)))
leak13=(in_box($DV_X, vector($DS_X8, $DS_Y9,
$DS_Z4), vector($DS_X9, $DS_Y12, $DS_Z5)))
leak14=(in_box($DV_X, vector($DS_X8, $DS_Y9,
$DS_Z3), vector($DS_X9, $DS_Y10, $DS_Z4)))
leak15=(in_box($DV_X, vector($DS_X8, $DS_Y11,
$DS_Z3), vector($DS_X9, $DS_Y12, $DS_Z4)))
leak16=(in_box($DV_X, vector($DS_X8, $DS_Y9,
$DS_Z2), vector($DS_X9, $DS_Y12, $DS_Z3)))
ad1=(in_box($DV_X, vector($DS_X3, $DS_Y8, $DS_Z6),
vector($DS_X4, $DS_Y13, $DS_Z11)))
ex1=(in_box($DV_X, vector($DS_X3, $DS_Y2, $DS_Z6),
vector($DS_X4, $DS_Y5, $DS_Z11)))
ad2=(in_box($DV_X, vector($DS_X10, $DS_Y9,
$DS_Z6), vector($DS_X11, $DS_Y12, $DS_Z11)))
ex2=(in_box($DV_X, vector($DS_X10, $DS_Y3,
$DS_Z6), vector($DS_X11, $DS_Y4, $DS_Z11)))
firepool=(in_box($DV_X, vector($DS_X2, $DS_Y6,
$DS_Z1), vector($DS_X5, $DS_Y7, $DS_Z2)))
END MODULE holes
concrete_name="GE_PerforatedMeshing"
type="perforated_meshing"
END MODULE GE_Meshing
MODULE split_on_processes
splitting_strategy="coordinate_splitting"
coordinate_splitting_formula=(segm3D_sort($DV_X,
$DV_MESH_X, 2, $DV_MESH_Y, 2, $DV_MESH_Z, 2))
END MODULE split_on_processes
type="structured_mesh"
geometry="cartesian_3D"
local_refinement="disabled"
END MODULE meshing
MODULE time_management
MODULE automatic_time_step
MODULE velocity_prediction_error
target=0.1
END MODULE velocity_prediction_error
CFL_control="disabled"
velocity_prediction_control="fixed_target"
velocity_increment_control="disabled"
enthalpy_increment_control="disabled"
k_increment_control="disabled"
epsilon_increment_control="disabled"
minimal_time_step=0.05
maximal_time_step=0.5
minimum_acceleration_factor=0.8
maximum_acceleration_factor=1.2
number_of_fixed_initial_time_steps=10
number_of_fixed_increasing_time_steps=3
END MODULE automatic_time_step
initial_time=($DS_tinit)
time_order="order1"
final_time=($DS_tend)
time_step=($DS_dt)
END MODULE time_management
MODULE problem_description
MODULE initial_values
velocity=<0.0 0.0 0.0>
k=($DS_k0)
epsilon=($DS_epsilon0)
mixture_fraction=0.0
fuel_mass_fraction=0.0
temperature=300.0
thermodynamical_pressure=101188.0
END MODULE initial_values
MODULE physical_properties
MODULE density
type="ideal_gas"
END MODULE density
MODULE conductivity
type="turbulent"
turbulent_Prandtl=0.7
END MODULE conductivity
MODULE enthalpy
type="turbulent_combustion"
reference_temperature=($DS_Tref)
END MODULE enthalpy

```

```

MODULE specific_heat
type="constant"
value=(SDS_Cp)
END MODULE specific_heat
MODULE laminar_viscosity
type="sutherland"
reference_viscosity=1.68E-5
reference_temperature=273.0
sutherland_coefficient=110.5
exponent=(3.e+00/2.e+00)
END MODULE laminar_viscosity
MODULE species_diffusivity
type="turbulent"
turbulent_Schmidt=0.7
END MODULE species_diffusivity
MODULE soot_density
type="constant"
value=(SDS_rhoSoot)
END MODULE soot_density
MODULE gas_absorption
type="gray-medium_assumption"
path_length="cell_characteristic_size"
gas_emissivity="wsggm_H2O_CO2"
END MODULE gas_absorption
MODULE soot_absorption
type="temperature_dependent_function"
soot_coefficient=1264.0
END MODULE soot_absorption
END MODULE physical_properties
MODULE gravity_force
type="standard"
gravity_field=<0.0 0.0 -9.81>
END MODULE gravity_force
MODULE macro_boundary_conditions
MODULE BC#adiabatic
MODULE velocity
type="wall_law"
field="velocity"
END MODULE velocity
MODULE radiative_intensity
type="null_radiative_flux"
field="radiative_intensity"
END MODULE radiative_intensity
MODULE temperature
type="adiabatic"
field="temperature"
END MODULE temperature
type="wall"
color="adiabatic_walls"
END MODULE BC#adiabatic
MODULE BC#concrete_wall
MODULE velocity
type="wall_law"
field="velocity"
END MODULE velocity
MODULE radiative_intensity
type="gray_surface"
field="radiative_intensity"
surface_emissivity=0.7
END MODULE radiative_intensity
MODULE temperature
MODULE wall_properties
specific_heat=736.0
density=2430.0
conductivity=1.5
meshing=(stretched_vector(0.e+00, 1.e-04, 5.e-02, 3.e-01))
T_initial=(SDS_Tref+5.e-01)
END MODULE wall_properties
MODULE heat_exchange_coefficient
type="wall_law"
laminar_prandtl=0.7
turbulent_prandtl=0.7
END MODULE heat_exchange_coefficient
MODULE boundary_condition_with_external
type="adiabatic"
END MODULE boundary_condition_with_external
type="wall_conduction"
field="temperature"
END MODULE temperature
type="wall"
color="concrete_walls"
END MODULE BC#concrete_wall
MODULE BC#ceiling
MODULE velocity
type="wall_law"
field="velocity"
END MODULE velocity
MODULE radiative_intensity
type="gray_surface"
field="radiative_intensity"
surface_emissivity=0.95
END MODULE radiative_intensity
MODULE temperature
MODULE wall_properties
specific_heat=840.0
density=140.0
conductivity=0.102
meshing=(stretched_vector(0.e+00, 1.e-04, 1.e-02, 3.e-01))
T_initial=(SDS_Tref)
END MODULE wall_properties
MODULE heat_exchange_coefficient
type="wall_law"
laminar_prandtl=0.7
turbulent_prandtl=0.7
END MODULE heat_exchange_coefficient
MODULE boundary_condition_with_external
type="adiabatic"
END MODULE boundary_condition_with_external
type="wall_conduction"
field="temperature"
END MODULE temperature
type="wall"
color="ceiling"
END MODULE BC#ceiling
MODULE Bc#pool_fire
MODULE velocity
MODULE mass_flow_rate
concrete_name="IS_MassFlowRate_BC#fixed"
type="fixed"
value=(SDS_Q)
END MODULE mass_flow_rate
type="fixed_mass_flow_rate"
field="velocity"
mode="imposed_velocity"

```



```

END MODULE velocity
MODULE mixture_fraction
type="inflow_mixture_fraction"
field="mixture_fraction"
value=(SDS_FuelInj)
END MODULE mixture_fraction
MODULE fuel_mass_fraction
type="inflow_fuel_mass_fraction"
field="fuel_mass_fraction"
value=(SDS_FuelInj)
END MODULE fuel_mass_fraction
MODULE k
type="fixed_k"
field="k"
value=(SDS_k_pool)
END MODULE k
MODULE epsilon
type="fixed_epsilon"
field="epsilon"
value=(SDS_epsilon_pool)
END MODULE epsilon
MODULE radiative_intensity
type="gray_surface"
field="radiative_intensity"
surface_emissivity=1.0
surface_temperature=(SDS_TFuel)
END MODULE radiative_intensity
MODULE density
type="fixed_density"
field="density"
value=(SDS_rhoFuel)
END MODULE density
MODULE temperature
type="inflow_temperature"
field="temperature"
value=(SDS_TFuel)
END MODULE temperature
type="inflow"
color="pool_fire_front"
END MODULE Bc#pool_fire
MODULE BC#admission
MODULE velocity
MODULE resistance
flow_exponent=2.0
density_exponent=1.0
R=(SDS_R_ADM)
END MODULE resistance
type="pipe_mass_flow_rate"
field="velocity"
mode="mixed"
external_pressure=(SDS_Pref+SDS_DP_ADM)
pipe_modelling="stationnary"
END MODULE velocity
MODULE mixture_fraction
type="inlet_outlet_mixture_fraction"
field="mixture_fraction"
inlet_value=0.0
END MODULE mixture_fraction
MODULE fuel_mass_fraction
type="inlet_outlet_fuel_mass_fraction"
field="fuel_mass_fraction"
inlet_value=0.0
END MODULE fuel_mass_fraction
MODULE radiative_intensity
type="incoming_radiation"
field="radiative_intensity"
external_temperature=(SDS_Tref)
END MODULE radiative_intensity
MODULE k
type="inlet_outlet_turbulent_intensity"
field="k"
inlet_turbulent_intensity=0.01
END MODULE k
MODULE epsilon
type="inlet_outlet_mixing_length_scale"
field="epsilon"
inlet_mixing_length_scale=0.03
END MODULE epsilon
END MODULE fuel_mass_fraction
MODULE radiative_intensity
type="incoming_radiation"
field="radiative_intensity"
external_temperature=(SDS_Tref)
END MODULE radiative_intensity
MODULE k
type="inlet_outlet_turbulent_intensity"
field="k"
inlet_turbulent_intensity=0.01
END MODULE k
MODULE epsilon
type="inlet_outlet_mixing_length_scale"
field="epsilon"
inlet_mixing_length_scale=0.03
END MODULE epsilon

```

```

MODULE temperature
type="inlet_outlet_temperature"
field="temperature"
inlet_value=(SDS_Tref)
END MODULE temperature
type="pipe_junction"
color="extraction"
END MODULE BC#extraction
MODULE BC#admission2
MODULE velocity
MODULE resistance
flow_exponent=2.0
density_exponent=1.0
R=(SDS_R_ADM2)
END MODULE resistance
type="pipe_mass_flow_rate"
field="velocity"
mode="mixed"
external_pressure=(SDS_Pref+SDS_DP_ADM2)
pipe_modelling="stationnary"
END MODULE velocity
MODULE mixture_fraction
type="inlet_outlet_mixture_fraction"
field="mixture_fraction"
inlet_value=0.0
END MODULE mixture_fraction
MODULE fuel_mass_fraction
type="inlet_outlet_fuel_mass_fraction"
field="fuel_mass_fraction"
inlet_value=0.0
END MODULE fuel_mass_fraction
MODULE radiative_intensity
type="incoming_radiation"
field="radiative_intensity"
external_temperature=(SDS_Tref)
END MODULE radiative_intensity
MODULE k
type="inlet_outlet_turbulent_intensity"
field="k"
inlet_turbulent_intensity=0.01
END MODULE k
MODULE epsilon
type="inlet_outlet_mixing_length_scale"
field="epsilon"
inlet_mixing_length_scale=0.03
END MODULE epsilon
MODULE temperature
type="inlet_outlet_temperature"
field="temperature"
inlet_value=(SDS_Tref)
END MODULE temperature
type="pipe_junction"
color="extraction2"
END MODULE BC#extraction2
MODULE insulationwall
MODULE velocity
type="wall_law"
field="velocity"
END MODULE velocity
MODULE temperature
MODULE wall_properties
specific_heat=840.0
density=140.0
conductivity=0.102
meshing=(stretched_vector(0.e+00, 1.e-04, 1.e-02, 3.e-01))
T_initial=(SDS_Tref)
END MODULE wall_properties
MODULE heat_exchange_coefficient
type="wall_law"
laminar_prandtl=0.7
turbulent_prandtl=0.7
END MODULE heat_exchange_coefficient
MODULE boundary_condition_with_external
type="adiabatic"
END MODULE boundary_condition_with_external
type="wall_conduction"
field="temperature"
END MODULE temperature

```

```

MODULE radiative_intensity
type="gray_surface"
field="radiative_intensity"
surface_emissivity=0.95
END MODULE radiative_intensity
type="wall"
color="insulation_walls"
END MODULE insulationwall
END MODULE macro_boundary_conditions
MODULE volumetric_heat_source
type="none"
END MODULE volumetric_heat_source
MODULE turbulence
MODULE wall_law
type="log_law"
delta="cell_size"
cell_size_fraction=0.25
END MODULE wall_law
MODULE parameters
C_mu=0.09
sigma_k=1.0
sigma_epsilon=1.3
sigma_g=0.7
C_k_P=1.0
C_k_G=1.0
C_k_W=0.0
C_k_Eps=1.0
C_epsilon_P=1.44
C_epsilon_G1=0.0
C_epsilon_G2=1.44
C_epsilon_W=0.0
C_epsilon_Rf=0.0
C_epsilon_Eps=1.92
turbulent_production="SGDH"
END MODULE parameters
maximal_mixing_length=($DS_LY)
END MODULE turbulence
MODULE combustion
MODULE injection
oxidizer_mass_fraction_in_oxidizer_injection=0.23
fuel_mass_fraction_in_fuel_injection=1.0
END MODULE injection
MODULE chemistry
type="combustion_soot"
fuel_molar_mass=0.17
fuel_stoichiometric_coefficient=1.0
oxidizer_molar_mass=0.032
oxidizer_stoichiometric_coefficient=(1.85e+01-
$DS_s_soot)
inert_molar_mass=0.028
gas_product_molar_masses=<0.018 0.044>
gas_product_stoichiometric_coefficients=(vector(1.3e+01,
(1.2e+01-$DS_s_soot)))
soot_fraction=0.0239
heat_release=($DS_HcFuel)
description="dodecane incomplete combustion in air:
C12H26+(18.5-s)O2+N2 -> 13H2O+(12-s)CO2+N2+sC
with s=0.338"
fuel="c12h26"
oxidizer="O2"
inert="N2"
gas_products=<"H2O" "CO2">
END MODULE chemistry
END MODULE combustion
MODULE radiation
angular_discretization="automatic"
N=4
END MODULE radiation
Navier_Stokes="low_mach"
energy_balance="enabled"
turbulence_model="k_epsilon"
combustion_model="EBU"
radiation_model="FVM"
soot_model="fixed_soot_fraction"
END MODULE problem_description
MODULE save_for_restarting
type="none"
END MODULE save_for_restarting
MODULE post_processing
MODULE formats
GMV=false
ParaView=true
FieldView=false
TIC=false
Pelicans=false
END MODULE formats
MODULE fields
MODULE state_law
density=true
density_name="RHO"
thermodynamical_pressure=true
END MODULE state_law
MODULE Navier_Stokes
velocity=true
velocity_name="VELO"
pressure=true
effective_viscosity=true
effective_viscosity_name="VISC"
laminar_viscosity=false
turbulent_viscosity=false
pressure_name="P"
inflow_mass_flow_rate=true
vorticity=false
END MODULE Navier_Stokes
MODULE energy_balance
temperature=true
temperature_name="T"
enthalpy=true
wall_heat_fluxes=true
wall_heat_exchange_coefficients=true
conductivity=true
conductivity_name="COND"
wall_heat_exchange_coefficients_name="HCON"
wall_heat_fluxes_name="FTOT_FCON_FRAD"
enthalpy_name="H"
enthalpy_radiative_source_terms=false
END MODULE energy_balance
MODULE turbulence
k=true
k_name="XK"
epsilon=true
epsilon_name="XEPS"
k_epsilon_source_terms=false
y_plus=true

```

```

wall_shear_stress=true
y_plus_name="YPL"
wall_shear_stress_name="TAU"
END MODULE turbulence
MODULE combustion
mixture_fraction=true
mixture_fraction_name="XZ"
fuel_mass_fraction=true
fuel_mass_fraction_name="YF"
oxidizer_mass_fraction=true
inert_mass_fraction=true
product_mass_fraction=true
product_mass_fraction_name="YP"
fuel_mole_fraction=false
oxidizer_mole_fraction=false
inert_mole_fraction=false
product_mole_fraction=false
Yf_source_term=false
oxidizer_mass_fraction_name="YO"
inert_mass_fraction_name="YI"
END MODULE combustion
MODULE radiation
radiative_intensity=true
radiative_intensity_name="RI"
boundary_radiative_flux=true
boundary_radiative_flux_name="QRAD"
gas_absorption=false
soot_absorption=false
END MODULE radiation
MODULE soot
soot_volume_fraction=true
soot_volume_fraction_name="FVS"
END MODULE soot
saving_location="at_cell_centers"
END MODULE fields
MODULE visu_toolkit
MODULE points_R3_NE
MODULE fields
MODULE temperature
name="temperature"
component=0
END MODULE temperature
END MODULE fields
MODULE field_compositions
END MODULE field_compositions
MODULE expressions
END MODULE expressions
MODULE points_definition
type="list_of_points"
points = (array(< 9.050000000000001e+00 4.5e+00 5.e-02 > , < 9.050000000000001e+00 4.5e+00 3.e-01 > , < 9.050000000000001e+00 4.5e+00 5.5e-01 > , < 9.050000000000001e+00 4.5e+00 8.e-01 > , < 9.050000000000001e+00 4.5e+00 1.05e+00 > , < 9.050000000000001e+00 4.5e+00 1.3e+00 > , < 9.050000000000001e+00 4.5e+00 1.55e+00 > , < 9.050000000000001e+00 4.5e+00 1.8e+00 > , < 9.050000000000001e+00 4.5e+00 2.05e+00 > , < 9.050000000000001e+00 4.5e+00 2.3e+00 > , < 9.050000000000001e+00 4.5e+00 2.55e+00 > , < 9.050000000000001e+00 4.5e+00 2.8e+00 > , < 9.050000000000001e+00 4.5e+00 3.05e+00 > , < 9.050000000000001e+00 4.5e+00 3.3e+00 > , < 9.050000000000001e+00 4.5e+00 3.55e+00 > , < 9.050000000000001e+00 4.5e+00 3.8e+00 > , < 9.050000000000001e+00 4.5e+00 3.85e+00 > , < 9.050000000000001e+00 4.5e+00 3.9e+00 > ))
ignore_exterior_points=true
END MODULE points_definition
MODULE post_processing
type="one_file"
file_name="RESULTS_POINTS_R3_NE"
banner=true
END MODULE post_processing
MODULE parameters
END MODULE parameters
concrete_name="FE_FieldValue"
END MODULE points_R3_NE
MODULE points_R3_SW
MODULE fields
MODULE temperature
name="temperature"
component=0
END MODULE temperature
END MODULE fields
MODULE field_compositions
END MODULE field_compositions
MODULE expressions
END MODULE expressions
MODULE points_definition
type="list_of_points"
points = (array(< 6.55e+00 4.5e+00 5.e-02 > , < 6.55e+00 4.5e+00 3.e-01 > , < 6.55e+00 4.5e+00 5.5e-01 > , < 6.55e+00 4.5e+00 8.e-01 > , < 6.55e+00 4.5e+00 1.05e+00 > , < 6.55e+00 4.5e+00 1.3e+00 > , < 6.55e+00 4.5e+00 1.55e+00 > , < 6.55e+00 4.5e+00 1.8e+00 > , < 6.55e+00 4.5e+00 2.05e+00 > , < 6.55e+00 4.5e+00 2.3e+00 > , < 6.55e+00 4.5e+00 2.55e+00 > , < 6.55e+00 4.5e+00 2.8e+00 > , < 6.55e+00 4.5e+00 3.05e+00 > , < 6.55e+00 4.5e+00 3.3e+00 > , < 6.55e+00 4.5e+00 3.55e+00 > , < 6.55e+00 4.5e+00 3.8e+00 > , < 6.55e+00 4.5e+00 3.85e+00 > , < 6.55e+00 4.5e+00 3.9e+00 > ))
ignore_exterior_points=true
END MODULE points_definition
MODULE post_processing
type="one_file"
file_name="RESULTS_POINTS_R3_SW"
banner=true
END MODULE post_processing
MODULE parameters
END MODULE parameters
concrete_name="FE_FieldValue"
END MODULE points_R3_SW
MODULE points_R2_centre_CC
MODULE fields
MODULE temperature
name="temperature"
component=0
END MODULE temperature
END MODULE fields
MODULE field_compositions
END MODULE field_compositions
MODULE expressions
END MODULE expressions

```

```

MODULE points_definition
type="list_of_points"
points = (array(< 2.5e+00 3.e+00 5.5e-01 > , < 2.5e+00
3.e+00 8.e-01 > , < 2.5e+00 3.e+00 1.05e+00 > , < 2.5e+00
3.e+00 1.3e+00 > , < 2.5e+00 3.e+00 1.55e+00 > , <
2.5e+00 3.e+00 1.8e+00 > , < 2.5e+00 3.e+00 2.05e+00 > ,
< 2.5e+00 3.e+00 2.3e+00 > , < 2.5e+00 3.e+00
2.55e+00 > , < 2.5e+00 3.e+00 2.8e+00 > , < 2.5e+00
3.e+00 3.05e+00 > , < 2.5e+00 3.e+00 3.3e+00 > , <
2.5e+00 3.e+00 3.55e+00 > , < 2.5e+00 3.e+00 3.8e+00 > ,
< 2.5e+00 3.e+00 3.85e+00 > , < 2.5e+00 3.e+00
3.9e+00 > ))
ignore_exterior_points=true
END MODULE points_definition
MODULE post_processing
type="one_file"
file_name="RESULTS_POINTS_R2_centre"
banner=true
END MODULE post_processing
MODULE parameters
END MODULE parameters
concrete_name="FE_FieldValue"
END MODULE points_R2_centre_CC
MODULE points_R3_centre
MODULE fields
MODULE temperature
name="temperature"
component=0
END MODULE temperature
END MODULE fields
MODULE field_compositions
END MODULE field_compositions
MODULE expressions
END MODULE expressions
MODULE points_definition
type="list_of_points"
points = (array(< 7.8e+00 3.e+00 5.e-02 > , < 7.8e+00
3.e+00 3.e-01 > , < 7.8e+00 3.e+00 5.5e-01 > , < 7.8e+00
3.e+00 8.e-01 > , < 7.8e+00 3.e+00 1.05e+00 > , < 7.8e+00
3.e+00 1.3e+00 > , < 7.8e+00 3.e+00 1.55e+00 > , <
7.8e+00 3.e+00 1.8e+00 > , < 7.8e+00 3.e+00 2.05e+00 > ,
< 7.8e+00 3.e+00 2.3e+00 > , < 7.8e+00 3.e+00
2.55e+00 > , < 7.8e+00 3.e+00 2.8e+00 > , < 7.8e+00
3.e+00 3.05e+00 > , < 7.8e+00 3.e+00 3.3e+00 > , <
7.8e+00 3.e+00 3.55e+00 > , < 7.8e+00 3.e+00 3.8e+00 > ,
< 7.8e+00 3.e+00 3.85e+00 > , < 7.8e+00 3.e+00
3.9e+00 > ))
ignore_exterior_points=true
END MODULE points_definition
MODULE post_processing
type="one_file"
file_name="RESULTS_POINTS_R3_centre"
banner=true
END MODULE post_processing
MODULE parameters
END MODULE parameters
concrete_name="FE_FieldValue"
END MODULE points_R3_centre
MODULE points_R2_NE
MODULE fields
MODULE temperature
name="temperature"

```

```

component=0
END MODULE temperature
END MODULE fields
MODULE field_compositions
END MODULE field_compositions
MODULE expressions
END MODULE expressions
MODULE points_definition
type="list_of_points"
points = (array(< 3.75e+00 4.5e+00 5.e-02 > , < 3.75e+00
4.5e+00 3.e-01 > , < 3.75e+00 4.5e+00 5.5e-01 > , <
3.75e+00 4.5e+00 8.e-01 > , < 3.75e+00 4.5e+00
1.05e+00 > , < 3.75e+00 4.5e+00 1.3e+00 > , < 3.75e+00
4.5e+00 1.55e+00 > , < 3.75e+00 4.5e+00 1.8e+00 > , <
3.75e+00 4.5e+00 2.05e+00 > , < 3.75e+00 4.5e+00
2.3e+00 > , < 3.75e+00 4.5e+00 2.55e+00 > , < 3.75e+00
4.5e+00 2.8e+00 > , < 3.75e+00 4.5e+00 3.05e+00 > , <
3.75e+00 4.5e+00 3.3e+00 > , < 3.75e+00 4.5e+00
3.55e+00 > , < 3.75e+00 4.5e+00 3.8e+00 > , < 3.75e+00
4.5e+00 3.85e+00 > , < 3.75e+00 4.5e+00 3.9e+00 > ))
ignore_exterior_points=true
END MODULE points_definition
MODULE post_processing
type="one_file"
file_name="RESULTS_POINTS_R2_NE"
banner=true
END MODULE post_processing
MODULE parameters
END MODULE parameters
concrete_name="FE_FieldValue"
END MODULE points_R2_NE
MODULE points_R2_SW
MODULE fields
MODULE temperature
name="temperature"
component=0
END MODULE temperature
END MODULE fields
MODULE field_compositions
END MODULE field_compositions
MODULE expressions
END MODULE expressions
MODULE points_definition
type="list_of_points"
points = (array(< 1.25e+00 1.5e+00 5.e-02 > , < 1.25e+00
1.5e+00 3.e-01 > , < 1.25e+00 1.5e+00 5.5e-01 > , <
1.25e+00 1.5e+00 8.e-01 > , < 1.25e+00 1.5e+00
1.05e+00 > , < 1.25e+00 1.5e+00 1.3e+00 > , < 1.25e+00
1.5e+00 1.55e+00 > , < 1.25e+00 1.5e+00 1.8e+00 > , <
1.25e+00 1.5e+00 2.05e+00 > , < 1.25e+00 1.5e+00
2.3e+00 > , < 1.25e+00 1.5e+00 2.55e+00 > , < 1.25e+00
1.5e+00 2.8e+00 > , < 1.25e+00 1.5e+00 3.05e+00 > , <
1.25e+00 1.5e+00 3.3e+00 > , < 1.25e+00 1.5e+00
3.55e+00 > , < 1.25e+00 1.5e+00 3.8e+00 > , < 1.25e+00
1.5e+00 3.85e+00 > , < 1.25e+00 1.5e+00 3.9e+00 > ))
ignore_exterior_points=true
END MODULE points_definition
MODULE post_processing
type="one_file"
file_name="RESULTS_POINTS_R2_SW"
banner=true
END MODULE post_processing

```

```

MODULE parameters
END MODULE parameters
concrete_name="FE_FieldValue"
END MODULE points_R2_SW
MODULE wall_R2_NE030
MODULE post_processing
type="interface"
file_name="RESULTS_WALL_R2_NE030"
format="gnuplot"
banner=true
END MODULE post_processing
concrete_name="IS_WallValue"
interface_coordinates=<4.15 5.97 0.28>
color="insulation_walls"
END MODULE wall_R2_NE030
MODULE wall_R2_NE155
MODULE post_processing
type="interface"
file_name="RESULTS_WALL_R2_NE155"
format="gnuplot"
banner=true
END MODULE post_processing
concrete_name="IS_WallValue"
interface_coordinates=<4.15 5.97 1.55>
color="insulation_walls"
END MODULE wall_R2_NE155
MODULE wall_R2_NE260
MODULE post_processing
type="interface"
file_name="RESULTS_WALL_R2_NE260"
format="gnuplot"
banner=true
END MODULE post_processing
concrete_name="IS_WallValue"
interface_coordinates=<4.15 5.97 2.61>
color="insulation_walls"
END MODULE wall_R2_NE260
MODULE wall_R2_NE355
MODULE post_processing
type="interface"
file_name="RESULTS_WALL_R2_NE355"
format="gnuplot"
banner=true
END MODULE post_processing
concrete_name="IS_WallValue"
interface_coordinates=<4.15 5.97 3.55>
color="insulation_walls"
END MODULE wall_R2_NE355
MODULE cutline_ceiling_r2
MODULE post_processing
type="wall_cutline"
file_basename="RESULTS_WALLCUT_ceiling_values_R
2_PL_CE"
format="gnuplot"
saving_times=(regular_vector(0.e+00,      $IS_SAVE2,
$DS_tend))
banner=true
END MODULE post_processing
concrete_name="IS_WallValue"
interface_coordinates=<4.32 3.04 3.95>
color="ceiling"
END MODULE cutline_ceiling_r2

```

```

MODULE ceiling_R2
MODULE post_processing
type="interface"
format="gnuplot"
banner=true
file_name="ceiling_R2_PL_CE"
END MODULE post_processing
concrete_name="IS_WallValue"
interface_coordinates=<4.32 3.04 3.95>
color="ceiling"
END MODULE ceiling_R2
MODULE point_admission
MODULE fields
MODULE temperature
name="temperature"
component=0
END MODULE temperature
MODULE pressure
name="pressure"
component=0
END MODULE pressure
END MODULE fields
MODULE field_compositions
MODULE soot_volume_fraction
name="soot_volume_fraction"
component=0
END MODULE soot_volume_fraction
MODULE oxidizer_mass_fraction
name="oxidizer_mass_fraction"
component=0
END MODULE oxidizer_mass_fraction
MODULE density
name="density"
component=0
END MODULE density
MODULE inert_mass_fraction
name="inert_mass_fraction"
component=0
END MODULE inert_mass_fraction
MODULE fuel_mass_fraction
name="fuel_mass_fraction"
component=0
END MODULE fuel_mass_fraction
MODULE product_mass_fraction
name="product_mass_fraction"
END MODULE product_mass_fraction
END MODULE field_compositions
MODULE expressions
END MODULE expressions
MODULE points_definition
type="list_of_points"
points = (array(< 2.3e+00 5.4e+00 3.4e+00 > ))
END MODULE points_definition
MODULE post_processing
type="one_file"
file_name="RESULTS_POINT_admission"
END MODULE post_processing
MODULE parameters
END MODULE parameters
concrete_name="FE_FieldValue"
END MODULE point_admission
MODULE point_extraction

```

```

MODULE fields
END MODULE fields
MODULE field_compositions
MODULE density
name="density"
component=0
END MODULE density
MODULE oxidizer_mass_fraction
name="oxidizer_mass_fraction"
component=0
END MODULE oxidizer_mass_fraction
MODULE inert_mass_fraction
name="inert_mass_fraction"
component=0
END MODULE inert_mass_fraction
MODULE fuel_mass_fraction
name="fuel_mass_fraction"
component=0
END MODULE fuel_mass_fraction
MODULE product_mass_fraction
name="product_mass_fraction"
END MODULE product_mass_fraction
MODULE soot_volume_fraction
name="soot_volume_fraction"
component=0
END MODULE soot_volume_fraction
END MODULE field_compositions
MODULE expressions
END MODULE expressions
MODULE points_definition
type="list_of_points"
points = (array(< 2.3e+00 6.e-01 3.4e+00 > ))
ignore_exterior_points=true
END MODULE points_definition
MODULE post_processing
type="one_file"
file_name="RESULTS_POINT_extraction"
END MODULE post_processing
MODULE parameters
END MODULE parameters
concrete_name="FE_FieldValue"
END MODULE point_extraction
MODULE post_admission
MODULE post_processing
file_name="admission_flux"
saving_times=(regular_vector(-1.e+00, 1, 0.e+00) <<
regular_vector(0.e+00, $IS_SAVE2, $DS_tend))
banner=true
format="gnuplot"
END MODULE post_processing
concrete_name="IS_FluxValue#boundary"
color="admission"
END MODULE post_admission
MODULE post_extraction
MODULE post_processing
file_name="extraction_flux"
saving_times=(regular_vector(-1.e+00, 1, 0.e+00) <<
regular_vector(0.e+00, $IS_SAVE2, $DS_tend))
banner=true
format="gnuplot"
END MODULE post_processing
concrete_name="IS_FluxValue#boundary"
color="extraction"
END MODULE post_extraction
MODULE point_admission2
MODULE fields
END MODULE fields
MODULE field_compositions
MODULE soot_volume_fraction
name="soot_volume_fraction"
component=0
END MODULE soot_volume_fraction
MODULE oxidizer_mass_fraction
name="oxidizer_mass_fraction"
component=0
END MODULE oxidizer_mass_fraction
MODULE density
name="density"
component=0
END MODULE density
MODULE inert_mass_fraction
name="inert_mass_fraction"
component=0
END MODULE inert_mass_fraction
MODULE fuel_mass_fraction
name="fuel_mass_fraction"
component=0
END MODULE fuel_mass_fraction
MODULE product_mass_fraction
name="product_mass_fraction"
END MODULE product_mass_fraction
END MODULE field_compositions
MODULE expressions
END MODULE expressions
MODULE points_definition
type="list_of_points"
points = (array(< 8.e+00 5.4e+00 3.4e+00 > ))
END MODULE points_definition
MODULE post_processing
type="one_file"
file_name="RESULTS_POINT_admission2"
END MODULE post_processing
MODULE parameters
END MODULE parameters
concrete_name="FE_FieldValue"
END MODULE point_admission2
MODULE point_extraction2
MODULE fields
END MODULE fields
MODULE field_compositions
MODULE density
name="density"
component=0
END MODULE density
MODULE oxidizer_mass_fraction
name="oxidizer_mass_fraction"
component=0
END MODULE oxidizer_mass_fraction
MODULE inert_mass_fraction
name="inert_mass_fraction"
component=0
END MODULE inert_mass_fraction
MODULE fuel_mass_fraction
name="fuel_mass_fraction"

```

```

component=0
END MODULE fuel_mass_fraction
MODULE product_mass_fraction
name="product_mass_fraction"
END MODULE product_mass_fraction
MODULE soot_volume_fraction
name="soot_volume_fraction"
component=0
END MODULE soot_volume_fraction
END MODULE field_compositions
MODULE expressions
END MODULE expressions
MODULE points_definition
type="list_of_points"
points = (array(< 8.e+00 6.e-01 3.4e+00 > ))
END MODULE points_definition
MODULE post_processing
type="one_file"
file_name="RESULTS_POINT_extraction2"
END MODULE post_processing
MODULE parameters
END MODULE parameters
concrete_name="FE_FieldValue"
END MODULE point_extraction2
MODULE post_admission2
MODULE post_processing
file_name="admission2_flux"
saving_times=(regular_vector(-1.e+00, 1, 0.e+00) <<
regular_vector(0.e+00, $IS_SAVE2, $DS_tend))
banner=true
format="gnuplot"
END MODULE post_processing
concrete_name="IS_FluxValue#boundary"
color="admission2"
END MODULE post_admission2
MODULE post_extraction2
MODULE post_processing
file_name="extraction2_flux"
saving_times=(regular_vector(-1.e+00, 1, 0.e+00) <<
regular_vector(0.e+00, $IS_SAVE2, $DS_tend))
banner=true
format="gnuplot"
END MODULE post_processing
concrete_name="IS_FluxValue#boundary"
color="extraction2"
END MODULE post_extraction2
MODULE leakdown
MODULE fields
MODULE pressure
name="pressure"
component=0
END MODULE pressure
MODULE temperature
name="temperature"
component=0
END MODULE temperature
MODULE field_compositions
MODULE density
name="density"
component=0
END MODULE density
END MODULE field_compositions
MODULE expressions
END MODULE expressions
MODULE points_definition
type="list_of_points"
ignore_exterior_points=true
points = (array(< 5.15e+00 5.41e+00
5.6000000000000001e-01 > ))
END MODULE points_definition
MODULE post_processing
type="one_file"
banner=true
file_name="leakdown"
END MODULE post_processing
MODULE parameters
END MODULE parameters
concrete_name="FE_FieldValue"
END MODULE leakdown
MODULE leakdown2
MODULE fields
MODULE pressure
name="pressure"
component=0
END MODULE pressure
MODULE temperature
name="temperature"
component=0
END MODULE temperature
END MODULE fields
MODULE field_compositions
MODULE density
name="density"
component=0
END MODULE density
END MODULE field_compositions
MODULE expressions
END MODULE expressions
MODULE points_definition
type="list_of_points"
ignore_exterior_points=true
points = (array(< 4.4e+00 5.41e+00 5.6000000000000001e-
01 > ))
END MODULE points_definition
MODULE post_processing
type="one_file"
banner=true
file_name="leakdown2"
END MODULE post_processing
MODULE parameters
END MODULE parameters
concrete_name="FE_FieldValue"
END MODULE leakdown2
MODULE leakdown3
MODULE fields
MODULE pressure
name="pressure"
component=0
END MODULE pressure
MODULE temperature
name="temperature"
component=0
END MODULE temperature

```



```

END MODULE fields
MODULE field_compositions
MODULE density
name="density"
component=0
END MODULE density
END MODULE field_compositions
MODULE expressions
END MODULE expressions
MODULE points_definition
type="list_of_points"
ignore_exterior_points=true
points = (array(< 5.9e+00 5.41e+00 5.600000000000001e-
01 > ))
END MODULE points_definition
MODULE post_processing
type="one_file"
banner=true
file_name="leakdown2"
END MODULE post_processing
MODULE parameters
END MODULE parameters
concrete_name="FE_FieldValue"
END MODULE leakdown3
MODULE leakup
MODULE fields
MODULE pressure
name="pressure"
component=0
END MODULE pressure
MODULE temperature
name="temperature"
component=0
END MODULE temperature
END MODULE fields
MODULE field_compositions
MODULE density
name="density"
component=0
END MODULE density
END MODULE field_compositions
MODULE expressions
END MODULE expressions
MODULE points_definition
type="list_of_points"
ignore_exterior_points=true
points = (array(< 5.15e+00 5.41e+00 3.4e+00 > ))
END MODULE points_definition
MODULE post_processing
type="one_file"
banner=true
file_name="leakup"
END MODULE post_processing
MODULE parameters
END MODULE parameters
concrete_name="FE_FieldValue"
END MODULE leakup2
MODULE leakup3
MODULE fields
MODULE pressure
name="pressure"
component=0

```

```

END MODULE pressure
MODULE temperature
name="temperature"
component=0
END MODULE temperature
END MODULE fields
MODULE field_compositions
MODULE density
name="density"
component=0
END MODULE density
END MODULE field_compositions
MODULE expressions
END MODULE expressions
MODULE points_definition
type="list_of_points"
ignore_exterior_points=true
points = (array(< 4.4e+00 5.41e+00 3.4e+00 > ))
END MODULE points_definition
MODULE post_processing
type="one_file"
banner=true
file_name="leakup2"
END MODULE post_processing
MODULE parameters
END MODULE parameters
concrete_name="FE_FieldValue"
END MODULE leakup2
MODULE leakup3
MODULE fields
MODULE pressure
name="pressure"
component=0
END MODULE pressure
MODULE temperature
name="temperature"
component=0
END MODULE temperature
END MODULE fields
MODULE field_compositions
MODULE density
name="density"
component=0
END MODULE density
END MODULE field_compositions
MODULE expressions
END MODULE expressions
MODULE points_definition
type="list_of_points"
ignore_exterior_points=true
points = (array(< 5.9e+00 5.41e+00 3.4e+00 > ))
END MODULE points_definition
MODULE post_processing
type="one_file"
banner=true
file_name="leakup3"
END MODULE post_processing
MODULE parameters
END MODULE parameters
concrete_name="FE_FieldValue"
END MODULE leakup3
MODULE point_02BAS_R2

```

```

MODULE fields
END MODULE fields
MODULE field_compositions
MODULE density
name="density"
component=0
END MODULE density
MODULE oxidizer_mass_fraction
name="oxidizer_mass_fraction"
component=0
END MODULE oxidizer_mass_fraction
MODULE product_mass_fraction
name="product_mass_fraction"
END MODULE product_mass_fraction
MODULE soot_volume_fraction
name="soot_volume_fraction"
component=0
END MODULE soot_volume_fraction
MODULE inert_mass_fraction
name="inert_mass_fraction"
component=0
END MODULE inert_mass_fraction
MODULE fuel_mass_fraction
name="fuel_mass_fraction"
component=0
END MODULE fuel_mass_fraction
MODULE oxidizer_mole_fraction
name="oxidizer_mole_fraction"
component=0
END MODULE oxidizer_mole_fraction
MODULE product_mole_fraction
name="product_mole_fraction"
END MODULE product_mole_fraction
MODULE inert_mole_fraction
name="inert_mole_fraction"
component=0
END MODULE inert_mole_fraction
MODULE fuel_mole_fraction
name="fuel_mole_fraction"
component=0
END MODULE fuel_mole_fraction
END MODULE field_compositions
MODULE expressions
END MODULE expressions
MODULE points_definition
type="list_of_points"
points = (array(< 9.050000000000001e+00 1.5e+00 8.e-01 >))
ignore_exterior_points=true
END MODULE points_definition
MODULE post_processing
type="one_file"
file_name="RESULTS_POINT_O2BAS_R2"
banner=true
END MODULE post_processing
MODULE parameters
END MODULE parameters
concrete_name="FE_FieldValue"
END MODULE point_02BAS_R2
MODULE post_fire
MODULE post_processing
file_name="fire_flux"
saving_times=(regular_vector(-1.e+00, 1, 0.e+00) <<
regular_vector(0.e+00, $IS_SAVE2, $DS_tend))
banner=true
format="gnuplot"
END MODULE post_processing
concrete_name="IS_FluxValue#boundary"
color="pool_fire_front"
END MODULE post_fire
MODULE FLT_R2_EC260
MODULE post_processing
type="interface"
file_name="FLT_R2_EC260"
banner=true
format="gnuplot"
END MODULE post_processing
concrete_name="IS_WallValue"
color="insulation_walls"
interface_coordinates=<4.97 2.9 2.35>
END MODULE FLT_R2_EC260
MODULE FLT_R3_EC260
MODULE post_processing
type="interface"
file_name="FLT_R3_EC260"
banner=true
format="gnuplot"
END MODULE post_processing
concrete_name="IS_WallValue"
color="concrete_walls"
interface_coordinates=<10.3 2.98 2.55>
END MODULE FLT_R3_EC260
MODULE FLT_R2_NC260
MODULE post_processing
type="interface"
file_name="FLT_R2_NC260"
banner=true
format="gnuplot"
END MODULE post_processing
concrete_name="IS_WallValue"
color="insulation_walls"
interface_coordinates=<2.5 5.97 2.58>
END MODULE FLT_R2_NC260
MODULE FLT_R3_NC260
MODULE post_processing
type="interface"
file_name="FLT_R3_NC260"
banner=true
format="gnuplot"
END MODULE post_processing
concrete_name="IS_WallValue"
color="concrete_walls"
interface_coordinates=<7.83 5.97 2.55>
END MODULE FLT_R3_NC260
MODULE FLT_R2_WC260
MODULE post_processing
type="interface"
file_name="FLT_R2_WC260"
banner=true
format="gnuplot"
END MODULE post_processing
concrete_name="IS_WallValue"
color="insulation_walls"
interface_coordinates=<0.03 2.93 2.6>

```

```

END MODULE FLT_R2_WC260
MODULE FLT_R3_WC260
MODULE post_processing
type="interface"
file_name="FLT_R3_WC260"
banner=true
format="gnuplot"
END MODULE post_processing
concrete_name="IS_WallValue"
color="concrete_walls"
interface_coordinates=<5.3 3.0 2.53>
END MODULE FLT_R3_WC260
MODULE FLT_R2_SC260
MODULE post_processing
type="interface"
file_name="FLT_R2_SC260"
banner=true
format="gnuplot"
END MODULE post_processing
concrete_name="IS_WallValue"
color="insulation_walls"
interface_coordinates=<2.56 0.03 2.6>
END MODULE FLT_R2_SC260
MODULE FLT_R3_SC260
MODULE post_processing
type="interface"
file_name="FLT_R3_SC260"
banner=true
format="gnuplot"
END MODULE post_processing
concrete_name="IS_WallValue"
color="concrete_walls"
interface_coordinates=<7.77 0.03 2.55>
END MODULE FLT_R3_SC260
MODULE FLT_R2_PL1
MODULE post_processing
type="interface"
file_name="FLT_R2_PL1"
banner=true
format="gnuplot"
END MODULE post_processing
concrete_name="IS_WallValue"
color="ceiling"
interface_coordinates=<1.62 1.54 3.95>
END MODULE FLT_R2_PL1
MODULE FLT_R3_PL
MODULE post_processing
type="interface"
file_name="FLT_R3_PL"
banner=true
format="gnuplot"
END MODULE post_processing
concrete_name="IS_WallValue"
color="ceiling"
interface_coordinates=<7.8 2.82 3.95>
END MODULE FLT_R3_PL
MODULE FLT_R2_PL2
MODULE post_processing
type="interface"
file_name="FLT_R2_PL2"
banner=true
format="gnuplot"
END MODULE post_processing
concrete_name="IS_WallValue"
color="ceiling"
interface_coordinates=<1.6 1.51 3.95>
END MODULE FLT_R2_PL2
MODULE FLT_R2_SOL_1
MODULE post_processing
type="interface"
file_name="FLT_R2_SOL_1"
banner=true
format="gnuplot"
END MODULE post_processing
concrete_name="IS_WallValue"
color="concrete_walls"
interface_coordinates=<4.85 3.0 0.0>
END MODULE FLT_R2_SOL_1
MODULE FLT_R3_SOL
MODULE post_processing
type="interface"
file_name="FLT_R3_SOL"
banner=true
format="gnuplot"
END MODULE post_processing
concrete_name="IS_WallValue"
color="concrete_walls"
interface_coordinates=<7.13 3.0 0.0>
END MODULE FLT_R3_SOL
MODULE FLT_R2_SOL_2
MODULE post_processing
type="interface"
file_name="FLT_R2_SOL_2"
banner=true
format="gnuplot"
END MODULE post_processing
concrete_name="IS_WallValue"
color="concrete_walls"
interface_coordinates=<3.0 3.0 0.0>
END MODULE FLT_R2_SOL_2
MODULE FLT_R2_SOL_CE
MODULE post_processing
type="interface"
file_name="FLT_R2_SOL_CE"
banner=true
format="gnuplot"
END MODULE post_processing
concrete_name="IS_WallValue"
color="concrete_walls"
interface_coordinates=<3.9 3.0 0.0>
END MODULE FLT_R2_SOL_CE
MODULE WallT_TP_L2_EC260
MODULE post_processing
type="interface"
saving_times=(regular_vector(0.e+00,          $IS_SAVE2,
$DS_tend))
banner=true
format="gnuplot"
file_name="TP_L2_EC260"
END MODULE post_processing
concrete_name="IS_WallValue"
color="insulation_walls"
interface_coordinates=<4.97 3.0 2.6>
END MODULE WallT_TP_L2_EC260

```

```

MODULE WallT_TP_L2_NC260
MODULE post_processing
type="interface"
saving_times=(regular_vector(0.e+00,      $IS_SAVE2,
$DS_tend))
banner=true
format="gnuplot"
file_name="TP_L2_NC260"
END MODULE post_processing
concrete_name="IS_WallValue"
color="insulation_walls"
interface_coordinates=<2.66 5.97 2.62>
END MODULE WallT_TP_L2_NC260
MODULE WallT_TP_L2_SC260
MODULE post_processing
type="interface"
saving_times=(regular_vector(0.e+00,      $IS_SAVE2,
$DS_tend))
banner=true
format="gnuplot"
file_name="TP_L2_SC260"
END MODULE post_processing
concrete_name="IS_WallValue"
color="insulation_walls"
interface_coordinates=<2.41 0.03 2.6>
END MODULE WallT_TP_L2_SC260
MODULE WallT_TP_L2_WC260
MODULE post_processing
type="interface"
saving_times=(regular_vector(0.e+00,      $IS_SAVE2,
$DS_tend))
banner=true
format="gnuplot"
file_name="TP_L2_WC260"
END MODULE post_processing
concrete_name="IS_WallValue"
color="insulation_walls"
interface_coordinates=<0.03 3.16 2.6>
END MODULE WallT_TP_L2_WC260
MODULE WallT_TP_L3_EC255
MODULE post_processing
type="interface"
saving_times=(regular_vector(0.e+00,      $IS_SAVE2,
$DS_tend))
banner=true
format="gnuplot"
file_name="TP_L3_EC255"
END MODULE post_processing
concrete_name="IS_WallValue"
color="concrete_walls"
interface_coordinates=<10.3 3.14 2.52>
END MODULE WallT_TP_L3_EC255
MODULE WallT_TP_L3_NC255
MODULE post_processing
type="interface"
saving_times=(regular_vector(0.e+00,      $IS_SAVE2,
$DS_tend))
banner=true
format="gnuplot"
file_name="TP_L3_NC255"
END MODULE post_processing
concrete_name="IS_WallValue"
color="concrete_walls"
interface_coordinates=<7.67 5.97 2.51>
END MODULE WallT_TP_L3_NC255
MODULE WallT_TP_L3_SC255
MODULE post_processing
type="interface"
saving_times=(regular_vector(0.e+00,      $IS_SAVE2,
$DS_tend))
banner=true
format="gnuplot"
file_name="TP_L3_SC255"
END MODULE post_processing
concrete_name="IS_WallValue"
color="concrete_walls"
interface_coordinates=<7.62 0.03 2.55>
END MODULE WallT_TP_L3_SC255
MODULE WallT_TP_L3_WC255
MODULE post_processing
type="interface"
saving_times=(regular_vector(0.e+00,      $IS_SAVE2,
$DS_tend))
banner=true
format="gnuplot"
file_name="TP_L3_WC255"
END MODULE post_processing
concrete_name="IS_WallValue"
color="concrete_walls"
interface_coordinates=<5.3 2.84 2.49>
END MODULE WallT_TP_L3_WC255
MODULE WallT_TP_L2_PL
MODULE post_processing
type="interface"
saving_times=(regular_vector(0.e+00,      $IS_SAVE2,
$DS_tend))
banner=true
format="gnuplot"
file_name="TP_L2_PL"
END MODULE post_processing
concrete_name="IS_WallValue"
color="ceiling"
interface_coordinates=<4.85 3.0 3.95>
END MODULE WallT_TP_L2_PL
MODULE WallT_TP_L2_SOL
MODULE post_processing
type="wall_cutline"
file_basename="TP_L2_SOL"
saving_times=(regular_vector(0.e+00,      $IS_SAVE2,
$DS_tend))
banner=true
format="gnuplot"
END MODULE post_processing
concrete_name="IS_WallValue"
color="concrete_walls"
interface_coordinates=<3.73 3.0 0.0>
END MODULE WallT_TP_L2_SOL
MODULE flowup
MODULE post_processing
file_name="results_flow_leakup"
banner=true
format="gnuplot"
END MODULE post_processing
concrete_name="IS_FluxValue#inner_surface"

```

```

color="leaku"
flux_orientation=<1.0 0.0 0.0>
END MODULE flowup
MODULE flowdown
MODULE post_processing
file_name="results_flow_leakdown"
banner=true
format="gnuplot"
END MODULE post_processing
concrete_name="IS_FluxValue#inner_surface"
color="leakd"
flux_orientation=<1.0 0.0 0.0>
END MODULE flowdown
MODULE concentration_L2_BAS
MODULE parameters
END MODULE parameters
MODULE fields
END MODULE fields
MODULE field_compositions
MODULE product_mass_fraction
name="product_mass_fraction"
END MODULE product_mass_fraction
MODULE product_mole_fraction
name="product_mole_fraction"
END MODULE product_mole_fraction
MODULE oxidizer_mole_fraction
name="oxidizer_mole_fraction"
component=0
END MODULE oxidizer_mole_fraction
MODULE oxidizer_mass_fraction
name="oxidizer_mass_fraction"
component=0
END MODULE oxidizer_mass_fraction
MODULE soot_volume_fraction
name="soot_volume_fraction"
component=0
END MODULE soot_volume_fraction
END MODULE field_compositions
MODULE expressions
END MODULE expressions
MODULE points_definition
type="list_of_points"
points = (array(< 3.75e+00 1.6e+00 7.3e-01 > ))
END MODULE points_definition
MODULE post_processing
type="one_file"
banner=true
file_name="concentration_L2_BAS"
END MODULE post_processing
concrete_name="FE_FieldValue"
END MODULE concentration_L2_BAS
MODULE concentration_L3_BAS
MODULE parameters
END MODULE parameters
MODULE fields
END MODULE fields
MODULE field_compositions
MODULE product_mass_fraction
name="product_mass_fraction"
END MODULE product_mass_fraction
MODULE product_mole_fraction
name="product_mole_fraction"
END MODULE product_mole_fraction
MODULE oxidizer_mole_fraction
name="oxidizer_mole_fraction"
component=0
END MODULE oxidizer_mole_fraction
MODULE oxidizer_mass_fraction
name="oxidizer_mass_fraction"
component=0
END MODULE oxidizer_mass_fraction
MODULE soot_volume_fraction
name="soot_volume_fraction"
component=0
END MODULE soot_volume_fraction
END MODULE field_compositions
MODULE expressions
END MODULE expressions
MODULE points_definition
type="list_of_points"
points = (array(< 3.7e+00 3.4e+00 3.5e-01 > ))
END MODULE points_definition
MODULE post_processing
type="one_file"
banner=true
file_name="concentration_L2_FP"
END MODULE post_processing
MODULE oxidizer_mole_fraction
name="oxidizer_mole_fraction"
component=0
END MODULE oxidizer_mole_fraction
MODULE oxidizer_mass_fraction
name="oxidizer_mass_fraction"
component=0
END MODULE oxidizer_mass_fraction
MODULE soot_volume_fraction
name="soot_volume_fraction"
component=0
END MODULE soot_volume_fraction
END MODULE field_compositions
MODULE expressions
END MODULE expressions
MODULE points_definition
type="list_of_points"
points = (array(< 6.53e+00 4.52e+00 8.e-01 > ))
END MODULE points_definition
MODULE post_processing
type="one_file"
banner=true
file_name="concentration_L3_BAS"
END MODULE post_processing
concrete_name="FE_FieldValue"
END MODULE concentration_L3_BAS
MODULE concentration_L2_FP
MODULE parameters
END MODULE parameters
MODULE fields
END MODULE fields
MODULE field_compositions
MODULE product_mass_fraction
name="product_mass_fraction"
END MODULE product_mass_fraction
MODULE product_mole_fraction
name="product_mole_fraction"
END MODULE product_mole_fraction
MODULE oxidizer_mole_fraction
name="oxidizer_mole_fraction"
component=0
END MODULE oxidizer_mole_fraction
MODULE oxidizer_mass_fraction
name="oxidizer_mass_fraction"
component=0
END MODULE oxidizer_mass_fraction
MODULE soot_volume_fraction
name="soot_volume_fraction"
component=0
END MODULE soot_volume_fraction
END MODULE field_compositions
MODULE expressions
END MODULE expressions
MODULE points_definition
type="list_of_points"
points = (array(< 3.75e+00 1.6e+00 7.3e-01 > ))
END MODULE points_definition
MODULE post_processing
type="one_file"
banner=true
file_name="concentration_L2_FP"
END MODULE post_processing

```

```

END MODULE post_processing
concrete_name="FE_FieldValue"
END MODULE concentration_L2_FP
MODULE concentration_L2_HAUT
MODULE parameters
END MODULE parameters
MODULE fields
END MODULE fields
MODULE field_compositions
MODULE product_mass_fraction
name="product_mass_fraction"
END MODULE product_mass_fraction
MODULE product_mole_fraction
name="product_mole_fraction"
END MODULE product_mole_fraction
MODULE oxidizer_mole_fraction
name="oxidizer_mole_fraction"
component=0
END MODULE oxidizer_mole_fraction
MODULE oxidizer_mass_fraction
name="oxidizer_mass_fraction"
component=0
END MODULE oxidizer_mass_fraction
MODULE soot_volume_fraction
name="soot_volume_fraction"
component=0
END MODULE soot_volume_fraction
END MODULE field_compositions
MODULE expressions
END MODULE expressions
MODULE points_definition
type="list_of_points"
points = (array(< 3.73e+00 1.61e+00 3.33e+00 > ))
END MODULE points_definition
MODULE post_processing
type="one_file"
banner=true
file_name="concentration_L2_HAUT"
END MODULE post_processing
concrete_name="FE_FieldValue"
END MODULE concentration_L2_HAUT
MODULE concentration_L3_HAUT
MODULE parameters
END MODULE parameters
MODULE fields
END MODULE fields
MODULE field_compositions
MODULE product_mass_fraction
name="product_mass_fraction"
END MODULE product_mass_fraction
MODULE product_mole_fraction
name="product_mole_fraction"
END MODULE product_mole_fraction
MODULE oxidizer_mole_fraction
name="oxidizer_mole_fraction"
component=0
END MODULE oxidizer_mole_fraction
MODULE oxidizer_mass_fraction
name="oxidizer_mass_fraction"
component=0
END MODULE oxidizer_mass_fraction
MODULE soot_volume_fraction
name="soot_volume_fraction"
component=0
END MODULE soot_volume_fraction
END MODULE field_compositions
MODULE expressions
END MODULE expressions
MODULE points_definition
type="list_of_points"
points = (array(< 6.56e+00 4.57e+00 3.27e+00 > ))
END MODULE points_definition
MODULE post_processing
type="one_file"
banner=true
file_name="concentration_L3_HAUT"
END MODULE post_processing
concrete_name="FE_FieldValue"
END MODULE concentration_L3_HAUT
MODULE soot_l2_bas
MODULE parameters
END MODULE parameters
MODULE fields
END MODULE fields
MODULE field_compositions
MODULE soot_volume_fraction
name="soot_volume_fraction"
component=0
END MODULE soot_volume_fraction
MODULE density
name="density"
component=0
END MODULE density
END MODULE field_compositions
MODULE expressions
END MODULE expressions
MODULE points_definition
type="list_of_points"
points = (array(< 4.5e+00 5.76e+00 0.31e+00 > ))
END MODULE points_definition
MODULE post_processing
type="one_file"
banner=true
file_name="soot_l2_bas"
END MODULE post_processing
concrete_name="FE_FieldValue"
END MODULE soot_l2_bas
MODULE soot_l2_haut
MODULE parameters
END MODULE parameters
MODULE fields
END MODULE fields
MODULE field_compositions
MODULE soot_volume_fraction
name="soot_volume_fraction"
component=0
END MODULE soot_volume_fraction
MODULE density
name="density"
component=0
END MODULE density
END MODULE field_compositions
MODULE expressions
END MODULE expressions

```

```

MODULE points_definition
type="list_of_points"
points = (array(< 4.79e+00 5.76e+00 3.4e+00 > ))
END MODULE points_definition
MODULE post_processing
type="one_file"
banner=true
file_name="soot_l2_bas"
END MODULE post_processing
concrete_name="FE_FieldValue"
END MODULE soot_l2_haut
MODULE soot_l3_haut
MODULE parameters
END MODULE parameters
MODULE fields
END MODULE fields
MODULE field_compositions
MODULE soot_volume_fraction
name="soot_volume_fraction"
component=0
END MODULE soot_volume_fraction
MODULE density
name="density"
component=0
END MODULE density
END MODULE field_compositions
MODULE expressions
END MODULE expressions
MODULE points_definition
type="list_of_points"
points = (array(< 4.79e+00 5.76e+00 3.4e+00 > ))
END MODULE points_definition
MODULE post_processing
type="one_file"
banner=true
file_name="soot_l3_haut"
END MODULE post_processing
concrete_name="FE_FieldValue"
END MODULE soot_l3_haut
MODULE soot_l3_bas
MODULE parameters
END MODULE parameters
MODULE fields
END MODULE fields
MODULE field_compositions
MODULE soot_volume_fraction
name="soot_volume_fraction"
component=0
END MODULE soot_volume_fraction
MODULE density
name="density"
component=0
END MODULE density
END MODULE field_compositions
MODULE expressions
END MODULE expressions
MODULE points_definition
type="list_of_points"
points = (array(< 4.79e+00 5.76e+00 1.12e+00 > ))
END MODULE points_definition
MODULE post_processing
type="one_file"
banner=true
file_name="p_l2_moy"
END MODULE post_processing
concrete_name="FE_FieldValue"
END MODULE p_l2_moy
MODULE p_l3_moy
MODULE parameters
END MODULE parameters
MODULE fields
MODULE pressure
name="pressure"
component=0
END MODULE pressure
END MODULE fields
MODULE field_compositions
END MODULE field_compositions
MODULE expressions
END MODULE expressions
MODULE points_definition
type="list_of_points"
points = (array(< 5.75e+00 3.e+00 0.75e+00 > ))
END MODULE points_definition
MODULE post_processing
type="one_file"
banner=true
file_name="p_l3_moy"
END MODULE post_processing
concrete_name="FE_FieldValue"
END MODULE p_l3_moy
END MODULE visu_toolkit
output_times=(regular_vector(-1.e+00, 1, 0.e+00) <<
regular_vector(0.e+00, $IS_SAVE, $DS_tend))
END MODULE post_processing
MODULE space_discretization
velocity="finite_elements"
scalar="finite_volumes"
END MODULE space_discretization
concrete_name="ISIS"

```

```

revision=2.5
application="ISIS"
execution_mode="parallel"
END MODULE ISIS

```

9.2 Sylvia script

```

MODULE PEL_Application
$$$__file_name="data2.syl"
$$$__short_name="data2"
$DS_tinfl=(pow($DS_surface, 5.e-01)/$DS_vinfl)
$DS_surface=0.6
$DS_vinfl=0.02
$DS_masse=17.5
$DV_maillage_pos=<0.0010 0.0020 0.0040 0.0080 0.015
0.03 0.06 0.09 0.09>
$DV_maillage_neg=<0.09 0.09 0.06 0.03 0.015 0.0080
0.0040 0.0020 0.0010>
$DS_temperatur_init=300.0
$DS_conv_coef=10.0
$DV_maillage_double=<0.0010 0.0020 0.0040 0.0080
0.015 0.03 0.06 0.06 0.06 0.03 0.015 0.0080 0.0040 0.0020
0.0010>
$$$__created_by="vauxsa"
$$$__creation_date="Tue Apr 13 13:36:44 GMT+01:00
2010"
$DV_maillage_thermipan_pos=(vector(1.e-03, 2.e-03, 4.e-
03, 8.e-03, 1.5e-02, 2.e-02))
$DV_maillage_thermipan_neg=(vector(1.e-03, 2.e-03, 4.e-
03, 8.e-03, 1.5e-02, 2.e-02))
$DV_maillage_protege_pos=<0.0010 0.0020 0.0040
0.0080 0.015 0.03 0.05 0.06 0.06 0.07>
$DV_maillage_protege_neg=<0.07 0.06 0.06 0.05 0.03
0.015 0.0080 0.0040 0.0020 0.0010>
$DV_maillage_protege_double=<0.0010 0.0020 0.0040
0.0080 0.015 0.025 0.03 0.04 0.05 0.04 0.025 0.03 0.015
0.0080 0.0040 0.0020 0.0010>
$DS_Resist_locaux=322.0
$DS_Resist_amont=1550.0
$DS_Decharge=100000.0
$DS_Babraus_Infinite_MLR=0.048
$DS_Babraus_kb=2.0
$DS_Resist_FireRoom=322.0
$DS_Resist_Leak=12000.0
$DS_Resist_TargetRoom=7646.56
$DV_maillage_thermipan_pos_bis=(vector(1.e-03, 2.e-03,
4.e-03, 8.e-03, 1.5e-02))
$DV_maillage_thermipan_neg_bis=(vector(1.5e-02, 8.e-03,
4.e-03, 2.e-03, 1.e-03))
$DS_height=3.95
$DS_delta_rock2=0.05
$DS_delta_conc=0.3
$DS_delta_rock=0.03
$DS_length=5.94
$DS_width=4.94
MODULE ELEMENTS_LIST
MODULE Fluxmetre_top
MODULE TEMPERATURE
type="constant"
value=($DS_temperatur_init)
END MODULE TEMPERATURE
type="BC_TARGET"
name="Fluxmetre_top"

```

```

save=true
savelevel="all"
node="FireRoom"
orientation="bottom_top"
material="black_body"
center=<3.0 10.165 4.0>
END MODULE Fluxmetre_top
MODULE Flux_ceiling
MODULE TEMPERATURE
type="constant"
value=($DS_temperatur_init)
END MODULE TEMPERATURE
type="BC_TARGET"
name="Flux_ceiling"
save=true
savelevel="all"
node="FireRoom"
orientation="bottom_top"
material="black_body"
center=<4.82 7.8 4.44>
END MODULE Flux_ceiling
MODULE Fluxmetre_bottom
MODULE TEMPERATURE
type="constant"
value=($DS_temperatur_init)
END MODULE TEMPERATURE
type="BC_TARGET"
name="Fluxmetre_bottom"
save=true
savelevel="all"
node="FireRoom"
orientation="bottom_top"
material="black_body"
center=<3.0 10.165 1.0>
END MODULE Fluxmetre_bottom
MODULE N9JUP
type="ROOM1Z"
name="N9JUP"
coordinate=<0.0 0.0 0.0>
height=12.0
length=15.0
width=20.0
save=true
savelevel="all"
pressure=-101.0
temperature=($DS_temperatur_init)
measured_pressure=-101.0
_graphics="4:4:-16777216:-2105377:0:1:0:Monospaced-
plain-10:"
END MODULE N9JUP
MODULE N17
type="ROOM1Z"
name="N17"
coordinate=<0.0 0.0 9.7>
save=true
savelevel="unknowns"
pressure=-935.0
temperature=($DS_temperatur_init)
height=1.0
length=1.0
width=1.0
measured_pressure=-935.0

```



```

_graphics="6:4:-16777216:-2105377:0:1:0:Monospaced-
plain-10:"
END MODULE N17
MODULE N19
type="ROOM1Z"
name="N19"
coordinate=<0.0 0.0 1.1>
save=true
savelevel="unknowns"
pressure=-937.0
temperature=(SDS_temperatur_init)
height=1.0
length=1.0
width=1.0
measured_pressure=-937.0
_graphics="6:6:-16777216:-2105377:0:1:0:Monospaced-
plain-10:"
END MODULE N19
MODULE N3
type="ROOM1Z"
name="N3"
coordinate=<0.0 0.0 7.3>
save=true
savelevel="unknowns"
pressure=589.0
temperature=(SDS_temperatur_init)
height=1.0
length=1.0
width=1.0
measured_pressure=589.0
_graphics="2:6:-16777216:-2105377:0:1:0:Monospaced-
plain-10:"
END MODULE N3
MODULE N4
type="ROOM1Z"
name="N4"
coordinate=<0.0 0.0 11.3>
save=true
savelevel="unknowns"
pressure=535.0
height=1.0
length=1.0
width=1.0
measured_pressure=535.0
_graphics="2:4:-16777216:-2105377:0:1:0:Monospaced-
plain-10:"
END MODULE N4
MODULE B4_9
MODULE UPSTREAM
section=1.0
elevation=11.3
take="between"
put="plume"
node="N4"
_graphics="-16777216:0:1:true:true:Monospaced-plain-10"
END MODULE UPSTREAM
MODULE DOSTREAM
section=1.0
elevation=11.3
take="between"
put="plume"
node="N9JUP"

```

```

_graphics="-16777216:0:1:true:true:Monospaced-plain-10"
END MODULE DOSTREAM
MODULE RESIST
option="evaluated"
measured_volumetric_flow_rate=11760.0
compressible_correction=false
resistance=51.54269
END MODULE RESIST
type="RES_QUAD"
name="B4_9"
section=1.0
length=0.0
volumetric_flowrate=11760.0
save=true
savelevel="unknowns"
_graphics="3:4:-16777216:-2105377:0:1:0:Monospaced-
plain-10:"
END MODULE B4_9
MODULE B9_17
MODULE UPSTREAM
section=1.0
elevation=11.3
take="between"
put="plume"
node="N9JUP"
_graphics="-16777216:0:1:true:true:Monospaced-plain-10"
END MODULE UPSTREAM
MODULE DOSTREAM
section=1.0
elevation=9.7
take="between"
put="plume"
node="N17"
_graphics="-16777216:0:1:true:true:Monospaced-plain-10"
END MODULE DOSTREAM
MODULE RESIST
option="evaluated"
measured_volumetric_flow_rate=11760.0
compressible_correction=false
resistance=68.70564
END MODULE RESIST
type="RES_QUAD"
name="B9_17"
section=1.0
length=0.0
volumetric_flowrate=11760.0
save=true
savelevel="unknowns"
_graphics="5:4:-16777216:-2105377:0:1:0:Monospaced-
plain-10:"
END MODULE B9_17
MODULE B17_19
MODULE UPSTREAM
section=1.0
elevation=9.7
take="between"
put="plume"
node="N17"
_graphics="-16777216:0:1:true:true:Monospaced-plain-10"
END MODULE UPSTREAM
MODULE DOSTREAM
section=1.0

```

```

elevation=1.1
take="between"
put="plume"
node="N19"
_graphics="-16777216:0:1:true:true:Monospaced-plain-10"
END MODULE DOSTREAM
MODULE RESIST
option="evaluated"
measured_volumetric_flow_rate=13950.0
compressible_correction=false
resistance=0.1286571
END MODULE RESIST
type="RES_QUAD"
name="B17_19"
section=1.0
length=0.0
volumetric_flowrate=13950.0
save=true
savelevel="unknowns"
_graphics="6:5:-16777216:-2105377:0:1:90:Monospaced-plain-10:"
END MODULE B17_19
MODULE N20
MODULE PRESSURE
type="constant"
value=-2469.0
END MODULE PRESSURE
type="BCONDIT"
name="N20"
reference_altitude=0.0
save=false
savelevel="unknowns"
measured_pressure=-2469.0
_graphics="6:8:-16777216:-2105377:0:1:90:Monospaced-plain-10:"
END MODULE N20
MODULE N2
MODULE PRESSURE
type="constant"
value=1369.0
END MODULE PRESSURE
type="BCONDIT"
name="N2"
reference_altitude=0.0
save=true
savelevel="unknowns"
measured_pressure=1369.0
_graphics="2:8:-16777216:-2105377:0:1:90:Monospaced-plain-10:"
END MODULE N2
MODULE N25
MODULE PRESSURE
type="constant"
value=0.0
END MODULE PRESSURE
type="BCONDIT"
name="N25"
reference_altitude=0.0
save=true
savelevel="unknowns"
measured_pressure=0.0
_graphics="0:6:-16777216:-2105377:0:1:180:Monospaced-plain-10:"
END MODULE N25
MODULE N26
MODULE PRESSURE
type="constant"
value=0.0
END MODULE PRESSURE
type="BCONDIT"
name="N26"
reference_altitude=0.0
save=true
savelevel="unknowns"
measured_pressure=0.0
_graphics="8:6:-16777216:-2105377:0:1:0:Monospaced-plain-10:"
END MODULE N26
MODULE B19_20
MODULE UPSTREAM
section=1.0
elevation=1.1
take="between"
put="plume"
node="N19"
_graphics="-16777216:0:1:true:true:Monospaced-plain-10"
END MODULE UPSTREAM
MODULE DOSTREAM
section=1.0
elevation=5.0
take="between"
put="plume"
node="N20"
_graphics="-16777216:0:1:true:true:Monospaced-plain-10"
END MODULE DOSTREAM
MODULE RESIST
option="evaluated"
measured_volumetric_flow_rate=21836.0
compressible_correction=false
resistance=36.66437
END MODULE RESIST
type="RES_QUAD"
name="B19_20"
section=1.0
length=0.0
volumetric_flowrate=21836.0
save=true
savelevel="unknowns"
_graphics="6:7:-16777216:-2105377:0:1:90:Monospaced-plain-10:"
END MODULE B19_20
MODULE B2_3
MODULE UPSTREAM
section=1.0
elevation=2.0
take="between"
put="plume"
node="N2"
_graphics="-16777216:0:1:true:true:Monospaced-plain-10"
END MODULE UPSTREAM
MODULE DOSTREAM
section=1.0
elevation=7.3

```

```

take="between"
put="plume"
node="N3"
_graphics="-16777216:0:1:true:true:Monospaced-plain-10"
END MODULE DOSTREAM
MODULE RESIST
option="evaluated"
measured_volumetric_flow_rate=24688.0
compressible_correction=false
resistance=14.30588
END MODULE RESIST
type="RES_QUAD"
name="B2_3"
section=1.0
length=0.0
volumetric_flowrate=24688.0
save=true
savelevel="unknowns"
_graphics="2:7:-16777216:-2105377:0:1:270:Monospaced-
plain-10:"
END MODULE B2_3
MODULE B3_4
MODULE DOSTREAM
section=1.0
elevation=11.3
take="between"
put="plume"
node="N4"
_graphics="-16777216:0:1:true:true:Monospaced-plain-10"
END MODULE DOSTREAM
MODULE RESIST
option="evaluated"
measured_volumetric_flow_rate=13950.0
compressible_correction=false
resistance=3.127071
END MODULE RESIST
MODULE UPSTREAM
section=1.0
elevation=7.3
take="between"
put="plume"
node="N3"
_graphics="-16777216:0:1:true:true:Monospaced-plain-10"
END MODULE UPSTREAM
type="RES_QUAD"
name="B3_4"
section=1.0
length=0.0
volumetric_flowrate=13950.0
save=true
savelevel="unknowns"
_graphics="2:5:-16777216:-2105377:0:1:270:Monospaced-
plain-10:"
END MODULE B3_4
MODULE B3_25
MODULE UPSTREAM
section=1.0
elevation=7.3
take="between"
put="plume"
node="N3"
_graphics="-16777216:0:1:true:true:Monospaced-plain-10"

```

```

END MODULE UPSTREAM
MODULE DOSTREAM
section=1.0
elevation=20.0
take="between"
put="plume"
node="N25"
_graphics="-16777216:0:1:true:true:Monospaced-plain-10"
END MODULE DOSTREAM
MODULE RESIST
option="evaluated"
measured_volumetric_flow_rate=10738.0
compressible_correction=false
resistance=56.88011
END MODULE RESIST
type="RES_QUAD"
name="B3_25"
section=1.0
length=0.0
volumetric_flowrate=10738.0
save=true
savelevel="unknowns"
_graphics="1:6:-16777216:-2105377:0:1:180:Monospaced-
plain-10:"
END MODULE B3_25
MODULE B26_19
MODULE UPSTREAM
section=1.0
elevation=7.0
take="between"
put="plume"
node="N26"
_graphics="-16777216:0:1:true:true:Monospaced-plain-10"
END MODULE UPSTREAM
MODULE DOSTREAM
section=1.0
elevation=1.1
take="between"
put="plume"
node="N19"
_graphics="-16777216:0:1:true:true:Monospaced-plain-10"
END MODULE DOSTREAM
MODULE RESIST
option="evaluated"
measured_volumetric_flow_rate=11866.0
compressible_correction=false
resistance=75.56917
END MODULE RESIST
type="RES_QUAD"
name="B26_19"
section=1.0
length=0.0
volumetric_flowrate=11866.0
save=true
savelevel="unknowns"
_graphics="7:6:-16777216:-2105377:0:1:180:Monospaced-
plain-10:"
END MODULE B26_19
MODULE B4_6
MODULE UPSTREAM
section=1.0
elevation=11.3

```

```

take="between"
put="plume"
node="N4"
_graphics="-16777216:0:1:true:true:Monospaced-plain-10"
END MODULE UPSTREAM
MODULE DOSTREAM
section=1.0
elevation=8.6
take="between"
put="plume"
node="N6"
_graphics="-16777216:0:1:true:true:Monospaced-plain-10"
END MODULE DOSTREAM
MODULE RESIST
option="evaluated"
measured_volumetric_flow_rate=2190.0
compressible_correction=false
resistance=94.0801
END MODULE RESIST
type="RES_QUAD"
name="B4_6"
section=1.0
length=0.0
volumetric_flowrate=2190.0
save=true
savelevel="unknowns"
_graphics="2:3:-16777216:-2105377:0:1:270:Monospaced-plain-10:"
END MODULE B4_6
MODULE B16_17
MODULE UPSTREAM
section=1.0
elevation=8.2
take="between"
put="plume"
node="N16"
_graphics="-16777216:0:1:true:true:Monospaced-plain-10"
END MODULE UPSTREAM
MODULE DOSTREAM
section=1.0
elevation=9.7
take="between"
put="plume"
node="N17"
_graphics="-16777216:0:1:true:true:Monospaced-plain-10"
END MODULE DOSTREAM
MODULE RESIST
option="evaluated"
measured_volumetric_flow_rate=2197.0
compressible_correction=false
resistance=78.21373
END MODULE RESIST
type="RES_QUAD"
name="B16_17"
section=1.0
length=0.0
volumetric_flowrate=2197.0
save=true
savelevel="unknowns"
_graphics="6:3:-16777216:-2105377:0:1:90:Monospaced-plain-10:"
END MODULE B16_17

```

```

MODULE N6
type="ROOM1Z"
name="N6"
coordinate=<0.0 0.0 8.6>
save=true
savelevel="unknowns"
pressure=495.0
temperature=(SDS_temperatur_init)
height=1.0
length=1.0
width=1.0
measured_pressure=495.0
_graphics="2:2:-16777216:-2105377:0:1:270:Monospaced-plain-10:"
END MODULE N6
MODULE N16
type="ROOM1Z"
name="N16"
coordinate=<0.0 0.0 8.2>
save=true
savelevel="unknowns"
pressure=-902.0
temperature=(SDS_temperatur_init)
height=1.0
length=1.0
width=1.0
measured_pressure=-902.0
_graphics="6:2:-16777216:-2105377:0:1:270:Monospaced-plain-10:"
END MODULE N16
MODULE FireRoom
MODULE zone_inf
END MODULE zone_inf
MODULE zone_sup
END MODULE zone_sup
type="ROOM2Z"
name="FireRoom"
coordinate=(vector(0.e+00,
5.02e+00+SDS_delta_conc+SDS_delta_rock, 5.e-01))
height=(SDS_height)
length=(SDS_length)
width=(SDS_width)
residual_height=1.0E-4
save=true
savelevel="all"
pressure=-137.0
measured_pressure=-137.0
height_interface=(SDS_height*9.9e-01)
_graphics="4:2:-16777216:-2105377:0:1:0:Monospaced-plain-10:"
END MODULE FireRoom
MODULE TargetRoom
MODULE zone_inf
END MODULE zone_inf
MODULE zone_sup
END MODULE zone_sup
type="ROOM2Z"
name="TargetRoom"
coordinate=(vector(0.e+00, 2.e-02-SDS_delta_conc, 5.e-01))
height=(SDS_height)
length=6.0

```

```

width=5.0
pressure=-138.0
save=true
savelevel="all"
residual_height=1.0E-4
measured_pressure=-138.0
height_interface=(SDS_height*9.9e-01)
_graphics="4:0:-16777216:-2105377:0:1:0:Monospaced-
plain-10:"
END MODULE TargetRoom
MODULE B6_11
MODULE UPSTREAM
section=0.16
elevation=8.6
take="between"
put="plume"
node="N6"
_graphics="-16777216:0:1:true:true:Monospaced-plain-10"
END MODULE UPSTREAM
MODULE DOSTREAM
section=0.18
elevation=4.05
take="between"
put="mitler"
node="FireRoom"
_graphics="-16777216:0:1:true:true:Monospaced-plain-10"
END MODULE DOSTREAM
MODULE RESIST
option="evaluated"
measured_volumetric_flow_rate=1820.0
compressible_correction=false
resistance=2156.871
END MODULE RESIST
type="RES_QUAD"
name="B6_11"
section=0.018
length=0.0
volumetric_flowrate=1820.0
save=true
savelevel="unknowns"
_graphics="3:2:-16777216:-2105377:0:1:0:Monospaced-
plain-10:"
END MODULE B6_11
MODULE B11_16
MODULE UPSTREAM
section=0.18
elevation=4.05
take="between"
put="mitler"
node="FireRoom"
_graphics="-16777216:0:1:true:true:Monospaced-plain-10"
END MODULE UPSTREAM
MODULE DOSTREAM
section=0.16
elevation=8.2
take="between"
put="plume"
node="N16"
_graphics="-16777216:0:1:true:true:Monospaced-plain-10"
END MODULE DOSTREAM
MODULE RESIST
option="evaluated"

```

```

measured_volumetric_flow_rate=1820.0
compressible_correction=false
resistance=2574.315
END MODULE RESIST
type="RES_QUAD"
name="B11_16"
section=0.018
length=0.0
volumetric_flowrate=1820.0
save=true
savelevel="unknowns"
_graphics="5:2:-16777216:-2105377:0:1:0:Monospaced-
plain-10:"
END MODULE B11_16
MODULE Pool
MODULE MASS_LOSS_RATE
type="tabulation"
param=(vector(-3.e+02, 0.e+00, 2.20261e+01,
5.13941e+01, 8.07621e+01, 1.1013e+02, 1.39498e+02,
1.68866e+02, 1.98234e+02, 2.27602e+02, 2.5697e+02,
2.86339e+02, 3.15707e+02, 3.45075e+02, 3.74443e+02,
4.03811e+02, 4.33179e+02, 4.62547e+02, 4.91915e+02,
5.21283e+02, 5.50651e+02, 5.80019e+02,
6.093869999999999e+02, 6.38755e+02,
6.681230000000001e+02, 6.97491e+02, 7.26859e+02,
7.56228e+02, 7.85596e+02, 8.149640000000001e+02,
8.44332e+02, 8.737000000000001e+02, 9.03068e+02,
9.32436e+02, 9.61804e+02, 9.91172e+02, 1.02054e+03,
1.04991e+03, 1.07928e+03, 1.10864e+03, 1.13801e+03,
1.16738e+03, 1.19675e+03, 1.5e+03))
value=(vector(0.e+00, 0.e+00, 5.93489e-03, 1.67378e-02,
1.39612e-02, 1.03534e-02, 7.33095e-03, 7.66948e-03,
1.56565e-02, 1.88423e-02, 1.91958e-02, 1.974e-02,
1.8535e-02, 1.71508e-02, 1.77405e-02, 1.80731e-02,
1.73565e-02, 1.82423e-02, 1.79358e-02, 1.55566e-02,
1.70196e-02, 1.47081e-02, 2.01903e-02, 1.94154e-02,
2.06524e-02, 1.89331e-02, 1.65292e-02, 1.7579e-02,
2.17484e-02, 1.71418e-02, 1.68355e-02, 1.96515e-02,
2.15639e-02, 1.96212e-02, 1.59054e-02, 1.15524e-02,
9.434659999999999e-03, 7.41087e-03, 3.93795e-03,
4.41095e-03, 2.23465e-04, 0.e+00, 0.e+00, 0.e+00))
END MODULE MASS_LOSS_RATE
type="POOL"
name="Pool"
combustible_species="TPH"
save=true
savelevel="all"
ignition_time=0.0
mass=(SDS_masse)
verbose=true
coordinate=(vector(3.e+00, 7.8e+00, 7.e-01))
uptake_under_pool=0.0
additional_flux=true
exchange_surface="from_mass_loss_rate"
END MODULE Pool
MODULE WestWALL_thermipan
MODULE WALL_MESHING
type="constant"
value=1
END MODULE WALL_MESHING
MODULE STRIP_MESHING
type="tabulation"

```

```

value=$(SDV_maillage_thermipan_pos_bis)
END MODULE STRIP_MESHING
MODULE MIN_SIDE
element="FireRoom"
END MODULE MIN_SIDE
MODULE MAX_SIDE
element="WestWall_protege"
END MODULE MAX_SIDE
type="WALL"
name="WestWall_thermipan"
orientation="west"
material="rockwool"
save=true
savelevel="unknowns"
thickness=$(DS_delta_rock)
width=$(DS_length)
height=$(DS_height)
coordinate=(vector(0.e+00,
5.02e+00+$DS_delta_conc+$DS_delta_rock+$DS_width,
5.e-01))
END MODULE WestWALL_thermipan
MODULE Ceiling
MODULE STRIP_MESHING
type="constant"
value=6
END MODULE STRIP_MESHING
MODULE MIN_SIDE
element="Ceiling_thermipan"
END MODULE MIN_SIDE
type="SLAB"
orientation="top"
name="Ceiling"
material="concrete"
save=true
savelevel="unknowns"
thickness=$(DS_delta_conc)
dim_south_north=$(DS_length)
dim_east_west=$(DS_width)
center=(vector(5.e-01*$DS_length,
5.02e+00+$DS_delta_conc+$DS_delta_rock+5.e-
01*$DS_width, ($DS_height+$DS_delta_rock2+5.e-
01*$DS_delta_conc+5.e-01)))
END MODULE Ceiling
MODULE Floor
MODULE STRIP_MESHING
type="tabulation"
value=$(SDV_maillage_neg)
END MODULE STRIP_MESHING
MODULE MAX_SIDE
element="FireRoom"
END MODULE MAX_SIDE
type="SLAB"
orientation="bottom"
name="Floor"
material="concrete"
save=true
savelevel="unknowns"
thickness=$(DS_delta_conc)
dim_south_north=$(DS_length)
dim_east_west=$(DS_width)
center=(vector(5.e-01*$DS_length,
5.02e+00+$DS_delta_conc+$DS_delta_rock+5.e-
01*$DS_width, 3.5e-01))
END MODULE Floor
MODULE B12_16
MODULE UPSTREAM
section=0.18
elevation=4.05
take="between"
put="mitler"
node="TargetRoom"
_graphics="-16777216:0:1:true:true:Monospaced-plain-10"
END MODULE UPSTREAM
MODULE DOSTREAM
section=0.16
elevation=8.2
take="between"
put="plume"
node="N16"
_graphics="-16777216:0:1:true:true:Monospaced-plain-10"
END MODULE DOSTREAM
MODULE RESIST
option="evaluated"
measured_volumetric_flow_rate=361.0
compressible_correction=false
resistance=66603.09
END MODULE RESIST
type="RES_QUAD"
name="B12_16"
save=true
savelevel="unknowns"
section=0.018
length=0.0
volumetric_flowrate=361.0
_graphics="5:0:-16777216:-2105377:0:1:0:Monospaced-
plain-10:"
END MODULE B12_16
MODULE B6_12
MODULE UPSTREAM
section=0.16
elevation=8.6
take="between"
put="plume"
node="N6"
_graphics="-16777216:0:1:true:true:Monospaced-plain-10"
END MODULE UPSTREAM
MODULE DOSTREAM
section=0.18
elevation=4.05
take="between"
put="mitler"
node="TargetRoom"
_graphics="-16777216:0:1:true:true:Monospaced-plain-10"
END MODULE DOSTREAM
MODULE RESIST
option="evaluated"
measured_volumetric_flow_rate=373.0
compressible_correction=false
resistance=51226.02
END MODULE RESIST
type="RES_QUAD"
name="B6_12"

```

```

save=true
savelevel="unknowns"
section=0.018
length=0.0
volumetric_flowrate=373.0
_graphics="3:0:-16777216:-2105377:0:1:0:Monospaced-
plain-10:"
END MODULE B6_12
MODULE Ceiling_thermipan
MODULE STRIP_MESHING
type="tabulation"
value=($DV_maillage_thermipan_pos)
END MODULE STRIP_MESHING
MODULE MIN_SIDE
element="FireRoom"
END MODULE MIN_SIDE
MODULE MAX_SIDE
element="Ceiling"
END MODULE MAX_SIDE
type="SLAB"
orientation="top"
name="Ceiling_thermipan"
material="rockwool"
save=true
savelevel="unknowns"
thickness=($DS_delta_rock2)
dim_south_north=($DS_length)
dim_east_west=($DS_width)
center=(vector(5.e-01*$DS_length,
5.02e+00+$DS_delta_conc+$DS_delta_rock+5.e-
01*$DS_width, $DS_height+5.e-01*$DS_delta_rock2+5.e-
01))
END MODULE Ceiling_thermipan
MODULE SouthWall_target
MODULE WALL_MESHING
type="constant"
value=1
END MODULE WALL_MESHING
MODULE STRIP_MESHING
type="tabulation"
value=($DV_maillage_neg)
END MODULE STRIP_MESHING
MODULE MAX_SIDE
element="TargetRoom"
END MODULE MAX_SIDE
type="WALL"
name="SouthWall_target"
orientation="south"
material="concrete"
save=true
savelevel="unknowns"
thickness=($DS_delta_conc)
width=5.0
height=($DS_height)
coordinate=(vector(-3.e-01, 2.e-02-$DS_delta_conc, 5.e-
01))
END MODULE SouthWall_target
MODULE NorthWall_target
MODULE WALL_MESHING
type="constant"
value=1
END MODULE WALL_MESHING

```

```

MODULE STRIP_MESHING
type="tabulation"
value=($DV_maillage_pos)
END MODULE STRIP_MESHING
MODULE MIN_SIDE
element="TargetRoom"
END MODULE MIN_SIDE
type="WALL"
orientation="north"
name="NorthWall_target"
material="concrete"
save=true
savelevel="unknowns"
thickness=($DS_delta_conc)
width=5.0
height=($DS_height)
coordinate=(vector(6.e+00, 2.e-02-$DS_delta_conc, 5.e-
01))
END MODULE NorthWall_target
MODULE EastWall_target
MODULE WALL_MESHING
type="constant"
value=1
END MODULE WALL_MESHING
MODULE STRIP_MESHING
type="tabulation"
value=($DV_maillage_double)
END MODULE STRIP_MESHING
MODULE MAX_SIDE
element="TargetRoom"
END MODULE MAX_SIDE
type="WALL"
orientation="east"
name="EastWall_target"
material="concrete"
save=true
savelevel="unknowns"
thickness=($DS_delta_conc)
width=6.0
height=($DS_height)
coordinate=(vector(0.e+00, -2.8e-01-$DS_delta_conc, 5.e-
01))
END MODULE EastWall_target
MODULE Floor_target
MODULE STRIP_MESHING
type="tabulation"
value=($DV_maillage_neg)
END MODULE STRIP_MESHING
MODULE MAX_SIDE
element="TargetRoom"
END MODULE MAX_SIDE
type="SLAB"
orientation="bottom"
name="Floor_target"
material="concrete"
save=true
savelevel="unknowns"
thickness=($DS_delta_conc)
dim_south_north=6.0
dim_east_west=5.0
center=(vector(3.e+00, 2.52e+00-$DS_delta_conc, 3.5e-01))
END MODULE Floor_target

```

```

MODULE Ceiling_target_thermipan
MODULE STRIP_MESHING
type="tabulation"
value=($DV_maillage_thermipan_pos)
END MODULE STRIP_MESHING
MODULE MIN_SIDE
element="TargetRoom"
END MODULE MIN_SIDE
type="SLAB"
orientation="top"
name="Ceiling_target_thermipan"
material="rockwool"
save=true
savelevel="unknowns"
thickness=($DS_delta_rock2)
dim_south_north=6.0
dim_east_west=5.0
center=(vector(3.e+00, 2.52e+00-$DS_delta_conc,
$DS_height+5.e-01*$DS_delta_rock2+5.e-01))
END MODULE Ceiling_target_thermipan
MODULE Leak_up
MODULE UPSTREAM
section=0.03142
elevation=4.0
take="between"
put="mitler"
node="FireRoom"
_graphics="-16777216:0:1:true:true:Monospaced-plain-10"
END MODULE UPSTREAM
MODULE DOSTREAM
section=0.03142
elevation=4.0
take="between"
put="mitler"
node="TargetRoom"
_graphics="-16777216:0:1:true:true:Monospaced-plain-10"
END MODULE DOSTREAM
MODULE RESIST
option="evaluated"
measured_volumetric_flow_rate=91.0
compressible_correction=false
resistance=1369.131
END MODULE RESIST
type="RES_QUAD"
name="Leak_up"
save=true
savelevel="unknowns"
section=0.03142
length=1.5
volumetric_flowrate=110.0
_graphics="3:1:-16777216:-2105377:0:1:270:Monospaced-
plain-10:"
END MODULE Leak_up
MODULE Leak_dn
MODULE UPSTREAM
section=0.03142
elevation=1.0
take="between"
put="mitler"
node="FireRoom"
_graphics="-16777216:0:1:true:true:Monospaced-plain-10"
END MODULE UPSTREAM

```

```

MODULE DOSTREAM
section=0.03142
elevation=1.0
take="between"
put="mitler"
node="TargetRoom"
_graphics="-16777216:0:1:true:true:Monospaced-plain-10"
END MODULE DOSTREAM
MODULE RESIST
option="evaluated"
measured_volumetric_flow_rate=88.0
compressible_correction=false
resistance=1464.565
END MODULE RESIST
type="RES_QUAD"
name="Leak_dn"
save=true
savelevel="unknowns"
section=0.03142
length=1.5
volumetric_flowrate=8.0
_graphics="5:1:-16777216:-2105377:0:1:270:Monospaced-
plain-10:"
END MODULE Leak_dn
MODULE WestWALL_protege
MODULE WALL_MESHING
type="constant"
value=1
END MODULE WALL_MESHING
MODULE STRIP_MESHING
type="tabulation"
value=($DV_maillage_protege_pos)
END MODULE STRIP_MESHING
MODULE MIN_SIDE
element="WestWall_thermipan"
END MODULE MIN_SIDE
type="WALL"
name="WestWall_protege"
orientation="west"
material="concrete"
save=true
savelevel="unknowns"
thickness=($DS_delta_conc)
width=($DS_length)
height=($DS_height)
coordinate=(vector(0.e+00,
5.02e+00+$DS_delta_conc+2.e+00*$DS_delta_rock+$DS
_width, 5.e-01))
END MODULE WestWALL_protege
MODULE SouthWall_thermipan
MODULE WALL_MESHING
type="constant"
value=1
END MODULE WALL_MESHING
MODULE STRIP_MESHING
type="tabulation"
value=($DV_maillage_thermipan_neg_bis)
END MODULE STRIP_MESHING
MODULE MAX_SIDE
element="FireRoom"
END MODULE MAX_SIDE
MODULE MIN_SIDE

```



```

element="SouthWall_protege"
END MODULE MIN_SIDE
type="WALL"
name="SouthWall_thermipan"
orientation="south"
material="rockwool"
save=true
savelevel="unknowns"
thickness=($DS_delta_rock)
width=($DS_width)
height=($DS_height)
coordinate=(vector(-$DS_delta_rock,
5.02e+00+$DS_delta_conc+$DS_delta_rock, 5.e-01))
END MODULE SouthWall_thermipan
MODULE SouthWall_protege
MODULE WALL_MESHING
type="constant"
value=1
END MODULE WALL_MESHING
MODULE STRIP_MESHING
type="tabulation"
value=($DV_maillage_protege_neg)
END MODULE STRIP_MESHING
MODULE MAX_SIDE
element="SouthWall_thermipan"
END MODULE MAX_SIDE
type="WALL"
name="SouthWall_protege"
orientation="south"
material="concrete"
save=true
savelevel="unknowns"
thickness=($DS_delta_conc)
width=($DS_width)
height=($DS_height)
coordinate=(vector(-$DS_delta_rock-$DS_delta_conc,
5.02e+00+$DS_delta_conc+$DS_delta_rock, 5.e-01))
END MODULE SouthWall_protege
MODULE NorthWall_thermipan
MODULE WALL_MESHING
type="constant"
value=1
END MODULE WALL_MESHING
MODULE STRIP_MESHING
type="tabulation"
value=($DV_maillage_thermipan_pos_bis)
END MODULE STRIP_MESHING
MODULE MIN_SIDE
element="FireRoom"
END MODULE MIN_SIDE
MODULE MAX_SIDE
element="NorthWall_protege"
END MODULE MAX_SIDE
type="WALL"
orientation="north"
name="NorthWall_thermipan"
material="rockwool"
save=true
savelevel="unknowns"
thickness=($DS_delta_rock)
width=($DS_width)
height=($DS_height)
coordinate=(vector($DS_length,
5.02e+00+$DS_delta_conc+$DS_delta_rock, 5.e-01))
END MODULE NorthWall_thermipan
MODULE NorthWall_protege
MODULE WALL_MESHING
type="constant"
value=1
END MODULE WALL_MESHING
MODULE STRIP_MESHING
type="tabulation"
value=($DV_maillage_protege_pos)
END MODULE STRIP_MESHING
MODULE MIN_SIDE
element="NorthWall_thermipan"
END MODULE MIN_SIDE
type="WALL"
orientation="north"
name="NorthWall_protege"
material="concrete"
save=true
savelevel="unknowns"
thickness=($DS_delta_conc)
width=($DS_width)
height=($DS_height)
coordinate=(vector($DS_length+$DS_delta_rock,
5.02e+00+$DS_delta_conc+$DS_delta_rock, 5.e-01))
END MODULE NorthWall_protege
MODULE EastWall_thermipan
MODULE WALL_MESHING
type="constant"
value=1
END MODULE WALL_MESHING
MODULE STRIP_MESHING
type="tabulation"
value=($DV_maillage_thermipan_neg_bis)
END MODULE STRIP_MESHING
MODULE MIN_SIDE
element="EastWall_protege"
END MODULE MIN_SIDE
MODULE MAX_SIDE
element="FireRoom"
END MODULE MAX_SIDE
type="WALL"
orientation="east"
name="EastWall_thermipan"
material="rockwool"
save=true
savelevel="unknowns"
thickness=($DS_delta_rock)
width=($DS_length)
height=($DS_height)
coordinate=(vector(0.e+00, 5.02e+00+$DS_delta_conc,
5.e-01))
END MODULE EastWall_thermipan
MODULE EastWall_protege
MODULE WALL_MESHING
type="constant"
value=1
END MODULE WALL_MESHING
MODULE STRIP_MESHING
type="tabulation"
value=($DV_maillage_protege_double)

```

```

END MODULE STRIP_MESHING
MODULE MIN_SIDE
element="Westwall_target"
END MODULE MIN_SIDE
MODULE MAX_SIDE
element="EastWall_thermipan"
END MODULE MAX_SIDE
type="WALL"
orientation="east"
name="EastWall_protege"
material="concrete"
save=true
savelevel="unknowns"
thickness=($DS_delta_conc)
width=($DS_length)
height=($DS_height)
coordinate=(vector(0.e+00, 5.02e+00, 5.e-01))
END MODULE EastWall_protege
MODULE ceiling_target
MODULE STRIP_MESHING
type="constant"
value=6
END MODULE STRIP_MESHING
MODULE MIN_SIDE
element="Ceiling_target_thermipan"
END MODULE MIN_SIDE
type="SLAB"
name="ceiling_target"
save=true
savelevel="all"
center=(vector(3.e+00, 2.52e+00-$DS_delta_conc,
$DS_height+$DS_delta_rock2+5.e-01*$DS_delta_conc+5.e-01))
orientation="top"
thickness=($DS_delta_conc)
dim_south_north=6.0
dim_east_west=5.0
material="concrete"
END MODULE ceiling_target
MODULE Westwall_target
MODULE WALL_MESHING
type="constant"
value=1
END MODULE WALL_MESHING
MODULE STRIP_MESHING
type="tabulation"
value=($DV_maillage_double)
END MODULE STRIP_MESHING
MODULE MIN_SIDE
element="TargetRoom"
END MODULE MIN_SIDE
MODULE MAX_SIDE
element="EastWall_protege"
END MODULE MAX_SIDE
type="WALL"
name="Westwall_target"
save=true
savelevel="unknowns"
orientation="west"
material="concrete"
thickness=($DS_delta_conc)
width=6.0
height=($DS_height)
coordinate=(vector(0.e+00, 5.02e+00-$DS_delta_conc, 5.e-01))
END MODULE Westwall_target
MODULE Flux_N30
MODULE TEMPERATURE
type="constant"
value=($DS_temperatur_init)
END MODULE TEMPERATURE
type="BC_TARGET"
name="Flux_N30"
save=true
savelevel="all"
node="FireRoom"
orientation="south_north"
material="black_body"
center=<5.83 6.17 0.78>
END MODULE Flux_N30
MODULE Flux_N155
MODULE TEMPERATURE
type="constant"
value=($DS_temperatur_init)
END MODULE TEMPERATURE
type="BC_TARGET"
name="Flux_N155"
save=true
savelevel="all"
node="FireRoom"
orientation="south_north"
material="black_body"
center=<5.83 6.19 2.05>
END MODULE Flux_N155
MODULE Flux_N260
MODULE TEMPERATURE
type="constant"
value=($DS_temperatur_init)
END MODULE TEMPERATURE
type="BC_TARGET"
name="Flux_N260"
save=true
savelevel="all"
node="FireRoom"
orientation="south_north"
material="black_body"
center=<5.83 6.2 3.11>
END MODULE Flux_N260
MODULE Flux_N355
MODULE TEMPERATURE
type="constant"
value=($DS_temperatur_init)
END MODULE TEMPERATURE
type="BC_TARGET"
name="Flux_N355"
save=true
savelevel="all"
node="FireRoom"
orientation="south_north"
material="black_body"
center=<5.83 6.2 4.05>
END MODULE Flux_N355
END MODULE ELEMENTS_LIST
MODULE EXCHANGES_LIST

```

```

MODULE RadiaFireRoom
MODULE TARGET
name=<"Fluxmetre_top" "Fluxmetre_bottom" "Flux_N30"
"Flux_N155" "Flux_N260" "Flux_N355" "Flux_ceiling">
END MODULE TARGET
MODULE FIRE
name=<"Fire">
END MODULE FIRE
MODULE MIXTURE
MODULE SOOT
name="SOOT"
model="sarofim"
END MODULE SOOT
MODULE H2O
name="H2O"
model="viskanta"
END MODULE H2O
MODULE CO2
name="CO2"
model="viskanta"
END MODULE CO2
mixture_model="sfpe"
END MODULE MIXTURE
type="THERMAL_RADIATION"
name="RadiaFireRoom"
nodename="FireRoom"
wallsname=<"WestWall_thermipan"
"EastWall_thermipan" "NorthWall_thermipan"
"SouthWall_thermipan" "Ceiling_thermipan" "Floor">
save=true
savelevel="all"
END MODULE RadiaFireRoom
MODULE ConvTarget_Flu_top
MODULE CONVECTION
conv_coef_min_type="user_data"
conv_coef_max_type="user_data"
conv_coef_min=($DS_conv_coef)
conv_coef_max=($DS_conv_coef)
END MODULE CONVECTION
type="TARGET_CONV"
name="ConvTarget_Flu_top"
save=true
savelevel="all"
target="Fluxmetre_top"
END MODULE ConvTarget_Flu_top
MODULE ConvTarget_Flu_bottom
MODULE CONVECTION
conv_coef_min_type="user_data"
conv_coef_min=($DS_conv_coef)
conv_coef_max_type="user_data"
conv_coef_max=($DS_conv_coef)
END MODULE CONVECTION
type="TARGET_CONV"
name="ConvTarget_Flu_bottom"
save=true
savelevel="all"
target="Fluxmetre_bottom"
END MODULE ConvTarget_Flu_bottom
MODULE Fire
MODULE FLAME_TEMPERATURE
type="imposed"
imposed_flame_temperature=1200.0

```

```

END MODULE FLAME_TEMPERATURE
type="FIRE"
name="Fire"
node="FireRoom"
save=true
savelevel="all"
fuel="Pool"
plume="heskestad"
geometry="center"
END MODULE Fire
MODULE ConvFireR_WestW
MODULE CONVECTION
type="natural_convection_correlation"
END MODULE CONVECTION
type="WALL_CONVECTION"
name="ConvFireR_WestW"
wall="WestWall_thermipan"
node="FireRoom"
END MODULE ConvFireR_WestW
MODULE ConvFireR_EastW
MODULE CONVECTION
type="natural_convection_correlation"
END MODULE CONVECTION
type="WALL_CONVECTION"
name="ConvFireR_EastW"
wall="EastWall_thermipan"
node="FireRoom"
END MODULE ConvFireR_EastW
MODULE ConvFireR_SouthW
MODULE CONVECTION
type="user_data"
conv_coef=($DS_conv_coef)
END MODULE CONVECTION
type="WALL_CONVECTION"
name="ConvFireR_SouthW"
node="FireRoom"
wall="SouthWall_thermipan"
END MODULE ConvFireR_SouthW
MODULE ConvFireR_NorthW
MODULE CONVECTION
type="user_data"
conv_coef=($DS_conv_coef)
END MODULE CONVECTION
type="WALL_CONVECTION"
name="ConvFireR_NorthW"
node="FireRoom"
wall="NorthWall_thermipan"
END MODULE ConvFireR_NorthW
MODULE ConvFireR_Ceiling
MODULE CONVECTION
type="user_data"
conv_coef=($DS_conv_coef)
END MODULE CONVECTION
type="WALL_CONVECTION"
name="ConvFireR_Ceiling"
node="FireRoom"
wall="Ceiling_thermipan"
END MODULE ConvFireR_Ceiling
MODULE ConvFireR_Floor
MODULE CONVECTION
type="user_data"
conv_coef=($DS_conv_coef)

```

```

END MODULE CONVECTION
type="WALL_CONVECTION"
name="ConvFireR_Floor"
node="FireRoom"
wall="Floor"
END MODULE ConvFireR_Floor
MODULE ConvTargetR_WestW
MODULE CONVECTION
type="user_data"
conv_coef=(SDS_conv_coef)
END MODULE CONVECTION
type="WALL_CONVECTION"
name="ConvTargetR_WestW"
node="TargetRoom"
wall="Westwall_target"
END MODULE ConvTargetR_WestW
MODULE ConvTargetR_EastW
MODULE CONVECTION
type="user_data"
conv_coef=(SDS_conv_coef)
END MODULE CONVECTION
type="WALL_CONVECTION"
name="ConvTargetR_EastW"
node="TargetRoom"
wall="EastWall_target"
END MODULE ConvTargetR_EastW
MODULE ConvTargetR_SouthW
MODULE CONVECTION
type="user_data"
conv_coef=(SDS_conv_coef)
END MODULE CONVECTION
type="WALL_CONVECTION"
name="ConvTargetR_SouthW"
node="TargetRoom"
wall="SouthWall_target"
END MODULE ConvTargetR_SouthW
MODULE ConvTargetR_NorthW
MODULE CONVECTION
type="user_data"
conv_coef=(SDS_conv_coef)
END MODULE CONVECTION
type="WALL_CONVECTION"
name="ConvTargetR_NorthW"
node="TargetRoom"
wall="NorthWall_target"
END MODULE ConvTargetR_NorthW
MODULE ConvTargetR_Ceiling
MODULE CONVECTION
type="user_data"
conv_coef=(SDS_conv_coef)
END MODULE CONVECTION
type="WALL_CONVECTION"
name="ConvTargetR_Ceiling"
node="TargetRoom"
wall="Ceiling_target_thermipan"
END MODULE ConvTargetR_Ceiling
MODULE ConvTargetR_Floor
MODULE CONVECTION
type="user_data"
conv_coef=(SDS_conv_coef)
END MODULE CONVECTION
type="WALL_CONVECTION"
name="ConvTargetR_Floor"
node="TargetRoom"
wall="Floor_target"
END MODULE ConvTargetR_Floor
MODULE RadiaTargetRoom
MODULE MIXTURE
MODULE SOOT
name="SOOT"
model="sarofim"
END MODULE SOOT
MODULE H2O
name="H2O"
model="viskanta"
END MODULE H2O
MODULE CO2
name="CO2"
model="viskanta"
END MODULE CO2
mixture_model="sfpe"
END MODULE MIXTURE
type="THERMAL_RADIATION"
name="RadiaTargetRoom"
nodename="TargetRoom"
wallsname=<"Westwall_target" "EastWall_target"
"NorthWall_target" "SouthWall_target"
"Ceiling_target_thermipan" "Floor_target">
save=true
savelevel="all"
END MODULE RadiaTargetRoom
END MODULE EXCHANGES_LIST
MODULE MATERIALS_LIST
MODULE BLACK_BODY
MODULE ENTHALPY
type="polynom"
coefficient=<0.0 473.0>
END MODULE ENTHALPY
MODULE CONDUCTIVITY
type="tabulation"
param=<273.15 293.15 373.15 473.15 573.0 673.15 873.15
1073.15 1273.15 1473.15>
value=<43.0 43.0 43.0 42.0 40.0 36.0 33.0 29.0 28.0 29.0>
END MODULE CONDUCTIVITY
MODULE EMISSIVITY
type="constant"
value=1.0
END MODULE EMISSIVITY
name="black_body"
density=7801.0
comment="Steel with 1%C"
END MODULE BLACK_BODY
MODULE CONCRETE
MODULE ENTHALPY
type="polynom"
coefficient=<0.0 736.0>
END MODULE ENTHALPY
MODULE CONDUCTIVITY
type="constant"
value=1.5
END MODULE CONDUCTIVITY
MODULE EMISSIVITY
type="constant"
value=0.7

```

```

END MODULE EMISSIVITY
name="concrete"
density=2430.0
comment="Concrete, cinder Stone at 20°C"
END MODULE CONCRETE
MODULE ROCKWOOL
MODULE CONDUCTIVITY
type="constant"
value=0.102
END MODULE CONDUCTIVITY
MODULE ENTHALPY
type="polynom"
coefficient=<0.0 840.0>
END MODULE ENTHALPY
MODULE EMISSIVITY
type="constant"
value=0.95
END MODULE EMISSIVITY
name="rockwool"
density=140.0
END MODULE ROCKWOOL
END MODULE MATERIALS_LIST
MODULE TIME
begtime=-300.0
endtime=1500.0
END MODULE TIME
MODULE NUMERICS
bdf_order=1
stepmin=1.0E-4
stepmax=1.0
stepinit=0.1
upcoef=2.0
downcoef=2.0
END MODULE NUMERICS
MODULE DEFAULT_VALUES
MODULE MASS_FRACTIONS
MODULE TPH
type="gas"
name="TPH"
value=0.0
END MODULE TPH
MODULE O2
type="gas"
name="O2"
value=0.233
END MODULE O2
MODULE H2O
type="gas"
name="H2O"
value=0.0
END MODULE H2O
MODULE CO2
type="gas"
name="CO2"
value=0.0
END MODULE CO2
MODULE CO
type="gas"
name="CO"
value=0.0
END MODULE CO
MODULE SOOT
type="particle"
name="SOOT"
value=0.0
END MODULE SOOT
END MODULE MASS_FRACTIONS
pressure=0.0
temperature=(SDS_temperatur_init)
END MODULE DEFAULT_VALUES
MODULE VERBOSE
bdf=false
func=false
eqc=false
newton=false
pitch=false
gest_elt=false
gest_ech=false
END MODULE VERBOSE
MODULE REFERENCE
pressure=101325.0
density=1.176
constant_density=false
END MODULE REFERENCE
MODULE SAVE
filename=(SSS__short_name+".sav")
format="ASCII"
END MODULE SAVE
MODULE SPECIES_LIST
MODULE MAJOR_SPECIES
MODULE ENTHALPY
type="janaf"
molar_mass=0.028
formation_heat=0.0
cp_coef=<26.092 8.218801 -1.976141 0.159274 0.044434>
bound_min=200.0
bound_max=6000.0
END MODULE ENTHALPY
MODULE VISCOSITY
type="tabulation"
param=<80.0 90.0 100.0 110.0 120.0 130.0 140.0 150.0
160.0 170.0 180.0 190.0 200.0 210.0 220.0 230.0 240.0
250.0 260.0 270.0 280.0 290.0 300.0 310.0 320.0 330.0
340.0 350.0 360.0 370.0 380.0 390.0 400.0 410.0 420.0
430.0 440.0 450.0 460.0 470.0 480.0 490.0 500.0 510.0
520.0 530.0 540.0 550.0 560.0 570.0 580.0 590.0 600.0
610.0 620.0 630.0 640.0 650.0 660.0 670.0 680.0 690.0
700.0 710.0 720.0 730.0 740.0 750.0 760.0 770.0 780.0
790.0 800.0 810.0 820.0 830.0 840.0 850.0 860.0 870.0
880.0 890.0 900.0 910.0 920.0 930.0 940.0 950.0 960.0
970.0 980.0 990.0 1000.0 1010.0 1020.0 1030.0 1040.0
1050.0 1060.0 1070.0 1080.0 1090.0 1100.0 1110.0 1120.0
1130.0 1140.0 1150.0 1160.0 1170.0 1180.0 1190.0 1200.0
1210.0 1220.0 1230.0 1240.0 1250.0 1260.0 1270.0 1280.0
1290.0 1300.0 1310.0 1320.0 1330.0 1340.0 1350.0 1360.0
1370.0 1380.0 1390.0 1400.0 1410.0 1420.0 1430.0 1440.0
1450.0 1460.0 1470.0 1480.0 1490.0 1500.0 1550.0 1600.0
1650.0 1700.0 1750.0 1800.0 1850.0 1900.0 1950.0 2000.0
2100.0 2200.0 3000.0>
value=<5.59E-6 6.22E-6 6.87E-6 7.52E-6 8.15E-6 8.78E-6
9.4E-6 1.0E-5 1.059E-5 1.118E-5 1.175E-5 1.231E-5
1.286E-5 1.34E-5 1.393E-5 1.445E-5 1.496E-5 1.546E-5
1.596E-5 1.645E-5 1.692E-5 1.74E-5 1.786E-5 1.832E-5
1.877E-5 1.921E-5 1.965E-5 2.008E-5 2.05E-5 2.092E-5

```

```

2.133E-5 2.174E-5 2.214E-5 2.254E-5 2.293E-5 2.332E-5
2.37E-5 2.408E-5 2.4E-5 2.482E-5 2.518E-5 2.554E-5
2.59E-5 2.625E-5 2.66E-5 2.695E-5 2.729E-5 2.763E-5
2.796E-5 2.83E-5 2.863E-5 2.895E-5 2.927E-5 2.959E-5
2.991E-5 3.023E-5 3.054E-5 3.085E-5 3.115E-5 3.146E-5
3.176E-5 3.206E-5 3.235E-5 3.265E-5 3.294E-5 3.323E-5
3.352E-5 3.38E-5 3.409E-5 3.437E-5 3.465E-5 3.493E-5
3.52E-5 3.548E-5 3.575E-5 3.602E-5 3.629E-5 3.655E-5
3.682E-5 3.708E-5 3.734E-5 3.76E-5 3.786E-5 3.812E-5
3.837E-5 3.863E-5 3.888E-5 3.912E-5 3.938E-5 3.963E-5
3.987E-5 4.012E-5 4.036E-5 4.06E-5 4.08E-5 4.11E-5
4.13E-5 4.16E-5 4.18E-5 4.2E-5 4.23E-5 4.25E-5 4.27E-5
4.3E-5 4.32E-5 4.34E-5 4.36E-5 4.39E-5 4.41E-5 4.43E-5
4.45E-5 4.48E-5 4.5E-5 4.52E-5 4.54E-5 4.56E-5 4.58E-5
4.61E-5 4.63E-5 4.65E-5 4.67E-5 4.69E-5 4.71E-5 4.73E-5
4.75E-5 4.78E-5 4.8E-5 4.82E-5 4.84E-5 4.86E-5 4.88E-5
4.9E-5 4.92E-5 4.94E-5 4.96E-5 4.98E-5 5.0E-5 5.02E-5
5.04E-5 5.06E-5 5.08E-5 5.1E-5 5.12E-5 5.21E-5 5.31E-5
5.4E-5 5.49E-5 5.58E-5 5.67E-5 5.76E-5 5.85E-5 5.93E-5
6.01E-5 6.18E-5 6.34E-5 6.34E-5>
END MODULE VISCOSITY
MODULE CONDUCTIVITY
type="tabulation"
param=<100.0 110.0 120.0 130.0 140.0 150.0 160.0 170.0
180.0 190.0 200.0 210.0 220.0 230.0 240.0 250.0 260.0
270.0 280.0 290.0 300.0 310.0 320.0 330.0 340.0 350.0
360.0 370.0 380.0 390.0 400.0 410.0 420.0 430.0 440.0
450.0 460.0 470.0 480.0 490.0 500.0 510.0 520.0 530.0
540.0 550.0 560.0 570.0 580.0 590.0 600.0 610.0 620.0
630.0 640.0 650.0 660.0 670.0 680.0 690.0 700.0 710.0
720.0 730.0 740.0 750.0 760.0 770.0 780.0 790.0 800.0
810.0 820.0 830.0 840.0 850.0 860.0 870.0 880.0 890.0
900.0 910.0 920.0 930.0 940.0 950.0 960.0 970.0 980.0
990.0 1000.0 1050.0 1100.0 1150.0 1200.0 1250.0 1300.0
1350.0 1400.0 1450.0 1500.0 1550.0 1600.0 1650.0 1700.0
1750.0 1800.0 1850.0 1900.0 1950.0 2000.0 2100.0 2200.0
2300.0 2400.0 2500.0 2600.0 2700.0 2800.0 2900.0 3000.0
3100.0 3200.0 3300.0 3400.0 3500.0>
value=<0.00941 0.0103 0.01119 0.01208 0.01296 0.01385
0.01474 0.01562 0.01651 0.01739 0.01826 0.01908
0.01989 0.02067 0.02145 0.02222 0.02298 0.02374
0.02449 0.02524 0.02598 0.02671 0.02741 0.02808
0.02874 0.02939 0.03002 0.03065 0.03127 0.03189
0.03252 0.03314 0.03376 0.03438 0.03501 0.03564
0.03626 0.03688 0.03749 0.03808 0.03864 0.0392 0.0398
0.0403 0.0408 0.0414 0.042 0.0425 0.0431 0.0436 0.0441
0.0446 0.0452 0.0457 0.0462 0.0467 0.0472 0.0478 0.0483
0.0488 0.0493 0.0498 0.0503 0.0508 0.0513 0.0517 0.0522
0.0526 0.0531 0.0536 0.0541 0.0546 0.0551 0.0555 0.0559
0.0564 0.0569 0.0574 0.0578 0.0583 0.0587 0.0592 0.0596
0.06 0.0605 0.0609 0.0613 0.0618 0.0622 0.0626 0.0631
0.0651 0.0672 0.0693 0.0713 0.0733 0.0754 0.0775 0.0797
0.0819 0.0842 0.0867 0.0893 0.0921 0.095 0.0981 0.1013
0.1046 0.108 0.1113 0.1146 0.1207 0.1263 0.1314 0.1361
0.1406 0.1449 0.1494 0.1542 0.159 0.164 0.1691 0.1743
0.1795 0.1853 0.1915>
END MODULE CONDUCTIVITY
type="gas"
name="N2"
molar=0.028
heat_of_formation=0.0
verbose=false

```

```

END MODULE MAJOR_SPECIES
MODULE CARRIER_GAS
MODULE TPH
MODULE ENTHALPY
type="polynom"
coefficient=<-652950.0 2190.0>
END MODULE ENTHALPY
MODULE VISCOSITY
type="constant"
value=0.001235
END MODULE VISCOSITY
MODULE CONDUCTIVITY
type="polynom"
coefficient=<-0.035133 1.1783E-4>
END MODULE CONDUCTIVITY
MODULE COMBUSTION
MODULE PRODUCTS
MODULE CO2
type="gas"
name="CO2"
yield=3.02
END MODULE CO2
MODULE H2O
type="gas"
name="H2O"
yield=1.37647
END MODULE H2O
MODULE CO
type="gas"
name="CO"
yield=8.8E-4
END MODULE CO
MODULE SOOT
type="particle"
name="SOOT"
yield=0.023
END MODULE SOOT
END MODULE PRODUCTS
type="mass_constant"
name="TPH_combustion"
oxidant_name="O2"
oxidant_yield=3.42035
combustion_heat=4.55E7
verbose=true
END MODULE COMBUSTION
MODULE OXIDANT_LIMIT
type="no_limit"
END MODULE OXIDANT_LIMIT
MODULE MASS_LOSS_RATE
type="constant"
value=0.05
END MODULE MASS_LOSS_RATE
MODULE EXTINCTION
decrease_time_constant=10.0
pyrolysis_rate=0.01
flame_temperature=0.0
END MODULE EXTINCTION
type="liquid_fuel"
name="TPH"
molar=0.17
heat_of_formation=-0.2909
verbose=false

```

```

liquid_density=758.0
liquid_heat_capacity=2163.0
liquid_viscosity=0.001235
liquid_conductivity=0.133
vaporization_temperature=461.15
oxidant_name="O2"
radiated_fraction=0.35
vaporization_heat=361000.0
END MODULE TPH
MODULE O2
MODULE ENTHALPY
type="janaf"
molar_mass=0.032
formation_heat=0.0
cp_coef=<29.659 6.137261 -1.186521 0.09578 -0.219663>
bound_min=200.0
bound_max=6000.0
END MODULE ENTHALPY
MODULE VISCOSITY
type="tabulation"
param=<100.0 110.0 120.0 130.0 140.0 150.0 160.0 170.0
180.0 190.0 200.0 210.0 220.0 230.0 240.0 250.0 260.0
270.0 280.0 290.0 300.0 310.0 320.0 330.0 340.0 350.0
360.0 370.0 380.0 390.0 400.0 410.0 420.0 430.0 440.0
450.0 460.0 470.0 480.0 490.0 500.0 510.0 520.0 530.0
540.0 550.0 560.0 570.0 580.0 590.0 600.0 610.0 620.0
630.0 640.0 650.0 660.0 670.0 680.0 690.0 700.0 710.0
720.0 730.0 740.0 750.0 760.0 770.0 780.0 790.0 800.0
810.0 820.0 830.0 840.0 850.0 860.0 870.0 880.0 890.0
900.0 910.0 920.0 930.0 940.0 950.0 960.0 970.0 980.0
990.0 1000.0 1050.0 1100.0 1150.0 1200.0 1250.0 1300.0
1350.0 1400.0 1450.0 1500.0 1550.0 1600.0 1650.0 1700.0
1750.0 1800.0 1850.0 1900.0 1950.0 2000.0 3000.0>
value=<7.68E-6 8.39E-6 9.12E-6 9.85E-6 1.056E-5
1.127E-5 1.196E-5 1.265E-5 1.333E-5 1.399E-5 1.465E-5
1.529E-5 1.593E-5 1.655E-5 1.717E-5 1.777E-5 1.837E-5
1.896E-5 1.954E-5 2.011E-5 2.067E-5 2.123E-5 2.177E-5
2.231E-5 2.284E-5 2.337E-5 2.389E-5 2.44E-5 2.491E-5
2.541E-5 2.589E-5 2.639E-5 2.687E-5 2.735E-5 2.782E-5
2.828E-5 2.874E-5 2.92E-5 2.965E-5 3.01E-5 3.054E-5
3.1E-5 3.14E-5 3.18E-5 3.23E-5 3.27E-5 3.31E-5 3.35E-5
3.39E-5 3.43E-5 3.47E-5 3.52E-5 3.55E-5 3.59E-5 3.63E-5
3.67E-5 3.71E-5 3.74E-5 3.78E-5 3.82E-5 3.85E-5 3.89E-5
3.93E-5 3.96E-5 4.0E-5 4.03E-5 4.07E-5 4.11E-5 4.14E-5
4.17E-5 4.21E-5 4.24E-5 4.28E-5 4.31E-5 4.34E-5 4.38E-5
4.41E-5 4.44E-5 4.47E-5 4.51E-5 4.54E-5 4.57E-5 4.6E-5
4.63E-5 4.67E-5 4.7E-5 4.73E-5 4.76E-5 4.79E-5 4.82E-5
4.85E-5 5.0E-5 5.14E-5 5.29E-5 5.42E-5 5.56E-5 5.69E-5
5.82E-5 5.95E-5 6.07E-5 6.19E-5 6.31E-5 6.43E-5 6.55E-5
6.66E-5 6.77E-5 6.88E-5 6.99E-5 7.1E-5 7.21E-5 7.31E-5
7.31E-5>
END MODULE VISCOSITY
MODULE CONDUCTIVITY
type="tabulation"
param=<100.0 110.0 120.0 130.0 140.0 150.0 160.0 170.0
180.0 190.0 200.0 210.0 220.0 230.0 240.0 250.0 260.0
270.0 280.0 290.0 300.0 310.0 320.0 330.0 340.0 350.0
360.0 370.0 380.0 390.0 400.0 410.0 420.0 430.0 440.0
450.0 460.0 470.0 480.0 490.0 500.0 510.0 520.0 530.0
540.0 550.0 560.0 570.0 580.0 590.0 600.0 610.0 620.0
630.0 640.0 650.0 660.0 670.0 680.0 690.0 700.0 710.0
720.0 730.0 740.0 750.0 760.0 770.0 780.0 790.0 800.0

```

```

810.0 820.0 830.0 840.0 850.0 860.0 870.0 880.0 890.0
900.0 910.0 920.0 930.0 940.0 950.0 960.0 970.0 980.0
990.0 1000.0 1010.0 1020.0 1030.0 1040.0 1050.0 1060.0
1070.0 1080.0 1090.0 1100.0 1110.0 1120.0 1130.0 1140.0
1150.0 1160.0 1170.0 1180.0 1190.0 1200.0 1210.0 1220.0
1230.0 1240.0 1250.0 1260.0 1270.0 1280.0 1290.0 1300.0
1310.0 1320.0 1330.0 1340.0 1350.0 1360.0 1370.0 1380.0
1390.0 1400.0 1410.0 1420.0 1430.0 1440.0 1450.0 1460.0
1470.0 1480.0 1490.0 1500.0 3000.0>
value=<0.00905 0.00998 0.01092 0.01187 0.01281
0.01376 0.01466 0.01556 0.01646 0.01735 0.01824
0.01911 0.01997 0.02083 0.02168 0.02254 0.02339
0.02424 0.02509 0.02592 0.02674 0.02753 0.02831
0.02907 0.02982 0.03056 0.0313 0.03204 0.03276 0.03348
0.0342 0.0349 0.0356 0.0363 0.037 0.0377 0.0384 0.0391
0.0398 0.0405 0.0412 0.0419 0.0426 0.0433 0.044 0.0447
0.0453 0.046 0.0467 0.0474 0.048 0.0487 0.0493 0.05
0.0506 0.0513 0.0519 0.0525 0.0532 0.0538 0.0544 0.055
0.0556 0.0562 0.0568 0.0574 0.0579 0.0585 0.0591 0.0597
0.0603 0.0609 0.0615 0.062 0.0626 0.0632 0.0638 0.0644
0.065 0.0655 0.0661 0.0667 0.0672 0.0678 0.0684 0.0689
0.0695 0.0701 0.0706 0.0712 0.0717 0.0723 0.0728 0.0734
0.0739 0.0745 0.075 0.0755 0.076 0.0765 0.0771 0.0776
0.0781 0.0786 0.0791 0.0796 0.0801 0.0806 0.0811 0.0816
0.0821 0.0826 0.0831 0.0836 0.0841 0.0846 0.0851 0.0856
0.0861 0.0866 0.0871 0.0876 0.0881 0.0886 0.0891 0.0896
0.0901 0.0906 0.0911 0.0916 0.0921 0.0926 0.0931 0.0936
0.0941 0.0946 0.0951 0.0956 0.096 0.0965 0.097 0.097>
END MODULE CONDUCTIVITY
type="gas"
name="O2"
molar=0.032
heat_of_formation=0.0
verbose=false
END MODULE O2
MODULE CO2
MODULE ENTHALPY
MODULE FUNC_LIST
MODULE FUNCTION#1
type="janaf"
molar_mass=0.044
formation_heat=-393522.4
cp_coef=<24.99737 55.18696 -33.69137 7.948387 -
0.136638>
bound_min=200.0
bound_max=1200.0
END MODULE FUNCTION#1
MODULE FUNCTION#2
type="janaf"
molar_mass=0.044
formation_heat=-393522.4
cp_coef=<58.16639 2.720074 -0.492289 0.038844 -
6.447293>
bound_min=1200.0
bound_max=6000.0
END MODULE FUNCTION#2
END MODULE FUNC_LIST
type="piecewise_continuous"
END MODULE ENTHALPY
MODULE VISCOSITY
type="tabulation"

```

```

param=<170.0 180.0 190.0 200.0 210.0 220.0 230.0 240.0
250.0 260.0 270.0 280.0 290.0 300.0 310.0 320.0 330.0
340.0 350.0 360.0 370.0 380.0 390.0 400.0 410.0 420.0
430.0 440.0 450.0 460.0 470.0 480.0 490.0 500.0 510.0
520.0 530.0 540.0 550.0 560.0 570.0 580.0 590.0 600.0
610.0 620.0 630.0 640.0 650.0 660.0 670.0 680.0 690.0
700.0 710.0 720.0 730.0 740.0 750.0 760.0 770.0 780.0
790.0 800.0 810.0 820.0 830.0 840.0 850.0 860.0 870.0
880.0 890.0 900.0 910.0 920.0 930.0 940.0 950.0 960.0
970.0 980.0 990.0 1000.0 1050.0 1100.0 1150.0 1200.0
1250.0 1300.0 1350.0 1400.0 1450.0 1500.0 1550.0 1600.0
1650.0 1700.0 1750.0 1800.0 1850.0 1900.0 1950.0 2000.0
3000.0>
value=<8.79E-6 9.26E-6 9.74E-6 1.022E-5 1.071E-5
1.119E-5 1.168E-5 1.216E-5 1.263E-5 1.312E-5 1.359E-5
1.406E-5 1.453E-5 1.499E-5 1.545E-5 1.591E-5 1.636E-5
1.681E-5 1.726E-5 1.77E-5 1.814E-5 1.857E-5 1.9E-5
1.942E-5 1.985E-5 2.026E-5 2.068E-5 2.109E-5 2.15E-5
2.19E-5 2.23E-5 2.269E-5 2.309E-5 2.348E-5 2.39E-5
2.43E-5 2.46E-5 2.5E-5 2.54E-5 2.57E-5 2.61E-5 2.65E-5
2.68E-5 2.72E-5 2.76E-5 2.79E-5 2.83E-5 2.86E-5 2.9E-5
2.93E-5 2.96E-5 3.0E-5 3.03E-5 3.06E-5 3.1E-5 3.13E-5
3.16E-5 3.2E-5 3.23E-5 3.26E-5 3.29E-5 3.32E-5 3.35E-5
3.39E-5 3.42E-5 3.45E-5 3.48E-5 3.51E-5 3.54E-5 3.57E-5
3.6E-5 3.63E-5 3.66E-5 3.69E-5 3.71E-5 3.74E-5 3.77E-5
3.8E-5 3.83E-5 3.86E-5 3.89E-5 3.91E-5 3.94E-5 3.97E-5
4.11E-5 4.24E-5 4.37E-5 4.49E-5 4.62E-5 4.74E-5 4.86E-5
4.97E-5 5.09E-5 5.2E-5 5.31E-5 5.42E-5 5.52E-5 5.63E-5
5.73E-5 5.83E-5 5.93E-5 6.03E-5 6.12E-5 6.22E-5 6.22E-5>
END MODULE VISCOSITY
MODULE CONDUCTIVITY
type="tabulation"
param=<200.0 210.0 220.0 230.0 240.0 250.0 260.0 270.0
280.0 290.0 300.0 310.0 320.0 330.0 340.0 350.0 360.0
370.0 380.0 390.0 400.0 410.0 420.0 430.0 440.0 450.0
460.0 470.0 480.0 490.0 500.0 510.0 520.0 530.0 540.0
550.0 560.0 570.0 580.0 590.0 600.0 610.0 620.0 630.0
640.0 650.0 660.0 670.0 680.0 690.0 700.0 710.0 720.0
730.0 740.0 750.0 760.0 770.0 780.0 790.0 800.0 810.0
820.0 830.0 840.0 850.0 860.0 870.0 880.0 890.0 900.0
910.0 920.0 930.0 940.0 950.0 960.0 970.0 980.0 990.0
1000.0 1010.0 1020.0 1030.0 1040.0 1050.0 1060.0 1070.0
1080.0 1090.0 1100.0 1110.0 1120.0 1130.0 1140.0 1150.0
1160.0 1170.0 1180.0 1190.0 1200.0 1210.0 1220.0 1230.0
1240.0 1250.0 1300.0 1350.0 1400.0 1450.0 1500.0 6000.0>
value=<0.00953 0.01017 0.01083 0.01151 0.01219
0.01289 0.0136 0.01433 0.01508 0.01585 0.01662 0.0174
0.01817 0.01895 0.01973 0.0205 0.02128 0.02206 0.02284
0.02362 0.02441 0.02519 0.02598 0.02677 0.02756
0.02834 0.02912 0.02991 0.0307 0.03149 0.03228 0.0331
0.0339 0.0347 0.0355 0.0363 0.0371 0.0379 0.0387 0.0395
0.0403 0.0412 0.0421 0.0429 0.0438 0.0446 0.0455 0.0463
0.0472 0.048 0.0487 0.0495 0.0503 0.051 0.0518 0.0525
0.0532 0.054 0.0547 0.0553 0.056 0.0566 0.0572 0.0578
0.0584 0.059 0.0597 0.0603 0.0609 0.0615 0.0621 0.0627
0.0633 0.0639 0.0645 0.0651 0.0656 0.0662 0.0668 0.0674
0.068 0.0685 0.0691 0.0696 0.0702 0.0707 0.0713 0.0718
0.0723 0.0728 0.0733 0.0738 0.0743 0.0747 0.0752 0.0757
0.0761 0.0766 0.0771 0.0775 0.078 0.0785 0.0789 0.0793
0.0798 0.0804 0.0825 0.0846 0.0867 0.0888 0.0909 0.0909>
END MODULE CONDUCTIVITY
type="gas"

```

```

name="CO2"
molar=0.044
heat_of_formation=-393520.0
verbose=false
END MODULE CO2
MODULE H2O
MODULE ENTHALPY
MODULE FUNC_LIST
MODULE FUNCTION#1
type="janaf"
molar_mass=0.018
formation_heat=-241826.4
cp_coef=<30.092 6.832514 6.793435 -2.53448 0.082139>
bound_min=200.0
bound_max=1700.0
END MODULE FUNCTION#1
MODULE FUNCTION#2
type="janaf"
molar_mass=0.018
formation_heat=-241826.4
cp_coef=<41.96426 8.622053 -1.49978 0.098119 -
11.15764>
bound_min=1700.0
bound_max=6000.0
END MODULE FUNCTION#2
END MODULE FUNC_LIST
type="piecewise_continuous"
END MODULE ENTHALPY
MODULE VISCOSITY
type="tabulation"
param=<200.0 280.0 290.0 300.0 310.0 320.0 330.0 340.0
350.0 360.0 370.0 380.0 390.0 400.0 410.0 420.0 430.0
440.0 450.0 460.0 470.0 480.0 490.0 500.0 510.0 520.0
530.0 540.0 550.0 560.0 570.0 580.0 590.0 600.0 610.0
620.0 630.0 640.0 650.0 660.0 670.0 680.0 690.0 700.0
710.0 720.0 730.0 740.0 750.0 760.0 770.0 780.0 790.0
800.0 810.0 820.0 830.0 840.0 850.0 860.0 870.0 880.0
890.0 900.0 910.0 920.0 930.0 940.0 950.0 960.0 970.0
980.0 990.0 1000.0 3000.0>
value=<8.32E-6 8.32E-6 8.73E-6 9.13E-6 9.54E-6 9.95E-6
1.035E-5 1.076E-5 1.117E-5 1.157E-5 1.198E-5 1.239E-5
1.28E-5 1.32E-5 1.361E-5 1.402E-5 1.442E-5 1.483E-5
1.524E-5 1.564E-5 1.605E-5 1.646E-5 1.687E-5 1.727E-5
1.768E-5 1.809E-5 1.849E-5 1.89E-5 1.931E-5 1.971E-5
2.012E-5 2.053E-5 2.094E-5 2.134E-5 2.175E-5 2.216E-5
2.256E-5 2.297E-5 2.338E-5 2.378E-5 2.419E-5 2.46E-5
2.501E-5 2.541E-5 2.582E-5 2.623E-5 2.663E-5 2.704E-5
2.745E-5 2.785E-5 2.825E-5 2.867E-5 2.908E-5 2.948E-5
2.989E-5 3.03E-5 3.07E-5 3.111E-5 3.152E-5 3.192E-5
3.233E-5 3.274E-5 3.315E-5 3.355E-5 3.396E-5 3.437E-5
3.477E-5 3.518E-5 3.559E-5 3.599E-5 3.64E-5 3.681E-5
3.722E-5 3.762E-5 3.762E-5>
END MODULE VISCOSITY
MODULE CONDUCTIVITY
type="tabulation"
param=<200.0 280.0 290.0 300.0 310.0 320.0 330.0 340.0
350.0 360.0 370.0 380.0 390.0 400.0 410.0 420.0 430.0
440.0 450.0 460.0 470.0 480.0 490.0 500.0 510.0 520.0
530.0 540.0 550.0 560.0 570.0 580.0 590.0 600.0 610.0
620.0 630.0 640.0 650.0 660.0 670.0 680.0 690.0 700.0
710.0 720.0 730.0 740.0 750.0 760.0 770.0 780.0 790.0

```



```

800.0 810.0 820.0 830.0 840.0 850.0 860.0 870.0 880.0
890.0 900.0 6000.0>
value=<0.0164 0.0164 0.0172 0.0181 0.0189 0.0197
0.0205 0.0214 0.0222 0.0231 0.0239 0.0248 0.0256 0.0264
0.0273 0.0282 0.0291 0.03 0.0307 0.0317 0.0327 0.0337
0.0347 0.0357 0.0368 0.0378 0.0389 0.04 0.0411 0.0422
0.0432 0.0443 0.0454 0.0464 0.0475 0.0486 0.0497 0.0508
0.0518 0.0529 0.054 0.0551 0.0562 0.0572 0.058 0.059
0.06 0.062 0.063 0.064 0.065 0.066 0.067 0.068 0.069 0.07
0.071 0.072 0.073 0.074 0.075 0.076 0.077 0.078 0.078>
END MODULE CONDUCTIVITY
type="gas"
name="H2O"
molar=0.018
heat_of_formation=-241830.0
verbose=false
END MODULE H2O
MODULE CO
MODULE ENTHALPY
MODULE FUNC_LIST
MODULE FUNCTION#1
type="janaf"
molar_mass=0.0280101
formation_heat=-110527.1
cp_coef=<25.56759 6.09613 4.054656 -2.671301 0.131021>
bound_min=200.0
bound_max=1300.0
END MODULE FUNCTION#1
MODULE FUNCTION#2
type="janaf"
molar_mass=0.0280101
formation_heat=-110527.1
cp_coef=<35.1507 1.300095 -0.205921 0.01355 -3.28278>
bound_min=1300.0
bound_max=6000.0
END MODULE FUNCTION#2
END MODULE FUNC_LIST
type="piecewise_continuous"
reference="http://webbook.nist.gov from Chase, M.W., Jr.,
NIST-JANAF Thermochemical Tables, Fourth Edition, J.
Phys. Chem. Ref. Data, Monograph 9, 1998"
END MODULE ENTHALPY
MODULE VISCOSITY
type="tabulation"
param=<80.0 90.0 100.0 110.0 120.0 130.0 140.0 150.0
160.0 170.0 180.0 190.0 200.0 210.0 220.0 230.0 240.0
250.0 260.0 270.0 280.0 290.0 300.0 310.0 320.0 330.0
340.0 350.0 360.0 370.0 380.0 390.0 400.0 410.0 420.0
430.0 440.0 450.0 460.0 470.0 480.0 490.0 500.0 510.0
520.0 530.0 540.0 550.0 560.0 570.0 580.0 590.0 600.0
610.0 620.0 630.0 640.0 650.0 660.0 670.0 680.0 690.0
700.0 710.0 720.0 730.0 740.0 750.0 760.0 770.0 780.0
790.0 800.0 810.0 820.0 830.0 840.0 850.0 860.0 870.0
880.0 890.0 900.0 910.0 920.0 930.0 940.0 950.0 960.0
970.0 980.0 990.0 1000.0 1010.0 1020.0 1030.0 1040.0
1050.0 1060.0 1070.0 1080.0 1090.0 1100.0 1110.0 1120.0
1130.0 1140.0 1150.0 1160.0 1170.0 1180.0 1190.0 1200.0
1210.0 1220.0 1230.0 1240.0 1250.0 1260.0 1270.0 1280.0
1290.0 1300.0 1310.0 1320.0 1330.0 1340.0 1350.0 1360.0
1370.0 1380.0 1390.0 1400.0 1410.0 1420.0 1430.0 1440.0
1450.0 1460.0 1470.0 1480.0 1490.0 1500.0 3000.0>

```

```

value=<5.4E-6 6.06E-6 6.7E-6 7.34E-6 7.98E-6 8.61E-6
9.23E-6 9.84E-6 1.044E-5 1.103E-5 1.161E-5 1.218E-5
1.274E-5 1.329E-5 1.382E-5 1.435E-5 1.487E-5 1.538E-5
1.588E-5 1.638E-5 1.687E-5 1.734E-5 1.781E-5 1.827E-5
1.873E-5 1.918E-5 1.962E-5 2.005E-5 2.048E-5 2.091E-5
2.132E-5 2.174E-5 2.214E-5 2.254E-5 2.294E-5 2.333E-5
2.372E-5 2.41E-5 2.448E-5 2.485E-5 2.522E-5 2.559E-5
2.595E-5 2.63E-5 2.67E-5 2.7E-5 2.74E-5 2.77E-5 2.8E-5
2.84E-5 2.87E-5 2.9E-5 2.94E-5 2.97E-5 3.0E-5 3.03E-5
3.07E-5 3.1E-5 3.13E-5 3.16E-5 3.19E-5 3.22E-5 3.25E-5
3.28E-5 3.31E-5 3.34E-5 3.37E-5 3.4E-5 3.43E-5 3.45E-5
3.48E-5 3.51E-5 3.54E-5 3.57E-5 3.59E-5 3.62E-5 3.65E-5
3.68E-5 3.7E-5 3.73E-5 3.76E-5 3.78E-5 3.81E-5 3.83E-5
3.86E-5 3.89E-5 3.91E-5 3.94E-5 3.96E-5 3.99E-5 4.01E-5
4.04E-5 4.06E-5 4.08E-5 4.11E-5 4.13E-5 4.16E-5 4.18E-5
4.21E-5 4.23E-5 4.25E-5 4.28E-5 4.3E-5 4.32E-5 4.35E-5
4.37E-5 4.39E-5 4.42E-5 4.44E-5 4.46E-5 4.49E-5 4.51E-5
4.53E-5 4.55E-5 4.57E-5 4.6E-5 4.62E-5 4.64E-5 4.66E-5
4.68E-5 4.71E-5 4.73E-5 4.75E-5 4.77E-5 4.79E-5 4.81E-5
4.83E-5 4.85E-5 4.87E-5 4.9E-5 4.92E-5 4.94E-5 4.96E-5
4.98E-5 5.0E-5 5.02E-5 5.04E-5 5.06E-5 5.08E-5 5.1E-5
5.12E-5 5.14E-5 5.16E-5 5.16E-5>
reference="Touloukian, Viscosity, Thermophysical
properties of matter, The TPRC Data Series, 1970"
END MODULE VISCOSITY
MODULE CONDUCTIVITY
type="tabulation"
param=<100.0 110.0 120.0 130.0 140.0 150.0 160.0 170.0
180.0 190.0 200.0 210.0 220.0 230.0 240.0 250.0 260.0
270.0 280.0 290.0 300.0 310.0 320.0 330.0 340.0 350.0
360.0 370.0 380.0 390.0 400.0 410.0 420.0 430.0 440.0
450.0 460.0 470.0 480.0 490.0 500.0 510.0 520.0 530.0
540.0 550.0 560.0 570.0 580.0 590.0 600.0 610.0 620.0
630.0 640.0 650.0 660.0 670.0 680.0 690.0 700.0 710.0
720.0 730.0 740.0 750.0 760.0 770.0 780.0 790.0 800.0
810.0 820.0 830.0 840.0 850.0 860.0 870.0 880.0 890.0
900.0 910.0 920.0 930.0 940.0 950.0 960.0 970.0 980.0
990.0 1000.0 1010.0 1020.0 1030.0 1040.0 1050.0 1060.0
1070.0 1080.0 1090.0 1100.0 1110.0 1120.0 1130.0 1140.0
1150.0 1160.0 1170.0 1180.0 1190.0 1200.0 1210.0 1220.0
1230.0 1240.0 1250.0 3000.0>
value=<0.00875 0.00962 0.01049 0.01138 0.01228
0.01318 0.01406 0.01492 0.01577 0.01661 0.01745
0.01825 0.01904 0.01983 0.02062 0.02141 0.0222 0.0229
0.0237 0.0244 0.0252 0.0259 0.0266 0.0274 0.0281 0.0288
0.0295 0.0302 0.0309 0.0316 0.0323 0.0329 0.0336 0.0342
0.0349 0.0355 0.0362 0.0367 0.0374 0.038 0.0386 0.0392
0.0398 0.0404 0.041 0.0416 0.0421 0.0427 0.0433 0.0438
0.0444 0.045 0.0455 0.046 0.0465 0.0471 0.0476 0.0481
0.0486 0.0491 0.0497 0.0502 0.0508 0.0513 0.0518 0.0523
0.0528 0.0533 0.0538 0.0544 0.0549 0.0553 0.0558 0.0563
0.0568 0.0572 0.0577 0.0582 0.0587 0.0592 0.0596 0.0601
0.0606 0.0611 0.0616 0.0621 0.0625 0.063 0.0635 0.0639
0.0644 0.0649 0.0654 0.0659 0.0663 0.0668 0.0673 0.0677
0.0683 0.0687 0.0692 0.0697 0.0701 0.0706 0.071 0.0715
0.072 0.0725 0.0729 0.0733 0.0738 0.0743 0.0747 0.0752
0.0756 0.0761 0.0761>
reference="Touloukian, Thermal Conductivity -
nonmetallic liquids and gases, Thermophysical properties
of matter, The TPRC Data Series, 1970"
END MODULE CONDUCTIVITY
type="gas"

```

```

name="CO"
molar=0.0280101
heat_of_formation=-110530.0
reference="http://webbook.nist.gov/cgi/cbook.cgi?ID=C63
0080&Units=SI&Mask=1#Thermo-Gas"
END MODULE CO
MODULE SOOT
MODULE ENTHALPY
type="polynom"
coefficient=<-208705.0 700.0>
reference="The SFPE Handbook of Fire Protection
Engineering, 1995, 2nd Edition, The National Fire
Protection Association, 1-97"
END MODULE ENTHALPY
MODULE CONDUCTIVITY
type="constant"
value=140.0
reference="HandBook of Chemistry and Physics, 85th
Edition, CRC Press, 12-221"
END MODULE CONDUCTIVITY
MODULE VISCOSITY
type="constant"
value=1.0E-5
reference="Dummy value"
END MODULE VISCOSITY
MODULE REPARTITION
type="mass_lognormal"
geometric_standard_deviation=1.8
mass_median_diameter=1.0E-6
class_number=1
bound_coef=4.0
END MODULE REPARTITION
MODULE SOLID_DATA
shape_factor=1.0
density=1800.0
END MODULE SOLID_DATA
type="particle"
name="SOOT"
heat_of_formation=0.0
comment="particle de suie (generique)"
END MODULE SOOT
END MODULE CARRIER_GAS
END MODULE SPECIES_LIST
MODULE CONDITION_LAWS
END MODULE CONDITION_LAWS
MODULE PREPROCESSOR
static_check=true
dynamic_check=true
compute_densities=true
compute_resistances=true
END MODULE PREPROCESSOR
concrete_name="Transient"
filename=($$$_file_name)
revision=1.423
show_additional_data=true
problem_description="thermic"
END          MODULE          PEL_Application

```

